BIOSORPTIVE REMOVAL OF HEAVY METALS USING *SARGASSUM FILIPENDULA* FROM WASTEWATER

Ph.D Thesis

by

AYUSHI VERMA

DEPARTMENT OF CHEMICAL ENGINEERING
INDIAN INSTITUTE OF TECHNOLOGY ROORKEE
ROORKEE-247 667 (INDIA)
JANUARY, 2018

BIOSORPTIVE REMOVAL OF HEAVY METALS USING *SARGASSUM FILIPENDULA* FROM WASTEWATER

A THESIS

Submitted in partial fulfilment of the requirements for the award of the degree

of

DOCTOR OF PHILOSOPHY

in

CHEMICAL ENGINEERING

by

AYUSHI VERMA

DEPARTMENT OF CHEMICAL ENGINEERING
INDIAN INSTITUTE OF TECHNOLOGY ROORKEE
ROORKEE-247 667 (INDIA)
JANUARY, 2018

INDIAN INSTITUTE OF TECHNOLOGY ROORKEE

CANDIDATE'S DECLARATION

I hereby certify that the work which is being presented in the thesis entitled **"BIOSORPTIVE REMOVAL OF HEAVY METALS USING *SARGASSUM FILIPENDULA* FROM WASTEWATER"** in partial fulfilment of the requirements for the award of the degree of Doctor of Philosophy and submitted in the Department of Chemical Engineering of the Indian Institute of Technology Roorkee, Roorkee is an authentic record of my own work carried out during a period from January, 2013 to January, 2018 under the supervision of Dr. C.B. Majumder, Professor and Late Dr. Shashi Kumar, Professor, Department of Chemical Engineering, Indian Institute of Technology Roorkee, Roorkee, India.

The matter presented in this thesis has not been submitted by me for the award of any other degree of this or any other Institution.

Signature of the Candidate

This is to certify that the above statement made by the candidate is correct to the best of my knowledge.

Signature of Supervisor

The Ph. D. Viva-Voce Examination of Ayushi Verma, Research Scholar, has been held on 13th June 2018.

Chairman, SRC **Signature of External Examiner**

This is to certify that the student has made all the corrections in the thesis.

Signature of Supervisor **Head of the Department**

Date:

ACKNOWLEDGEMENTS

I would like to express my heartiest gratitude to my research supervisors Dr. C.B. Majumder, Professor and Late Dr. Shashi Kumar Professor, Department of Chemical Engineering, Indian Institute of Technology Roorkee, for their precious guidance, interest, stimulating suggestions and supervision at every level of this thesis. I am obliged forever for their kind inspiration, encouragement, useful criticism and constant support without which it was not possible to complete this work. I have gained enormous knowledge from them during my research work that would be immensely useful to me for all my future endeavours.

I am thankful to Dr. Surendra Kumar, Professor, Department of Chemical Engineering, Indian Institute of Technology Roorkee, for his support and guidance during my research work. My sincere and grateful thanks are also due to student research committee (SRC) members Dr. Amit Dhiman, Associate Professor, Department of Chemical Engineering and Dr. Bijan Choudhury, Associate Professor, Department of Biotechnology, Indian Institute of Technology Roorkee, for their time and invaluable input to my research.

I would like to express my gratitude to my lab mates and special thanks to my dear friends Neetu, Komal, Shweta, Rimpi, Rashmi and Uttam whose love and support had made me overcome the lows and highs of research tenure.

My humble thanks to all the technical and ministerial staff of the Department of Chemical Engineering for their assistance. I am sincerely grateful to Annu, Vandana, Aarti, Mr. Akhilesh Sharma, Mr. Manga Ram, staff members of I.A. Laboratory, Department of Chemical Engineering, Indian Institute of Technology, Roorkee for their constant support.

I am also thankful to the Head and technical staffs of the Institute Instrumentation Centre for their help in the analysis of the samples.

I would deeply appreciate to my parents, brother and sister for their generous support, motivation and trust in me, without which it was not possible for me to complete my research work.

I am profoundly thankful to the Ministry of Human Resource Development (MHRD), Government of India for proving a financial assistance.

Above all, I thank 'Almighty God' for encouraging me in every possible way to reach this far.

(AYUSHI VERMA)

ABSTRACT

Environmental pollution particularly from heavy metals in the wastewater is the most severe worldwide problem. Heavy metals are major pollutants in marine, ground, industrial surface and even treated wastewater. Effluents from large number of industries like textile, leather, tannery, electroplating, wood processing, paint, photographic film production, petroleum refining, dyes and pigment, etc. contains significant amount of heavy metals in their wastewater. The heavy metals are non-biodegradable and persistent in nature which can accumulate in the food chain. They are toxic and carcinogenic which causes a serious threat to the human health. To avoid health hazards it is necessary to eradicate these toxic heavy metals from waste water before its dumping into wastewater stream. Several conventional methods are available for removal of heavy metals from wastewater such as chemical oxidation, electro dialysis, ion exchange, chemical precipitation, reverse osmosis, membrane separation etc. These methods are costly, require high energy input, associated with generation of toxic sludge, and less effective. Biosorption has emerged out as a better economical and effective alternative treatment methods. In general low concentrations of heavy metals are present in the wastewater which can be removed by biosorption. This makes biosorption an economical and favorable technology for heavy metal removal from wastewater.

For this study brown marine algae *Sargassum filipendula* was used as biosorbent for Pb^{2+}, Cd^{2+}, and Ni^{2+} ions biosorption from aqueous solution. The biosorbent was characterized by FESEM-EDS, and FTIR analysis. Batch experimentation was carried out for single and dual metal ion systems to examine the effect of various process parameters like temperature, initial metal ions concentration, pH, biosorbent dosage and contact time on effective removal of Pb^{2+}, Cd^{2+}, and Ni^{2+} ions. Response surface methodology was used to optimize the biosorption process parameters. Simultaneous removal of dual metal ions (Pb^{2+} and Cd^{2+}) were also examined.

The optimum process parameters for Pb^{2+} ions biosorption were obtained as temperature (34.8 °C), pH (4.99), initial Pb^{2+} ions concentration (152.10 mg/L) and biosorbent dosage (0.49 g/L) with 96 % of Pb^{2+} ions removal were achieved. The optimum values of four process parameters for

Cd^{2+} ions biosorption were obtained as pH (5.7), temperature (34.2 °C), initial Cd^{2+} ions concentration (50.8 mg/L), and biosorbent dosage (0.99 g/L) with 99.56 % removal of Cd^{2+} ions. The optimum values of four process parameters for Ni^{2+} ions biosorption were obtained as temperature (41.47 °C), pH (5.4), biosorbent dosage (1.97 g/L), and initial Ni^{2+} ions concentration (83.18 mg/L) with 68.45 % removal of Ni^{2+} ions.

The experimental data of Pb^{2+}, Cd^{2+}, and Ni^{2+} ions biosorption were fitted to six isotherm models. Non-linear regression analysis was used to identify the best-fitted isotherm model on the basis of normalized standard deviation and correlation coefficients. The parameters of isotherm models was examined by MATLAB 2013. The maximum biosorption capacity of *S. filipendula* estimated for Pb^{2+}, Cd^{2+}, and Ni^{2+} ions using Langmuir model were obtained as 367.942, 103.5, and 34.3 mg/g, respectively. The best fitted isotherm models were found to be Fritz (for Pb^{2+}) and Redlich-Peterson (for Cd^{2+} and Ni^{2+}). The experimental data of Pb^{2+}, Cd^{2+}, and Ni^{2+} ions biosorption were fitted to six kinetic models to determine removal rate of solute, rate controlling step and the biosorption mechanism. The kinetic data of Pb^{2+}, Cd^{2+}, and Ni^{2+} ions followed Bangham, pseudo second order, and pseudo first order kinetic models, respectively. Thermodynamic parameters were also examined. The overall biosorption process of Pb^{2+}, Cd^{2+}, and Ni^{2+} ions was spontaneous, endothermic and feasible in nature. Desorption study was also carried out to examine the regeneration and reuse capacity of *S. filipendula.* Desorption study shows the better reusability of *S. filipendula* during four consecutive cycles of biosorption and desorption without any significant loss of their biosorption capacities. According to physiochemical properties of metal ions, the order of metal ions uptake on *S. filipendula* was found to be $Pb^{2+} > Cd^{2+} > Ni^{2+}$.

The experiments for simultaneous removal of Pb^{2+} and Cd^{2+} ions from dual metal ions system were carried out to study the competitive effect of metal ions. For dual metal ion system: (a) the concentration of Pb^{2+} ions was changed from 0 to 300 mg/L with 50 mg/L of Cd^{2+} ions concentration (b) the concentration of Cd^{2+} ions was changed from 0 to 300 mg/L with 50 mg/L of Pb^{2+} ions concentration. The six multicomponent isotherm models were fitted to experimental data of dual metal ions biosorption. The best fitted isotherm models for dual metal ions biosorption system was found to be extended Freundlich isotherm model. The effect of presence of Pb^{2+} and Cd^{2+} ions on each other was found to be antagonistic in nature which results in less removal of both the metal ions.

TABLE OF CONTENTS

LIST OF TABLES

LIST OF FIGURES

NOMENCLATURE

Symbols

A	Cross sectional area of metal ion (m^2)
a	Radke-Prausnitz model exponent
a_t	Toth isotherm constant (mg/L)
b	Langmuir isotherm constant indicates the affinity between the biosorbent and biosorbate (L/mg)
B_F	Bias factor (–)
b_i	Modified Langmuir model constant for i^{th} component estimated from single component Langmuir isotherm models (L/mg)
b_o	Redlich-Peterson isotherm exponent (–)
C_e	Equilibrium concentration of metal ion (mg/L)
C_i	Initial concentration of metal ion (mg/L)
C	Intercept of the intraparticle diffusion plot (mg/g)
$C_{e,i}$	equilibrium concentration of component '*i*' in a multicomponent system consisting *N* components (mg/L)
h	Initial biosorption rate (mg/g.min)
K	Pseudo second order equilibrium rate constant (g/mg.min)
k	Number of variables (–)
K	Adsorption equilibrium constant (L/g)
K_1	Redlich-Peterson isotherm constant (L/g)
K_2	Redlich-Peterson isotherm constant $(L/mg)^{bo}$
k_b	Bangham model constant (mL/g.L)

k_f	Freundlich isotherm constant ((mg/g)(L/mg)$^{1/n}$)
K_{id}	Intraparticle diffusion rate constant (mg/g.min$^{0.5}$)
K_o	Radke-Prausnitz equilibrium constant (L/mg)
k_3	Modified Freundlich uptake rate constant (L/g.min)
k_o	Biosorption rate constant of pseudo first order kinetics (min^{-1})
m_1	Kuo-Lotse constant (–)
M	Molecular weight of metal ion (g/mol)
m	Mass of biosorbent (g)
N	Avogadro number (–)
n	Freundlich model exponent (–)
N	Total data points (–)
n_1	Toth isotherm exponent, a measure of surface heterogeneity (–)
η_i	Correction factor of component '*i*' (–)
N_o	Number of experiments carried out at the center (–)
q_e	Biosorption capacity of a biosorbent represent the amount of biosorbate biosorbed on the biosorbent surface at equilibrium (mg/g)
$q_{e,cal}$	Predicted value of q_e obtained by models
$q_{e,exp}$	Experimental value of q_e (mg/g)
q_m	Monolayer biosorption capacity (g/g)
q_o	Maximum monolayer adsorption capacity predicted by Langmuir isotherm (mg/g)
$q_{o,i}$	Modified Langmuir model constant for ith component estimated from single component Langmuir isotherm models (mg/g)
q_t	Amount of metal ions biosorbed at time 't' (mg/g)
R	Universal gas constant (kJ/mol.K)

S	Specific surface area of biosorbent (m^2/g)
t	Contact time (min)
T	Temperature (Kelvin)
V	Volume of solution (L)
x_i	Uncoded real value of the i^{th} independent variable
Y	Predicted response (%)

Greek Symbols

α_o	Bangham model constant (–)
α	Elovich coefficient representing the initial rate of biosorption (mg/ g.min)
α_1	Fritz isotherm constant ((mg/g) (L/mg) $^{\beta 1}$)
α_2	Fritz isotherm constant ((L/mg) $^{\beta 2}$)
β	Elovich coefficient representing the desorption constant (g/mg)
β_0	Independent term of regression equation (–)
β_1	Fritz equation exponent (–)
β_2	Fritz equation exponent (–)
β_i,	linear of regression equation (–)
β_{ii}	Second order term of regression equation (–)
β_{ij}	Interactive term of regression equation (–)
$\Delta G°$	Gibb's free energy change (kJ/mol)
$\Delta H°$	Enthalpy change (kJ/mol)
$\Delta S°$	Entropy change (J/mol.K)

ABBREVIATIONS

AAS	Atomic Absorbtion Spectroscopy
ARE	Average Relative Error
CCD	Central Composite Design
FESEM	Field Emission Scanning Electron Microscope
EDS	Energy-dispersive X-ray spectroscopy
FTIR	Fourier-transform infrared spectroscopy
NSD	Normalized standard deviation
RMSE	Root mean square error
RSM	Response Surface Methodology

CHAPTER I

INTRODUCTION

1.0 GENERAL

Environmental pollution caused by rapid growth in industry, agriculture, hospital and health-care facilities has become a global concern contributing to the destruction of the biosphere. Especially the pollutants which are released from industries and discharged into the environment, affect the soil, air and water [25]. Among all the environmental pollutions, water is the most effected natural resource. Water is a vital natural resource for all the living organisms which exist in the universe. The water pollution due to the indiscriminate discharge of industrial wastewaters is a worldwide concern for the last few decades [106, 178]. It results into several health issues and low quality of life. Everyday 14000 people lose their life because of water pollution. The pollutants present in water make it unsuitable for irrigation, drinking and many other valuable purposes. The other main sources of water pollution are marine dumping, radioactive waste, oil pollution, sewage, atmospheric deposition, global warming, and underground storage leakages. Besides, some of the industrial effluents contain heavy metals, which may contaminate the natural water bodies due to which aquatic ecosystem are at a great risk [7]. The direct discharged wastewater containing heavy metals causes detrimental effects on all living organisms. The main causes of industrial pollution are lack of policies to control pollution, use of outdated technologies, unplanned industrial growth, and inefficient waste disposal [29, 172]. It is a major problem in both developing and industrialized countries. However, advanced and effective waste water treatment technologies are available which may suitably treat the industrial wastewater before its discharge into the water bodies [100].

Among several toxic and harmful pollutants such as pesticides, dyes, heavy metals, fluorides etc, heavy metal contamination is more severe pollutant for flora and fauna, and human health [302, 324]. In priority list of hazardous substances prepared by EPA, heavy metals are present at the top position among all the inorganic pollutants [116]. The metals with high atomic weight (63.5-200.6) and density (> 6 g/cm^3) are referred to as "heavy metals". Heavy metals exist naturally in ore minerals and rock formation. The industrial effluents are the anthropogenic source of heavy metals for water bodies. The natural biogeochemical cycles of metals has been disturbed by cumulative release of heavy metals into the environment by anthropogenic source in ecosystem [211, 226]. Several industries from which heavy metals are released into wastewater are metal plating, pulp and paper, tanneries, battery making, pesticides, electric appliance manufacturing, metal surface treating, leather working, paint, electroplating, ceramic and glass manufacturing, textile, plastic, fertilizer industries, photography, iron and steel manufacturing, metallurgical processes, dye and pigment industries [17, 88, 100, 285, 307]. Many heavy metals are toxic and carcinogenic even at low concentration [117, 245]. The heavy metals, which are extensively toxic to ecological environments and human beings, include copper (Cu), lead (Pb), chromium (Cr), zinc (Zn), manganese (Mn), mercury (Hg), nickel (Ni), cadmium (Cd), and iron (Fe) etc [57, 112, 205, 337]. Heavy metals are persistent, non-biodegradable and toxic in nature [259]. Bioaccumulation of heavy metals occurs in the entire food chain where they bind with the biomolecules of human body and form a stable and non-dissociated bio toxic compound which results in several diseases and disorders [59, 121, 250, 289]. Some past history of disasters caused by heavy metals contamination in water are 'Itai-Itai' due to contamination of cadmium in Jintsu river of Japan and 'Minamata' tragedy in Japan due to mercury contamination [307].

Generally, the heavy metals are categorized in two groups: (i) essential heavy metals which are required within permissible limit for physiological and biological functions of normal body (Co, Zn, Cu, Fe, Mn, Mg, Ni, Se), and (ii) non-essential heavy metals which are not required for normal growth and they are toxic even at low concentration (Pb, Cd, As, Hg) [230, 341, 342]. Lead cadmium and nickel are significant heavy metals, and their toxicity is a big issue for evolutionary, ecological, environmental and nutritional reasons [151, 245]. They along with high doses of nickel are also acknowledged by EPA as toxic and priority heavy metals that should be treated before releasing into wastewater. Therefore, in present work our focus is on the removal of lead, cadmium and nickel ions from wastewaters.

1.1 ABOUT Pb^{2+}, Cd^{2+} AND Ni^{2+} IONS

Based on the Agency for Toxic Substances and Disease Registry pollutants priority list (ASTDR 2015) the lead is present on second position as hazardous heavy metal after arsenic which is classified as carcinogenic to humans [88]. Lead (Pb) is a ductile, malleable, soft, and gray colored metal with high melting point (327.4 °C), boiling point (1749 °C), density (11.34 g/cm^3) and atomic weight (207.2 u). It exists in 0 and + 2 oxidation states. Lead forms low solubility complexes with organic (fulvic and humic acids, amino acids, EDTA) and inorganic ligands (PO_4^{3-}, Cl^{1-}, CO_3^{2-}, SO_4^{3-}). Mainly the lead ions are present in effluents of lead and lead processing industries [49, 344]. According to WHO and EPA the maximum limits of discharge of lead ions in wastewater is 0.5 mg/L, for drinking water is 0.05 mg/L and for sewage slurry applied to agriculture land is 420 mg/L [24, 58, 85]. Thus, the concentration of lead ions in wastewater must be reduced to a level of 0.05 mg/L before discharging to water bodies [27, 97, 109]. The list of some industries from which lead ions are discharged beyond a permissible limit is given in **Table 1.1**.

Table 1.1 Concentration of Pb^{2+} ions in wastewater of various industries

S. No.	Industry	Pb^{2+} ions concentration in wastewater (mg/L)	Reference
1	Chemical manufacturing plant, Glubczyce (Poland)	326.4	[315]
2	-	200-500*	[21]
3	Oil	125-150	[308]
4	Battery manufacturing plant	5-15	[350]
5	Electroplating units	116.42	[206]
6	Industrial plant	19.1	[135]
*Industry not mentioned			

According to ASTDR 2015 cadmium is ranked on 7^{th} number among other hazardous environmental pollutants. It exists in form of complex oxides with zinc, lead, copper ore, sulfides and carbonates. The solubility of cadmium chloride and cadmium sulphate in water is more than cadmium oxide. The properties of cadmium (Cd) are given as: atomic mass (112.41 u), density (8.65 g/cm^3), melting point (321.07 °C), and boiling point (767 °C). It is tasteless and odorless element. It does not dissolve in alkaline medium while dissolves in acidic medium to produce Cd^{2+}

ions. When it reacts with bases it forms cadmium hydroxides [Cd $(OH)_2$] as precipitate. It exists as inorganic compounds and complexes with chelating agents. Cadmium is harmful heavy metal because of its high stability and toxicity. The new ways of cadmium application and emission increased day by day because of its low market price. According to WHO and EPA the permitted limit of cadmium in drinking water is 0.005 mg/L [171]. The list of some industries from which cadmium ions are discharged beyond a permissible limit is given in **Table 1.2**.

Table 1.2 Concentration of Cd^{2+} ions in wastewater of various industries

S.No.	Industry	Cd^{2+} ions concentration in wastewater (mg/L)	References
1	Electroplating industry	0.01-3.2	[67]
2	Electroplating industry	1504	[61]
3	Electronic industry	1-10	[217]
4	Washing baths in electroplating process	7-50	[29]
5	Electroplating baths	23000	[29]
6	Passivation bath of electro polishing	2000-5000	[29]

Nickel (Ni) is hard, silvery-white, ductile, and malleable metal. The properties of nickel are given as: atomic mass (58.69 u), density (8.9 g/cm^3), melting point (1453 °C), and boiling point (2730 °C). Various industries like mineral processing, copper sulfate manufacture, refining, pulp and paper mills, electroplating, welding, porcelain enameling, battery and accumulator manufacturing are the main source of nickel ions into wastewater streams [18, 48]. The permissible limit set by WHO and EPA for nickel in drinking water is 0. 5 mg/L [229, 269]. **Table 1.3** shows the concentration of nickel ions in wastewater of various industries.

Table 1.3 Concentration of Ni^{2+} ions in wastewater of various industries

S. No.	Industry	Ni^{2+} ions concentration in wastewater (mg/L)	Reference
1	Nickel plating industry	1250	[155]
2	Chemical manufacturing plant	249.3	[315]
3	Electroplating industry	2240	[247]
4	Electrical Industries	10.21	[179]

1.1.1 Hazardous health effects of Pb^{2+}, Cd^{2+} and Ni^{2+} ions

Lead is a broad-spectrum toxic which can affect all the metabolic function of living beings [50]. The metabolism of lead is closely mimic to that of calcium, mainly at the membranes receptor site, where it replaces calcium ions and severely affects both neuromuscular and synaptic transmissions [266]. It results into accumulation of lead in bones. The lethal and toxic effects of lead are well known [36, 38, 115]. The low level exposure of lead is neurotoxin and linked to pre-senile dementia of Alzheimer's type [138, 229]. It affects the central nervous system during developmental stage and childhood. The adverse effects of lead are more susceptible to infants, developing fetus, pregnant woman, and children up to 6 years of age which results in abortion, stillbirths, sterility, and neo-natal deaths [107, 236]. In addition to this it can damage central nervous system. Lead poisoning results in various unwanted human health effects like sleeplessness, mental retardation, reduction in hemoglobin formation, hypertension, headache, memory loss, kidney and liver damage [199, 227, 252, 347, 354]. The three general disease syndromes are caused by chronic lead poisoning: (a) Central nervous system effects or CNS syndrome that may result to coma and death (b) Neuromuscular effects (lead lapsy) weakness, fatigue muscular atrophy (c) Gastrointestinal disorders, constipation, abdominal pain, etc. [205].

Cadmium shows toxic effect on animals, plants, and humans even at low concentration. Cadmium entering the ecosystem results in bioaccumulation, geo-accumulation, and bio-magnification [63, 127]. International Agency for Research on Cancer (IARC 1993) categorized the cadmium and cadmium compounds in the carcinogenic group of pollutants for humans. Some studies show the evidences of cadmium exposure on human health such as cancer of lungs, breast, prostate and renal [33, 176]. The various lethal effects of cadmium are renal dysfunction, emphysema, damage of nervous system, hypertension, liver injury, muscles cramp, diarrhea, vomiting, nausea, anemia and testicular atrophy [274]. The prolonged exposure of cadmium results in a yellow stain that gradually appears on the joints of the teeth and anemia [167, 178].

The trace amount of nickel is beneficial as an activator of some enzyme systems while intake of nickel beyond permissible limit results in various types of diseases. The International Agency for Research on Cancer (IARC) categorized nickel in group 2B (agents which are possibly carcinogenic to humans) and its compounds in group 1 (there is adequate evidence of

carcinogenicity in humans). Studies of human cell cultures show that Ni^{2+} ions is teratogenic and embryo toxin [49, 311]. The acute poisoning effects of Ni^{2+} ions at higher concentration are dizziness, headache, tightness of the chest, nausea, vomiting, dry cough, chest pain, rapid respiration, lung fibrosis, cyanosis, shortness of breath, and extreme weakness [40, 125, 126, 197]. The exposure of nickel containing coins and jewelry to skin causes an allergic dermatitis called "Nickel Itch" which is lethal [205].

1.2 TREATMENT TECHNIQUES FOR HEAVY METALS REMOVAL

The techniques generally used for heavy metals removal from wastewater consist of physical and chemical methods [37, 238]. Chemical methods are chemical precipitation, ion exchange, coagulation-flocculation and electrochemical methods [31, 35, 125, 258]. Physical methods are flotation, membrane filtration and adsorption.

1.2.1 Chemical methods

(i) Chemical precipitation

Chemical precipitation is a conventional and most widely used technique for the removal of heavy metals from wastewater. In this process at highly alkaline conditions (pH: 9-11), the dissolved metal ions are converted to the insoluble precipitates of carbonate, hydroxide and sulfide by chemical reaction with a precipitating agent like lime. These precipitates can be separated from aqueous solution by sedimentation and filtration. Alkaline reagents such as sodium hydroxide etc. are used to adjust pH of the solution during chemical precipitation. This method is usually able to remove high concentration of heavy metals [48]. It may become too expensive or ineffective to treat wastewater with metal ion concentrations < 10 mg/L [130]. Moreover, lime precipitation can be used to effectively treat inorganic effluent with a metal concentration of higher than 1000 mg/L [177]. In a batch or continuous system lime precipitation was used to remove metal ions like Cd^{2+}, Mn^{2+} and Zn^{2+} with initial metal ions concentrations of 150, 1085 and 450 mg/L, respectively [60]. This method is simple and safe. While the drawbacks of these methods are requirement of large amount of chemicals, slow process due to poor settling of solids, strict process conditions

have to be maintained which is not easy, aggregation of metal precipitates, and the production of excessive sludge, which requires further treatment and creates sludge disposal problem [19].

(ii) Ion exchange

Ion exchange is also one of the most frequently used technique to treat wastewater laden with heavy metals. In this technique metal ions present in aqueous solution are exchanged with cations of insoluble ion exchange resin. The commonly used cation exchangers for the removal of heavy metals are weakly acidic resin with carboxyl acid groups (-COOH) and strongly acidic resin with sulfonic acid groups ($-SO_3H$). Hydrogen ions in carboxylic group or sulfonic group of resin are replaced with metal ions. Among the most commonly studied ion exchange resins, natural zeolites, clinoptilolite shows a high selectivity for some heavy metal ions like Cd^{2+}, Pb^{2+}, Cu^{2+} and Zn^{2+} [77]. This technique is applicable for the removal of metal ions concentration < 100 mg/L [130]. Several other advantages of this technique are high regeneration of materials, metal selective operation, no sludge disposal problem and quick process. However, this technique also has some disadvantages like high capital cost, it cannot be used for large scale, and removes less number of metal ions.

(iii) Coagulation-flocculation

Coagulation–flocculation can be used to remove heavy metals from wastewater. It involves two steps, first step is coagulation in which coagulants (alum, ferric chloride and ferrous sulfate) are added to destabilize the colloidal particles by neutralization of repulsive forces between them. In second step coagulation is followed by the flocculation in which the destabilized unstable neutral particles are aggregated into bulky floccules by adding flocculants (polyacrylamide and polyferric sulfate). Coagulation and flocculation are followed by sedimentation and filtration. Like chemical precipitation, pH varying from 11.0-11.5 was found to be effective to improve the removal of heavy metal by this technique. It can be applicable for large scale wastewater treatment plants. The lime based coagulation involves some more advantages like improved dewatering characteristics, improved sludge settling, sludge stability, bacterial inactivation capability [65, 92]. The disadvantages of this technique are high operational cost due to use of costly reagents, production of sludge in large quantity and sludge disposal problem.

(iv) Electrochemical methods

In this treatment method current is passed in a metal ion containing solution which results in migration of positively charged metal ions towards negatively charged cathode and then the deposited metal ions can be recovered [53]. It can be used to treat wastewater with a metal ion concentration > 10 mg/L [130]. Electrochemical treatments methods are classified as electro dialysis (< 20 mg/L), electrochemical precipitation / electro-coagulation (> 2000 mg/L) and membrane electrolysis (suitable for small, medium and large scales) [3]. The application of electrochemical methods for wastewater treatment involves removal of effluents containing oil, suspended solids, grease, inorganic and organic pollutants. It is widely used for effluent treatment of metal recovery and food processing industries [300]. The advantages of this method are less use of chemicals, metal selective, and recovery of pure metal. However, it requires high capital cost for designing and implementing, not applicable for large volume of wastewater, less efficient at dilute concentration, and corrosion of electrodes during process.

1.2.2 Physical methods

(i) Flotation

It is the only physical separation process which is extensively used for removal of heavy metal at industrial scale [204]. It involves separation of heavy metals from aqueous phase using bubble attachment. Flotation can be classified as: (i) dissolved air flotation (ii) electroflotation (iii) dispersed air flotation (iv) biological flotation (v) vaccum air flotation. Low cost materials like chabazite and zeolite were found to be effective collectors for initial metal ion concentration ranging from 60 to 500 mg/L with removal efficiency of > 95%. Dissolved air flotation is used for clarification of refinery wastewater while dispersed air flotation is well known to treat effluents of mineral processing, and petrochemical industry. Eletroflotation can be applicable for the removal of heavy metals from small, medium, and large scales [79]. The other advantages of this technique are low cost, high metal selectivity, better removal of small particles, high removal efficiency and high flow rate. While disadvantages of this technique are high initial capital and maintenance costs [202, 203, 265].

(ii) Membrane filtration

Membrane filtration is a pressure driven separation process. In this technique membrane provides a physical barrier that permits the passage of particles up to specific size. On the basis of size of particles that have to be retained, different types of membrane filtration techniques are classified as ultrafiltration, nano filtration and reverse osmosis which can be used to remove heavy metals from wastewater. The membrane filtration is employed for the treatment of various effluents of chemical, textile, petrochemical, dye, food, electrochemical, tanning, pulp and paper industries as well as in the treatment of municipal waste waters [89, 110, 353]. Reverse osmosis can achieve 97 % of removal efficiency for metal ion concentration of 20 to 200 mg/L. While ultrafiltration can achieve more than 90 % of removal efficiency for 10 to 112 mg/L metal ion concentration [119]. The advantages of membrane filtration technique are less use of chemicals, less solid waste produced, high efficiency, reuse of wastewater and recovery of valuable materials. While it has some disadvantages like high initial and running cost, less efficient at low metal ion concentration, membrane fouling and low flow rates [329].

(iii) Adsorption

Adsorption process is a potential alternative to physiochemical methods for heavy metal removal from wastewater stream. It is an economic and effective method [31, 122, 294]. Adsorption is based on mass transfer process by which metal ions are transferred from aqueous solution to the surface of adsorbent and bind through physical or chemical interactions [154, 290, 332]. Generally activated carbon is used as an efficient adsorbent [84, 268, 295]. A granular or powdered form of activated carbon consists of porous structure with network of interconnected mesopores, micropores, and macropores which provide a high surface area for the adsorption of heavy metals [4, 40, 283]. The adsorption is suitable for removal of metal ions at concentrations as low as 1 mg/L [318]. However, the use of activated carbon is associated with some disadvantages e.g. thermal and chemical regeneration of spent activated carbon is costly, and higher the quality greater will be the cost, produces additional effluent and results in significant loss of the adsorbent [35, 118, 266]. To overcome these disadvantages, an emerging and economical treatment technology called “Biosorption” has been developed as it involves the use of naturally available

and non-hazardous adsorbents called biosorbents to remove heavy metals from industrial wastewater [355].

1.3 BIOSORPTION OF Pb^{2+}, Cd^{2+} AND Ni^{2+} IONS FROM AQUEOUS SOLUTION

Biosorption is a property of naturally occurring biomass to bind and concentrate heavy metals from aqueous solution on its cellular structure through physiochemical process [13, 83, 281]. The cell wall structure of algae, fungi, yeast and bacteria is responsible for the passive uptake of heavy metals [27, 160, 261, 299, 304]. The main advantages of biosorption are the use of inexpensive biosorbents, it can remove the heavy metal ions even at very low concentration effectively, low sludge production, non-hazardous and it may permit recovery of the metals from the sorbing biomass [68, 152, 306, 322]. The biosorption process involves one or more mechanisms like complexation, coordination, ionic exchange, chelation, inorganic micro-precipitation and physical or chemical adsorption [234, 239, 307].

Marine algae, usually known as seaweeds, are abundantly available in many parts of the world and it can be obtained economically from the ocean at a large scale [149]. The marine algae are proved to be more effective for metal binding activity because of their low cost, high capacity of metal biosorption, and renewable nature [43, 48, 123, 189].They can efficiently remove very low concentration of metal ions ranging from few ppm to several hundred ppm [63]. The cell wall of marine algae consists of sodium, calcium and magnesium salts which act as efficient ion exchangers for removal of metal ions present in an effluent solution [73]. The main mechanism involved in metals ions removal by the algal biosorbents is the ionic exchange. There are three types of algae, red (Rhodophyta), brown (Phaeophyta), and green (Chlorophyta). These types of algae are mainly differing in their cell wall composition, where sorption takes place [136]. Among these, brown algae are proved to be more efficient for biosorption of metal ions because of their acidic polysaccharide content which are present in their cell wall. In brown algae, carboxyl and sulphate are the predominant active groups [244, 260, 314]. The partial or complete esterification of the carboxylic sites results in reduction of Cd^{2+} and Pb^{2+} ions uptake on dried *Sargassum* biomass which shows a clear evidence that carboxylic groups plays main role in the biosorption process [82]. The sulfonic acid groups play a secondary role in metal binding. The effectiveness of biosorption to remove metal ions depends on the pH of the solution, effluent

composition, biosorbent concentration, reaction temperature and kinetics [1, 2, 338]. Compared to different types of marine alga, biosorptive performance shown by *Sargassum* genus of brown alga is proved to be the best due to its high biosorption capacity for metal ions at a low equilibrium concentration [76]. This genus of brown alga is widely distributed in most of the tropical countries and is available in large quantities as a waste seaweed biomass [73, 102, 325, 333]. The main constituents of *Sargassum* sp. brown alga are polysaccharides alginate, usually Ca and Na alginates [104, 301, 312]. Thus it has a high efficiency to accumulate metal ions in comparison to alga of other genera [78]. **Fig 1.1** shows the raw form of *Sargassum filipendula*.

The bacterial strains *Bacillus cereus* and *Bacillus pumilus* were used for the removal of Pb^{2+} ions from aqueous solution. The effects of operating variables contact time, initial metal concentration, adsorbent dosage, and pH were examined in the batch system. The Langmuir and Freundlich model were fitted to the experimental data. The kinetics of Pb^{2+} ions biosorption was studied by using Pseudo first order and Pseudo second order kinetic models. The adsorption capacities of *B. pumilus* and *B. cereus* were found to be 28.06 and 22.1 mg/g, respectively [69].

The biosorption of Pb^{2+} ions was investigated by eight brown, green and red marine algae. Three species of brown algae (*S. natans, S. hystrix* and *Padina pavonia*) efficiently removed Pb^{2+} ions from aqueous solution. It shows that biosorption of metal ions by marine brown algae was done in similar manner as ion-exchange resins. Thus, biosorption of Pb^{2+} ions by using marine brown alga can be considered, as an alternative method for existing lead-removal technology [149].

The potential of a fungal strain *Aspergillus niger* to remove Cd^{2+} ions from aqueous solution was investigated. The effects of initial concentration, pH, temperature, contact time, and agitation rate on the biosorption of Cd^{2+} ions were examined. The maximum uptake capacity of 15.5 mg/g was obtained at initial concentration of 75 mg/L and at pH of 4.0. The experimental equilibrium and kinetic data were analyzed by isotherm and kinetic models, respectively [187].

Fig. 1.1 Raw biomass of *Sargassum filipendula.*

The biosorption of Cd^{2+} ions was done by using a dried brown alga *Fucus spiralis*. The uptake capacity of alga was strongly depends on pH. In less than 1 h 90 % removal efficiency was achieved. The experimental data was fitted to Langmuir, Freundlich, Langmuir-Freundlich and Toth isotherm models to examine the adsorption parameters [71].

The biosorption of Ni^{2+} ions was done by using deactivated protonated baker's yeast. The effects of sorbent dose, pH and initial metal ion concentration were investigated. The kinetics data was analyzed by pseudo first and pseudo second order models. The equilibrium data were explained by Langmuir isotherm model. The maximum adsorption capacity was found to be 11.4 mg/g at pH of 6.75 [150].

The potential of *Bacillus sphaericus* biomass was examined for Ni^{2+} ions biosorption. The biosorption process was affected by various operating conditions such as biomass dosage, pH, temperature, initial Ni^{2+} ions concentration and contact time. The equilibrium data and sorption kinetics were described with isotherm models and the kinetic models, respectively. The maximum uptake capacity of *Bacillus sphaericus* was calculated as 55.55 mg/g using the Langmuir isotherm model. The thermodynamic study was done to find the spontaneity of the biosorption process. The interaction of *Bacillus sphaericus* surface functional groups with Ni^{2+} ions was confirmed by FTIR analysis [28].

The biosorption of Ni^{2+} ions was done by using the brown algae (*Nizmuddinia zanardini, Sargassum glaucescens, Padina australis* and *Cystoseria indica*). The effect of various operating parameters such as contact time, pH, temperature and initial metal concentration were examined. To investigate the controlling mechanism of biosorption process such as chemical reaction and mass transfer dynamic models were fitted to experimental data. The thermodynamic study was carried out to determine whether a process will occur spontaneously or not [243].

The efficacy of different types of algae (green, red and brown) was evaluated for the biosorption of Cd^{2+}, Ni^{2+}, Pb^{2+}, Cu^{2+} and Zn^{2+} in a single metal ion system. It was found that the maximal biosorption capacity was achieved by a brown algae *Fucus spiralis* in the following order: $Pb^{2+} > Cd^{2+} \geqslant Cu^{2+} > Zn^{2+} > Ni^{2+}$. The optimum conditions for biosorption of Pb^{2+} ions were found to be pH 3.0 and biomass dosage 0.5 g/L with 204.1 mg/g biosorption capacity [260].

The biosorption capacity of different marine algae (*Sargassum* sp., *Padina* sp., *Ulva* sp., and *Gracillaria* sp.,) was investigated for the biosorption of copper, zinc, cadmium, nickel, and lead from dilute aqueous solutions. The optimum pH for Pb^{2+} and Cu^{2+} was 5.0 and 5.5 for Ni^{2+}, Zn^{2+} and Cd^{2+}.The maximum uptake capacity was obtained for *Sargassum* sp. (0.61 to 1.16 mmol/g) and *Padina* sp (0.63 to 1.25 mmol/g). The sequence of affinity for *Sargassum* sp. was $Pb^{2+} > Zn^{2+} > Cd^{2+} > Cu^{2+} > Ni^{2+}$ and for *Padina* sp. was $Pb^{2+} > Cu^{2+} > Cd^{2+} > Zn^{2+} > Ni^{2+}$ [284].

On the basis of literature review, it has been found that various biomasses were used as biosorbent for the removal of heavy metals from wastewater (**Table 1.4**). Among various biosorbents brown algae is by far the most exploited biosorbent owing to its ability to act as ion exchangers and its large surface area for removal of heavy metals. Most of the studies have been reported on the removal of heavy metals using brown algae from which very few of them were on *Sargassum filipendula* species of brown algae for Cd^{2+} and Ni^{2+} ions only. So, it has been concluded that research work may be pursued for the removal of Pb^{2+}, Cd^{2+} and Ni^{2+} ions from aqueous solution using *Sargassum filipendula* species of brown algae. Biosorption studies for the removal of metal ions from aqueous solution containing more than one solute (metal ions) are also of interest to simulate industrial environment and therefore may also be conducted.

Table 1.4 Various biomasses used as biosorbent for the removal of Pb^{2+}, Cd^{2+}, and Ni^{2+} ions from wastewater

Type of biomass	Biosorbent	Metal ion	Metal ion concentration (mg/L)	Biosorption capacity (mg/g)	Reference
Red alga	*Hypneavalentiae*	Cd^{2+}	50-250	28.65	[256]
	Galaxaura oblongata	Pb^{2+}	50-300	88.6	[143]
	Galaxaura oblongata	Cd^{2+}	50-300	85.6	[143]
	Gracilaria caudata	Ni^{2+}	0-150	50.1	[43]
Brown alga	*Cystosera indica*	Ni^{2+}	30	7	[253]
	Cystosera indica	Cd^{2+}	56	8.35	[253]
	Cystosera indica	Pb^{2+}	103	47.22	[253]
	Sargassum glaucescens	Pb^{2+}	103	45.84	[253]
	Sargassum glaucescens	Ni^{2+}	30	6.35	[253]
	Sargassum glaucescens	Cd^{2+}	56	4.23	[253]
	Nizimuddinia zanardini	Pb^{2+}	103	50.41	[253]
	Nizimuddinia zanardini	Ni^{2+}	30	6.38	[253]
	Nizimuddinia zanardini	Cd^{2+}	56	4.04	[253]
	Padina australis	Pb^{2+}	103	46.51	[253]
	Padina australis	Ni^{2+}	30	5.96	[253]
	Padina australis	Cd^{2+}	56	3.49	[253]
	Undaria pinnatifida	Ni^{2+}	5-50	24.71	[64]
	Sargassum muticum	Ni^{2+}	0-150	75.6	[43]
	Laminaria hyperboria	Cd^{2+}	75-100	31.3	[105]
	Bifurcaria bifurcata	Cd^{2+}	75-100	30.3	[105]
	Fucus	Cd^{2+}	75-100	42.1	[105]
	Laminaria hyperboria	Pb^{2+}	75-100	50.3	[105]
	Bifurcaria bifurcata	Pb^{2+}	75-100	52.7	[105]
	Fucus	Pb^{2+}	75-100	43.5	[105]
	Sargassum filipendula	Cd^{2+}	11.2-1008	115.36	[193]
	Sargassum filipendula	Ni^{2+}	29.3-263.7	62.7	[162]
Green alga	*Spirogyra*	Pb^{2+}	50-300	90.91	[182]
	Cladophora	Pb^{2+}	50-300	46.51	[182]
	Anabaena sphaerica	Cd^{2+}	50-300	111.1	[32]
	Anabaena sphaerica	Pb^{2+}	50-300	121.9	[32]
	Oedogonium hatei	Ni^{2+}	20-100	40.9	[125]
	Enteromorpha prolifera	Ni^{2+}	50-150	36.8	[240]
	Oedogonium sp.	Pb^{2+}	20-200	145	[123]
	Nostoc	Pb^{2+}	20-200	93.5	[123]
Fungi	*Trichoerma resei*	Pb^{2+}	30	82.64	[111]
	Trichoerma resei	Ni^{2+}	30	70.92	[111]
	Mucor hiemalis	Ni^{2+}	50-300	15.83	[287]
	Mucor indicus	Pb^{2+}	5-25	22	[150]
	Rhizopus cohnii	Cd^{2+}	20-100	40.5	[148]
	Pleurotus platypus	Cd^{2+}	10-100	32.73	[330]

Table 1.4 Continued…

Type of biomass	Biosorbent	Metal ion	Metal ion concentration (mg/L)	Biosorption capacity (mg/g)	Reference
Bacteria	*Bacillus cereus*	Pb^{2+}	10-80	22.1	[69]
	Pseudomonas sp.	Cd^{2+}	10-100	27.69	[142]
	Pseudomonas sp.	Pb^{2+}	10-100	81.74	[142]
	Rhodococcus opacus	Ni^{2+}	5	7.63	[55]
	Aeromonas hydrophila	Pb^{2+}	51-259	163.3	[134]
Yeast	*Yarrowia lipolytica*	Ni^{2+}	1000	95.33	[286]
	Baker's yeast	Ni^{2+}	10-400	9.8	[286]
	Aspergillus niger	Cd^{2+}	8-30	10.14	[22]
	Saccharomyces cerevisiae	Cd^{2+}	8-30	6.71	[114]

1.4 OBJECTIVES

Based on the detailed literature review presented in Chapter II, objectives of the present doctoral thesis have been formulated. In the present thesis efficacy of *S. filipendula* for the biosorption of Pb^{2+}, Ni^{2+}, and Cd^{2+} ions from aqueous solution in single and dual metal ion system have been studied in detail. Response surface methodology has been used to design the experiment and to determine optimized biosorption process parameters. Main objectives for present research work are:

1. To characterize *S. filipendula*, by FESEM analysis to find the surface structure of *S. filipendula*, by EDS analysis, to find the chemical composition of *S. filipendula*, and by FTIR analysis to confirm the presence of functional groups on its surface.

2. To conduct biosorption experiments for the removal of Pb^{2+}, Ni^{2+}, and Cd^{2+} as single metal ion from aqueous solution at the designed process parameters (pH, temperature, initial metal ion concentration, contact time, and biosorbent dosage).

3. To study the effect of different process parameters like pH, initial metal ion concentration, biosorbent dosage, temperature and contact time on biosorption.

4. To study the kinetics, equilibrium, and thermodynamics of Pb^{2+}, Ni^{2+}, and Cd^{2+} ions biosorption on *S. filipendula.*

5. To study the biosorption of multisolute aqueous system (containing Pb^{2+} and Cd^{2+}) and determine appropriate process conditions, and models for design.

1.5 ORGANIZATION OF THE THESIS

The entire work presented in this thesis has been divided into six chapters. A brief account of the contents of these chapters has been furnished below:

The ***first chapter*** presents a brief introduction on water pollution due to heavy metals, their discharge from different industries, removal technologies, significance of biosorption over conventional technologies and the importance of marine alga for biosorption purpose. Besides this a brief review of different biosorbents used for removal of Pb^{2+}, Cd^{2+} and Ni^{2+} ions is also given in this chapter. This chapter also enumerates the objectives of the present work.

The ***second chapter*** presents the detailed review of previous biosorption studies done on single and dual metal ions systems. The available data in literature on biosorption of metal ions by using other brown marine algae were compared with the results of present work.

The ***third chapter*** furnish experimental details of the used materials/reagents, equipment and techniques. A brief account of the methodologies used for performing their characterization, isotherm, kinetics and thermodynamic modeling, different equations and formulae used for the data analyses have been provided. It also includes the experimental procedure used for batch study of biosorption process.

The ***fourth chapter*** explained the results obtained for single metal ion (Pb^{2+}, Cd^{2+} and Ni^{2+} ions) biosorption process.

The ***fifth chapter*** explained the results of simultaneous removal of Pb^{2+} and Cd^{2+} from dual metal ions system in detail.

The ***sixth chapter*** presents the conclusions arrived from fourth and fifth chapters. The future directions for this type of work has also been proposed.

CHAPTER II

LITERATURE REVIEW

2.0 INTRODUCTION

The present thesis concerns with the biosorption of heavy metals present in wastewater. The metals considers herein are Pb^{2+}, Cd^{2+}, and Ni^{2+} ions. Accordingly this chapter on literature review has been planned. First adsorption / biosorption have been described along with effect of various operating parameters on the performance of removal of pollutants. Thereafter, various biosorbents and their selection have been discussed. Then the studies available in literature pertaining to the removal of Pb^{2+}, Cd^{2+}, and Ni^{2+} ions by biosorbents have been described. The aspects such as optimization of operating conditions of biosorption process, kinetics of biosorption, thermodynamic study, equilibrium study and desorption study have been critically evaluated. Lastly the motivation for the proposed study has been discussed.

2.1 HEAVY METAL POLLUTION

Heavy metal pollution is the major concern which is released into the environment by agriculture, mining and industrial activities [123, 175]. In toxicological studies it has been identified that heavy metals are toxic for plants, animals and humans. They persist in tissues for a long time once they are absorbed. It cannot be metabolized from tissues by metabolic degradation like other organic chemicals. In the environment heavy metals are accumulated in the food chain which increases the danger for humans. With the help of high precision detection analysis, concentration of the metal ions can be analyzed up to nano levels and it can be reduced to their permissible limits by using different techniques. Although many studies related to the removal of heavy metals by using different techniques are available but our focus is on the review of literature related to adsorption.

2.2 ADSORPTION / BIOSORPTION

Adsorption was first studied by Lowitz in 1785 which was applied for the removal of color removal from sugar during refining. In the later half of the 19th century, inactivated charcoal filters was used for the purpose of water purification in American water treatment plants. The first granular activated carbon units for water supply treatment were designed in 1929 at Hamm Germany and in 1930 at Bay City, Michigan [220]. Nowadays activated carbon is used for the adsorption process to remove the heavy metals from wastewater. However, the high cost of activated carbon limits its use in adsorption. The use of low cost and easily available agricultural and biological origin materials as adsorbent was found as an alternative of activated carbon [129].

Biosorption is an emerging alternative technology for the removal of various pollutants from industrial wastewater. Researchers defined biosorption as – "The removal of metal or metalloid species, compounds and particulates from solution by biological material" [95]. Biosorption is the surface phenomenon where metal ions bind to biosorbent surface by van der Waal's or covalent forces. It is a biotechnological process which utilizes naturally abundant or waste biomass for removing of different heavy metals from wastewater. This process involves a liquid phase containing dissolved species like metal ions to be sorbed (sorbate) and a solid phase biomaterial (sorbent). The biosorbents can be referred to as natural ion exchangers [334]. The biosorbents are cost effective, highly selective and efficient as compared to activated carbon that used in classical methods. The biosorption method has major advantages over conventional techniques for removal of metal ions such as high efficiency, low cost, no additional nutrient requirement, no sludge problem, possibility of metal recovery and regeneration of biosorbent [232, 165, 208].

On the basis of bonding between the biosorbent and the biosorbate, the nature of biosorption may be divided into two types of sorption as given below:

(i) Physisorption (physical adsorption)

It involves long ranged weak van der waal's attraction of the bisorbate to the biosorbent surface and the heat of adsorption are low i.e. about 20-40 kJ/mol. During the process of physisorption, the chemical identity of the biosorbate remains intact. It forms multilayer.

Physisorption, being a spontaneous thermodynamic process, must have a negative ΔG^o. This usually takes place at low temperature and decreases with the increase in temperature.

(ii) Chemisorption (chemical adsorption)

In this process strong chemical bonds are formed between the biosorbate and the surface of biosorbent. It forms monolayer. It is usually irreversible in nature. The heat of adsorption are high i.e. about 40-400 kJ/mol. This interaction is much stronger than physisorption, and, in general, chemisorption required the compatibility in between the biosorbate and the binding site of biosorbent than physisorption. The chemisorption may be stronger than the bonds internal to the free adsorbate, which results in the dissociation of the biosorbate upon adsorption (dissociative adsorption). In some cases $\Delta S^o > 0$ for dissociative adsorption, which indicates endothermic chemisorption is possible. This takes place at high temperature and increases with the increase in temperature. A comparison between physisorption and chemisorption for various adsorption properties is given in **Table 2.1**.

2.2.1 Factors controlling biosorption

The amount of biosorbate from the liquid phase biosorbed on the biosorbent surface is influenced by a number of factors such as: (a) pH of solution, (b) contact time, (c) initial concentration, (d) nature of adsorbent, (e) temperature (f) biosorbent concentration [328].

(i) pH of solution

The pH seems to be the most significant parameter in the biosorptive process as it affects the activity of the functional groups in the biomass, the solution chemistry of the metal ions, and the competition of metallic ions. As pH value increases, biosorption of cations increases while that of the anions decreases. It is important to assess pH_{pzc} of the biosorbents to understand the biosorption mechanism. In case of $pH < pH_{pzc}$, H^+ ions are available which favors the biosorption of anions, whereas $pH > pH_{pzc}$, deposition of OH^- ions favors the biosorption of cations.

Table 2.1 Comparison of chemisorption and physisorption

Properties	Physisorption	Chemisorption
Nature of adsorption	(a) Van der Waal's adsorption (b) Non-dissociative and reversible	(a) Activated adsorption (b) Often dissociative and irreversible in many cases
Energy	Activation energy is not involved in adsorption process.	Activation energy may be involved in adsorption process.
Saturation	Multi layer adsorption occurs often.	Usually mono layer adsorption occurs.
Crystallographic specificity	Independent of surface geometry	Marked difference between crystal planes
Dependent	Extent of adsorption depends upon the properties of adsorbent.	Extent of adsorption depends on both adsorbate and adsorbent.
Rate of adsorption	(a) Controlled by resistance to mass transfer. (b) Rapid rate at low temperature	(a) Controlled by resistance to surface reaction (b) Low rate at low temperature
Quantity adsorbed per unit mass	High (entire surface is participating)	Low (only active surface sites are participating)
Adsorption temperature	Adsorption can occur near or less than boiling point temperature of the adsorbate.	Adsorption can occur even at high temperature above the boiling point.

(ii) Contact time

Contact time affects the biosorption capacity, where the time required to reach equilibrium varies based on the available biosorption sites and the nature of biosorbent [346]. In physical adsorption, most of the biosorbate species are biosorbed in less contact time. While strong chemical binding of biosorbate with biosorbent requires a longer contact time to achieve equilibrium condition. Initially, the uptake capacity is high due to a presence of large number of available binding sites for biosorption. Thereafter, the rate of biosorption becomes slower and found to be nearly constant due to the repulsion between solute molecules adsorbed on the surface. In the reported literature, the increase in the uptake capacity of Pb^{2+}, Cd^{2+} and Ni^{2+}, using modified rice straw increases with time until equilibrium was attained beyond which no further increase was observed [284]. Similarly the adsorption of Cu^{2+}, Cd^{2+} and Pb^{2+} ions using modified sugarcane bagasse also increases with contact time until equilibrium [336].

(iii) Initial metal ion concentration

The initial concentration of biosorbate significantly affects the uptake capacity of biosorbent. Initially the uptake capacity of biosorbent increases with increase in initial metal ion concentration due to the availability of more number of metal ions in solution for biosorption. The initial metal ion concentration provides the essential driving force to overcome the mass transfer resistance by metal ions between the aqueous phase and the solid phase.

(iv) Nature of biosorbent

Many non living biomasses can be used as biosorbents to remove the metal ions from waste water. The network of small pores inside the particles provides the surface area for biosorption of metal ions. Biosorption capacity is directly proportional to the exposed surface.

(v) Temperature

In biosorption process, temperature is an important controlling parameter. Generally, the biosorption process is exothermic in nature. According to Le chatlier's principle, the magnitude of biosorption should increase with the decrease in temperature. The van der waal's forces involve in physisorption process are strong at low temperature. While, in chemisorption process the chemical reactions need activation energy which shows the increase in biosorption initially with rise in temperature and then starts decreasing. The reasons behind an increase in biosorption tendency with an increasing temperature are (i) an increased mobility of the metal ions and a decrease in the retarding forces acting on the diffusing ions, (ii) an increase in the number of biosorption sites due to breakage of the internal bonds near the edge of the biosorbent active surface sites.

(vi) Effect of biosorbent concentration

The number of active sites for biosorption increases with the increase in biosorbent concentration which results in increase of percent removal of metal ions. However after certain time, an equilibrium condition is attained at which there is no further increase of percent removal even with the increase in biosorbent concentration under the same experimental conditions [165].

2.2.2 Selection and types of biosorbents

(i) Algae

Algae contain several polyfunctional metal-binding sites for both anionic and cationic metal complexes. They have large surface area which makes it suitable to be used as biosorbent in sorption process. The components of metal binding sites in algae contain amine, carboxyl, phosphate, imidazole, sulfhydryl, hydroxyl, sulphate, and other chemical functional groups contained in cell sugars and proteins [9]. The brown alga has proved to be a very good biosorbent of heavy metals [260].Their cell walls contain alginic acid and fucoidin. The alginic acid provides sulfate and carboxylate ions at neutral pH. Volesky *et al* (1999) studied the uptake capacity of one of the best metal-sorbing biomass types, ubiquitous genus of alga *Sargassum* [336]. They compared the uptake capacity of three different *Sargassum* species for Cu and Cd uptakes from aqueous solutions. Uptakes of Cu at pH 4.5 were q_{max} = 59 mg/g for *S. vulgare*, 56 mg/g for *S. filipendula*, and 51 mg/g for *S. fluitans*. Uptakes of Cd^{2+} ions at the optimum pH 4.5 were q_{max} = 87 mg/g, for *S. vulgare*, 80 mg/g for *S. fluitans*, and 74 mg/g for *S. filipendula*.

(ii) Fungi and yeast

The cell wall of fungi consists of chitin framework embedded on an amorphous polysaccharide matrix [346]. The cell walls are rich in polysaccharides and glycoproteins such as chitin (β- 1 -4 linked N-acetyl-D- glucosamine), glycans (β- 1 -6 andβ- 1 -3 linked D-glucose residues), mannans (β- 1 -4 linked mannose), chitosan (β- 1 -4 linked D-glucosamine), and phosphormannans (phosphorylated mannans). The different metal binding groups, like imidazole, amine, sulphate, phosphate, hydroxyl and sulfhydryl are present in polymers [75].

The yeast cells contain some chemical compounds which can also act as ion exchangers with rapid reversible binding of cations [326]. Volesky *et al* (1993) studied the biosorption of Cd^{2+} ions by *Saccharomyces cerevisiae* and observed that this yeast could be used as potent biosorbent for metal ion biosorption [335].

(iii) Bacteria

According to Beveridge (1989), bacteria can be used as an efficient biosorbent due to their high surface-to-volume ratios and a high content of potentially active chemisorption sites such as on teichoic acid in their cell walls [45, 156]. Fein *et al* (1997) used *Bacillus subtilis* to study the interaction of bacteria with Cu^{2+}, Cd^{2+}, Al^{2+} and Pb^{2+}. Their results notified the stability constants for biosorption of metal ions onto the individual sites and deprotonation constants for some important organic functional groups on the bacterial cell wall [99, 305]. In acidic conditions, bacterial cell walls are negatively charged and functional groups of cell wall show a high affinity for metal ions in solution [70].

2.3 SINGLE METAL ION STUDIES

Gupta *et al*. (2008) investigated the use of green algae *Spirogyra* sp. for Pb^{2+} ions biosorption from wastewater [124]. The maximum adsorption capacity of Pb^{2+} ions was obtained as 140 mg metal/g at algal dose 0.5 g/L, pH 5.0 in 100 min with 200 mg/L of initial concentration. The equilibrium is well explained by Langmuir isotherm and uptake kinetics follows the pseudo-second-order model. FTIR analysis of algal biomass indicates the presence of carboxyl, amino, carbonyl and hydroxyl groups, which are responsible for Pb^{2+} ions biosorption.

Amini *et al*. (2008) worked on optimization of Pb^{2+} ions removal from aqueous solution by using response surface methodology on *Aspergillus niger* [18]. The optimum conditions were obtained as initial lead ion concentration (30 mg/L), pH (4.27) and biomass dosage (2.17 g/L) at which maximum removal efficiency was achieved 96.21 %.

Gupta *et al*. (2008) also investigated the dried non-living biomass of two fresh water algae, *Oedogonium* sp. and *Nostoc* sp. as biosorbent for Pb^{2+} ions removal from aqueous solutions in a batch system [123]. The optimum conditions for Pb^{2+} ions biosorption were biosorbent dose 0.5 g/L, contact time 90 and 70 min, initial Pb^{2+} ions concentration 200 mg/L and pH 5.0. The maximum uptake capacity for *Oedogonium* sp. and *Nostoc* sp. was 145.0 mg/g and 93.5 mg/g, respectively. It shows that the biomass of *Oedogonium* sp. was found to be more efficient biosorbent for the removal of Pb^{2+} ions from aqueous solution as comparison to *Nostoc* sp. The Langmuir isotherm model was fitted well to the equilibrium data. Thus it indicates the monolayer

biosorption of Pb^{2+} ions on both the algal biomass. The biosorption of Pb^{2+} ions on both the alga followed the second-order kinetics. The thermodynamic study indicates that Pb^{2+} ions biosorption process was endothermic in nature. The FTIR analysis suggested that carboxyl and amino groups on the surface of algal biomass were involved in binding of Pb^{2+} ions. The biosorbents were reused for five successive biosorption-desorption cycles without any loss of biosorption capacity (with 90 % recovery).

Hansen *et al*. (2013) used the brown algae *Durvillaea antarctica* for biosorption of Pb^{2+} ions from aqueous solution [132]. The uptake capacity of Pb^{2+} ions was determined at different process conditions ranging from (a) initial Pb^{2+} ions concentration, 200-1200 mg/L, (b) pH, 1.5-4, (c) contact time, 10-80 min. The biosorption process was described by pseudo second order kinetic model. The Langmuir isotherm model was the best fitted model for biosorption equilibrium experimental data. The maximum uptake capacity and affinity constant obtained by Langmuir isotherm were 135.1 mg/g and 2.55 mg/L, respectively. The value of optimum pH was found to be 1.5.

Tabaraki *et al*. (2014) investigate the biosorption of Pb^{2+} ions on *Sargassum ilicifolium* in a batch system [313]. The response surface methodology was used to optimize the biosorption process parameters which were obtained at biosorbent concentration, 0.2 g/L, initial Pb^{2+} ions concentration, 200 mg/L and pH, 3.7. At optimum conditions, the maximum uptake capacity of *S. ilicifolium* for Pb^{2+} ions was found to be 195 mg/g. The experimental data were best fitted with both Langmuir and Freundlich isotherm models. The equilibrium time was 2 h and the kinetic of Pb^{2+} ions biosorption on *S. ilicifolium* was best explained by second-order kinetic model. Thermodynamic studies demonstrated that the biosorption process was spontaneous and endothermic.

Deng *et al*. (2006) investigated the capacity of green alga *Cladophora fascicularis* for Pb^{2+} ions biosorption as a function of temperature, initial metal ion concentration, pH and other co-existing ions [87]. The equilibrium data were well explained by Langmuir and Freundlich isotherm models. The maximum biosorption capacity was obtained as 198.91 mg/g for Pb^{2+} ions at pH 5.0 and 298 K. The biosorption heats calculated by the Langmuir constant ‘b’ was found to be 29.6 kJ/mol which shows the endothermic nature of Pb^{2+} ions biosorption process. The biosorption

kinetics followed the pseudo-second order model. Desorption experiments proved that 0.01 mol/L Na_2EDTA was an efficient desorbent for Pb^{2+} ions recovery from biomass.

Vieira *et al*. (2007) studied the biosorption of Pb^{2+} ions using the brown alga *Sargassum filipendula* [325]. They have performed all the experiments only at 30 ºC. The optimum pH value for Pb^{2+} ions biosorption was found to be pH 4.0. The equilibrium data were well explained by Langmuir isotherm model. Isotherms indicated that for solutions containing 0.03 to 3.27 mmol/L of Pb^{2+} ions, 2.0 g /L was the optimum biosorbent dose. The equilibrium was achieved in 30 min. The kinetic data of Pb^{2+} ions biosorption followed the pseudo second order kinetic model. The continuous system operated for 56 h results in 100 % binding of Pb^{2+} ions, which corresponds to an accumulation of 168 g Pb^{2+} ions, equivalent to a load of 1.7 mmol/g.

Singh (2007) were screened non-living biomass of five filamentous algae belonging to *Cyanophyta* and *Chlorophyta* group for their removal efficiency of Pb^{2+} ions in a batch system [291]. The equilibrium data were best fitted by Langmuir isotherm model. The removal efficiency of 89 and 97 % Pb^{2+} ions was achieved in 30 min for *Spirogyra neglecta* and *Pithophora odeogonia*, respectively from a solution containing 5 mg/L initial concentration of Pb^{2+} ions with 1 g/L biomass dosage. *S. neglecta* was able to remove > 70 % Pb^{2+} ions even from a solution containing 75 mg/L of Pb^{2+} ions. The removal efficiency of Pb^{2+} ions by the test algae decreased with the increase in initial metal ion concentration in the solution. Other tested algae, namely, *Aulosira fertilissima, Cladophora calliceima* and *Hydrodictyon reticulatum* were comparatively less efficient for removing the metal ions from solution.

Wierzba *et al*. (2015) studied Pb^{2+} and Ni^{2+} ions biosorption from industrial wastewater using two live bacterial strains *Bacillus subtilis* and S*tenotrophomonas maltophilia* [339]. The biosorption performances were strongly affected by parameters like contact duration, pH, and initial metal ion concentration. For both the two bacterial species, the optimum pH for Pb^{2+} and Ni^{2+} ions biosorption was achieved as pH 5.0–6.0 for 30 min. The experimental data were analyzed using Langmuir and Freundlich isotherms. Langmuir isotherm model was best fitted to the equilibrium data of Pb^{2+} and Ni^{2+} ions biosorption. The maximum biosorption capacity of *S. maltophilia* for Pb^{2+} and Ni^{2+} ions were found to be 133.3 and 54.3 mg/g, respectively. While the

maximum biosorption capacity of *B. subtilis* for Pb^{2+} and Ni^{2+} ions were 166.7 and 57.8 mg/g, respectively but *B. subtilis* biomass was more favorable for Pb^{2+} and Ni^{2+} ions biosorption.

Lee *et al.* (2011) evaluated the biosorption capacity of the green algae species, *Cladophora* and *Spirogyra* for Pb^{2+} ions biosorption [182]. The equilibrium data of Pb^{2+} ions biosorption for both the algae were showed a better fit with the Langmuir isotherm model. These two genera of green alga involved physical and chemical biosorption of particles which was more significant than diffusion and adsorption between particles. FTIR analysis showed that the functional groups of both algae were similar, but varied in their adsorption efficiency. This study found that *Spirogyra* sp. was more efficient than *Cladophora* sp. for Pb^{2+} ions biosorption.

Kowanga *et al.* (2015) used a red alga *Spyridia filamentosa* for Pb^{2+} ions biosorption from aqueous solutions [164]. The maximum uptake capacity was found to be 178.7 mg/g at pH of 5.0. The effect of light metal ions was found not to significantly affect the uptake of Pb^{2+} ions. The kinetics of adsorption was rapid within 30 min. It was confirmed that *S. filamentosa* can be used in fixed-bed operations and could be used as an efficient biosorbent for the removal of Pb^{2+} ions from wastewater streams.

Selatnia *et al.* (2015) investigated Pb^{2+} ions biosorption capacity of a NaOH (0.1 M) treated bacterial strain *Streptomyces rimosus* in the batch mode [278]. The equilibrium data were best fitted by Langmuir isotherm equation. The optimum process conditions were contact time (3 h), stirring speed (250 rpm), biosorbent dosage (3.0 g/L) and biomass particle size between 50 and 160 µm at which maximum biosorption capacity of 135 mg/g was achieved. The cell wall of *S. rimosus* consists of anionic functional groups like –COO, –C–O, –NH, –C=O, –OH which were responsible for Pb^{2+} ions biosorption. The dead biomass of *S. rimosus* was found to be an efficient biosorbent of Pb^{2+} ions in dilute solutions.

Amirnia *et al.* (2015) studied the behavior of unmodified yeast cells of *Saccharomyces cerevisiae* to remove Pb^{2+} and Cu^{2+} ions from aqueous solutions in continuous mode [21]. Though live cells were used, the biosorption on the cell surface was the major metal separation mechanism. The maximum uptake capacity of yeast cells for Pb^{2+} ions was found to be 72.5 mg/g. The removal efficiencies of the test metals were decreased with the increase in initial metal ion concentration.

Equilibrium adsorption data of the metals by yeast cells were well described by the Langmuir isotherm model. The kinetics data of biosorption was fitted to diffusion-based and chemical reaction-based models. At low metal ion concentration, intracellular diffusion was found as the rate controlling step. The result of this work showed that live cells of yeast in a continuous biosorption system was an effective method for metal ions removal from industrial effluents reducing biomass pretreatment and preparation steps.

Munoz *et al*. (2016) studied the removal of Pb^{2+} ions from aqueous solution using *Klebsiella* sp. 3S1 strain of bacterium in a fixed-bed column [224]. FTIR spectra showed that *Klebsiella* sp. 3S1 provides extra binding sites for the retention of Pb^{2+} ions. In continuous mode, the dynamic behavior of the column was well-described by breakthrough curves, with experimental data fitting by using different mathematical models, mainly the Yang model. The biosorption equilibrium data better fitted to the Freundlich model, which implies the heterogeneous surface conditions. In each cycle up to 70 mg of Pb^{2+} ions was retained per gram of microbial biofilm without loss of biosorption capacity. Four biosorption-desorption cycles were carried out with 100 % of desorption efficiency in a continuous sequential manner without a significant loss in removal efficiency of Pb^{2+} ions. The results obtained revealed that the developed packed bed biosorption column loaded with *Klebsiella* sp. 3S1 biofilm can be efficiently use for the removal of Pb^{2+} ions from industrial wastewater.

Hackbarth *et al*. (2014) worked on removal of Pb^{2+} and Cd^{2+} ions from aqueous solution using marine brown macroalgae *Pelvetia canaliculata* [128]. Batch kinetic and equilibrium experiments were carried out at different pH values using Na-loaded algae. FTIR was used to analyze the main functional groups present on the surface of the algae responsible for binding metals. The biosorption capacity of Cd^{2+} at pH 4.5 was 140 mg/g and for Pb^{2+} ions at pH 4.0 was 259 mg/g. The mass action law for the ternary mixture was able to predict the equilibrium data, with the selectivity coefficients $\alpha_{Na}^{Pb} = 941$ and $\alpha_{Na}^{Cd} = 337$ for carboxylic and $\alpha_{Na}^{Pb} = 1695$ and $\alpha_{Na}^{Cd} = 38$ for sulfonic groups, indicating a higher affinity of the biomass towards Pb^{2+} ions. A mass transfer model, considering equilibrium given by the mass action law, and a linear driving force model for intraparticle diffusion, was able to fit well to the batch kinetic data. The increasing order of Na-loaded algae selectivity coefficients is $Na^+ < H^+ < Cd^{2+} < Pb^{2+}$, which shows that sulfonic and carboxylic groups have a higher affinity for Pb^{2+} ions. Due to high uptake capacity of

Pelvetia canaliculata in comparison to commercially available ion exchange resins, this renewable biomass can be used as an effective and cheap natural metal ion exchanger for a large scale process.

Anayurt *et al*. (2009) worked on biosorption of Pb^{2+} and Cd^{2+} ions from aqueous solution using macrofungus (*Lactarius scrobiculatus*) [22]. The optimum conditions for biosorption process were found to be as: contact time (60 min), pH (5.5), temperature (20 ºC) and biomass concentration (4.0 g/L) of solution. The maximum uptake capacity of *L. scrobiculatus* was found to be 53.1 mg/g for Cd^{2+} ions and 56.2 mg/g for Pb^{2+} ions. The kinetic data of Pb^{2+} and Cd^{2+} ions biosorption followed pseudo-second order model. The mean free energy values calculated by Dubinin–Radushkevich (D–R) model showed that the biosorption of the Pb^{2+} and Cd^{2+} ions onto *L. scrobiculatus* biomass involved chemical ion-exchange Pb^{2+} and Cd^{2+} ions. The calculated thermodynamic parameters showed that Pb^{2+} and Cd^{2+} ions biosorption onto *L. scrobiculatus* biomass was spontaneous, feasible and exothermic in nature. The reusability of the biosorbent was good after six consecutive sorption–desorption cycles. The recovery tests indicated that 1M HNO_3 solution was able to elute 95 % of Pb^{2+} and Cd^{2+} ions from the biomass.

Tuzun *et al*. (2005) studied the biosorption of Pb^{2+} and Cd^{2+} ions on microalgae *Chlamydomonas reinhardtii* [320]. FTIR analysis of *Chlamydomonas reinhardtii* biomass revealed the presence of carboxyl, amino, carbonyl and hydroxyl groups, which were responsible for biosorption of metal ions. The maximum biosorption capacities of microalgae for Pb^{2+} and Cd^{2+} ions were obtained as 96.3 mg/g at pH 5.0 and 42.6 mg/g at pH 6.0, respectively. The affinity order for algal biomass was $Pb^{2+} > Cd^{2+}$. The experimental data were well described by the Freundlich adsorption isotherm models and biosorption equilibrium was established in about 60 min. The biosorption capacity was not affected by change in temperature from 5–35 ºC. After 6 successive biosorption–desorption cycles, 98 % recovery was achieved without any considerable loss of biosorption capacity.

Aty *et al*. (2013) worked on the biosorption of Pb^{2+} and Cd^{2+} ions from aqueous solution on biomass of blue green alga *Anabaena sphaerica* [32]. Langmuir, Freundlich, and Dubinin – Radushkevich (D–R) models were fitted to explain the Pb^{2+} and Cd^{2+} ions biosorption isotherm. The equilibrium data of Pb^{2+} and Cd^{2+} ions biosorption follows the Freundlich and Langmuir

isotherm models. The maximum biosorption capacities for Pb^{2+} and Cd^{2+} ions were found to be 121.95 and 111.1 mg/g, respectively. From D–R isotherm model, the mean free energy was determined as 14.3 and 11.7 kJ/mol for Pb^{2+} and Cd^{2+} ions, respectively. It showed that the biosorption mechanism of Pb^{2+} and Cd^{2+} ions by *A. sphaerica* was chemisorption. The FTIR analysis for biomass surface functional group revealed the existence of hydroxyl, carboxyl, carbonyl and amino groups, which were responsible for Pb^{2+} and Cd^{2+} ions biosorption. This work suggested that *A. sphaerica* can be used as efficient biosorbent for the removal of Pb^{2+} and Cd^{2+} ions from aqueous solution.

Sulaymon *et al.* (2013) studied the removal of Cd^{2+} and Pb^{2+} ions using algae. Effect of parameters like temperature, pH and initial metal concentrations were studied [309]. The biosorption of these metals was based on ion exchange mechanism accompanied by the release of light metals such as sodium, magnesium, and calcium. The biosorption process depends significantly on pH of the solution. The optimum pH for Cd^{2+} and Pb^{2+} ions biosorption was found as 5.0 and 3.0, respectively. FTIR analysis was used to find the effects of functional groups of algae in biosorption process. The kinetic of Cd^{2+} and Pb^{2+} ions biosorption well fitted to the pseudo second order kinetics model. The optimum agitation speed to reach 90 % removal efficiency was 300 and 600 rpm for biosorption of Pb^{2+} and Cd^{2+} ions, respectively.

Sun *et al.* (2010) studied the biosorption of Pb^{2+} and Cd^{2+} ions by using fungal strain *Aspergillus terreus* immobilized in a natural matrix [310]. The biosorption selectivity of immobilized *Aspergillus terreus* was in the order of $Pb^{2+} > Cd^{2+}$. The maximum biosorption capacity was obtained as 247.2 and 23.8 mg/g for Pb^{2+} and Cd^{2+} ions, respectively. Metal uptake by immobilized *Aspergillus terreus* was dependent on pH of the metal solution, but independent of temperature. The equilibrium data was well explained by Langmuir model. The regenerated biosorbent was found to be efficiently used for five repeated cycles without any significant loss of biosorption capacity. This work revealed that immobilized *Aspergillus terreus* exhibit excellent biosorption capacity for Pb^{2+} ions from aqueous solution and industrial wastewaters.

Shanab *et al.* (2012) studied the removal efficiency of three fresh water microalgal isolates *Pseudochlorococcum typicum* for Pb^{2+} and Cd^{2+} ions [282]. Transmission electron microscopy (TEM) was used to examine the interaction between heavy metal ions and *P. typicum* cells. The

maximum removal efficiency of Cd^{2+} and Pb^{2+} ions was found to be 86 and 70 %, respectively by *P. typicum* from aqueous solution.

Kumar *et al*. (2012) examined the biosorption capacity of dried biomass of *Spirogyra hyalina* for removal of Cd^{2+} and Pb^{2+} ions from aqueous solutions at different initial metal ion concentrations and contact time [170]. The results showed that highest amount of Pb^{2+} was adsorbed when the initial Cd^{2+} ion concentration was 80 mg/L whereas Cd^{2+} ions exhibited greatest removal at 40 mg/L. The values of Langmuir separation factor values (R_L) varied between 0.114 and 0.719 and the values of Freundlich model constant (1/n) for different metals ranged from 0.342 to 0.693 that showed favorable biosorption by the biomass. The order of metal uptake for the dried biomass was found to be $Pb^{2+} > Cd^{2+}$.

Vilar *et al*. (2006) compared the biosorption capacity of industrial algal waste from agar extraction and red alga *Gelidium* sp. for Cd^{2+} ions from aqueous solutions [327]. The equilibrium data followed both Langmuir and Redlich-Peterson isotherm models. The adsorptive behavior of biosorbent particles was modelled using a batch reactor mass transfer kinetic model. Kinetic experiments were conducted at initial Cd^{2+} ions concentrations in the range 6-91 mg/L. The pseudo first and second order kinetic models were well fitted to kinetic data of Cd^{2+} ions. Diffusion of the metal ion inside the particle is the limiting step on mass transfer. The obtained kinetic parameters can be used for bioreactor design. Both sorbents can be considered for sequestering Cd^{2+} ions from industrial effluents in continuous flow processes.

Selatnia *et al*. (2004) studied the biosorption of Cd^{2+} ions by using a biomass of bacterial strain (*Streptomyces rimosus*) in batch mode [277]. The operating conditions for Cd^{2+} ions biosorption were as follows: biomass particle size (50 and 160 µm), contact time of 1 h, biosorbent dosage (2.5-3 g/L) and a stirring speed (200-250 rpm), respectively. The equilibrium data could be fitted by Langmuir isotherm equation. The maximum biosorption capacity of *Streptomyces rimosus* was obtained as Cd^{2+} ions 63.3 mg/g. The external mass transfer was found to be the controlling step in the overall sorption process. The biosorption of Cd^{2+} ions followed the pseudo second order biosorption kinetics on *S. rimosus*.

Loukidou *et al*. (2005) studied the biosorption of Cd^{2+} ions from aqueous solution using non-living form of bacterial strain (*Aeromonas caviae*) in a well-stirred batch reactor [190]. The kinetic and equilibrium experiments were performed at various temperatures, initial metal ion concentrations, biomass dosage, and ionic background. The equilibrium experimental data were well described by Langmuir and Freundlich isotherm models. It implies that both monolayer biosorption and heterogenous surface conditions exist under the experimental conditions studied. The kinetic data of Cd^{2+} ions biosorption on *A. caviae* followed the pseudo second order kinetic model which shows chemisorptions process.

Lu *et al*. (2006) studied the removal of Pb^{2+} and Cd^{2+} ions using *Enterobacter* sp. J1. The recovery of metal ions and regeneration of biosorbent were also done [192]. The equilibrium biosorption capacities of Pb^{2+} and Cd^{2+} ions was found to be 50 and 46.2 mg/g, respectively. Langmuir and Freundlich models were able to describe biosorption isotherm. The removal efficiency of 90 % for Pb^{2+} and 100 % for Cd^{2+} ions was achieved at pH 2.0 and 3.0, respectively. After four consecutive biosorption/desorption cycles, the regenerated biosorbent can achieve 75-90 % of its original adsorption capacity. *Enterobacter* sp. J1 can be used as adsorbent for the removal and recovery of heavy-metals from polluted wastewater as it exhibit good metal uptake capacity and high resistance to various heavy metals.

Li *et al*. (2006) worked on biosorption of Cd^{2+} ions from aqueous solution using *Rhodotorula* sp. [185]. The influences of initial pH of the solution and temperature on biosorption were studied. The presence of competing metal ions like Cu^{2+}, Mg^{2+} and Ag^{+}, except Na^{+} ions, extensively interfered with the metal uptake. Caustic and heat treatments effects the biosorption capacity of yeast cells, and the maximum metal uptake value (19.38 mg/g) was attained by boiling treated yeast cells. The equilibrium data were best explained by Langmuir isotherm model. Chemical modifications of the biomass indicated that amide and carboxyl groups play a significant role in Cd^{2+} ions biosorption.

Sarada *et al*. (2014) studied the removal of Cd^{2+} ions from aqueous solution by using *Caulerpa fastigiata* (Macro algae) [270]. The removal efficiency of Cd^{2+} ions biosorption was increased from 21.5 to 92.01 % for Cd^{2+} ions when pH was increased from 2.5 to 5.5 at fixed initial Cd^{2+} ions concentration of 30.29 mg/L. The pH value beyond 5.5 showed a rapid decline in

the biosorption yield for Cd^{2+} ions. The maximum removal efficiency was found to be 92.01 % at pH 5.5. The equilibrium was well described by Freundlich model and uptake kinetics followed the pseudo second order model. The thermodynamic study showed that Cd^{2+} ions biosorption on *C. fastigiata* was spontaneous, feasible and exothermic in nature. The XRD pattern of the biosorbent was found to be mostly amorphous in nature. The FTIR analysis indicated that the functional groups predominantly involved in the biosorption were -OH, -CH, COO^-, -C-C-, C=S and C=C groups.

Bulgariu *et al.* (2016) used the algae waste obtained after oil extraction for biosorption of Cd^{2+} ions in batch and column systems [52]. For batch systems, the effect of contact time and initial Cd^{2+} ions concentration was studied at optimal experimental conditions (8 g/L of biomass, pH of 5.0). The well fitted kinetic and isotherm model to experimental data were found to be pseudo-second order kinetic and Langmuir isotherm models. For column studies, to prevent the clogging of column the alkaline treated algae waste biomass was mixed with an industrial cation exchange resin (Purolite A-100). Five biosorption / desorption cycles have yielded between 98.83 and 92.39 % biosorbent regeneration. The breakthrough curves were fitted to Thomas, Bohart-Adams, and Yoon-Nelson models under varying conditions. Batch studies shows that Cd^{2+} ions biosorption onto alkaline treated algae waste required a short contact time (10 min) and has higher biosorption capacity (41.88 mg/g) in comparison to untreated algae waste biomass (30 min, 33.71 mg/g). It indicates that after alkaline treatment the availability of functional groups on biosorbent surface will be more. The maximum biosorption capacity of alkaline treated algae waste for Cd^{2+} ions was 53.68 % higher than that of untreated algae waste biomass.

Arivalagan *et al.* (2014) studied the removal of Cd^{2+} ions from aqueous solution using *Bacillus cereus* in batch mode [26]. The effect of process parameters on Cd^{2+} ions biosorption like contact time, temperature, initial metal concentration and pH were examined. The surface characterization was examined by SEM–EDX and XRD techniques. It was analyzed that the functional groups like -C=O, -OH, -C=C and -C-C were involved in Cd^{2+} ions biosorption. The maximum removal efficiency was found to be 82 % at initial Cd^{2+} ions concentration (200 mg/L), temperature (35 ºC) and pH (6.0).

Homaidan *et al.* (2015) investigated the uptake capacity of *Spirulina platensis* for Cd^{2+} ions biosorption [141]. Batch study were carried out at 150 rpm to study the effects of various process parameters such as biomass concentration (0.25-2 g), pH (3-9), temperature (18-46 ºC), contact time (30-120 min) and initial Cd^{2+} ions concentration (40-200 mg/L). After 90 min of contact time the maximal removal efficiency of Cd^{2+} ions was attained as 87.69 % at optimal process conditions of biosorbent (2 g), pH (8.0), initial Cd^{2+} ions concentration (60 mg/L) and temperature (26 ºC). The equilibrium data were well fitted to Langmuir isotherm model [17].

Delshab *et al.* (2015) used a brown alga *Sargassum oligocystum* as biosorbent for Cd^{2+} ions biosorption [86]. The characterization of biosorbent was done by using various instrumental techniques (FTIR and XPS). The maximum biosorption capacity was obtained as 153.85 mg/g. The biosorption equilibrium data were analyzed by using four different isotherm models: Langmuir, Freundlich, Temkin and Hasley. The kinetic data was fitted to four kinetic models: Pseudo first order, Pseudo second order, Intra particle diffusion and Bangham models. The best fitted isotherm and kinetic models were found to be Langmuir and pseudo second order, respectively. Thermodynamic study shows that the Cd^{2+} ions biosorption on *S. oligocystum* was spontaneous, feasible and exothermic in nature.

Ghorbani *et al.* (2008) evaluated the biosorption capacity of *Saccharomyces cerevisiae* for Cd^{2+} ions [114]. The optimization of Cd^{2+} ions biosorption process was done by using a central composite design of response surface methodology. The optimum conditions were obtained as *S. cerevisiae* biomass dosage of 2.13 g/L and initial cadmium ion concentration of 26.46 mg/L at which 6.71 mg/g biosorption capacity was achieved. The Langmuir model and intra-particle diffusion model were the best fitted isotherm and kinetic models for Cd^{2+} ions biosorption process, respectively.

Sari *et al.* (2008) elucidated the Cd^{2+} ions biosorption onto red alga (*Ceramium virgatum*) from aqueous solution [271]. The maximum uptake capacity of *C. virgatum* biomass for Cd^{2+} ions was obtained as 39.7 mg/g. The mean free energy (12.7 kJ/mol) calculated from D–R isotherm model showed that the Cd^{2+} ions biosorption was occured by chemisorption. The biosorption kinetics showed that the Cd^{2+} ions biosorption on *C. virgatum* followed pseudo-second-order

kinetics. The thermodynamic study indicated that the biosorption of Cd^{2+} ions on *C. virgatum* was spontaneous, feasible and exothermic in nature.

Chen *et al.* (2008) used the byproduct of brown-rot fungus *Lentinus edodes* for Cd^{2+} ions biosorption from water [62]. The effect of different process conditions like biomass dosage, pH and the initial Cd^{2+} ions concentration were examined. The removal efficiency was decreased with increase in biomass dosage while increased with the increase in initial Cd^{2+} ions concentration. Uptake of Cd^{2+} ions was higher in weak acid condition than in strong acid condition. At pH < 2.0, no removal was occurred. Three adsorption isotherm models namely, Langmuir, Freundlich and Temkin were fitted to simulate the biosorption data. The equilibrium data was well explained by Freundlich isotherm model. The maximum uptake capacity was found to be 5.58 mmol/g in weak acidic condition. FTIR spectrum and X-ray energy spectrum revealed the ion exchange mechanism occurring between protons on biomass functional groups and inorganic metal ions.

Sjahrul *et al.* (2012) used the live form of marine phytoplankton, *Tetracelmis chuii* and *Chaetoceros calcitrans* for the removal of Cd^{2+} ions [297]. The effect of the medium pH, initial Cd^{2+} ions concentration, and interacting time on accumulation of Cd^{2+} ions in the phytoplankton was evaluated. The optimum accumulation occurred after 15 min at the pH of 8.0, i.e. 1055.27 and 13.46 mg/g for *C. Calcitrans* and *T. Chuii*, respectively. The functional groups of *T. chuii* involved in the bioaccumulation of Cd^{2+} ions were S=O, -CN, OH, S-S, M-S and N-O, while that of *C. Calcitrans* were S-S, C=O, C=C, OH and M-S.

Monteiro *et al.* (2011) worked on the removal of Cd^{2+} ions by using two microalgae, *Desmodesmus pleiomorphus* and *Scenedesmus obliquus* [218]. The maximum uptake amount of Cd^{2+} ions by *S. obliquus* and *D. pleiomorphus* was found to be 60.8 mg/g and 58.6 mg/g, respectively. *D. pleiomorphus* showed a higher metal sorption capacity than *S. obliquus*.

Lodeiro *et al.* (2005) tested five different brown seaweeds, *Pelvetia caniculata, Saccorhiza polyschides, Laminaria ochroleuca, Ascophyllum nodosum* and *Bifurcaria bifurcata* for the removal of Cd^{2+} ions from aqueous solution [188]. The removal of Cd^{2+} ions was fast, with 90 % of total adsorption occurring in less than 1 h. The kinetic of Cd^{2+} ions biosorption was well described by pseudo-second-order kinetic model. A Langmuir isotherm determine the value of

maximum uptake capacity of Cd^{2+} ions and an affinity parameter indicative of the binding energy between the adsorbent and adsorbed solute molecules. The value of sorption rate constant 'k' was ranged between 1.66 x 10^{-3} and 9.92 x 10^{-3} g/mg.min. Acid–base properties of algae were studied by potentiometry to decide the total number of acid groups and pK_a values (from 3.54 to 3.98). The pK_a values obtained were in good agreement with those corresponding to carboxyl groups from alginate which was responsible for the biosorption of Cd^{2+} ions. The solution pH was a significant factor affecting Cd^{2+} ions biosorption, the uptake was almost negligible at pH ≤ 2.0 and reached a plateau at around 4.0.

Mokaddem *et al.* (2009) investigated Cd^{2+} ions removal from aqueous solutions by using *Paenibacillus polymyxa* [216]. The equilibrium data were best fitted to Dubinin–Radushkevich isotherm model. The maximum biosorption capacity was attained as 520.09 mg/g. The optimization of biosorption process parameters was done by using a 2^3 full factorial design. The initial Cd^{2+} ions concentration and pH were found to be the most significant parameters for Cd^{2+} ions biosorption process.

Prado *et al.* (2011) tested the efficiency of two brown algae *Sargassum sinicola* and *Sargassum lapazeanum* for Cd^{2+} ions biosorption [248]. The biosorption capacity of *S. sinicola* and *S. lapazeanum* for Cd^{2+} ions was obtained as 62.42 mg/g and 71.20 mg/g, respectively. Langmuir isotherm model was fitted to equilibrium experimental data of Cd^{2+} ions biosorption.

Ghoneim *et al.* (2014) examined the efficiency of green alga, *Ulva lactuca* for the removal of Cd^{2+} ions from the aqueous solution [113]. The maximum removal efficiency achieved was 99.2 % at the optimum process conditions: pH (5.5), biosorbent dosage (0.1 g), temperature (30 ºC), and initial Cd^{2+} ions concentration (10 mg/L). The adsorption equilibrium data fitted very well to both the Langmuir and Freundlich model.

Hannachi *et al.* (2014) carried out Cd^{2+} ions biosorption studies with the brown alga (*Dictyota dichotoma*) [131]. The maximum uptake capacity of *D. dichotoma* was obtained to be 75 mg/g at biomass concentration of 4.0 g/L, contact time of 30 min, temperature of 20 ºC and pH 5.0. The studied thermodynamic parameters indicated that Cd^{2+} ions biosorption onto *D. dichotoma* was spontaneous, feasible and exothermic. The kinetic study showed that the biosorption process

followed pseudo-second-order model. FTIR analysis confirmed that the ether, carboxyl, amino and alcoholic functional groups were involved in Cd^{2+} ions biosorption.

Zhang *et al*. (2016) used *Scenedesmus obliquus* for the removal of Cd^{2+} ions from aqueous solution [352]. The maximum removal efficiency of 93.39 % was achieved by *S. obliquus* AS-6-1 for Cd^{2+} ions at 30 °C, pH 6.0, 0.8 g/L biomass and initial Cd^{2+} ions concentration of 50 mg/L in 20 min. The Langmuir or Freundlich isotherm models could be used to explain the adsorption equilibrium of *S. obliquus* AS-6-1. The maximum uptake capacity was 144.93 mg/g determined by Langmuir isotherm. The regeneration of Cd^{2+} ions loaded *S. obliquus* AS-6-1 biomass was done by using 0.1 M HCl.

Gutierrez *et al*. (2015) investigated the sorption capacity of two brown macroalgae *Lessonia nigrescens* and *Durvillaea antarctica* for the removal of Cd^{2+} ions [127]. To achieve the equilibrium, optimum pH was 3.7 ± 0.2, and 5 days of contact time were required for both biosorbents. The maximum uptake capacities of *D. antarctica* and *L. nigrescens* for Cd^{2+} ions were obtained as 95.3 mg/g and 109.5 mg/g, respectively. The equilibrium data were well described by Langmuir isotherm model for both biosorbents. The biosorption kinetic followed by pseudo second order model for *D. Antarctica* and pseudo first order model for *L. nigrescens* satisfactorily.

Kim *et al*. (2015) used bacterial strain *Bacillus catenulatus* JB-022 for biosorption of Cd^{2+} ions from industrial wastes [161]. The surface morphology and functional groups were analyzed by using field emission scanning electron microscope, X-ray diffraction, energy-dispersive X-ray spectrometer and Fourier transform infrared spectroscopy. The maximal removal efficiency of Cd^{2+} ions was achieved as 66 % at initial Cd^{2+} ions concentration of 150 mg/L. The experimental data were well fitted by the pseudo second order kinetic and Langmuir isotherm models. The biosorption kinetics showed that the equilibrium was reached within 5 min for Cd^{2+} ions. The maximum uptake capacity was found to be 64.28 mg/g.

Kulkarni *et al*. (2014) studied the biosorption of Cd^{2+} and Ni^{2+} ions by dead biomass of *Bacillus laterosporus*, MTCC 1628 [167]. The effects of various process parameters like pH, biosorbent dosage, contact time and initial metal ion concentration were examined. All the experiments were performed in batch mode. The equilibrium was attained in 120 min, for both the

metals. The maximum biosorption capacity for Ni^{2+} and Cd^{2+} ions was found to be 44.44 mg/g and 85.47 mg/g, respectively. The kinetic data showed that the biosorption of Cd^{2+} and Ni^{2+} ions followed the pseudo-second order kinetics. Thermodynamic study indicated that Cd^{2+} and Ni^{2+} ions biosorption was an endothermic process. The SEM and FTIR analysis confirmed the interaction between metal ions and biosorbent. Adsorption, ion exchange, and complexation were the main mechanisms involved in biosorption of Cd^{2+} and Ni^{2+} ions on *B. laterosporus*. Desorption studies revealed that the biomass can be effectively regenerated using 0.1 N HCl.

Cechinel *et al.* (2016) used four brown algae, *Fucus spiralis*, *Laminaria hyperborea Pelvetia canaliculata,* and *Ascophyllum nodosum* for the removal of Ni^{2+} ions from a petrochemical wastewater [56]. The binding of Ni^{2+} ions take place by the release of light metals (Na, K and Mg), initially bound to the functional groups. *L. hyperborea* species showed a higher affinity for Ni^{2+} ions than the other brown algae. The treatment strategy consists of two consecutive packed bed columns, Ni^{2+} ions were retained in the second column. 1.0 g of biomass was sufficient to treat approximately 3.1 and 0.4 liters of the petrochemical wastewater, in the second column Ni^{2+} ions.

Wierzba (2017) investigated the biosorption capacity of *Yarrowia lipolytica* dead biomass for Ni^{2+} ions biosorption from an aqueous solution [340]. The characterization of biosorbent was done by FTIR, which showed the involvement of carboxyl, hydroxyl, amine and amide groups in the binding process of Ni^{2+} ions. The optimum parameters for Ni^{2+} ions biosorption process by the dead biomass of *Y. lipolytica* yeast were found as pH 6.0 and 2 g/L of biosorbent dosage. The maximum biosorption capacity of *Y. lipolytica* dead biomass for Ni^{2+} ions was found to be 30.12 mg/g. Most of the Ni^{2+} ions were biosorbed in the initial 20 min and equilibrium was attained in 60 min. The equilibrium data of Ni^{2+} ions at 20, 30 and 40 ºC were well fitted to Langmuir isotherm models. The bisorption of Ni^{2+} ions followed pseudo-second order kinetics. The mechanism of biosorption includes both intraparticle diffusion and chemical reactions. The thermodynamic study showed that the biosorption of Ni^{2+} ions onto the *Y. lipolytica* was spontaneous, feasible, and endothermic in nature. The value of ΔG^o less than –20 kJ/mol signified the involvement of physical adsorption in Ni^{2+} ions biosorption by the biomass of *Y. lipolytica*.

Pundir *et al*. (2016) worked on the removal of Ni^{2+} ions by growing *Aspergillus* sp. in batch reactor using Taguchi method [251]. The biosorption process parameters were optimized by Taguchi experimental design with L9 orthogonal array. The optimized process parameters were initial metal Ni^{2+} ions concentration (50 mg/L), inoculum concentration (15 % v/v), temperature (30 °C) and pH 4.0. The role of each parameter for the removal percentage of Ni^{2+} ions was of the following order: concentration of inoculum (38.4 %), initial metal concentration (49 %), temperature (0.10 %) and pH (7.45 %). The optimization using a different set of process parameters assist in the enhancement of process efficacy. 'Design of Experiment' technique with large number of experimental runs and more parameters provide a better understanding for biosorption process.

Barquilha *et al*. (2017) studied the biosorption of Ni^{2+} ions in batch and fixed-bed columns by free and immobilized *Sargassum* sp. [39]. The biosorption equilibrium data were well described by the Langmuir model. In continuous system, biosorbents exhibited higher uptake capacities than those predicted by Langmuir model in batch process. In fixed-bed columns, the uptake capacity of free and immobilized biosorbent for Ni^{2+} ions were obtained as 72 mg/g and 99.1 mg/g, respectively. The high metal uptake of the immobilized biosorbent indicated good bed distribution. The immobilized biosorbent also facilitated the bed packing due to its regular spherical shape. Hence it was proved that the immobilization was a good alternative for the scale up of biosorption process in fixed-bed column.

Shroff *et al*. 2011 investigated the equilibrium and kinetics of Ni^{2+} ions biosorption from aqueous solution using physico-chemically treated dead biomass of *Mucor hiemalis* in a batch system [287]. The effect of different biosorption process parameters were studied with varying ranges of operating process parameters like pH (2-8), initial Ni^{2+} ion concentration (50-500 mg/L), stirring speed (60-210 rpm), temperature (10-60 ºC) and biosorbent dosage (0.5-3 g/L). The optimized conditions obtained were as pH (8.0), biosorbent dosage (0.5 g/L), stirring speed (150 rpm), temperature (40 ºC) and initial Ni^{2+} ions concentration (50 mg/L) at which maximum uptake capacity of 15.83 mg/g was achieved. The biosorption equilibrium was established in about 150 min. The kinetic data of Ni^{2+} ions biosorption were analyzed using pseudo first and pseudo second order kinetic models as well as intra-particular rate expressions. The biosorption of Ni^{2+} ions on *M. hiemalis* followed the second-order kinetic model. The equilibrium data were well fitted to both

Langmuir and Freundlich isotherm models. The biosorbent could be regenerated and reused at least five times in biosorption-desorption cycles successively.

Liu *et al*. (2009) studied the biosorption of Cd^{2+} and Ni^{2+} ions by chemically modified brown algae *Laminaria japonica* [186]. The equilibrium data were analyzed by using Langmuir, Freundlich and Redlich-Peterson isotherm models. The biosorption equilibrium data was well described by both the Langmuir and Redlich-Peterson isotherms. The biosorption kinetic of Cd^{2+} and Ni^{2+} ions was well fitted to pseudo first order kinetic model. The optimum pH values for Ni^{2+} and Cd^{2+} ions biosorption was found to be 5.0 and 5.5, respectively. The optimum biosorbent dose ratio was 3.0 g/L corresponding to the high removal rate and the cost efficiency. The metal uptake capacity was increased with time, and equilibrium was achieved in 2 h.

Ferreira *et al*. (2011) used the dry biomass of *Arthrospira platensis* and *Chlorella vulgaris* for the biosorption of Ni^{2+} and Pb^{2+} ions as a function of initial metal concentration and contact time [101]. The pH_{pzc} for *Arthrospira platensis* and *Chlorella vulgaris* was found as 4.0 and 3.4, respectively. By conducting additional pH tests, it was concluded that pH range of 5.0–5.5 was suitable for the experiments. The pseudo first and second order kinetic models were fitted to interpret the experimental data. The best fitted kinetic model was found as pseudo second order. The equilibrium data was well described by both Langmuir and Freundlich isotherm models, thus indicating an intermediate mono/multilayer sorption mechanism. The maximum biosorption capacity of *A. platensis* for Ni^{2+} and Pb^{2+} ions was obtained as 20.77 and 102.56 mg/g, respectively. While the maximum biosorption capacity of *C. vulgaris* for Ni^{2+} and Pb^{2+} ions was obtained as 0.499 and 0.634 mmol/g, respectively. It showed that *C. vulgaris* behaved as a better biosorbent as compared to *A. platensis*. The removal efficiency was decreased with increasing initial metal ion concentration, indicating that the process was a passive adsorption process involving the active sites of biomass. The FTIR analysis indicated mainly carboxylate groups present on cell wall, which were mainly involved in coordination and/or ionic exchange of bivalent ions.

Tabaraki *et al*. (2014) studied the biosorption of Ni^{2+} ions using *Sargassum ilicifolium* [313]. The optimization of biosorption process parameters like pH, time and biosorbent dose was done by using response surface methodology (RSM). The optimum value of pH for Ni^{2+} ions

biosorption was found to be 5.0. The equilibrium data were best fitted to Dubinin–Redushkevich (D–R) isotherm model. The kinetic sorption data were best explained by the pseudo second-order kinetic model. The maximum uptake capacity of *S. ilicifolium* for Ni^{2+} ions was obtained as 133.8 mg/g. FTIR analysis showed that carboxylic group was involved as active binding site. The thermodynamic study showed that the Ni^{2+} ions biosorption process on *S. ilicifolium* was spontaneous and endothermic in nature. *S. ilicifolium* is a natural biosorbent for metal ions which can be used for scale-up purpose due to its low cost, availability in abundance, and reusability.

Doshi *et al*. (2006) studied the sorption of Ni^{2+} ions by using live and dead *Spirulina* sp. [91]. The metabolic activities in live *Spirulina* sp. possibly help in higher uptake of metal ions compared to dead species. The uptake of Ni^{2+} ions by live *Spirulina* sp. follows pseudo second-order while dead *Spirulina* sp. follows pseudo first-order kinetic model. The equilibrium data of sorption process obeyed Freundlich isotherm. The FTIR analysis indicated that uptake of Ni^{2+} ions involved the participation of hydroxyl group of polysaccharides, carboxylate, amide and phosphate groups.

Padmavathy (2008) investigated the baker's yeast for Ni^{2+} ions biosorption as a function of temperature at different initial Ni^{2+} ion concentrations [241]. The highest Ni^{2+} ions biosorption capacity was found to be 9.1 mg/g at temperature 27 ºC, pH 6.75 and initial Ni^{2+} ions concentration of 400 mg/L. The equilibrium data was well described by Freundlich and Redlich–Peterson isotherm models as comparison to Langmuir model in the concentration range studied (10–400 mg/L). The biosorption of Ni^{2+} ions followed the pseudo-second order kinetic model. Desorption studies have shown that 0.1N HCl regenerate the protonated yeast biomass which can be reused.

Amini *et al*. (2009) studied the biosorption of Ni^{2+} ions by using *Aspergillus niger* as biosorbent [18]. The optimization of batch experiments for Ni^{2+} ions biosorption was carried out by using a response surface methodology. The optimum conditions for Ni^{2+} ions biosorption were obtained as biomass dosage (2.98 g/L), pH (6.25) and initial Ni^{2+} ions concentration (30 mg/L) at which 4.82 mg/g of uptake capacity and 70.30 % of removal efficiency were attained. The biosorption equilibrium was reached in 240 min. Langmuir and Freundlich isotherm models well

described the biosorption experimental data. The FTIR analysis confirmed that carbonyl and hydroxyl groups on surface of *A. niger* biomass were responsible for Ni^{2+} ions biosorption.

Gupta *et al*. (2010) used *Oedogonium hatei* to develop adsorbent for the removal of Ni^{2+} ions from aqueous solution [125]. The optimum process conditions were obtained as 0.7 g/L algal dose, 80 min contact time, 298 K temperature and 5.0 pH. The maximum uptake capacity of untreated and acid-treated algae was found to be 40.9 and 44.2 mg/g, respectively. The thermodynamic study indicated that Ni^{2+} ions adsorption on algal biomass was spontaneous, feasible, and exothermic in nature. The adsorption kinetics followed both first and second order models. The Langmuir and Freundlich models were better fitted to adsorption equilibrium data at all the temperatures studied. The regeneration and recovery study showed that 70 % recovery was achieved by using 0.1 M NaOH solution.

Bermudez *et al*. (2010) examined the uptake capacity of two seaweeds (*Sargassum muticum*, S.m. and *Gracilaria caudata*, G.c.) for Ni^{2+} ions biosorption [43]. The optimum values of pH for S.m. and G.c. were found to be 3.0 and 5.0, respectively. The maximum uptake capacity of S.m. and G.c. was achieved as 70 mg/g and 45 mg/g for Ni^{2+} ions biosorption, respectively. The Langmuir isotherm model was the best fitted to the experimental data. The biosorption kinetics was explained by using intra particle diffusion and the pseudo-second order kinetic models. The biosorption process of Ni^{2+} ions on both the seaweeds was exothermic in nature.

Fan *et al*. (2010) used alginate bead containing immobilized brown algae (*Laminaria japonica*) for Ni^{2+} ions biosorption [94]. The equilibrium experimental results were well fitted by both the Langmuir and Freundlich isotherm models. The biosorption of Ni^{2+} ions on immobilized *Laminaria japonica* followed a pseudo second order model. It confirms that rate limiting step was chemisorption. The maximum uptake capacity of immobilized algae beads for Ni^{2+} ions biosorption was observed as 39.43 mg/g. FTIR analysis of biosorbent indicated that $–NH_2$, –OH, $–CH_3$, CH_2, –N–H, –C=O, –C–O,–C–H and –C=O functional groups present on surface of alga involved in the biosorption of Ni^{2+} ions biosorption.

Aryal (2015) used the bacterial biomass (*Bacillus sphaericus*) to study the Ni^{2+} ions biosorption [28]. The equilibrium data and sorption kinetics were described well with Freundlich

isotherm model and the pseudo-second order kinetic model. The maximum uptake capacity of *Bacillus sphaericus* biomass for Ni^{2+} ions biosorption was found to be 55.55 mg/g calculated from the Langmuir isotherm model. The thermodynamic study indicates that Ni^{2+} ions biosorption was spontaneous and exothermic in nature. FTIR results confirmed that amine and carboxylic groups were responsible for Ni^{2+} ions biosorption on *Bacillus sphaericus* cells.

Romera *et al*. (2007) investigated the biosorption capacity of six different algae (red, brown and green) for Cd^{2+}, Ni^{2+} and Pb^{2+} ions from aqueous solution [260]. The best results were obtained with the lowest biomass concentration used (0.5 g/L). The optimum pH for the removal of Cd^{2+} and Ni^{2+} ions was found to be 6.0 and < 5.0 for Pb^{2+} ions. The equilibrium experimental data were well described by Langmuir isotherm model. The sequence of the biosorption capacity was $Pb^{2+} > Cd^{2+} > Ni^{2+}$. The maximum removal was obtained with a brown alga *Fucus spiralis*. The theoretical and experimental results were compared by a software computer program (PHREEQCI 6.2) which indicated minimum differences between both types of data.

2.3.1 Biosorption of Pb^{2+} ions: Isotherm and kinetic study

Studies done on the removal of Pb^{2+} ions from aqueous solution are reviewed and their summary is given in **Table 2.2** to **Table 2.4**. **Table 2.4** pertains to adsorption isotherm models proposed by various researchers. In most of the studies Langmuir and Freundlich isotherms have been observed to describe the biosorption behavior of biosorbate on the biosorbent. Parameters of isotherm models have been given in these tables. In some of the papers these parameter values were given in different units. In order to be consistent these have been converted into units mentioned in the table. pH, temperature, biomass dosage and initial metal ion concentration used in these studies are given **Table 2.2**. Most of the authors have not done kinetic studies. Studies available on kinetic models are given in **Table 2.3** with the values of kinetic constants.

2.3.2 Biosorption of Cd^{2+} ions: Isotherm and kinetic study

In order to analyze the equilibrium data of Cd^{2+} ions biosorption, various isotherm models were fitted by different researchers. In most of the studies, Langmuir and Freundlich isotherm models were used. **Table 2.5** shows the studied isotherm models and their parameters for different

studies. In previous research work, the kinetic data of Cd^{2+} ions biosorption were studied by using different kinetic models (**Table 2.6**). The pseudo first and pseudo second order kinetic models were found to be more frequently used kinetic models. **Table 2.7** shows the comparison of biosorption capacity of different biosorbents for Cd^{2+} ions biosorption at various process parameters.

2.3.3 Biosorption of Ni^{2+} ions: Isotherm and kinetic study

For Ni^{2+} ions biosorption, most of the researchers used pseudo first and pseudo second order kinetic models to analyze the kinetic data (**Table 2.8**). In most of the studies Langmuir and Freundlich isotherm models have been used to study the equilibrium data of Ni^{2+} ions biosorption (**Table 2.9**). **Table 2.10** shows the comparison of biosorption capacity of different biosorbents for Ni^{2+} ions biosorption at various process parameters.

2.3.4 Thermodynamic study for Pb^{2+} / Ni^{2+} / Cd^{2+} ions biosorption

The thermodynamic study was done by various researchers for Pb^{2+} / Ni^{2+} / Cd^{2+} ions biosorption on various biosorbents. **Table 2.11** shows that biosorption process of these ions is spontaneous and feasible. Some of the studies show the endothermic nature of biosorption with positive value of ΔH^o. While the negative value of ΔH^o shows the exothermic nature of biosorption process. The positive value of ΔS^o indicated that there was an increment in the randomness of the system solid/solution interface during the biosorption process.

2.4 DUAL METAL IONS BIOSORPTION STUDIES

Li *et al*. (2004) used the filamentous fungus (*Phanerochaete chrysosporium)* for the competitive biosorption of Pb^{2+} and Cd^{2+} ions together [184]. The experimental results showed that biosorption of metal ions were suppressed in presence of the other metal ions. In binary metal ions solution *P. chrysosporium* has higher selectivity for Pb^{2+} ions in comparison of Cd^{2+} ions. The optimum pH and temperature for both metal ions biosorption were found to be 4.5 and 27 °C. The experimental equilibrium data were well described by Freundlich isotherm model. At initial concentration of 50 mg/L, biosorption capacity of Pb^{2+} and Cd^{2+} ions was achieved as 12.34 mg/g and 15.2 mg/g, respectively.

Aksu *et al*. (2006) used the green alga (*Chlorella vulgaris) for the* competitive biosorption of Ni^{2+} and Cd^{2+} ions from the binary metal ion mixture [11]. All the batch experiments were carried out at pH 4.0 to investigate the biosorption capacity of *Chlorella vulgaris* for Ni^{2+} and Cd^{2+} ions *in single and dual metal ions system*. It was found that the uptake capacity of both the metal ions was increased with the increasing initial metal ion concentration up to 150 mg/L. In binary metal ions system the uptake capacity of *Chlorella vulgaris* for a metal ion was decreased with increasing concentrations of the other metal ion. For single and binary systems, both Langmuir and Freundlich isotherm models well described the equilibrium data. In single metal ion system, maximum uptake capacity of *Chlorella vulgaris* for Ni^{2+} and Cd^{2+} ions was obtained as 58.4 mg/g and 86.6 mg/g, respectively. While for binary metal ion system due to antagonistic effect of metal ions, uptake capacity was decreased to 28.3 mg/g for Ni^{2+} ions and 68.5 mg/g for Cd^{2+} ions.

Seker *et al*. (2008) investigated the efficacy of *Spirulina platensis* for Pb^{2+}, Cd^{2+} and Ni^{2+} ions biosorption from aqueous solution [276]. The experimental data were well explained by Freundlich, Temkin and Dubinin–Radushkevich isotherm models. The uptake of metal ions by *S. platensis* seemed to be quite rapid and the experimental data obeyed well the pseudo-second-order model. The rate of Pb^{2+} ions adsorption was higher in comparison to Cd^{2+} ions. The calculated activation energy for Pb^{2+}, Cd^{2+} and Ni^{2+} ions was found to be 44 kJ/mol, −16 kJ/mol and 54 kJ/mol, respectively. The results of competitive biosorption showed that *S. platensis* was more selective for Pb^{2+} ions biosorption.

Mahamadi *et al*. (2010) used *Eichhornia crassipes* to study the competitive biosorption of Pb^{2+}, Cd^{2+} and Zn^{2+} ions in binary and ternary systems at pH 4.84 and temperature of 30 °C [194]. The combined metal ions effect was found to be antagonistic. The following order of metal ion biosorption on *Eichhornia crassipes* was observed: $Pb^{2+} > Cd^{2+} > Zn^{2+}$. The Langmuir Competitive Model shows the better fitting to Pb^{2+}–Cd^{2+} and Pb^{2+}–Zn^{2+} ions systems but not fitted to Cd^{2+}–Zn^{2+} data. In conclusion, Pb^{2+} ions could still be effectively removed from aqueous solution. In the presence of both Cd^{2+} and Zn^{2+}ions, effective Pb^{2+} ions biosorption was occurred while the presence of Pb^{2+} ions shows the suppressive effect on Cd^{2+} and Zn^{2+} ions biosorption.

Luna et al. (2010) studied the competitive biosorption of Cd^{2+} and Zn^{2+} ions from single component and binary systems using *Sargassum filipendula* [193]. They have performed all the experiments at 25 ºC with the purpose of determining multiple component isotherms. Seven isotherm models were tested with the equilibrium data for modeling of the binary system. The Langmuir–Freundlich isotherm model was found to be best fitted to the binary adsorption data. The influence of binary metal ions on the behavior of Cd^{2+} and Zn^{2+} ions was analyzed by comparing single component and binary isotherms. It was observed that interference of Cd^{2+} ions on the sorption of Zn^{2+} ions was considerably less intense while Zn^{2+} ions had a relevant effect on the Cd^{2+} ions biosorption.

Kleinubing et al. (2011) studied the removal of Cu^{2+} and Ni^{2+} ions from single and binary systems using *Sargassum filipendula* [163]. The low ranges of initial concentrations were used with the purpose of conducting column studies. The equilibrium data was fitted to Langmuir isotherm model for single and binary systems to represent the equilibrium between liquid and solid phases. In fixed-bed columns the biosorption was described by using a mathematical model. This model considered that the mass transfer in the biosorbent was the controlling step, which was described by the LDF (Linear Driving Force) concept. The higher affinity of Cu^{2+} ions for biosorbent was confirmed by the values of binary isotherm parameters, and by the presence of an overshoot for the competitor metal (Ni^{2+} ions) on the breakthrough curves. It showed that *S. filipendula* can be used for the efficient removal of metal ions in fixed-bed columns from industrial wastewater containing, Cu^{2+} and Ni^{2+} ions in solution.

2.5 MOTIVATION FOR THE PROPOSED RESEARCH WORK

On the basis of critical assessment of literature review on the biosorption of Pb^{2+}/ Cd^{2+}/ Ni^{2+} ions in single and multiple metal ions systems. Following observations have been made:

(i) Though *S. filipendula* has been used for the removal of single metal ion (Pb^{2+}/ Cd^{2+}/ Ni^{2+}) from wastewater, but these studies are preliminary in nature or at particular operating conditions. Therefore, it is desired to conduct the comprehensive studies on biosorption of single metal ions (Pb^{2+}/ Cd^{2+}/ Ni^{2+}) present in wastewater by using *S. filipendula*.

(ii) Normally two or more metal ions are present in wastewater. However, there is no single study on the biosorption of multiple metal ions (Pb^{2+} and Cd^{2+}) on *S. filipendula*.

On the basis of above, objectives of research work in the present thesis have been formulated and are given in section 1.5 of Chapter I.

2.6 CONCLUSIONS

Biosorption is a cost effective and efficient technique for the removal of heavy metals ions from wastewater. The summarized form of all the available reviewed studies on metal ions biosorption provides sufficient information on metal ions biosorption. This review work explains the equilibrium and kinetic study of metal ion biosorption with uptake capacity of different biosorbents in single and binary metal ion systems.

Table 2.2 Summary of studies done on biosorption of Pb^{2+} ions

S.No.	Biosorbent	pH	T (°C)	Initial Pb^{2+} ions concentration (g/L)	Biosorbent dosage (g/L)	q_e (mg/g)	Reference
1	*Cladophora fascucularis*	5.0	25	41-828	0.1	198.91	[87]
2	*Saccharomyces cerevisiae*	5.0	22	10-180	1.5	72.5	[21]
3	*Chlamydomonas reinherdtii*	6.0	25	20-400	0.8	42.6	[320]
4	*Streptomyces rimosus*	-	25	100	3	135	[278]
5	*Lactarius scrobiculatus*	5.5	20	10	4	56.2	[22]
6	*Anabaena sphaerica*	5.5	25	50-300	0.2	111.1	[32]
7	*Stenotrophomonas maltophilia*	5.0	30	98.4	1.0	133.3	[339]
8	*S. filipendula*	4.0	30	6.2-677	2.0	261.07	[325]
9	*Chlorella vulgaris*	3.0	25	1-30	2.0	20.48	[180]
10	*Bacillus subtilis*	5.0	30	8.4	1.0	166.7	[339]
11	*Aspergillus terreus*	5.0	30	6000	0.1	247.2	[310]
12	*Pleurotus florida*	7.0	30	10	0.2	12.195	[249]
13	*Trichoderma viride*	6.0	30	10	0.2	10.98	[249]
14	*Spyridia filamentosa*	5.0	25	414	2	178.19	[164]
15	*Aspergillus niger*	5.0	30	50	0.91	2.47	[228]
16	*Spirogyra* sp.	5.0	25	200	0.05	140	[124]
17	*Cladohpora* sp.	5.0	25	100	10	46.51	[182]
18	*P. oedogonia*	5.0	25	5-200	1.0	90.19	[291]
19	*Codium vermilara*	5	-	-	0.5	21.8	[260]
20	*Spirogyra hyalina*	-	-	80	0.25	31.25	[170]
21	*A. platensis*	-	25	-	2	113.13	[101]
22	*C. vulgaris*	-	25	-	2	138.27	[101]
23	*S. neglecta*	5.0	25	5.0	0.01	90.19	[291]
24	*Enterobacter* sp.	2	25	100	-	50	[192]
25	*Pelvetia canaliculata*	4.0	25	30-320	0.5	259	[128]
26	*Ulva latuca*	5.5	30	10	0.1	29.1	[113]

Table 2.3 Comparison of kinetic models parameters studied for Pb^{2+} ions biosorption

S.No.	Biosorbent	Pseudo first order	Pseudo second order	Intraparticle diffusion	Reference
1	*Cladophora fascicularis*	-	K = 0.078 g/mmol.min q_e = 0.70 mmol/g	-	[87]
2	*Sacchormyces cerevisiae*	k_o = 0.4202 1/min q_e = 9.73 mg/g	K = 0.1712 g/mg.min q_e = 23.70 mg/g	-	[21]
3	*Chlamydomonas reinherdtii*	k_o = 7.7 x 10^2 1/min q_e =1.26 mmol/g	K = 3.0 x10^2 g/mmol.min q_e = 0.46 mmol/g	-	[320]
4	*Streptomyces rimosus*	k_o = 3.56x10^{-4} 1/min	-	K_{id} = 0.863 mg/g.$sec^{0.5}$	[278]
5	*Lactarius scrobiculatus*	k_o = 4.3×10^{-2}1/min q_e = 0.46 mg/g	K = 0.25 g/mmol.min q_e = 1.56 mg/g	-	[22]
6	Alga	k_o = 6.0.028 1/min	K = 0.169 mg/g.min	-	[309]
7	*Chlorella vulgaris*	k_o = 0.007 1/min q_e = 2.662 mg/g	K = 0.273 g/mg.min q_e = 3.952 mg/g	K_{id} = 0.233 mg/g.$min^{0.5}$ C = 2.835	[180]

Table 2.4 Comparison of isotherm model parameters for Pb^{2+} ions biosorption on some reported biosorbents

S. No.	Biosorbent	Biosorption Isotherm Models			Reference
		Langmuir	Freundlich	Dubnin-Radushkevich	
1	*Cladophora fascicularis*	q_e = 196.65 mg/g b = 0.040 L/mg	k_f = 0.789 n = 3.62	-	[87]
2	*Saccharomyces cerevisae* (Live)	q_e = 72.46 mg/g b = 0.086 L/mg	-	-	[21]
3	*Chlamydomonas reinhardtii*	q_e = 147.11 mg/g b = $7.8x10^4$ L/mg	k_f = $9.46x10^3$ n = 1.42	-	[320]
4	*Streptomyces rimosus*	q_e = 137 mg/g b = 0.172 L/mg	k_f = 30.1 n = 3.41	-	[278]
5	*Lactarius scrobiculatus*	q_e = 56.2 mg/g b = 0.02 L/mg	k_f = 6.26 n = 2.56	q_m = 9.5 x 10^{-4} mol/g E= 10.3 kJ/mol	[22]
6	*Anabaena sphaerica*	q_e = 121.95 mg/g b = 0.0521 L/mg	k_f = 28.28 n = 3.80	-	[32]
7	*Stenotrophomonas maltophilia*	q_e = 133.3 mg/g b = 0.016 L/mg	k_f = 36.4 n = 3.91	-	[339]
8	*Sargassum filipendula*	q_e = 1.35 mg/g b = 20.2 L/mg	-	-	[325]
9	*Chlorella vulgaris*	q_e = 20 mg/g b = 0.892 L/mg	k_f = 8.57 n = 1.5	-	[180]
10	*Bacillus subtilis*	q_e = 166.7 mg/g b = 0.019 L/mg	k_f = 52.5 n = 4.81	-	[339]
11	*Aspergillus terreus*	q_e = 253.16 mg/g b = 0.01 L/mg	k_f = 57.68 n = 0.18	-	[310]
12	*Pleurotus florida*	q_e = 12.195 mg/g b = 0.058 L/mg	k_f = 0.954 n = 1.61	-	[249]
13	*Trichoderma viride*	q_e = 10.98 mg/g b = 0.057 L/mg	k_f = 0.935 n = 1.623	-	[249]
14	*Spyridia filamentosa*	q_e = 178.19 mg/g b = 8.06 L/mg	-	-	[164]

Table 2.4 Continued…

S. No.	Biosorbent	Biosorption Isotherm Models			Reference
		Langmuir	Freundlich	Dubnin-Radushkevich	
15	*Aspergillus niger*	q_e = 2.17 mg/g b = 2.8 L/mg	-	-	[228]
16	*Spirogyra* sp.	q_e = 140.84 mg/g b = 0.021 L/mg	k_f = 8.01 n = 1.87	-	[124]
17	*Cladophora* sp.	q_e = 46.51 mg/g b = 0.025 L/mg	k_f = 6.63 n = 3.03	-	[182]
18	*P. oedogonia*	q_e = 71.13 mg/g b = 0.020 L/mg	k_f = 5.28 n = 0.461	-	[291]
19	*Codium vermilara*	q_e = 63.3 mg/g b = 0.11 L/mg	-	-	[242]
20	*Spirogyra hyalina*	q_e = 31.25 mg/g b = 0.096 L/mg	n = 1.50	-	[170]
21	*A. platensis*	q_e = 113.13 mg/g b = 0.0137 L/mg	k_f = 78.73 n = 3.21	-	[101]
22	*C. vulgaris*	q_e = 138.40 mg/g b = 0.545 L/mg	k_f = 127.22 n = 3.66	-	[101]
23	*S. neglecta*	q_e = 90.19 mg/g b = 0.015 L/mg	k_f = 4.75 n = 0.513	-	[291]
24	*Enterobacter* sp.	q_e = 30.6 mg/g b = 13.6 L/mg	k_f = 15.5 n = 4.2	-	[192]

Table 2.5 Comparison of isotherm model parameters for Cd^{2+} ions biosorption on some reported biosorbents

S. No.	Biosorbent	Biosorption Isotherm Models				Reference
		Langmuir	Freundlich	Temkin	Hasley	
1	*Aeromonas caviae*	q_e = 155.32 mg/g b = 0.019 L/mg	k_f = 10.85 L/g n = 2.12	-	-	[190]
2	*Chlamydomonas reinhardtii*	q_e = 77.28 mg/g b = 19.1x10^4 L/mg	k_f = 4.8x10^3 n = 1.27	-	-	[320]
3	*Chlorella vulgaris*	q_e = 13.15 mg/g b = 4.22 L/mg	k_f = 8.95 mg/g n = 3.41	-	-	[180]
4	Green alga	q_e = 53.19 mg/g b = 0.0193 L/mg	k_f = 3.81mg$^{(1-1/n)}$.L$^{1/n}$ /g n = 2.11	k_T = 0.161 L/mg b_T = 194.71 kJ/mol		[52]
5	*Spirogyra hyalina*	q_e = 18.18 mg/g b = 0.061 L/mg	n = 1.44	-	-	[170]
6	*Sargassum oligocystum*	q_e = 153.85 mg/g b = 0.005 L/mg	k_f = 1.128 L/mg n = 0.983	k_T = 0.115 L/mmol	k_H = 0.359 L/g n_H = - 0.687	[86]
7	*Caulerpa fastigiata*	q_e = 16.13 mg/g b = 0.082 L/mg	k_f = 1.584 n = 1.538	-	-	[270]
8	*Bacillus laterosporus*	q_e = 85.47 mg/g b = 11.09x103 L/mg	k_f = 1.003 n = 1.086	-	-	[166]
9	*D. antarctica*	q_e = 106.4 mg/g b = 0.086 L/mg	k_f = 7.667 mg/g n = 2.664	-	-	[132]
10	*Anabaena sphaerica*	q_e = 111.1 mg/g b = 0.052 L/mg	k_f = 15.31 n = 2.56	-	-	[32]
11	*Ulva latuca*	q_e = 29.06 mg/g b = 5.4x10^{-4} L/mg	k_f = 0.23 n = 1.002	-	-	[113]
12	*Codium vermilara*	q_e = 21.8 mg/g b = 0.10 L/mg	-	-	-	[260]
13	*Lentinus edodes*	q_e = 625.0mg/g b = 0.260 L/mg	k_f = 1.860 mg/g n = 1.282	a_T = 0.1063 L/mg b_T = 25.788	-	[62]
14	*Rhodotorulla* sp.	q_e = 14.03 mg/g b = 0.429 L/mg	k_f = 5.04 n = 4.20	-	-	[185]

Table 2.5 Continued…

S. No.	Biosorbent	Biosorption Isotherm Models				Reference
		Langmuir	Freundlich	Temkin	Hasley	
15	*Spirulina platensis*	q_e = 10.61 mg/g b = 0.093 L/mg	-	-	-	[101]
16	*Spirulina maxima*	q_e = 29.76 mg/g b = 0.325 L/mg	k_f = 6.33 mg/g n = 1.24	-	-	[26]
17	*S. neglecta*	q_e = 27.95 mg/g b = 0.047 L/mg	k_f = 5.01$mg^{(1-n)}.L^n$ /g n = 0.32	-	-	[291]
18	*P. oedogonia*	q_e = 13.07 mg/g b = 0.038 L/mg	k_f = 2.02 $mg^{(1-n)}.L^n$ /g n = 0.344	-	-	[291]
19	*Pelvetia caniculata*	q_e = 75 mg/g b = 0.075 L/mg	k_f = 13 n = 2.8	**Langmuir-Freundlich** q_e = 79 mg/g b = 0.06 n = 1.1	**Toth** q_e = 83 mg/g b = 0.09 n = 1.3	[188]
20	*Gelidium*	q_e = 18 mg/g b = 0.19 L/mg	**Redlich-Peterson** K_1 = 3.2 K_2 = 0.2 b = 0.95	-	-	[327]

Table 2.6 Comparison of kinetic models parameters studied for Cd^{2+} ions biosorption

S.No.	Biosorbent	Pseudo first order	Pseudo second order	Ritchie second order equation	Bangham	Reference
1	*Aeromonas caviae*	-	K = 0.132 g/mg.min q_e = 4.33 mg/g	q_e = 4.36 mg/g k_R= 0.48 1/min	-	[190]
2	*Chlamydomonas reinherdtii*	k_o = 7.7 x 10^2 1/min q_e =1.26 mmol/g	K = 3.0 x10^2 g/mmol.min q_e = 0.46 mmol/g	-	-	[320]
3	*Chlorella vulgaris*	k_o = 0.007 1/min q_e = 2.662 mg/g	K = 0.273 g/mg.min q_e = 3.952 mg/g	**Intraparticle diffusion** K_{id} = 0.233 mg/g.$min^{0.5}$ C = 2.835	-	[180]
4	Green alga	k_o = 0.0077 1/min q_e = 0.8914 mg/g	K = 0.0749 g/mg.min q_e = 6.9686 mg/g	K^I_{id} = 0.2388 mg/g.$min^{0.5}$ C^I = 5.2945 mg/L K^{II}_{id} = 0.0551mg/g.$min^{0.5}$ C^{II} = 6.2151 mg/L	-	[52]
5	*Gelidium*	k_o = 0.17 1/min q_e = 16.3 mg/g	K = 0.11 g/mg.min q_e = 18.9 mg/g	-	-	[327]
6	*Sarsassum oligocystum*	k_o = 0.041 1/min q_e = 0.610 mg/g	K = 0.702 g/mg.min q_e = 1.424 mg/g	K_{id} = 0.025 mg/g.$min^{0.5}$	k_b = 0.126 α_o = 5.99 x 10^{-4}	[86]
7	*Laminaria japonica*	k_o = 0.09 1/min q_e = 0.99 mmol/g	K = 0.17 g/mmol.min q_e = 1.02 mmol/g	-	-	[186]
8	Alga	k_o = 0.028 1/min	K = 0.169 mg/g.min	-	-	[309]
9	*Pelvetia caniculata*	-	K = 4.6 x 10^{-3} g/mg.min q_e = 67.62 mg/g	-	-	[188]
10	*Lactarius scrobiculatus*	k_o = 4.3×10^{-2}1/min q_e = 0.46 mg/g	K = 0.25 g/mmol.min q_e = 1.56 mg/g	-	-	[22]

Table 2.7 Summary of studies done on biosorption of Cd^{2+} ions

S.No.	Biosorbent	pH	T (°C)	Initial Cd^{2+} ions concentration (mg/L)	Biosorbent dosage (g/L)	q_e (mg/g)	Reference
1	*Aeromonas caviae*	7.0	20	5-350	1.0	155.32	[190]
2	*Chlamydomonas reinherdtii*	6.0	25	20-400	0.8	42.6	[320]
3	*Chlorella vulgaris*	4.5	25	10	2.0	13.15	[180]
4	*Green alga*	5.0	20	20-540	8.0	33.71	[52]
5	*S. neglecta*	5.0	25	0-200	0.01	27.95	[291]
6	*Spirogyra hyalina*	-	25	20-80	1.0	18.18	[170]
7	*Caulerpa fastigiata*	5.5	25	30.29	10	16.48	[270]
8	*Bacillus laterosporus*	7.0	30	10-50	4.0	85.47	[167]
9	*D. antarctica*	3.7	25	50-1200	2.0	95.3	[127]
10	*Anabaena sphaerica*	5.5	25	50-300	0.2	111.1	[32]
11	*Ulva latuca*	5.5	30	10	0.1	29.1	[113]
12	*Codium vermilara*	6.0	25	10-150	0.5	21.8	[260]
13	*Lentinus edodes*	6.5	25	1000	1.0	624.96	[62]
14	*Rhodotorulla* sp.	4.0	28	100	1.5	19.38	[185]
15	*Spirulina platensis*	8.0	20	60	2.0	10.61	[141]
16	*P. oedogonium*	5.0	25	5-200	0.01	13.07	[291]
17	*Sargassum oligocystum*	-	24	0-100	10	153.85	[86]
18	*Pelvitia caniculata*	4.8	25	250	2.5	75	[188]
19	*Gelidium*	5.3	20	6-91	0.2	18	[327]
20	*Ceramium virgatus*	5.0	20	10	10	39.7	[271]
21	Modified alga	5.0	25	360	8.0	34.15	[133]

Table 2.8 Comparison of kinetic models parameters studied for Ni^{2+} ions biosorption

S.No.	Biosorbent	Pseudo first order	Pseudo second order	Reference
1	*Yarrowia lipolytica*	k_o = 0.055 1/min q_e = 2.476 mg/g	K = 0.019 g/mg.min q_e = 15.97 mg/g	[340]
2	*Sargassum iliciform*	k_o = 0.057 1/min q_e = 169.61 mg/g	K = 0.013 g/mg.min q_e = 136.16 mg/g	[313]
3	*Laminaria japonica*	k_o = 0.09 1/min q_e = 0.99 mmol/g	K = 0.17 g/mmol.min q_e = 1.02 mmol/g	[186]
4	*Baker's yeast*	k_o = 0.0021 1/min q_e = 57 mg/g	K = 0.0035 g/mg.min q_e = 8.1 mg/g	[241]
5	*Mucor hiemalis*	k_o = 0.0414 1/min q_e = 18.84 mg/g	K = 0.046 g/mmol.min q_e = 20.83 mg/g	[287]
6	*Bacillus laterosporus*	k_o = 0.0792 1/min q_e = 7.033 mg/g	K = 0.0375 g/mg.min q_e = 9.66 mg/g	[166]

Table 2.9 Comparison of isotherm model parameters for Ni^{2+} ions biosorption on some reported biosorbents

S. No.	Biosorbent	Biosorption Isotherm Models					Reference
		Langmuir	Freundlich	Redlich-Peterson	Temkin	Dubnin-Radushkevich	
1	*Bacillus laterosporus*	q_e = 44.44 mg/g b = 1.44 x 10^{-3} L/mg	k_f = 0.068 n = 1.034	-	-	-	[166]
2	*Yarrowia lipolytica*	q_e = 30.12 mg/g b = 0.020 L/mg	k_f = 1.165 n = 1.61	-	-	-	[340]
3	*Baker's yeast*	q_e = 9.01 mg/g b = 0.212 L/mg	k_f =3.73 mg^{1-n}/g. L^n n = 5.88	K_1 = 4.12 K_2 = 0.813 b = 0.887	-	-	[241]
4	*Mucor hiemalis*	-	k_f = 1.922 n = 0.99	-	-	-	[287]
5	*S. ilicifolium*	q_e =133.81 mg/g b = 0.325 L/mg	k_f = 0.54 n = 1.51	-	k_T = 3.38 L/mg b_T = 0.494J/mol	q_m =110.9 mol/g E= 0.038 kJ/mol	[313]
6	*Laminaria japonica*	q_e = 66.3 mg/g b = 0.212 L/mg	k_f = 0.63 n = 3.78	K_1 = 2.29 K_2 = 10.3 b = 0.89	-	-	[186]
7	*Strenotrophomonas maltophilia*	q_e = 54.3 mg/g b = 0.036 L/mg	k_f = 23.6 L/mg n = 5.83	-	-	-	[339]
8	*Bacillus subtilis*	q_e = 57.8 mg/g b = 0.047 L/mg	k_f = 26 L/mg n = 5.71	-	-	-	[339]
9	*Sargassum sp.*	q_e = 53.58 mg/g b = 0.0276 L/mg	k_f = 0.542 n = 3.613	-	-	-	[39]
10	*Spirogyra neglecta*	q_e = 26.3 mg/g b = 0.042 L/mg	k_f = 74.2 mg^{1-n}/g. L^n n = 0.366	-	-	-	[291]
11	*P. oedogonia*	q_e = 11.81mg/g b = 0.039 L/mg	k_f = 1.84 mg^{1-n}/g. L^n n = 0.342	-	-	-	[291]
12	*S. filipendula*	q_e = 62.7 mg/g b = 0.0681 L/mg	-	-	-	-	[163]
13	*A. platensis*	q_e = 43.43 mg/g b = 0.0074 L/mg	k_f = 12.61 n = 1.36	-	-	-	[101]

Table 2.10 Summary of studies done on biosorption of Ni^{2+} ions

S.No.	Biosorbent	pH	T (ºC)	Initial Ni^{2+} ions concentration (mg/L)	Biosorbent dosage (g/L)	q_e (mg/g)	Reference
1	*Bacillus laterosporus*	7.0	30	10-50	4.0	44.44	[167]
2	*Yarrownia lipolytica*	6.0	40	100	2.0	30.12	[340]
3	*Baker's yeast*	6.7	27	400	1.0	9.8	[241]
4	*Mucor hiemalis*	8.0	40	50	0.5	15.83	[287]
5	*Sargassum iliciform*	5.0	25	100	6.1	218.91	[313]
6	*Laminaria japonica*	6.0	25	234.7	1	52.81	[186]
7	*Streptomonas maltophilia*	6.0	30	45.6	2.0	54.3	[339]
8	*Bacillus subtilis*	6.0	30	45.6	2.0	57.8	[339]
9	*Sargassum* sp.	5.0	30	0-410	0.1	53.58	[39]
10	*Spirogyra neglecta*	5.0	-	5-200	1	90.19	[291]
11	*P. oedogonia*	5.0	-	5-200	1	71.13	[291]
12	*Sargassum filipendula*	4.5	21	17.6-234.76	3	62.7	[163]
13	*A. platensis*	5.0	20	29.34-176.0	2	20.77	[101]
14	*Pelvetia canaliculata*	4.0	25	50	0.5	228.89	[46]
15	*Codium vermilara*	6.0	25	100-150	0.5	13.2	[260]

Table 2.11 Comparison of thermodynamic parameters for Pb^{2+} / Ni^{2+} / Cd^{2+} ions biosorption with different biosorbents

S. No.	Biosorbent	Metal ion	T (°C)	$\Delta G°$ (kJ/mol)	$\Delta H°$ (kJ/mol)	$\Delta S°$ (J/mol.K)	Reference
1	*Sargassum ilicifolium*	Pb^{2+}	20, 25, 30	-2.6 to -3.6	0.027	0.102	[313]
2	*Spirogyra sp.*	Pb^{2+}	25, 30, 35	-20.45 to -22.12	4.0	0.083	[124]
3	*Lactarius scrobiculatus*	Pb^{2+}	25, 35, 45	-19.1 to -18.3	-26.5	-25.2	[22]
4	*Halomonas sp.*	Cd^{2+}	20, 30, 40, 50	-20.08 to -7.69	-180.03	-545.91	[198]
5	*Caulerpa fastigiata*	Cd^{2+}	25	-2.59	-23.87	-61.34	[270]
6	*Sargassum oligocystum*	Cd^{2+}	24	-2.45	-18.52	0.0019	[86]
7	*Lactarius scrobiculatus*	Cd^{2+}	25, 35, 45	-18.4 to 17.5	-26.8	-28.6	[22]
8	Baker's yeast	Ni^{2+}	27, 40, 50, 60	-23.51 to -22.7	-30.70	-23.65	[241]
9	*Sargassum ilicifolium*	Ni^{2+}	30, 40, 50, 60	-3.1 to -4.19	8.98	39.41	[313]

CHAPTER III

MATERIALS AND METHODS

3.0 INTRODUCTION

In this chapter material required and experimental procedure followed for biosorption of Pb^{2+}, Cd^{2+}, and Ni^{2+} ions are given. The details of auxillary and analytical instruments required for experimentation, characterization and analysis purpose are given. Response surface methodology was also explained in this chapter for the optimization of biosorption process parameters. Besides, this statistical modeling for kinetic, isotherm, and thermodynamic study of single and dual metal ions biosorption systems is also described.

3.1 EXPERIMENTAL STUDIES

3.1.1 Materials

3.1.1.1 Biosorbent

The dried biomass of *Sargassum filipendula* (**Fig 3.1**) was bought from Aushadh Agri Science Private Limited, Gujarat (India).

3.1.1.2 Chemicals

All the chemicals utilized in the experimentation (HNO_3, NaOH, salts of lead nitrate,

Fig. 3.1 Dried biomass of *Sargassum filipendula.*

cadmium nitrate and nickel nitrate) were from Merck Germany, Himedia Laboratories Pvt. Ltd. Mumbai, and Ranbaxy Fine Chemicals Ltd. New Delhi.

3.1.1.3 Instruments

(i) Analytical instruments used in the present study

Fig 3.2 (a-e) shows pictorial representation of several analytical instruments which were used in the present study namely: Fourier Transform Infrared Spectrometer (FTIR), FESEM & EDS, Atomic Absorption Spectroscopy (AAS), pH meter, and weighing balance.

(ii) Auxiliary equipments used in the present study

The pictorial representation of auxiliary equipments which were used in the present study namely: Incubator shaker, Hot Air Oven, Millipore water unit and grinder are shown in **Fig 3.3 (a&d)**.

3.1.2 Methods

3.1.2.1 Biosorbent preparation

The collected biomass of *S. filipendula* was washed several times with deionized distilled water to remove impurities and ions such as Ca^{2+} or Na^{+} bound on biosorbent surface that can affect the biosorption process. After that, it was dried in an oven at 80 ^{o}C for 24 h and store in desiccator. The dried biomass was then grounded and sieved through 212 µm sieve. The obtained fraction was used as biosorbent for biosorption process.

3.1.2.2 Biosorbate preparation

The stock solution of 1000 mg/L metal ions was prepared by dissolving nitrate salts of lead (1.56 g), cadmium (2.1 g), and nickel (4.95 g) in deionized distilled water. The pH of solution was adjusted with 0.1 M HNO_3 and 0.1 M NaOH.

(a) FTIR Spectrometer (Thermo Model AVATR 370)

(b) Atomic Absorption Spectroscopy (GBC Scientific Equipmemts Ltd)

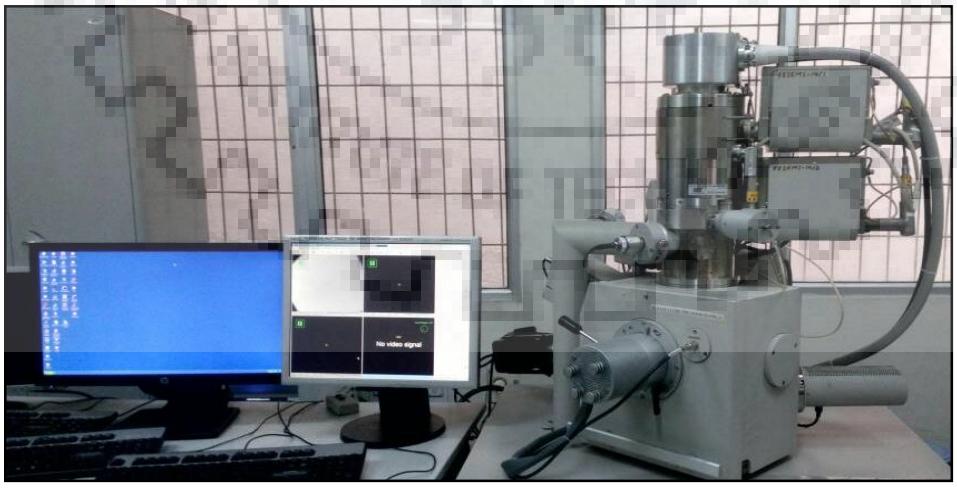

(c) FESEM & EDS (Quanta 200 F)

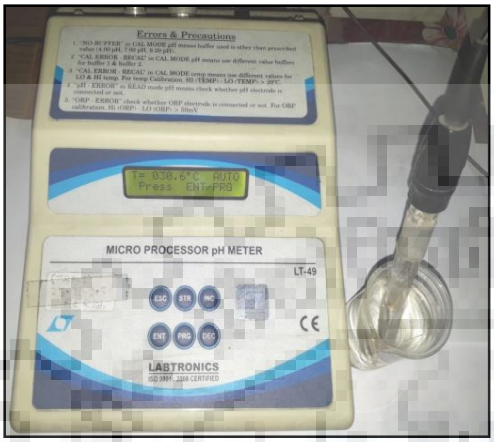

(d) pH meter (Labtronics)

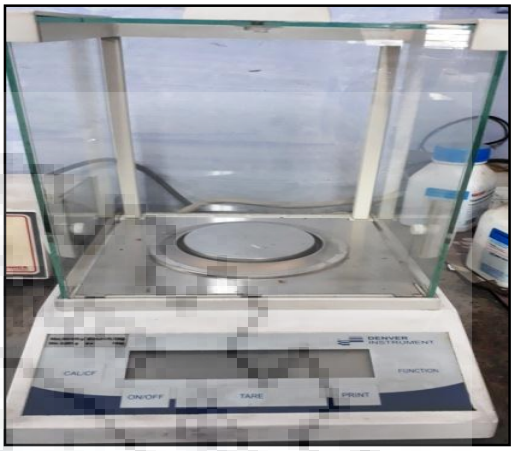

(e) Weighing balance (Denver Instrument)

Fig. 3.2 (a-e) Photographic images of analytical instruments used during the present investigation.

(a) Hot air oven

(b) Incubator shaker (Metrex Scientific)

(c) Millipore water unit

(d) Grinder

Fig. 3.3 (a-d) Photographic images of auxiliary instruments used during the present investigation.

3.1.2.3 FTIR analysis

The FTIR analysis was carried out to detect the functional groups present on the biosorbent surface and their interaction with metal ions [262, 272, 273]. Infra-red spectra were obtained by KBr disc method, in which a dried form of raw and metal ions loaded *S. filipendula* was added separately with KBr in 1:10 ratio to form a pellet. FTIR spectral analysis was carried out using the Perkin-Elmer model Lambda 35 double beam spectrophotometer in the range between wavelength of 2500-25000 nm.

3.1.2.4 FESEM and EDS analysis

The physical morphology of biosorbent surface was studied under Field Emission Electron microscopy (FESEM) combined with Energy Dispersive X-ray Spectroscopy (EDS) which gives information about the chemical composition of biosorbent before and after metal ions biosorption [120, 212, 298, 331]. FESEM and EDX analysis was carried out using FESEM QUANTA 200 FEG (FEI Netherlands).

3.1.2.5 Specific surface area of biosorbent

The maximum biosorption capacity 'q_m' determined by Langmuir isotherm can be used to determine the specific surface area of biosorbent by using equation [8] given below:

$$S = \frac{q_m N A}{M} \tag{3.1}$$

where M is molecular weight of metal ion, N is Avogadro number (6.022×10^{23}), A is cross sectional area of metal ion (m^2), and q_m is monolayer biosorption capacity (g/g).

3.1.2.6 Experimental procedure used to conduct biosorption experiments

The biosorption experiments were carried out in batch mode to check the removal efficiency of *S. filipendula* for Pb^{2+}, Cd^{2+} and Ni^{2+} ions. All the batch biosorption experiments were conducted to observe the effects of several experimental parameters like temperature, pH, initial metal ions

concentration, biosorption time, and biosorbent dosage on the removal of Pb^{2+}, Cd^{2+} and Ni^{2+} ions. The biosorption experiments were conducted separately in 250 mL conical flask with 100 mL of metal ion solution for 85 min on rotary shaker (Metrex Scientific Instruments Private Limited, India) at three different agitation speed namely 50, 100, and 150 rpm. It was found that the extent of biosorption at 100 and 150 rpm were the same. Therefore, further experiments were conducted at 150 rpm.

(i) Single metal ion biosorption study

The optimization of Pb^{2+} ion biosorption was studied by varying important reaction parameters such as pH (2.0-5.0), temperature (25-35 ºC), initial Pb^{2+} ion concentration (100-300 mg/L) and biosorbent dosage (0.2-0.5 g/L).

For Cd^{2+} ions biosorption the range of process parameters chosen as pH (2.0-7.0), biomass dosage (0.25-1.25 g/L), initial Cd^{2+} ions concentration (25-125 mg/L), and temperature (20-40 ºC).

For Ni^{2+} ions biosorption the effect of different process parameters were studied by varying pH (2.0-6.0), initial Ni^{2+} ions concentration (50-150 mg/L), temperature (20-40 ºC), and biomass dosage (1.0-2.5 g/L).

The initial pH of each metal ions solution was maintained to the requisite pH value by adding 0.1 M NaOH or 0.1 M HNO_3.

(ii) Dual metal ions biosorption study

For dual metal ion system: (a) the concentration of Pb^{2+} ions was changed from 0 to 300 mg/L with 50 mg/L of Cd^{2+} ions concentration (b) the concentration of Cd^{2+} ions was changed from 0 to 300 mg/L with 50 mg/L of Pb^{2+} ions concentration. The optimum temperature and pH were selected from a range of temperature 20 to 40 ºC and pH 2-6.

In all the experiments, samples were collected after a regular interval of time. In order to determine the concentration of metal ions in the solution, the treated solution was filtered with

Whatman No. 1 filter paper. The filtrate was examined for residual metal ions concentration using Atomic Absorption Spectrophotometer (GBC Avantha, Germany) and quantified against known standard solution of specific metal ion. Whenever it was necessary, the samples were diluted with distilled water to improve accuracy of estimation. All the experiments were conducted in triplicate and the results were statistically analyzed.

3.1.2.7 Desorption study

The recycling of biosorbent is a most important step from economical point of view. The possibility of regenerating and recycle of biosorbent enhances the attractiveness of biosorption process. It is very important factor to regenerate the biosorbent without losing its biosorption capacity. The selection of a suitable eluent is a significant step in desorption process which depends on the biosorbent type and biosorption mechanism to achieve a successful recovery of metal ion from biosorbent. The eluent should be cost effective, non-damaging to biomass, and environment friendly [313]. For this research work 0.2 M HCl was used as eluent.

Hence biosorption-desorption process were carried out up to 4 cycles by adding 0.5 g of metal ions loaded *S. filipendula* in 100 mL of 0.2 M HCl for each cycle. A single cycle sequence comprises of biosorption followed by desorption. This mixture was stirred for 65 min, then filtered and analyzed for metal ions desorbed in the solution by AAS. In order to reuse the biomass for next cycle, the biomass was washed with 0.2 M HCl solution and distilled water, consecutively. The percent desorbed of metal ions was given by the following equation:

$$\textit{Desorption efficiency (\%)} = \frac{Amount\ of\ desorbed\ metal\ ion}{Amount\ of\ biosorbed\ metal\ ion} \text{ x } 100 \qquad (3.2)$$

3.1.2.8 Determination of removal efficiency and biosorption capacity

The results were expressed in terms of % removal of metal ions, as given below by the following equation:

$$\textit{\% Removal} = \frac{C_i - C_e}{C_i} . 100 \qquad (3.3)$$

The biosorption capacity 'q_e' of a biosorbent is the amount of metal biosorbed per unit amount of biosorbent (mg/g) at equilibrium. It can be obtained by using Eq. (3.4):

$$q_e = \frac{(C_i - C_e)\,V}{C_i \,.\, m} \tag{3.4}$$

where 'q_e' is amount of biosorbate biosorbed at equilibrium (mg/g), 'V' is volume of solution (L), 'm' is mass of biosorbent (g), 'C_i' is initial concentration of metal ion and 'C_e' is equilibrium concentration of metal ion (mg/L).

3.2 KINETIC AND BIOSORPTION ISOTHERM MODELS

3.2.1 Kinetic modeling

The biosorption kinetic study explains the removal rate of solute, rate controlling step and the mechanism involve in Pb^{2+}, Cd^{2+}, and Ni^{2+} ions biosorption on to *S. filipendula* [225, 322]. The biosorption mechanism relies on the mass transfer process and physical or chemical properties of the biosorbent [191, 194]. The biosorption process involves several consecutive steps: bulk solution transport, pore diffusion, film diffusion, and biosorption on the surface or pores [223]. The slowest step limits the overall biosorption rate. The six kinetic models which were used to analyze the experimental kinetic data: Pseudo first order, Pseudo second order, Elovich, Intra particle diffusion, Bangham, and Modified Freundlich.

(i) Pseudo first order

According to pseudo first order model, the rate of biosorption is proportional to the number of remaining unoccupied sites on biosorbent surface. This model represents physisorption. The pseudo first order equation is given below [66, 293]:

$$\frac{dq_t}{dt} = k_o\,(q_e - q_t) \tag{3.5}$$

Eq. (3.5) may be integrated with initial conditions, at $t = 0$, $q_t = 0$ and at $t = t$, $q_t = q_t$. Its integrated equations are:

Linear equation:

$$ln\ (q_e - q_t) = ln\ q_{\ e} - k_o t \quad (3.6)$$

Nonlinear equation [217, 264]:

$$q_t = q_e\ (1 - e^{-k_o\ t}) \quad (3.7)$$

where k_o (min^{-1}) is biosorption rate constant of pseudo first order kinetics, q_t is the amount of metal ions biosorbed at time 't'. The value of k_o was calculated from the slope of plot of $ln\ (q_e - q_t)$ *vs. t*.

(ii) Pseudo second order

This model is applicable for chemisorption process. The kinetic behavior of biosorption process with chemisorption being the rate controlling step is more likely to be predicted by this model. The pseudo second order equation is given below [293]:

$$\frac{dq_t}{dt} = K(q_e - q_t)^2 \quad (3.8)$$

Eq. (3.8) may be integrated with initial conditions, at $t = 0$, $q_t = 0$ and at $t = t$, $q_t = q_t$. Its integrated equations are:

Linear equation [195, 214]:

$$\frac{t}{q_t} = \frac{1}{Kq_e^2} + \frac{1}{q_e} t \quad (3.9)$$

Nonlinear equation [217, 264]:

$$q_t = \frac{q_e^2\ K\ t}{1 + q_e\ K\ t} \quad (3.10)$$

The initial biosorption rate *h* (mg/g.min) at $t = 0$ is expressed as:

$$h = K\, q_e^2 \quad (3.11)$$

where K (g/mg.min) is pseudo second order equilibrium rate constant. The value of K was calculated from the slope of plot of $(\frac{1}{q_t} - \frac{1}{q_e})\ vs.\ \frac{1}{t}$.

(iii) Elovich model

This model is generally applicable for chemisorption kinetics and heterogenous biosorbing surface [246]:

$$\frac{dq_t}{dt} = \alpha\ exp\ (-\beta q_t) \quad (3.12)$$

Eq. (3.12) may be integrated with initial conditions, at $t = 0$, $q_t = 0$ and at $t = t$, $q_t = q_t$. Its integrated equations with the simplification by assuming $\alpha\beta t \gg 1$ are:

Linear equation [139]:

$$q_t = \frac{1}{\beta} ln\ (\alpha\beta) + \frac{1}{\beta} ln\ (t) \quad (3.13)$$

Nonlinear equation [139]:

$$q_t = \frac{1}{\beta}\ ln(\alpha\beta t) \quad (3.14)$$

where α (mg/g.min) represents initial rate of biosorption, β (g/mg) represents desorption constant related with the extent of surface coverage and activation energy for chemisorption. The value of both constants α and β were examined from the linear plot of q_t *vs.* $ln\ t$ and q_t (mg/g) was the amount of metal ions biosorbed at time t (min).

(iv) Bangham model

This model is used to assess whether the biosorption is pore-diffusion controlled. The

equation for this model is given below [234]:

$$\frac{dq_t}{dt} = \frac{k_b\, \alpha_o\, t^{\alpha_o - 1}}{V}(C_i - q_t\, m) \tag{3.15}$$

Eq. (3.15) may be integrated with initial conditions, at $t = 0$, $q_t = 0$ and at $t = t$, $q_t = q_t$. Its integrated equations are:

Linear equation:

$$ln(ln[\frac{C_i}{C_i - q_t\, m}]) = ln[\frac{k_b\, m}{V}] + \alpha_o ln\,(t) \tag{3.16}$$

Nonlinear equation [217]:

$$q_t = \frac{C_i}{m}[1 - \exp\,(-\frac{m\; k_b\; t^{\alpha_o}}{V})] \tag{3.17}$$

where α_o(<1) and k_b (mL/g.L) are constants which were determined from the intercept and slope of the straight line plot of $ln\,(ln\,[\frac{C_i}{C_i - q_t\, m}])$ *vs.* $ln\,(t)$.

(v) Intraparticle diffusion model

In intraparticle diffusion there is a movement of metal ions from liquid phase to the solid phase. According to Weber and Morris theory, equation for this model is given below [215, 245]:

$$q_t = K_{id}\, t^{0.5} + C \tag{3.18}$$

where K_{id} is intraparticle diffusion rate constant (mg/g.min$^{0.5}$), and C is constant. A linear relationship shows by the plot of q_t *vs.* $t^{0.5}$ indicates that the biosorption process involves the intraparticle diffusion. In intraparticle diffusion the uptake is proportional to $t^{0.5}$ instead of time t. The value of K_{id} and C were obtained from the slope and intercept of plot q_t *vs.* $t^{0.5}$, respectively. The value of intercept C is proportional to boundary layer thickness. It implies that larger the intercept

more will be the boundary layer effect. The value of *C* equal to zero shows that the intraparticle diffusion is the rate controlling step.

(vi) Modified Freundlich model

Modified Freundlich model equation for kinetics of biosorption is developed by Kuo and Lotse [234]. This model is expressed as follows:

$$\frac{dq_t}{dt} = \frac{k_3 C_i}{m_1}\ t^{\left(\frac{1-m_1}{m_1}\right)} \tag{3.19}$$

Eq. (3.19) may be integrated with initial conditions, at $t = 0$, $q_t = 0$ and at $t = t$, $q_t = q_t$. Its integrated equations are:

Linear equation:

$$ln\ q_t = lnk_3 C_i + \frac{1}{m_1} ln\ (t) \tag{3.20}$$

Nonlinear equation:

$$q_t = k_3\ C_i\ t^{\left(\frac{1}{m_1}\right)} \tag{3.21}$$

where m_1 is Kuo-Lotse constant, k_3 is uptake rate constant (L/g.min), and *t* is contact time (min). The values of m_1 and k_3 are used to observe the effect of ionic strength and surface loading on biosorption process. A plot of *ln* q_t *vs. ln t* should be linear if the modified Freundlich model fitted to experimental data of metal ions biosorption process.

Parameters of all the kinetic models were evaluated by linear regression analysis by using MS-Excel.

3.2.2 Biosorption isotherm modeling

The equilibrium biosorption isotherm study gives the relationship between biosorbed amount of biosorbate per unit mass of biosorbent q_e (mg/g) at equilibrium and biosorbate concentration in liquid phase at equilibrium C_e (mg/L). It informs about biosorption capacity of biosorbent or amount of biosorbent essential to biosorb a unit mass of biosorbate [168].

3.2.2.1 Isotherms for single metal ions system

For single metal ion system, the experimental data were fitted to six different isotherm models namely Langmuir, Freundlich, Redlich-Peterson, Radke-Prausnitz, Toth, and Fritz. From these isotherms, Langmuir and Freundlich both are two parameter models, Radke-Prausnitz, Toth, and Redlich-Peterson are three parameter models, and Fritz is a four parameter model [169].

(i) Langmuir isotherm

This model based on the assumptions that a single layer of biosorbate is biosorbed above uniform surface of biosorbent at a constant temperature. There is no interaction of biosorbed molecules with vacant sites of biosorbent. Thus, the Langmuir model signifies the equilibrium distribution of metal ions among the solid and liquid phases [80]. All the active sites are energetically same. The Langmuir isotherm model equation as follows:

$$q_e = \frac{q_o b C_e}{1 + b C_e} \tag{3.22}$$

where q_o (mg/g) is the maximum amount of metal ions biosorbed per gram of *S. filipendula* to form a complete single layer on biosorbent surface, b (L/mg) is Langmuir isotherm constant. These constants are associated to monolayer biosorption capacity and biosorption energy, respectively. The value of b indicates the affinity between the biosorbent and biosorbate [140, 294].

(ii) Freundlich isotherm

The Freundlich isotherm is an exponential equation and thus considers that the biosorbate concentration on the surface of biosorbent increases with the increase in biosorbate concentration.

This model is used to define multilayer metal ions biosorption over heterogeneous surface [294]. The expression for this model is given below [44]:

$$q_e = k_f \, C_e^{1/n} \tag{3.23}$$

where n and k_f both are Freundlich constants which signify the intensity of biosorption and uptake capacity, respectively [51]. According to this isotherm, the value of *1/n* must lies between *0* and *1* for good biosorption. If $n = 1$ then the biosorption process is independent of the concentration, $n > 1$ shows a normal and favorable biosorption, and $n < 1$ shows cooperative biosorption [80, 207, 213, 217]. The constraint of this isotherm model is that at high concentration it does not achieve a maximum biosorption and at low concentration it doesn't follow Henry's law [221].

(iii) Redlich-Peterson isotherm

This model comprises the features of both Langmuir and Freundlich isotherm equations [293]. The equilibrium data represents by an empirical equation which is given below [54]:

$$q_e = \frac{K_1 \, C_e}{1 + K_2 C_e^{b_o}} \tag{3.24}$$

where K_1 and K_2 are Redlich-Peterson isotherm constants and b_o is Redlich-Peterson isotherm exponent which lies between *0* and *1*. For $b_o = 1$ this model converts to Langmuir isotherm, and for $K_2 C_e^{b_o} >> 1$, it reduces to Freundlich isotherm, and for $K_2 C_e^{b_o} << 1$ it follows Henry's law. The ratio of $\frac{K_1 \, C_e}{K_2 C_e^{b_o}}$ indicates the biosorption capacity [42].

(iv) Radke-Prausnitz isotherm

Radke-Prausnitz is a modification to Langmuir equation which is given below:

$$q_e = \frac{q_o K_o C_e}{1 + q_o C_e^a} \tag{3.25}$$

where q_o is maximum biosorption capacities (mg/g), a is Radke-Prausnitz model exponent, and K_o is Radke-Prausnitz equilibrium constant. At low concentration, Radke-Prausnitz isotherm reduces to a linear isotherm and at high concentration it changes to Freundlich isotherm [253].

(v) Toth isotherm

Toth isotherm is derived from potential theory and best suited for biosorption of heterogenous systems. This model is a modified form of Langmuir isotherm which reduces the possible error between experimental data and predicted values of equilibrium biosorption data [103]. It obeys Henry's law at low concentration of biosorbate. The empirical equation for this model is given below:

$$q_e = \frac{q_o C_e}{(a_T + C_e)^{1/n_1}} \tag{3.26}$$

where a_T (mg/L) is Toth isotherm constant and n_1 is dimensionless constant generally $n_1 < 1$.

(vi) Fritz isotherm

This model can be used to fit a wide range of experimental data because of large number of coefficients in their equation, and which is given below [159].

$$q_e = \frac{\alpha_1 C_e^{\beta_1}}{1 + \alpha_2 C_e^{\beta_2}} \tag{3.27}$$

where α_1 and α_2 are Fritz isotherm constant, β_1 and β_2 are Fritz equation exponents.

3.2.2.2 Isotherms for dual metal ion system

The presence of other metal ion in solution leads to competition and interference for binding sites of biosorbent due to which mathematical expression for equilibrium becomes more complex [233]. Thus, the multicomponent biosorption isotherm models were studied to define the relationship between uptake of one metal ion and other metal ions present in aqueous solution [193, 280]. The

multicomponent biosorption behavior was explained by fitting of five multicomponent isotherm models (modified and non-modified models). The isotherm parameters of dual metal ions system were obtained by a trial and error method using the solver add in function, Microsoft Excel. The parameters of single metal ion models were used to derive the non-modified model parameters while correction factor was added for modified models [183, 343].

(i) Non-modified Langmuir isotherm

This model uses the biosorption data of single component of Langmuir isotherm to describe the biosorption behavior of multicomponent [174, 193]. This model determine the equilibrium uptake of '*i*' component per unit mass of *S. filipendula* ($q_{e,i}$) in presence of other components. The equation for this model is given below:

$$q_{e,i} = \frac{q_{o,i} b_i C_{e,i}}{1+\sum_{j=1}^{N} b_j C_{e,j}} \tag{3.28}$$

where $C_{e,i}$ is the equilibrium concentration of component '*i*' in a multicomponent system consisting *N* components; b_i and $q_{o,i}$ are the model parameters estimated from single component Langmuir isotherm models.

(ii) Modified Langmuir isotherm

The actual interaction in metal ions of multicomponent system was not defined by single component isotherm model parameters. Thus, to achieve better accuracy modified form of isotherm models with correction factor were used [174]. The modified form of Langmuir model is given below:

$$q_{e,i} = \frac{q_{o,i} b_i (C_{e,i}/\eta_i)}{1+\sum_{j=1}^{N} b_j (C_{e,j}/\eta_j)} \tag{3.29}$$

where b_i and $q_{o,i}$ are derived from single component Langmuir isotherm models; η_i is the correction factor of component '*i*', which depends on other components concentration in the solution. The correction factor value was obtained from the experimental data of multicomponent system.

(iii) Extended Freundlich isotherm

The extended Freundlich isotherm model equations for dual component system are given below [174]:

$$q_{e,1} = \frac{K_{F,1} C_{e,1}^{n_1+x_1}}{C_{e,1}^{x_1} + y_1 C_{e,2}^{z_1}} \tag{3.30}$$

$$q_{e,2} = \frac{K_{F,2} C_{e,2}^{n_2+x_2}}{C_{e,2}^{x_2} + y_2 C_{e,1}^{z_2}} \tag{3.31}$$

where n_1, n_2, $K_{F,1}$, and $K_{F,2}$ are the parameters examined by Freundlich isotherm model for single component and x_1, y_1, z_1, x_2, y_2, and z_2 are the parameters of first and second component which were examined through data of multicomponent biosorption.

(iv) Non-modified Redlich-Peterson isotherm

For multicomponent system, a non-modified Redlich-Peterson model is given by the following equation [15, 275]:

$$q_{e,i} = \frac{K_{1,i} C_{e,i}}{1 + \sum_{j=1}^{N} K_{2,j} C_e^{b_{o,j}}} \tag{3.32}$$

where $K_{1,i}$, $K_{2,j}$, and $b_{o,j}$ are parameters obtained from single component Redlich-Peterson isotherm model.

(v) Modified Redlich-Peterson isotherm

The modified form of Redlich Peterson model was developed by adding interaction term to non-modified Redlich-Peterson model [275]. The equation for this model is given below:

$$q_{e,i} = \frac{K_{1,i} (C_{e,i}/\eta_i)}{1 + \sum_{j=1}^{N} K_{2,j} (C_{e,j}/\eta_j)^{b_{o,j}}} \tag{3.33}$$

where $K_{1,i}$, $K_{2,j}$, and $b_{o,j}$ are parameters obtained from single component Redlich-Peterson isotherm model; η_i is the correction factor of component '*i*'.

3.2.3 Statistical modeling for optimization

A standard response surface methodology (RSM) design known as central composite design (CCD) was used to study the parameters of metal ion biosorption [6, 319, 351]. RSM is a mathematical and statistical tool which determines the independent and interaction effects of different process parameters and optimizes the operational conditions for desired results with less number of experiments [46, 147, 148, 321]. The RSM involves the following two steps (i) model formulation to examine which parameters and their interactions influence the response (ii) optimization of process parameters that affects the performance of the response [8, 222, 303]. The correlation between the parameters and response were examined by using central composite design (CCD) under RSM of Design Expert Software (version 10) Stat Ease Inc. USA. The CCD design was selected in this study as it is flexible, robust and efficient [20, 34].

A second order polynomial equation which was used to fit the experimental data is given below:

$$Y = \beta_o + \sum_{i=1}^{k} \beta_i x_i + \sum_{i=1}^{k} \beta_{ii} {x_i}^2 + \sum_{i=1}^{k} \sum_{j>i}^{k} \beta_{ij} \; x_i x_j \qquad (3.34)$$

where Y is predicted response (dependent), β_0 is constant coefficient, x_i and x_j are variables, β_i, β_{ii} and β_{ij} are interaction coefficients for linear, quadratic, and second order terms, respectively. In this study, four factors considered were pH, biosorbent dosage, initial metal ion concentration, and temperature. According to CCD, 30 runs were obtained in order to investigate the effect of four variables [219]. This experimental design consist of 16 factorial points, 8 axial points and 6 center points which can be calculated by using the given equation:

$$N = 2^k + 2k + N_o \qquad (3.35)$$

where k is number of variables, 2^k are factorial points, $2k$ are axial points and N_o is number of experiments carried out at the center. All the runs were performed in duplicate.

3.2.4 Thermodynamic modeling

The spontaneity of biosorption process was examined by thermodynamic parameters like Gibb's free energy change ($\Delta G°$), enthalpy change ($\Delta H°$), and entropy change ($\Delta S°$) [288, 296, 323]. The amount of metal ions biosorbed at different temperatures (298, 303, 308, and 313 K) were calculated to find thermodynamic parameters for the biosorption system.

$$M^{2+} + biosorbent \leftrightarrow M - biosorbent \tag{3.36}$$

Thermodynamic constants were evaluated by the following equations:

$$\Delta G° = - RT \ln K \tag{3.37}$$

$$\Delta G° = \Delta H° - T \Delta S° \tag{3.38}$$

where K is equilibrium constant, calculated as ratio of equilibrium metal concentration on the biosorbent surface C_a and in the solution C_e ($K = C_a / C_e$), R is universal gas constant (8.314×10^{-3} kJ/mol.K) and T is temperature in Kelvin. The value of $\Delta H°$ and $\Delta S°$ were calculated from intercept and slope of a plot of ΔG^o *vs.* T. The scale of the $\Delta H°$ value gives information about the type of biosorption, which can be either chemical or physical. The heat of biosorption, varying from 0.5 to 5 kcal/mol (2.1-20.9 kJ/mol), indicates physical biosorption, and the activation energy for chemical biosorption is of the same level as the heat of chemical reactions, 5-100 kcal/mol (20.9-418.4 kJ/mol) [146]. The negative value of ΔG^o shows the feasibility and spontaneous nature of biosorption process which does not require any external source of energy for the system [23, 47, 181]. The increase in biosorption with temperature can be either due to increase in the number of metal binding sites which are accessible for biosorption on surface of biosorbent or due to decrease in boundary layer thickness surrounding the biosorbent, which in turn reduces the mass transfer resistance of biosorbate [72]. The positive values of $\Delta S°$ indicate the enhancement in randomness of biosorbed species at solid and liquid interface with progress of biosorption. While the negative value of $\Delta S°$ indicates a decrease in randomness at solid/liquid interface. The negative values of $\Delta H°$ indicates the exothermic nature of the biosorption and its magnitude describe the type of biosorption, which can be either chemical or physical [257].

3.2.5 Model validation

For single component system the level of accuracy and adequacy of different isotherm models fitting with the biosorption experimental data, were examined by using the statistical formulae which are given below [174]:

$$B_F = 10^{(\sum log_{10}(q_{e,cal}/q_{e,exp})/N)} \quad (3.39)$$

$$\textit{Root mean square error (RMSE)} = \sqrt{\frac{(q_{e,exp} - q_{e,cal})^2}{N}} \quad (3.40)$$

$$\textit{Normalized standard deviation (NSD)} = 100\sqrt{\frac{\sum[(q_{e,exp} - q_{e,cal}/q_{e,exp}]^2}{N}} \quad (3.41)$$

where $q_{e,exp}$ is experimental value of q_e, $q_{e,cal}$ is the predicted value of q_e obtained by models, N represents the total data points.

For multicomponent system, the best fitted isotherm model was evaluated by using the following statistical formula, Average Relative Error (ARE) [12, 169, 174]:

$$ARE = \sqrt{\sum_{i=1}^{N}(1 - \frac{q_{e,i,cal}}{q_{e,i,exp}})^2} \cdot \frac{100}{N} \quad (3.42)$$

where, $q_{e,i,exp}$ is the equilibrium experimental uptake value of component '*i*', $q_{e,i,cal}$ is the predicted uptake value of component '*i*' obtained by model, and N represents the total experimental data points. The smaller value of statistical indices indicates the more precise estimation.

3.3 CONCLUSIONS

The materials and instruments which were used for this research work were given. The experimental methodology to examine the removal efficiency of metal ions and biosorption capacity of *S. filipendula* in single and dual metal ion systems was explained. The modeling of kinetic, isotherm and thermodynamic was done to find out the biosorption mechanism. Besides this computation techniques were explained to optimize the biosorption process conditions.

CHAPTER IV

BIOSORPTION OF Pb^{2+}, Cd^{2+}, Ni^{2+} IONS FROM SINGLE METAL ION SYSTEM

4.0 INTRODUCTION

In this Chapter, the ability of dead marine algae *S. filipendula* for the removal of Pb^{2+}, Cd^{2+}, and Ni^{2+} ions from aqueous solution is demonstrated. The batch experiments were planned to be conducted according to design of experiments using Response Surface Methodology (RSM). The effect of temperature, pH, initial metal ions concentration and biosorbent dosage were examined. The isotherm models were fitted to experimental data in order to examine the nature of biosorption. The mechanism of Pb^{2+}, Cd^{2+}, and Ni^{2+} ions biosorption, were investigated by fitting the experimental data to available kinetic models. Thermodynamic study was carried out to judge the feasibility of the process. Desorption study was also done to ascertain the regeneration and reuse capacity of *S. filipendula*.

4.1 REMOVAL OF Pb^{2+} IONS FROM AQUEOUS SOLUTION USING *S. FILIPENDULA*

This section explains the results of biosorbent characterization, experimental design, analysis of Pb^{2+} ions biosorption experimental data and optimization of Pb^{2+} ions biosorption process parameters. Besides this kinetic, equilibrium, thermodynamic and desorption study for Pb^{2+} ions biosorption are also described in this section.

4.1.1 Characterization of *S. filipendula*

4.1.1.1 FESEM - EDS analysis

Fig. 4.1 (a) shows rough surface *S. filipendula* before biosorption. **Fig. 4.1 (b)** shows that after biosorption of Pb^{2+} ions the pores and surface of *S. filipendula* were covered and the surface became smooth. It was evident that the structure of *S. filipendula* has changed after biosorption.

EDS analysis of biosorbent before and after biosorption of Pb^{2+} ions confirms this observation as shown in **Fig. 4.2 (a & b)**. A peak of Pb^{2+} ions were noticed when *S. filipendula* samples were exposed to $Pb(NO_3)_2$ solution. Some of the cations initially present on cell wall matrix were replaced with Pb^{2+} ions and created a strong cross linkage. EDS image shows that the main component of *S. filipendula* cell wall was C (Carbon) along with small amounts of Mg, Na, S, Ca, and K.

4.1.1.2 FTIR analysis

The FTIR study was carried out to detect the functional groups present on the biosorbent surface and their interaction with metal ions [292]. **Fig. 4.3** shows the peaks corresponding to functional groups of *S. filipendula* biomass before and after biosorption of Pb^{2+} ions. **Table 4.1** shows the change in vibrational frequency of *S. filipendula* functional groups after Pb^{2+} ions biosorption.

Table 4.1 IR vibration wavenumber and functional groups observed on untreated and Pb^{2+} ions treated *S. filipendula* biomass

Wavenumber (cm^{-1})		Functional groups
Unloaded biomass	Metal ion loaded biomass	
3407.9	3407.15	-OH stretching
-	3140.54	-OH stretching
2925.35	2924.43	-CH & -OH stretching
1633.89	1628.96	-C=C stretching
1426.39	1417.63	C-H stretching & -C=C bending
1245.13	1250.9	C-O stretching
1048.13	1049.47	C-O stretching
606.88	622.57	C-Cl stretching

(a)

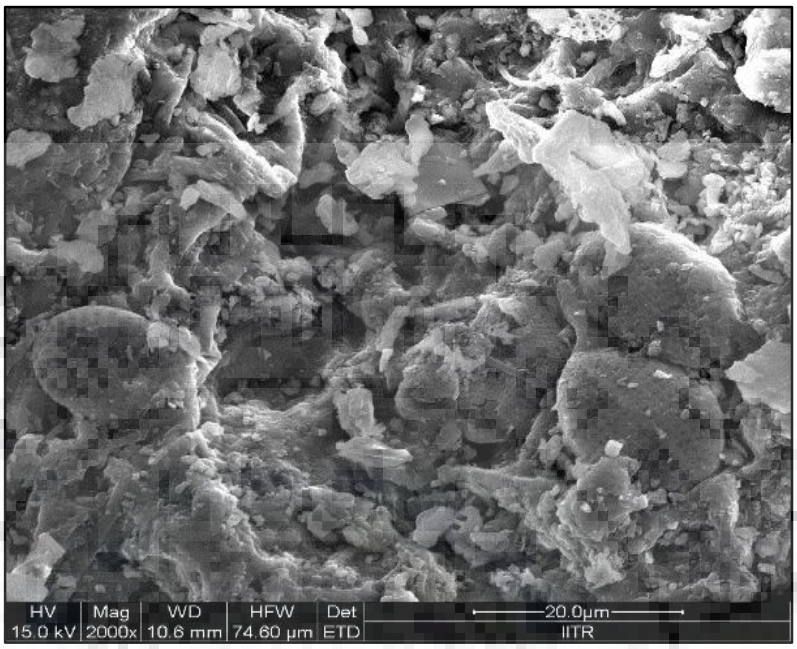

(b)

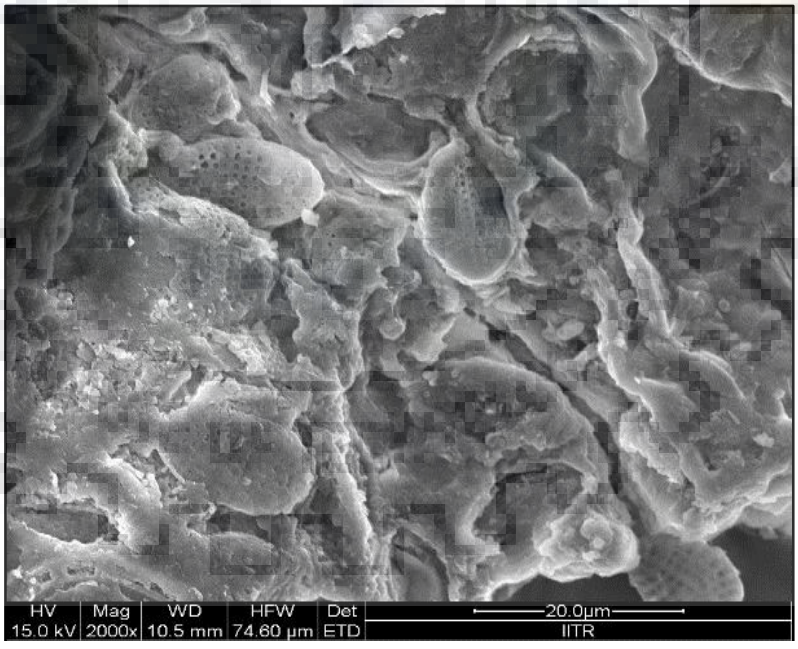

Fig. 4.1 FESEM images for Pb^{2+} ions biosorption on *S. filipendula* (a) before biosorption (b) after biosorption.

(a)

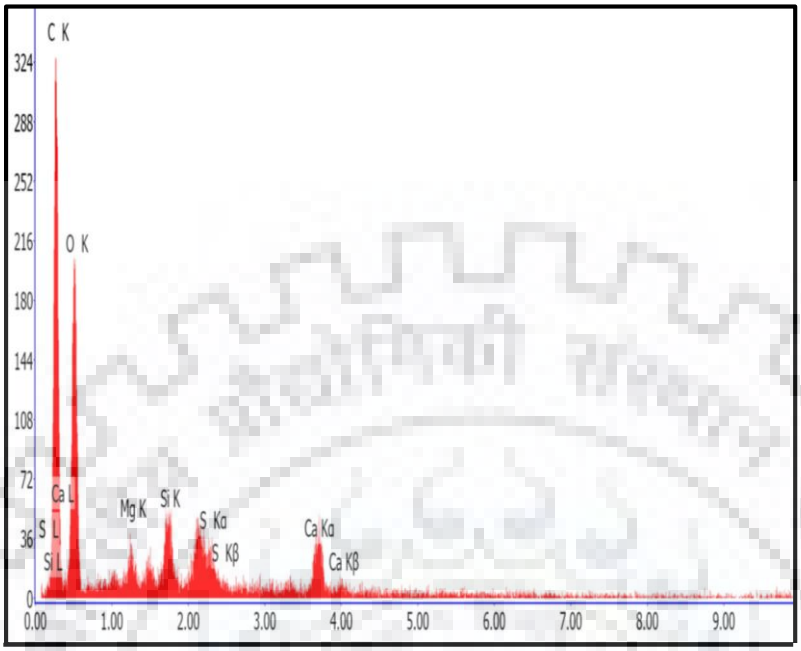

(b)

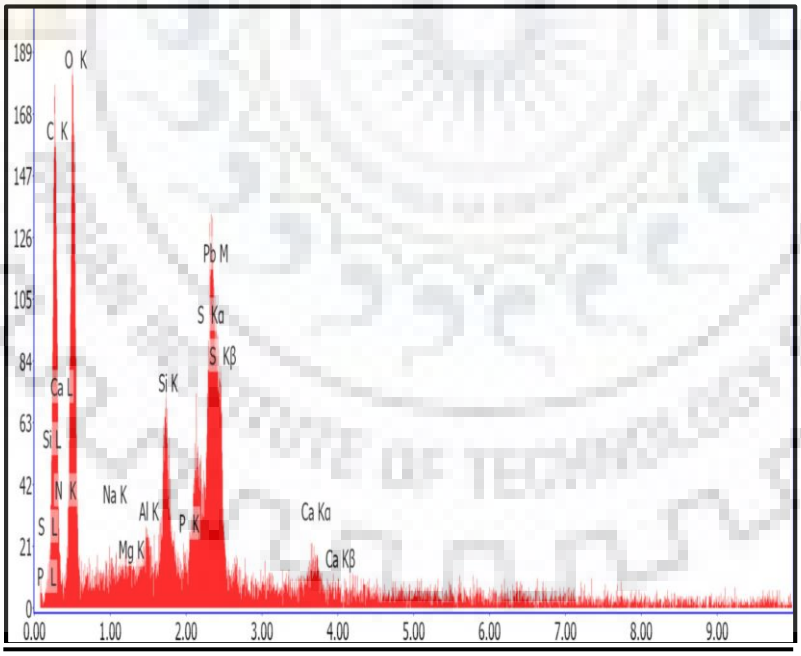

Fig. 4.2 EDS images for Pb^{2+} ions biosorption on *S. filipendula* (a) before biosorption (b) after biosorption.

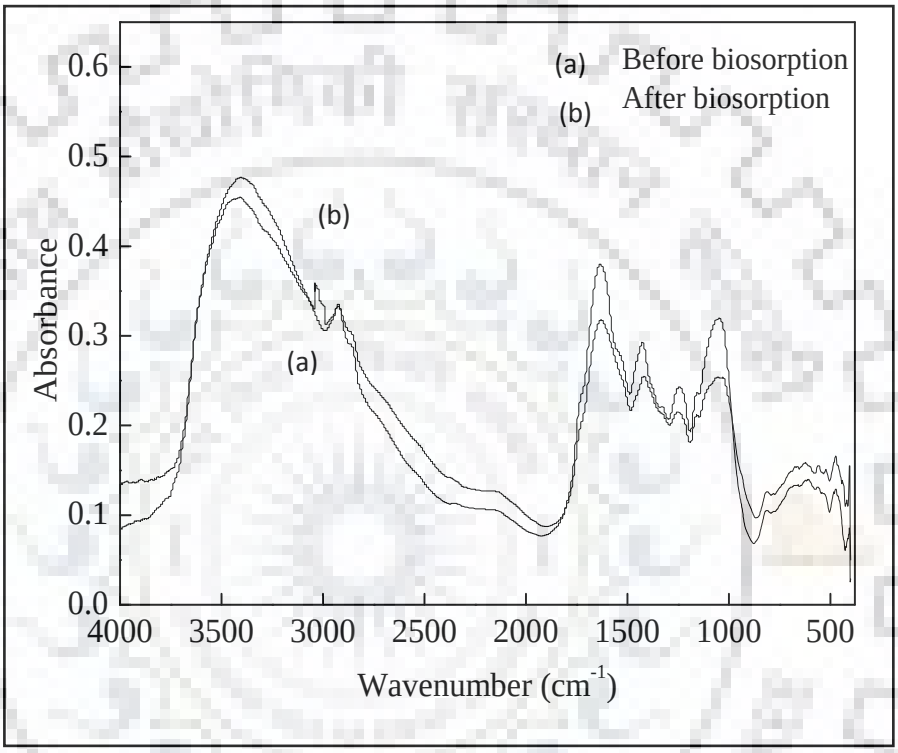

Fig. 4.3 FTIR image of *S. filipendula* surface before and after biosorption of Pb^{2+} ions.

The biosorption peak at 3407.9 cm^{-1} corresponds to stretching of –OH group shifted to 3405.9 cm^{-1}, 2925.35 cm^{-1} corresponds to stretching of –OH group and C-H group shifted to 2924.3 cm^{-1}, 1633.89 cm^{-1} corresponds to stretching of –C=C group shifted to 1628.96 cm^{-1}, 1426.39 cm^{-1} corresponds to C-H group stretching and –C=C group bending shifted to 1417.63 cm^{-1} and 606.88 cm^{-1} corresponds to –C-Cl group shifted to 622.57 cm^{-1}. The peaks at 1245.13 cm^{-1} and 1048.13 cm^{-1} corresponds to C-O groups stretching are shifted to 1250.90 cm^{-1} and 1049.47 cm^{-1}. The new peak at 3140.54 cm^{-1} corresponds to –OH group stretching appears. The change in vibrational frequency of functional groups after biosorption of Pb^{2+} ions shows that these groups were involved in biosorption process [145, 245].

4.1.2 Analysis of results of experiments

In this study, experimentation was designed by Central Composite Design (CCD) of Response Surface Methodology (RSM). The selection and development of proper models to analyze the results was carried out by using statistical software, Design-Expert 6.8. By using this software, the regression equations on the basis of coded and actual values of input parameters for the process performances were obtained. The responses were plotted against the process inputs to study the effects of process input parameters on the measures of process performance. The ANOVA (Analysis of Variance) has been carried out to analyze the results with the help of this software [98]. Finally optimization was performed to find out the optimum value of process inputs for confirmation experiments.

4.1.2.1 Experimental design and factorial model for Pb^{2+} ions biosorption process

In the experimental design, the selected range and level of variables were selected on the basis of literature reported for Pb^{2+} ions biosorption by other brown algae. The optimized conditions of higher biosorption efficiency for Pb^{2+} ions were analyzed by using CCD under RSM. The matrix of four variables pH, initial Pb^{2+} ions concentration, biosorbent dosage, and temperature were varied at 5 levels ($-\alpha$, -1, 0, +1, $+\alpha$) as shown in **Table 4.2**. The higher and lower levels of variables were symbolized as '+' and '-', respectively. Removal efficiency (%) of Pb^{2+} ions obtained from the experiments at the end of equilibrium time for each experiment is presented in **Table 4.3**.

Table 4.2 Range and level of the independent variables for Pb^{2+} ions biosorption

Independent variables	Range and levels (coded)			
	-α	**-1**	**0**	**+1**
Temperature, °C (A)	20	25	30	35
Initial Pb^{2+} ions concentration, mg/L (B)	75	150	225	300
Biosorbent dosage, g/L (C)	0.05	0.2	0.35	0.5
pH (D)	2	3	4	5

The mathematical expression of relationship of four independent variables with response is given as:

$$Y = +53.21 + 6.15\,A - 11.98\,B + 15.54\,C + 5.83\,D + 0.29\,AB + 1.42\,AC - 0.82\,AD - 3.23\,BC - 1.26\,BD + 1.78\,CD - 0.92\,A^2 + 2.69\,B^2 - 1.23\,C^2 - 3.06\,D^2 \quad (4.1)$$

where Y is percent removal of Pb^{2+} ions and A, B, C and D were coded values of temperature (°C), initial Pb^{2+} ions concentration (mg/L), biosorbent dosage (g/L), and pH, respectively. A^2, B^2, C^2 and D^2 were the measure of main effect of variables such as temperature (°C), initial Pb^{2+} ions concentration (mg/L), biosorbent dosage (g/L), and pH, respectively. Whereas, AB, BC, CD and AD represent interaction effect of temperature and initial Pb^{2+} ions concentration, initial Pb^{2+} ions concentration and biosorbent dosage, biosorbent dosage and pH, temperature and pH, respectively. The six runs were replicated for central point.

The statistical significance and interaction of factors were determined by ANOVA. Regression coefficient and analysis of variance for second-order polynomial models are given in **Table 4.4**. The *p-value* ($P < 0.0001$) and *F-value* (53.94) showed that the model was significant. The "Lack of fit *F-value*" of 21.36 shows that Lack of fit was significant. A low value of coefficient of variance (CV) 7.73 indicates that the deviation between experimental and predicted values was low. The goodness of fit of the model was tested by coefficient of determination (R^2). The R^2 value close to 1.0 showed that the model was more significant. For this model R^2 value was

Table 4.3 Experimental design based on CCD and its response for Pb^{2+} ions removal

Run	Temperature (°C)	Initial Pb^{2+} ions concentration (mg/L)	Biosorbent dosage (g/L)	pH	Removal (%)	
					Experimental	Predicted
1	25	150	0.2	3	33.98	33.33
2	35	150	0.2	3	41.64	43.85
3	25	300	0.2	3	16.48	17.78
4	35	300	0.2	3	34.9	29.46
5	25	150	0.5	3	61.84	64.47
6	35	150	0.5	3	78.56	80.65
7	25	300	0.5	3	33.67	36.00
8	35	300	0.5	3	54.17	53.33
9	25	150	0.2	5	42.68	45.58
10	35	150	0.2	5	57.33	52.83
11	25	300	0.2	5	29.26	25.00
12	35	300	0.2	5	33.97	33.40
13	25	150	0.5	5	80.59	83.85
14	35	150	0.5	5	96.50	96.76
15	35	300	0.5	5	50.49	50.34
16	35	300	0.5	5	65.94	64.41
17	20	225	0.35	4	40.96	37.22
18	40	225	0.35	4	57.95	61.80
19	30	75	0.35	4	92.34	87.93
20	30	375	0.35	4	35.50	40.03
21	30	225	0.05	4	12.78	17.23
22	30	225	0.65	4	83.71	79.38
23	30	225	0.35	2	31.18	29.31
24	30	225	0.35	6	50.64	52.63
25	30	225	0.35	4	53.53	53.21
26	30	225	0.35	4	51.53	53.21
27	30	225	0.35	4	54.53	53.21
28	30	225	0.35	4	53.59	53.21
29	30	225	0.35	4	52.53	53.21
30	30	225	0.35	4	53.53	53.21

Table 4.4 ANOVA results for response surface quadratic model of Pb^{2+} ions biosorption

Source	Sum of square	df	Mean square	*F value*	*p-value*	Remarks
Model	11832.02	14	845.14	53.94	<0.0001	Significant
A	906.51	1	906.51	57.86	<0.0001	Significant
B	3442.09	1	3442.09	219.69	<0.0001	Significant
C	5793.31	1	5793.31	369.76	<0.0001	Significant
D	815.97	1	815.97	52.08	<0.0001	Significant
AB	1.35	1	1.35	0.086	0.7735	Not significant
AC	32.04	1	32.04	2.04	0.1732	Not significant
AD	10.69	1	10.69	0.68	0.4217	Not significant
BC	167.06	1	167.06	10.66	0.0052	Significant
BD	25.35	1	25.35	1.62	0.2227	Not significant
CD	50.91	1	50.91	3.25	0.0916	Not significant
A^2	23.39	1	23.39	1.49	0.2406	Not significant
B^2	198.88	1	198.88	12.69	0.0028	Significant
C^2	41.23	1	41.23	2.63	0.1256	Not significant
D^2	256.8	1	256.8	16.39	0.0011	Significant
Residual	235.02	15	15.67	-	-	-
Lack of fit	229.64	10	22.96	21.36	0.0017	Significant
Pure error	5.38	5	1.08	-	-	-
Total	12067.03	29	-	-	-	-
R^2 = 0.9805; *Adjusted* R^2 = 0.9623; *Predicted* R^2 = 0.8897; *Adequate precision* = 28.415						

found to be 0.98 which shows that more than 98 % of the experimental data were compatible with predicted data. The value of *predicted* R^2 (0.88) was in reasonable agreement with *adjusted* R^2 value (0.96). *Adequate precision* measures the ratio of signal to noise. A ratio greater than 4 was desirable [157]. In this work, the ratio was 28.41 which indicate an adequate signal. The value of *Prob.>F* less than 0.050 indicates that the model terms are significant. Here, for biosorption of Pb^{2+} ions A, B, C, D, B^2, D^2 and BC were significant model terms. The *p-value* greater than 0.10 shows that model terms A^2, C^2, AB, AC, AD and BD were not significant. **Fig. 4.4** shows that the predicted response values of reduced quadratic model were well in agreement with actual ones in the range of operating variables. The 3D graphs for Pb^{2+} ions removal efficiency are presented in **Fig. 4.5 (a-c)**.

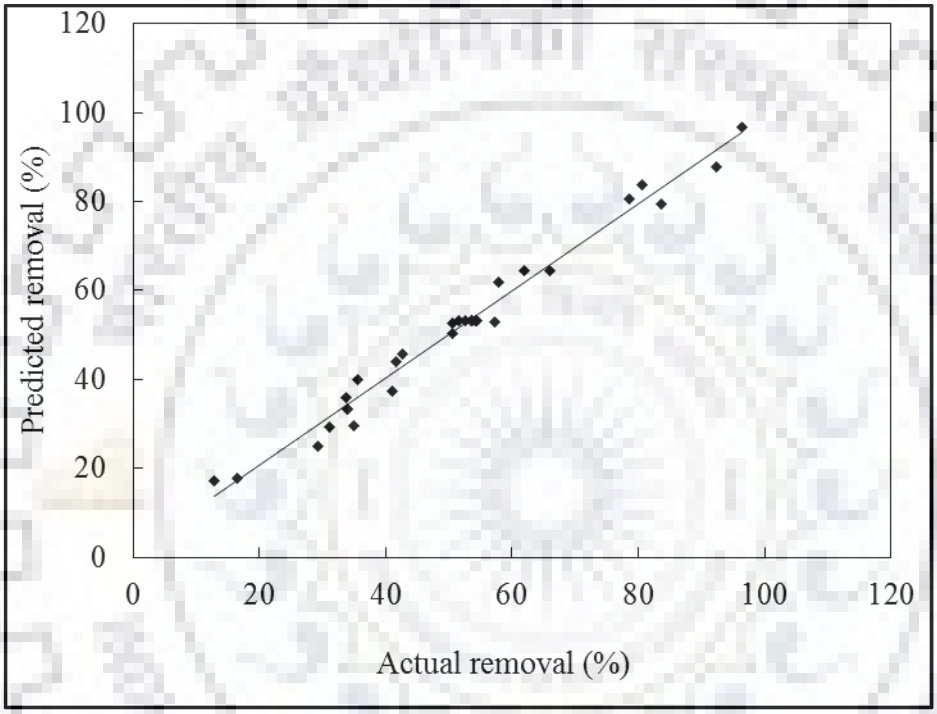

Fig. 4.4 Correlation of actual versus predicted removal of Pb^{+2} ions by *S. filipendula*.

4.1.2.2 Variation of process parameters on maximum Pb^{2+} ions removal efficiency

(i) Effect of contact time

It was noticed experimentally that initially biosorption rate was very high and 80 % removal efficiency has been achieved within initial 15 min. Thereafter, the biosorption rate was gradually decreased with time until it reaches the equilibrium (**Fig. 4.6**). It was due to the fact that initially large surface area of biosorbent was available for biosorption of metal ions but after a certain time period accessibility of active sites on biosorbent surface decreases which slows down the rate of biosorption [81]. The equilibrium time for Pb^{2+} ions biosorption onto *S. filipendula* was 85 min at which 96.54 % removal efficiency of Pb^{2+} ions was achieved.

(ii) Effect of pH

The pH of the solution plays a significant role in the protonation of functional group present on biosorbent surface. **Fig. 4.5 (a)** illustrates the effect of pH on removal efficiency of Pb^{2+} ions. It was noticed that removal efficiency of Pb^{2+} ions increases with the increase in pH from 3.0 to 5.0. At low pH, the biomass surface becomes positively charged due to which repulsion for binding of metal ions occurs [320, 349]. With rise in pH of the solution, the concentration of H^+ ions decreases and negatively charged ligands like phosphate, and carboxyl present on biomass surface was exposed because of deprotonation of metal binding sites which can interact with positively charged metal ions. At pH greater than 5.0, precipitation of Pb^{2+} ions occurs as lead hydroxides [349].

(iii) Effect of biosorbent dosage

The biosorbent dosage has a great impact on biosorption process at a specified initial metal ions concentration. The effect of biomass dosage on removal efficiency of Pb^{2+} ions was studied by changing biosorbent dosage from 0.2 to 0.5 g/L and the results are presented in **Fig. 4.5 (a)**. It was observed that Pb^{2+} ions removal efficiency increases with increase in dosage of *S. filipendula*. This trend was due to the availability of more active sites available on *S. filipendula* surface [112, 263, 339].

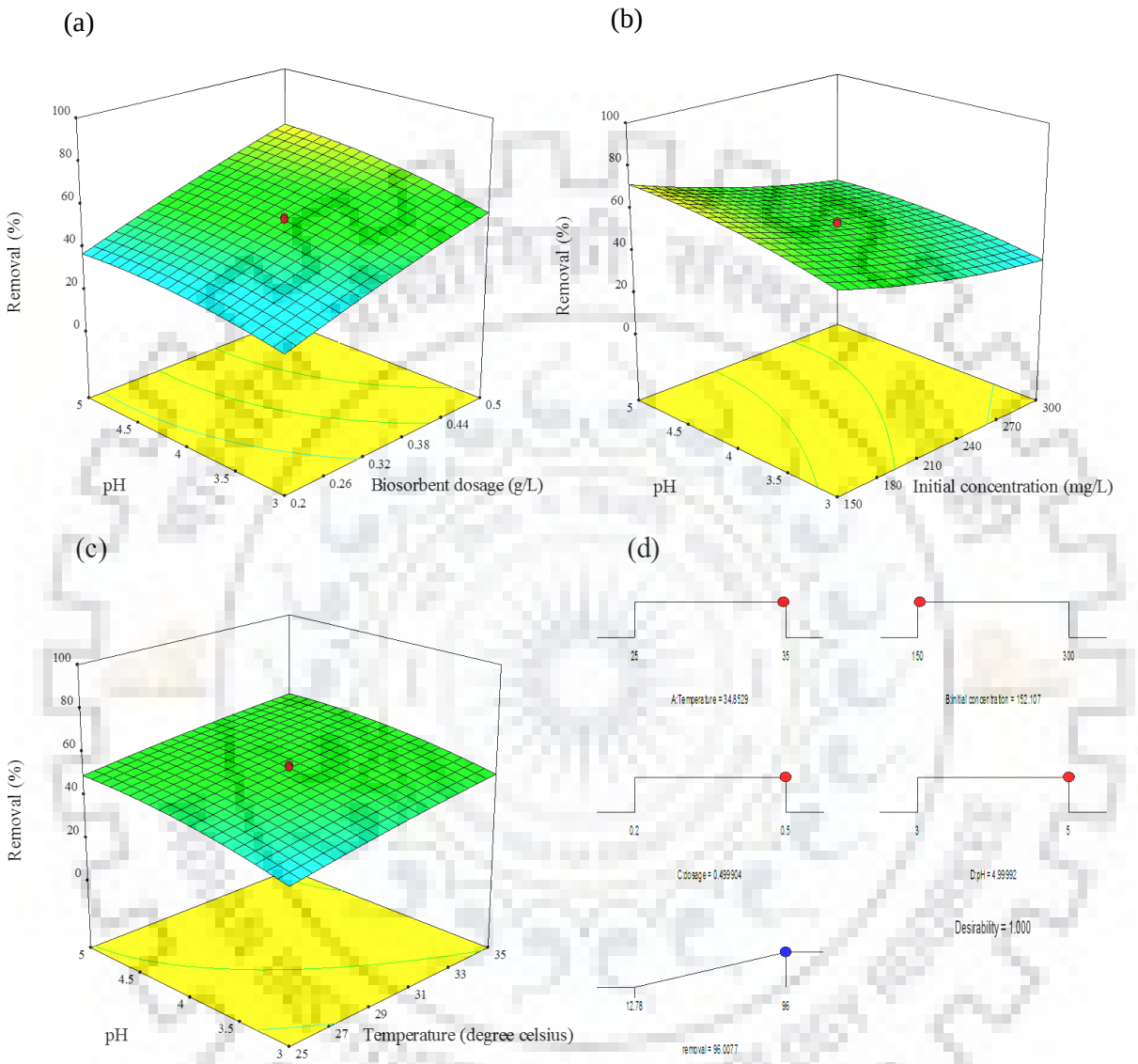

Fig. 4.5 (a) Interactive effect of pH and biosorbent dosage (b) Interactive effect of pH and initial concentration of Pb^{2+} ions (c) Interactive effect of pH and temperature (d) Desirability ramp for numerical optimization of four independent variables and the responses.

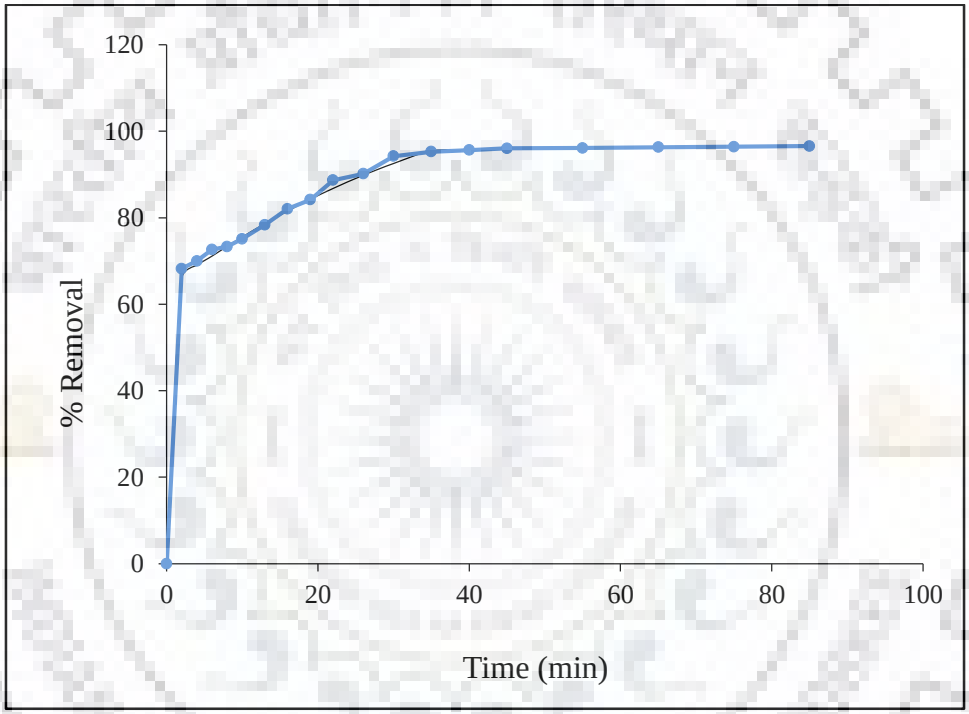

Fig. 4.6 Effect of contact time on biosorption of Pb^{2+} ions by *S. filipendula* (pH 5.0, temperature 35 ^{o}C, biosorbent dosage of 0.5 g/L, initial Pb^{2+} ions concentration 150 mg/L).

(iv) Effect of initial Pb^{2+} ions concentration

The effect of initial Pb^{2+} ions concentration on removal efficiency of Pb^{2+} ions was studied in the range 150-300 mg/L. The results are shown in **Fig. 4.5 (b)**. The removal efficiency of Pb^{2+} ions decreases on increasing the initial Pb^{2+} ions concentration. It could be possible that all the biosorbents have certain number of active binding sites which were accessible for binding of metal ions at low initial concentration while at high initial concentration the binding sites become saturated [308].

(v) Effect of temperature

Fig. 4.5 (c) illustrates the effect of temperature on Pb^{2+} ions removal efficiency. It was noticed that there was an increase in removal efficiency of Pb^{2+} ions with rise in temperature from 25-35 °C indicating that the reaction for Pb^{2+} ions biosorption was endothermic in nature [10]. On increasing temperature, the thickness of layer that surrounds the biosorbent decreases. This results in the decrease of external layer resistance. Micro-pores become widen and deepen which provide more surface area for biosorption and the increased availability of active sites in the biosorbent [135].

4.1.3 Optimization using the desirability function

To obtain the maximum point for desirability function, numerical optimization was done by fixing the values of reaction parameters within their ranges and maximizing the removal efficiency of Pb^{2+} ions [68]. It can be seen in **Fig. 4.5 (d)**, that the best local maximum value was noticed at initial solution pH of 4.99, temperature of 34.85 °C, initial Pb^{2+} ion concentration of 152.10 mg/L, and biosorbent dosage of 0.5 g/L. In this condition, Pb^{2+} ions removal efficiency and the desirability value were found to be 96.0 % and 1.0, respectively. This optimum condition was tested experimentally and results revealed that removal efficiency was 96.5 %. The high degree of agreement between the predicted optimum conditions and repeated experimental results shows that RSM can be used as an efficient and reliable tool to evaluate and optimize the effects of biosorption parameters on Pb^{2+} ions removal efficiency using *S. filipendula*.

4.1.4 Kinetic study

The experiments for kinetic study of Pb^{2+} ions biosorption on *S. filipendula* were performed at 35 °C by using five different initial Pb^{2+} ions concentrations: 100, 150, 200, 250, and 300 mg/L. In each flask, a fixed amount of biosorbent (0.5 g/L) was added in solution of pH 5.0. The values of parameters, R^2 and Δq % for all the kinetic models were evaluated and given in **Table 4.5** (values for Pseudo first order and Pseudo second order have not been mentioned as their R^2 values were very much lower). The R^2 values for Bangham, Elovich, Modified Freundlich, and Intra particle diffusion models were greater than 0.90 while the value of normalized standard deviation (Δq %) was low (1.36) in case of Bangham model in comparison to other kinetic models (**Table 4.5**). According to these results, it can be concluded that Bangham model gives a good correlation for Pb^{2+} ions biosorption on *S. filipendula*. **Fig. 4.7** shows the graphical representation of all the kinetic models for Pb^{2+} ions biosorption on *S. filipendula* at different initial Pb^{2+} ions concentrations.

4.1.5 Equilibrium study

In order to determine Pb^{2+} ions biosorption isotherms at different temperatures, experiments were performed at four different temperatures (20, 25, 30 and 35 °C) by varying initial Pb^{2+} ions concentration from 100 to 300 mg/L with constant biosorbent dosage of 0.5 g/L. The value of parameters for each isotherm model with their correlation coefficient (R^2) and normalized standard deviation (Δq %) are shown in **Table 4.6. Fig. 4.8** shows the comparison of different isotherm models with experimental results. The shape of isotherm models can be used to find out favorable biosorption system. For Fritz model, the value of R^2 was greater than 0.99 and Δq % was very small for all the temperatures. This shows that Fritz model was the best fitted isotherm model for Pb^{2+} ions biosorption on *S. filipendula.*

4.1.6 Thermodynamic study

The nature of biosorption process and feasibility, were assessed by thermodynamic study. From **Fig. 4.9** the values of ΔH^o (128.34 kJ/mol) and ΔS^o (0.443 J/mol.K) were evaluated from intercept and slope of a plot of ΔG^o vs. *T*. The positive value of ΔH^o indicates endothermic nature

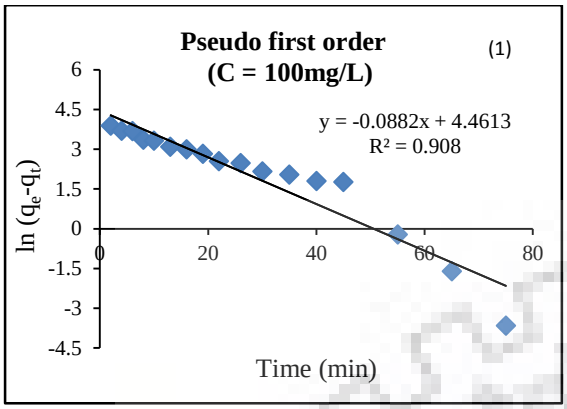
Pseudo first order
(C = 100mg/L)
(1)
y = -0.0882x + 4.4613
R² = 0.908
ln (qe-qt)
Time (min)

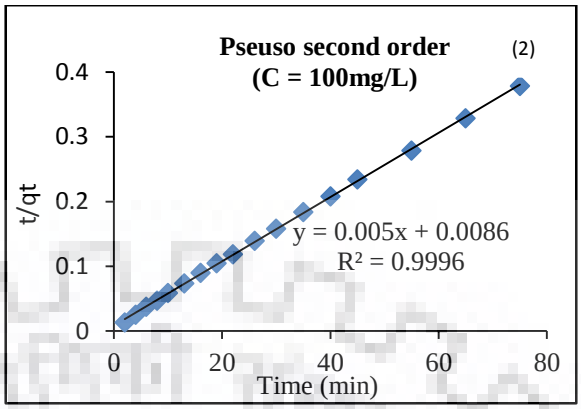
Pseuso second order
(C = 100mg/L)
(2)
y = 0.005x + 0.0086
R² = 0.9996
t/qt
Time (min)

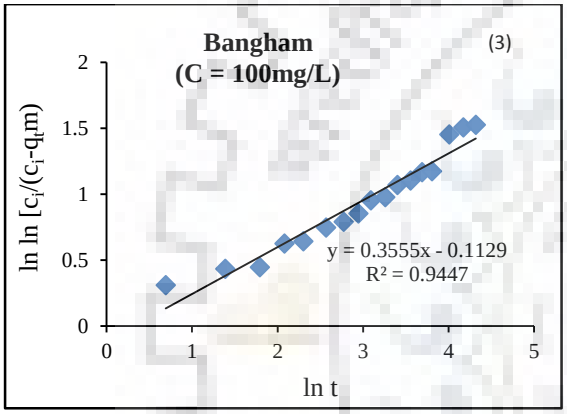
Bangham
(C = 100mg/L)
(3)
y = 0.3555x - 0.1129
R² = 0.9447
ln ln [Ci/(Ci-qtm)
ln t

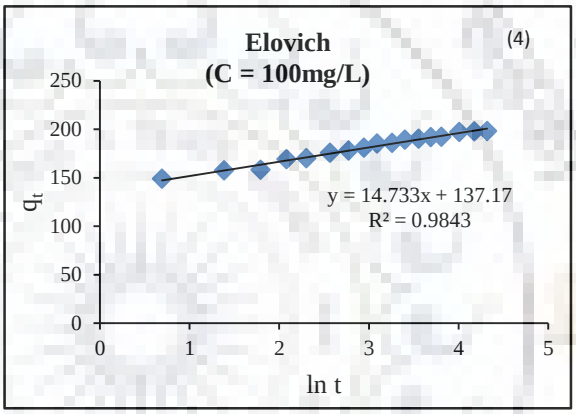
Elovich
(C = 100mg/L)
(4)
y = 14.733x + 137.17
R² = 0.9843
qt
ln t

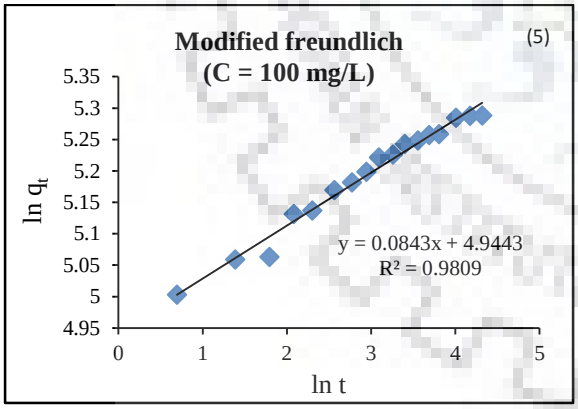
Modified freundlich
(C = 100 mg/L)
(5)
y = 0.0843x + 4.9443
R² = 0.9809
ln qt
ln t

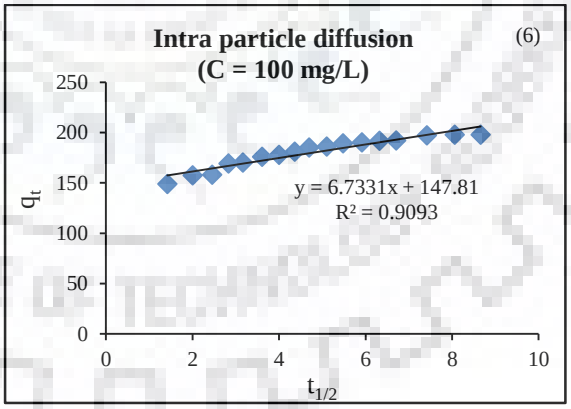
Intra particle diffusion
(C = 100 mg/L)
(6)
y = 6.7331x + 147.81
R² = 0.9093
qt
t1/2

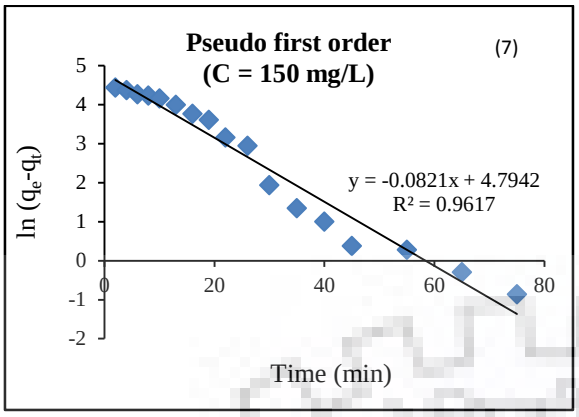
Pseudo first order
(C = 150 mg/L)
(7)
ln (qe-qt)
y = -0.0821x + 4.7942
R² = 0.9617
Time (min)

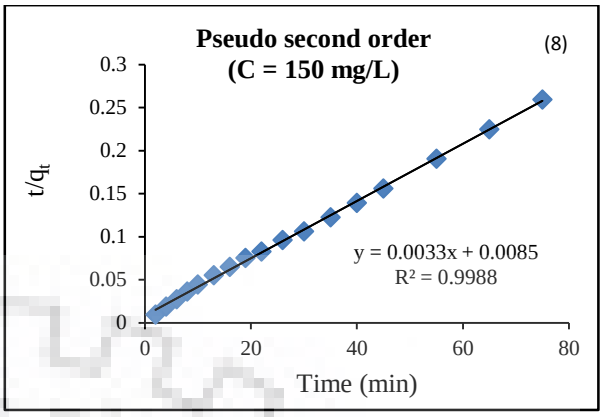
Pseudo second order
(C = 150 mg/L)
(8)
t/qt
y = 0.0033x + 0.0085
R² = 0.9988
Time (min)

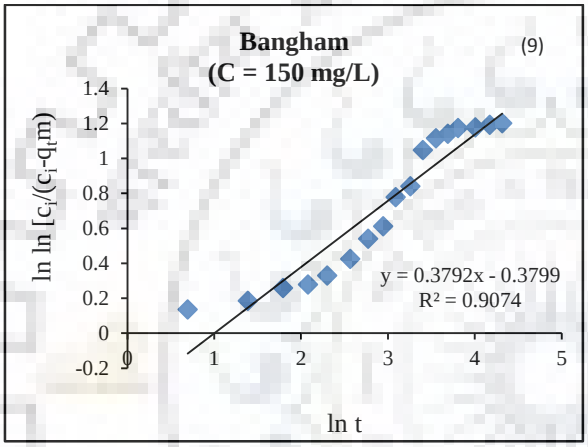
Bangham
(C = 150 mg/L)
(9)
ln ln [Ci/(Ci-qtm)]
y = 0.3792x - 0.3799
R² = 0.9074
ln t

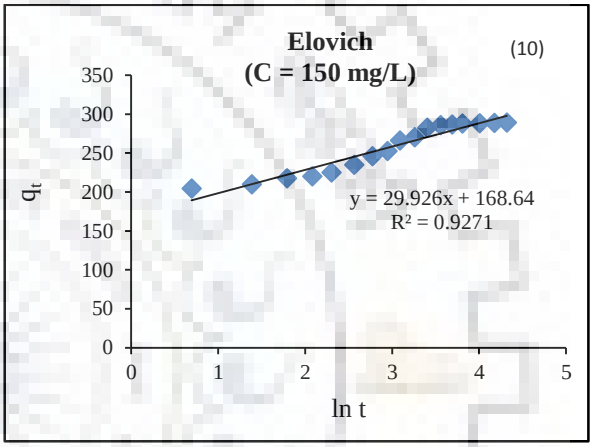
Elovich
(C = 150 mg/L)
(10)
qt
y = 29.926x + 168.64
R² = 0.9271
ln t

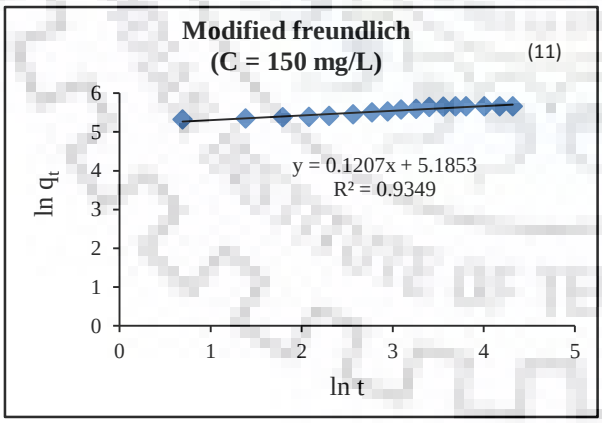
Modified freundlich
(C = 150 mg/L)
(11)
ln qt
y = 0.1207x + 5.1853
R² = 0.9349
ln t

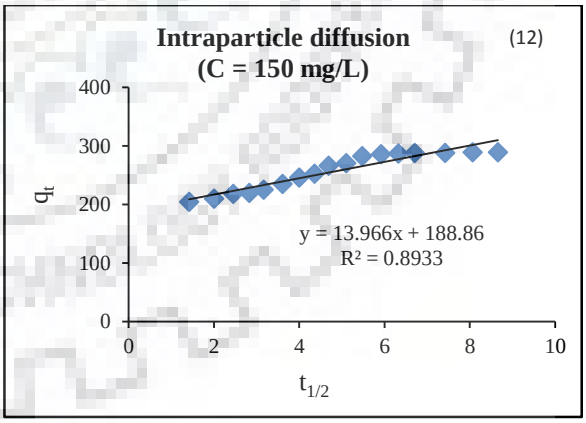
Intraparticle diffusion
(C = 150 mg/L)
(12)
qt
y = 13.966x + 188.86
R² = 0.8933
t1/2

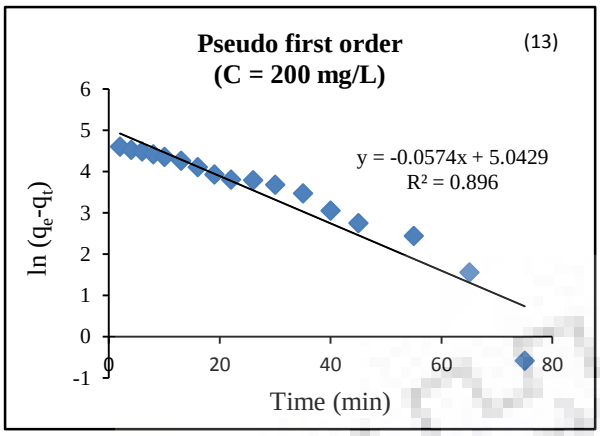
Pseudo first order
(C = 200 mg/L)
(13)
y = -0.0574x + 5.0429
R² = 0.896
ln (qe-qt)
Time (min)

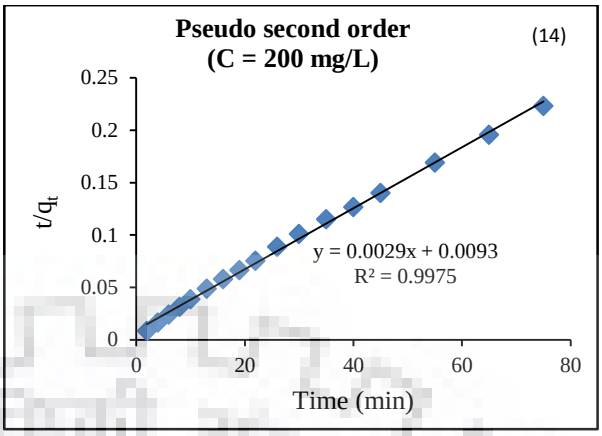
Pseudo second order
(C = 200 mg/L)
(14)
y = 0.0029x + 0.0093
R² = 0.9975
t/qt
Time (min)

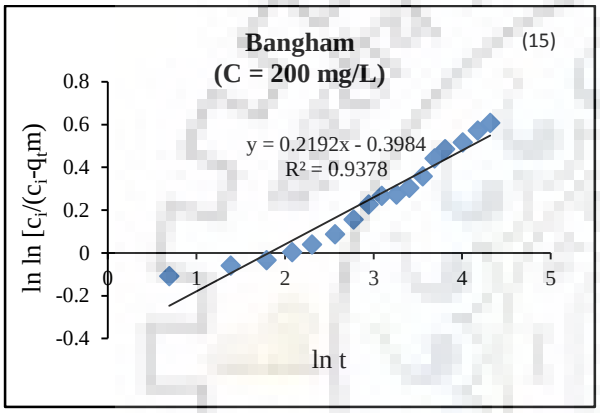
Bangham
(C = 200 mg/L)
(15)
y = 0.2192x - 0.3984
R² = 0.9378
ln ln [ci/(ci-qtm)
ln t

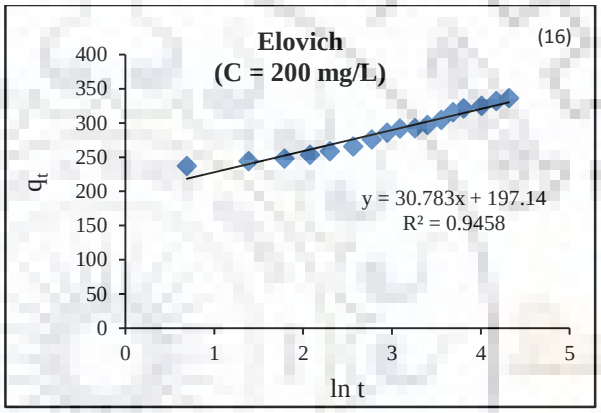
Elovich
(C = 200 mg/L)
(16)
y = 30.783x + 197.14
R² = 0.9458
qt
ln t

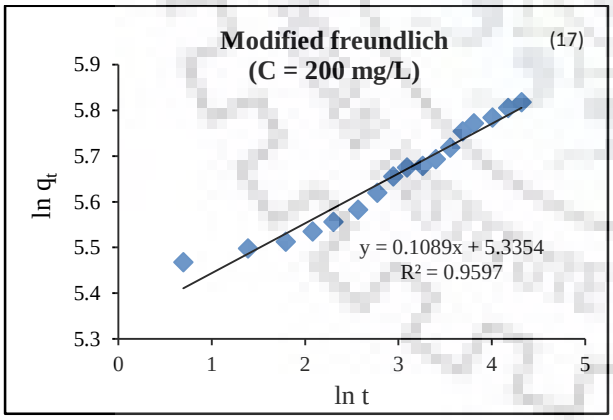
Modified freundlich
(C = 200 mg/L)
(17)
y = 0.1089x + 5.3354
R² = 0.9597
ln qt
ln t

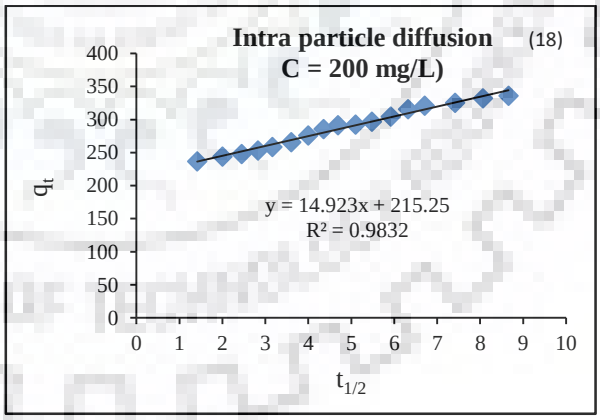
Intra particle diffusion
C = 200 mg/L
(18)
y = 14.923x + 215.25
R² = 0.9832
qt
t1/2

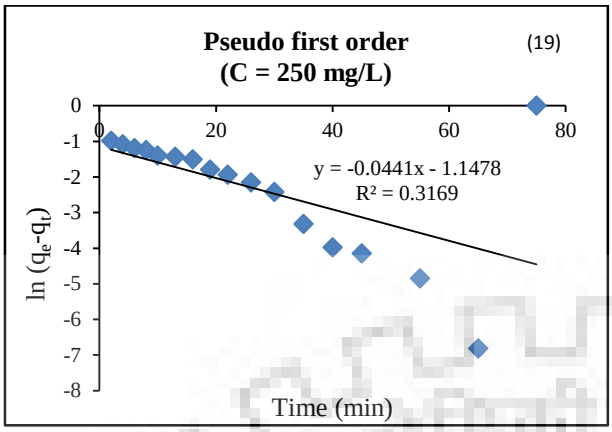
Pseudo first order
(C = 250 mg/L)
(19)
y = -0.0441x - 1.1478
R² = 0.3169
ln (qe-qt)
Time (min)

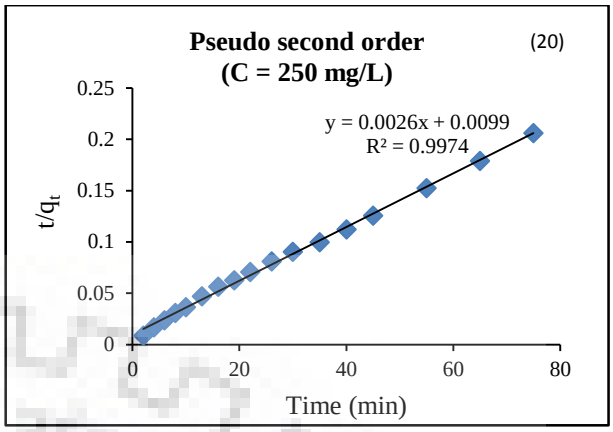
Pseudo second order
(C = 250 mg/L)
(20)
y = 0.0026x + 0.0099
R² = 0.9974
t/qt
Time (min)

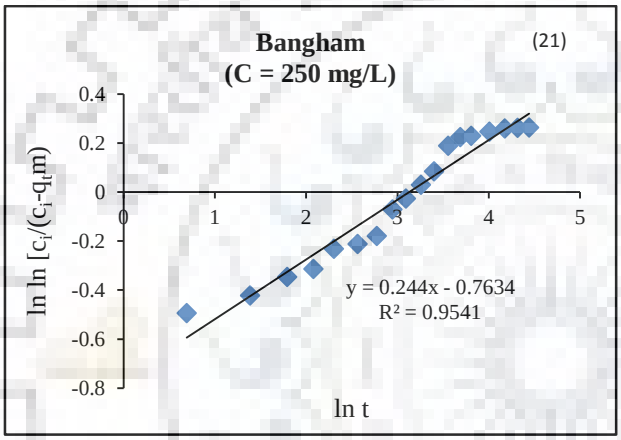
Bangham
(C = 250 mg/L)
(21)
y = 0.244x - 0.7634
R² = 0.9541
ln ln [Ci/(Ci-qtm)]
ln t

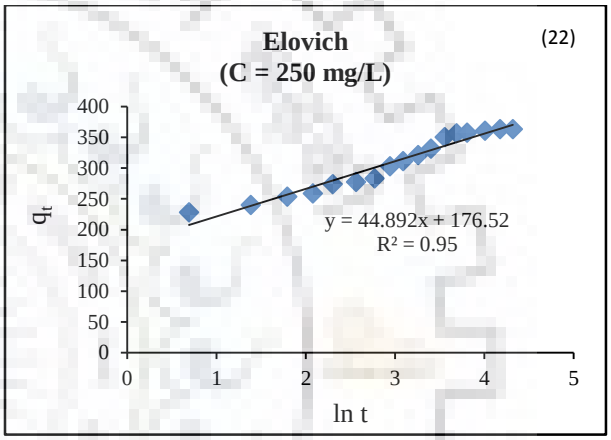
Elovich
(C = 250 mg/L)
(22)
y = 44.892x + 176.52
R² = 0.95
qt
ln t

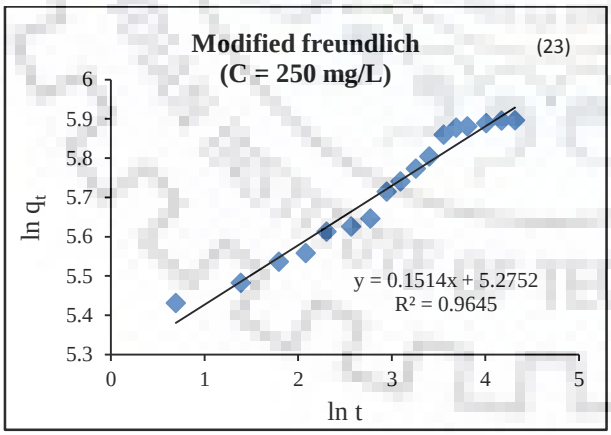
Modified freundlich
(C = 250 mg/L)
(23)
y = 0.1514x + 5.2752
R² = 0.9645
ln qt
ln t

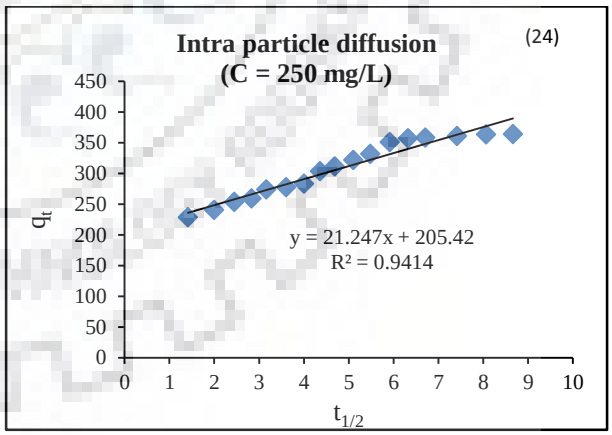
Intra particle diffusion
(C = 250 mg/L)
(24)
y = 21.247x + 205.42
R² = 0.9414
qt
t1/2

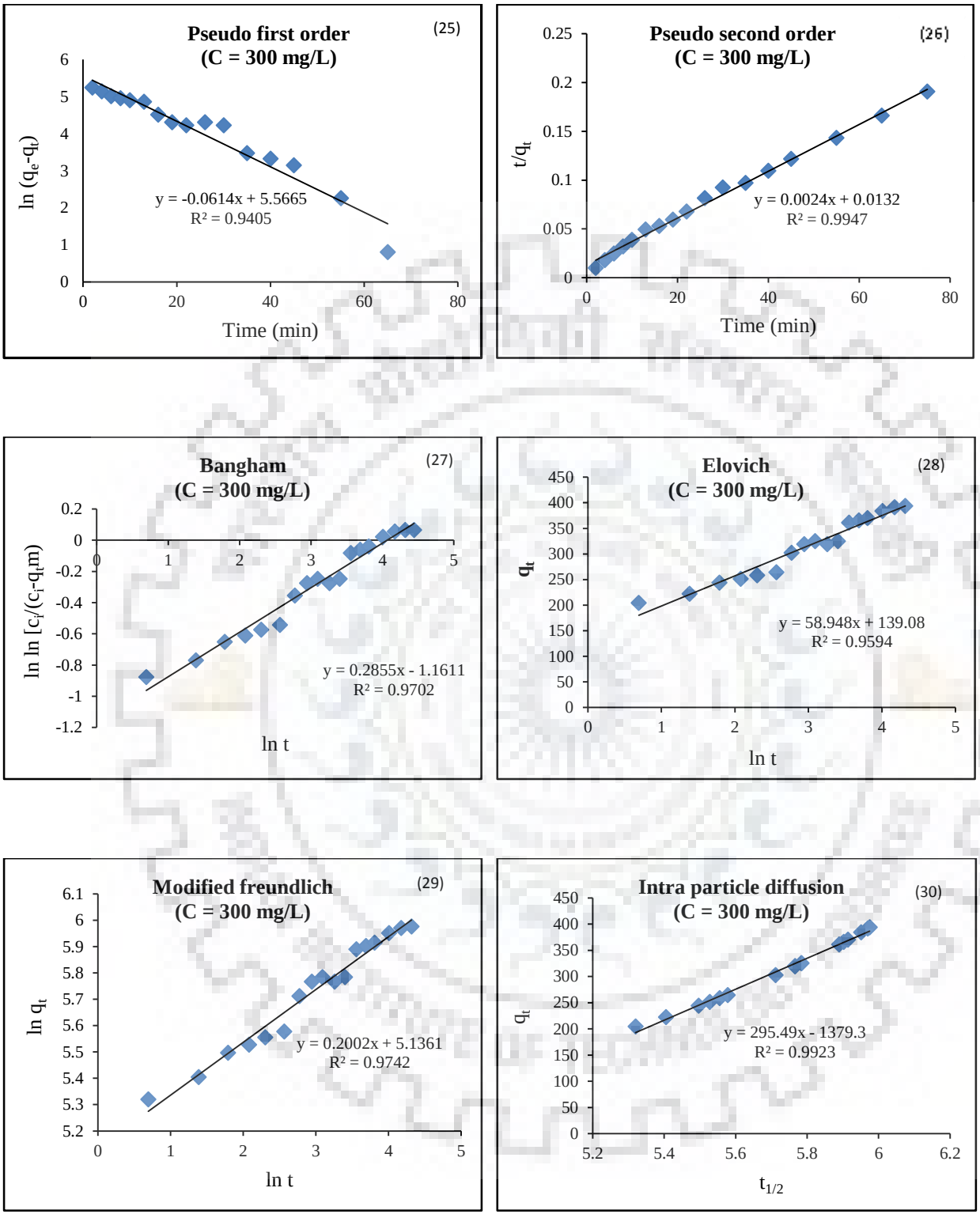

Fig. 4.7 (1-30) Graphical representation of kinetic models for biosorption of Pb^{2+} ions on *S. filipendula* at different initial Pb^{2+} ions concentrations.

Table 4.5 Kinetic model parameters for Pb^{2+} ions biosorption using *S. filipendula*

Kinetic model	Parameters	Initial concentration (mg/L)					Δq %
		100	150	200	250	300	
Elovich	q_e (mg/g)	198	289.22	336.32	363.78	393.6	1.94
	q_t (mg/g)	200.789	297.903	330.11	371.584	393.675	
	α	$1.628x10^5$	$8.364x10^3$	$1.86x10^4$	$2.297x10^3$	$6.24x10^2$	
	β	0.067	0.033	0.0324	0.022	0.0169	
	R^2	0.98	0.92	0.94	0.95	0.95	
Bangham	q_e (mg/g)	198	289.22	336.32	363.78	393.6	1.36
	q_t (mg/g)	196.831	291.083	329.069	370.407	396.725	
	α_o	0.355	0.3792	0.219	0.2491	0.289	
	k_o	89.32	68.392	67.139	46.06	31.04	
	R^2	0.94	0.90	0.93	0.95	0.968	
Intraparticle diffusion model	q_e (mg/g)	198	289.22	336.32	363.78	393.6	5.72
	q_t (mg/g)	206.093	309.757	344.461	389.363	418.86	
	K_{id} (mg $min^{0.5}$/g)	6.73	13.96	14.92	21.24	27.96	
	C	147.81	188.86	215.25	205.42	176.72	
	R^2	0.90	0.89	0.98	0.94	0.95	
Modified Freundlich	q_e (mg/g)	198	289.22	336.32	363.78	393.6	2.79
	q_t (mg/g)	201.995	300.78	331.897	375.72	403.58	
	k_3	1.403	1.190	1.037	0.781	0.566	
	m_1	11.862	8.825	9.182	6.605	4.995	
	R^2	0.98	0.93	0.95	0.96	0.97	

Table 4.6 Isotherm model constants for Pb^{2+} ions biosorption onto *S. filipendula* at different temperatures

Isotherm model	Parameters	Temperature (°C)			
		20	25	30	35
Langmuir	q_o	455.68	427.635	376.907	367.942
	b	0.021	0.0412	0.178	1.024
	R^2	0.983	0.986	0.979	0.923
	$\Delta q\%$	4.466	3.794	2.209	5.89
Freundlich	kf	43.023	75.308	152.69	215.342
	n	2.339	3.033	5.245	7.720
	R^2	0.957	0.929	0.929	0.96
	$\Delta q\%$	7.5	8.542	5.574	5.396
Radke-Prausnitz	q	0.009	0.013	0.247	3.139
	K	912.914	1051.8	318.721	263.832
	a	1.133	1.179	0.963	0.918
	R^2	0.984	0.994	0.996	0.988
	$\Delta q\%$	3.91	2.202	2.334	2.168
Redlich-Peterson	K_1	8.589	13.645	78.726	828.258
	K_2	0.009	0.013	0.247	3.139
	b	1.138	1.179	0.963	0.918
	R^2	0.984	0.994	0.996	0.988
	$\Delta q\%$	3.91	2.177	2.334	2.168
Toth	q_e	385.889	368.906	384.317	473.129
	a_T	329.596	385.194	4.176	0.314
	n_1	1.478	1.724	0.901	0.321
	R^2	0.985	0.996	0.996	0.981
	$\Delta q\%$	3.58	1.531	2.312	2.89
Fritz	α_1	69.8132	176.738	2.297	242.445
	α_2	1.1448×10^6	331.774	0.011	0.2245
	β_1	0.322	0.145	3.270	0.100
	β_2	- 4.733	-2.210	3.145	-13.896
	R^2	0.996	0.999	0.999	0.994
	$\Delta q\%$	2.10	0.442	0.732	1.505

of physical biosorption. It is evident that the extent of metal ion biosorption increases with the increase in the temperature of process. The negative value of ΔG^o (-1.75 to -8.52) shows the feasibility and spontaneous nature of biosorption [23, 47]. The increase in biosorption with temperature can be either due to increase in the number of metal binding sites which were accessible for biosorption on surface of biosorbent or due to decrease in boundary layer thickness surrounding the biosorbent, which intern reduces the mass transfer resistance of biosorbate [72]. The positive values of ΔS^o indicate the enhancement in randomness of biosorbed species at solid and liquid interface with progress of biosorption.

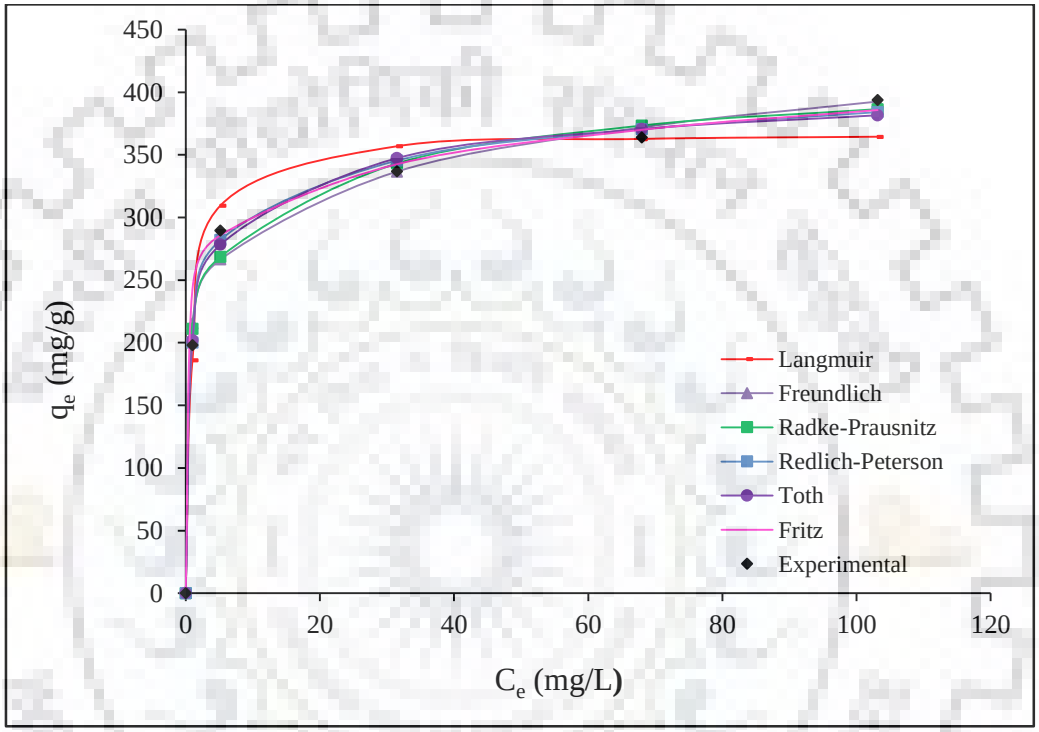

Fig. 4.8 Comparison of different isotherm models for biosorption of Pb^{2+} ions on *S. filipendula.*

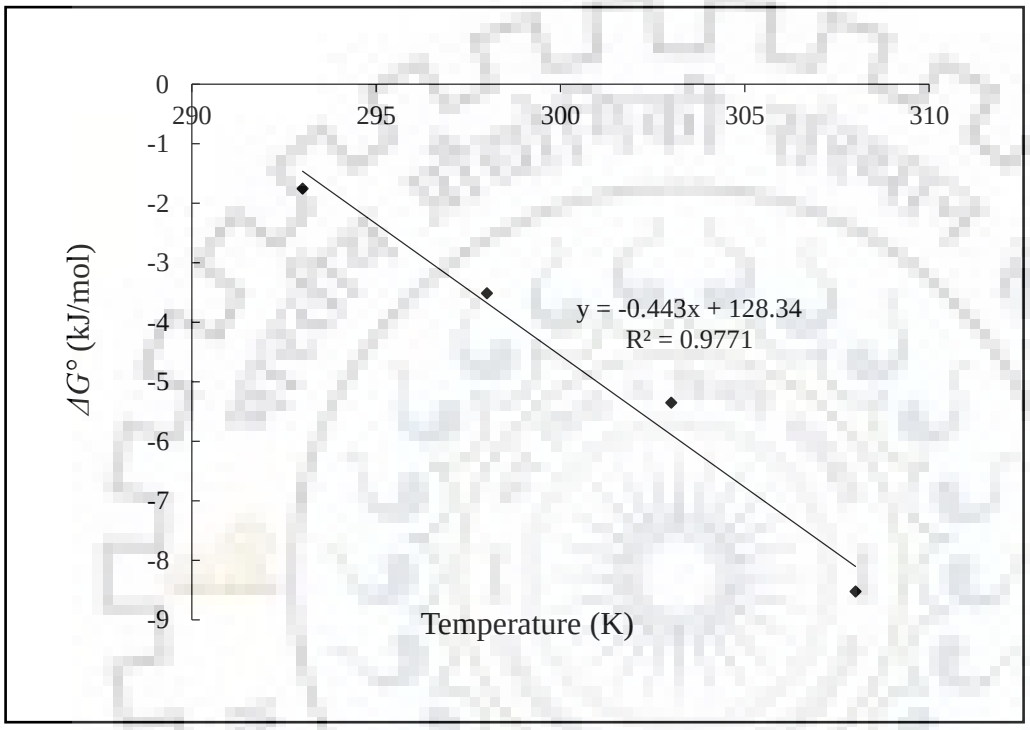

Fig. 4.9 Plot of *ΔG° vs.* T for the estimation of thermodynamic parameters for biosorption of Pb^{2+} ions on *S. filipendula*.

4.1.7 Desorption and reuse efficiency

Four consecutive cycles of biosorption and desorption for Pb^{2+} ions were carried out in a batch system to find the reusability of *S. filipendula* for Pb^{2+} ions biosorption (**Fig. 4.10**). After four cycles, the biosorption and desorption of Pb^{2+} ions was decreased by 5.7 % and 15.68 %, respectively. Hence, *S. filipendula* has shown the better reusability during four consecutive cycles of biosorption and desorption for Pb^{2+} ions. The results indicate that *S. filipendula* can be reused in Pb^{2+} ions biosorption studies without any significant loss of their biosorption capacities.

4.1.8 Specific surface area of *S. filipendula* for Pb^{2+} ions biosorption

As the molecular weight of Pb^{2+} ions is 207 and the cross sectional area is 5.56 m^2. The specific surface area of *S. filipendula* for Pb^{2+} ions biosorption was found to be 59.51 m^2/g

4.1.9 Conclusions

A batch experimental study for the biosorptive removal of Pb^{2+} ions on *S. filipendula* algae has been presented. The RSM was used to obtain the optimum conditions for biosorption of Pb^{2+} ions from the aqueous solution by *S. filipendula*. The optimum parameters for biosorption were obtained as pH (4.99), temperature (34.8 °C), initial Pb^{2+} ions concentration (152 mg/L), and biosorbent dosage (0.49 g/L) at which 96 % removal efficiency was achieved. The removal efficiency of Pb^{2+} ions was increased with increasing biosorbent dosage and reaction temperature while decreased with rise in initial Pb^{2+} ions concentration. The percentage of Pb^{2+} ions removal was decreased at both low and high pH. Therefore, further biosorption studies have been performed at pH of 5.0. The biosorption experimental data of Pb^{2+} ions removal using *S. filipendula* were very well fitted with Fritz isotherm and Bangham kinetic model. Thermodynamic studies has shown that the biosorption process of Pb^{2+} ions was spontaneous, feasible and endothermic in nature. After four consecutive cycles of biosorption-desorption, 77.53% of Pb^{2+} ions was recovered. The observations of this study indicates that *S. filipendula* can be used effectively as a biosorbent for the removal of Pb^{2+} ions from industrial wastewater.

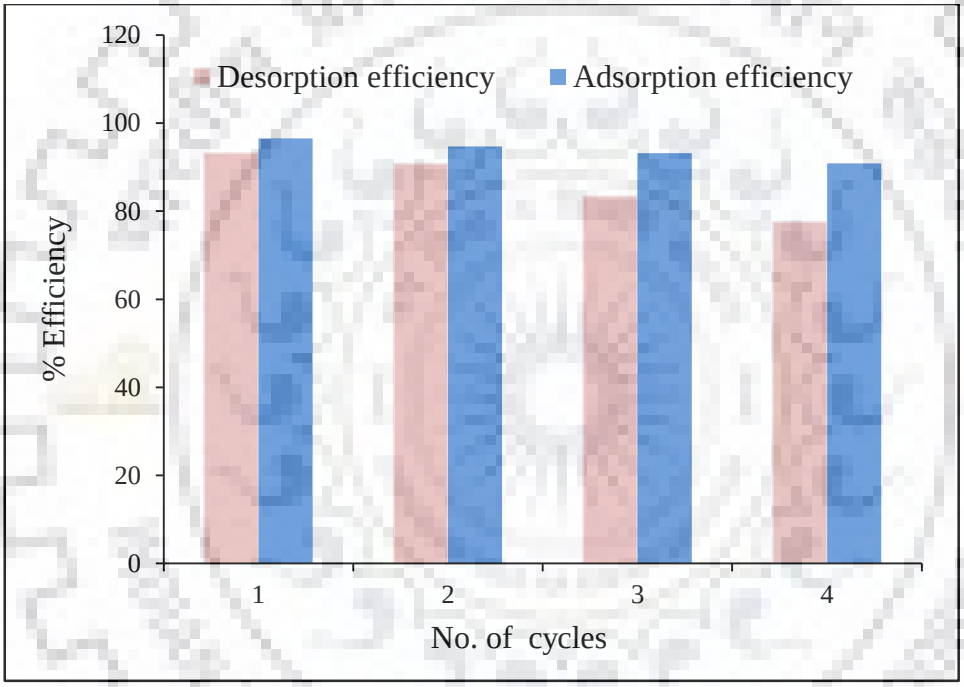

Fig. 4.10 Biosorption-desorption efficiency *vs.* the number of cycles.

4.2 REMOVAL OF Cd^{2+} IONS FROM AQUEOUS SOLUTION USING *S. FILIPENDULA*

4.2.1 Characterization of *S. filipendula*

4.2.1.1 FESEM - EDS analysis

FESEM analysis was used to observe the surface morphology of *S. filipendula* before and after biosorption of Cd^{2+} ions. The FESEM images of *S. filipendula* at magnification of 2,000 x are shown in **Fig. 4.11 (a & b)**. As shown in figure before biosorption the surface of *S. filipendula* was rough and porous while after biosorption of Cd^{2+} ions the surface becomes smooth. The smooth surface resulted due to filling of the pores by biosorbed Cd^{2+} ions.

The EDS analysis before and after Cd^{2+} ions biosorption was done to observe the elemental composition of *S. filipendula* as shown in **Fig. 4.12 (a & b)**. After biosorption, EDS shows the occurrence of Cd^{2+} ions which was biosorbed by *S. filipendula*.

4.2.1.2 FTIR analysis

FTIR analysis was carried out to examine the functional groups involved in the biosorption of Cd^{2+} ions and their interaction with *S. filipendula*. **Fig. 4.13** shows FTIR spectra for *S. filipendula* biosorbent before and after Cd^{2+} ions biosorption. The shifting of peaks was observed after Cd^{2+} ions biosorption. The peaks corresponding to different functional groups were shifted from 3407.90-3447.13 cm^{-1} (–OH group stretching), 2928.06-2925.35 cm^{-1} (stretching of C-H bonds in methyl and methylene groups), 1633.89-1637cm^{-1} (stretching of C=O bond in amide group), 1048.13-1067.01 cm^{-1} (stretching of C-O group) and 606.88-667.93 cm^{-1} (stretching of alkyl halide groups). The shifting of peaks shows that –OH, C-H, –COOH, C=O, and alkyl halide groups were involved in Cd^{2+} ions biosorption.

(a)

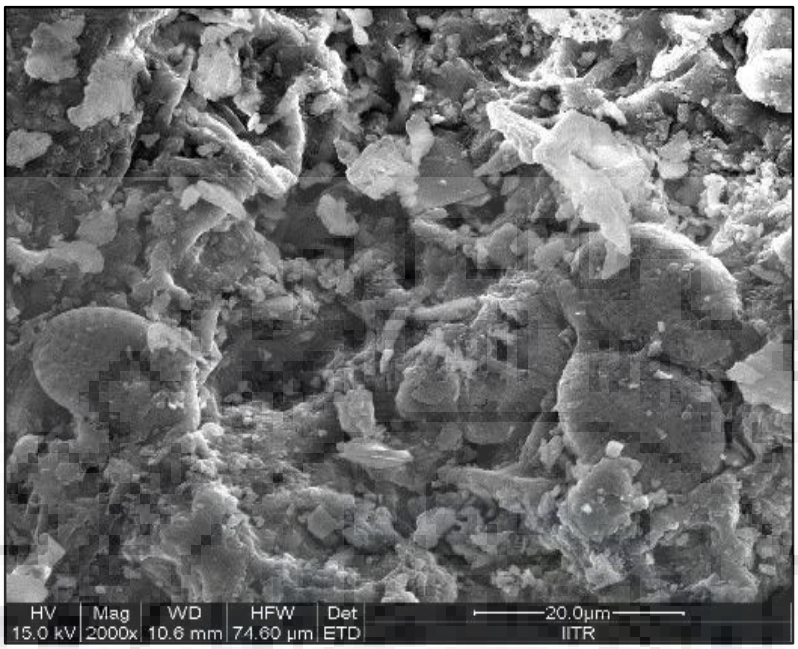

(b)

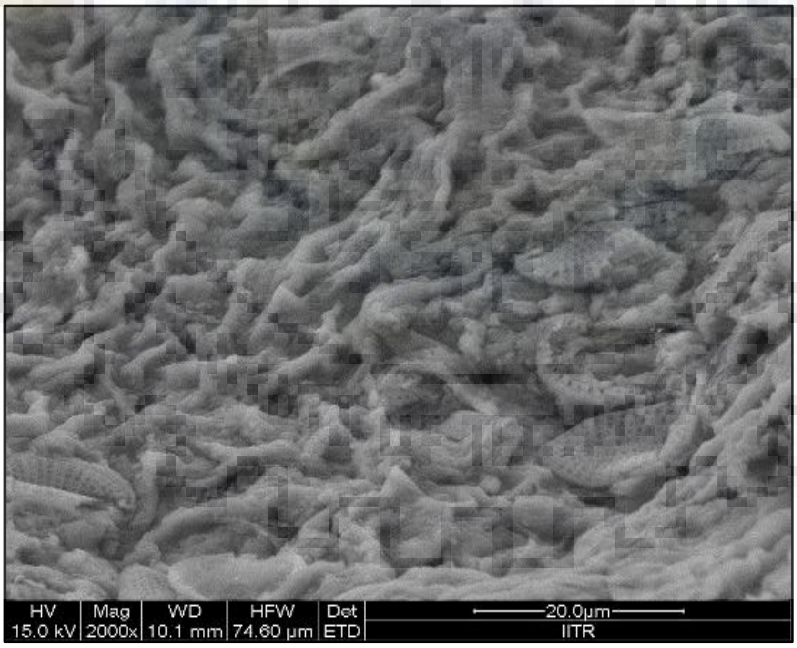

Fig. 4.11 FESEM image of *S. filipendula* (a) before biosorption (b) after biosorption of Cd^{2+} ions.

(a)

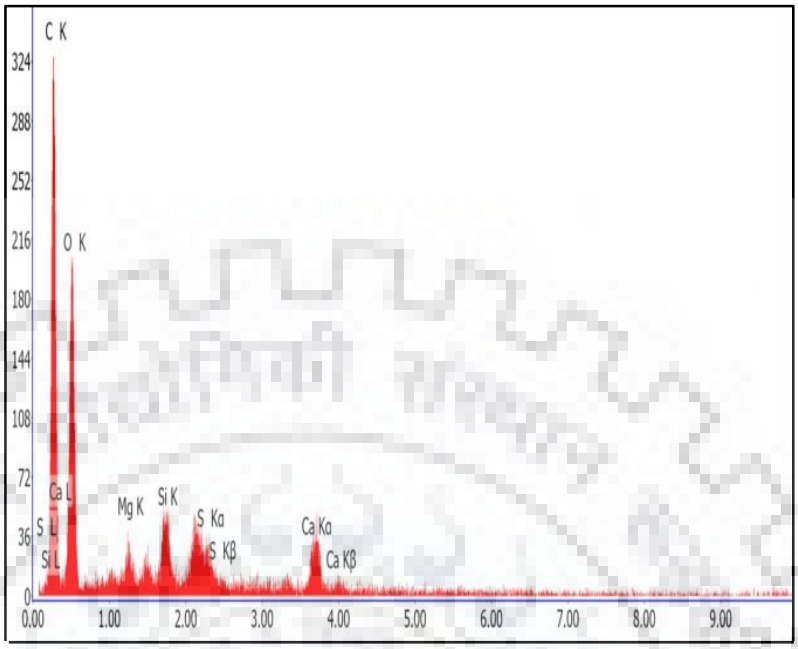

(b)

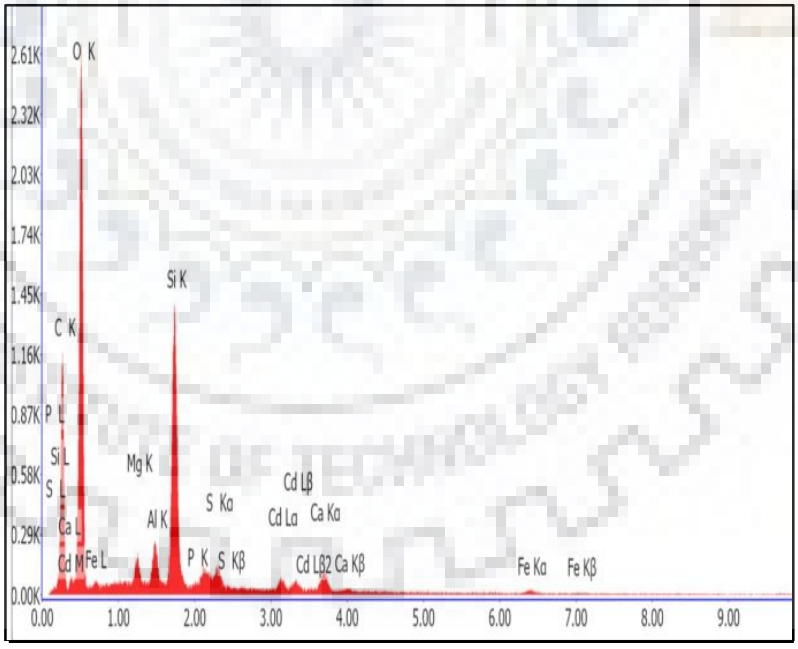

Fig. 4.12 EDS image of *S. filipendula* (a) before biosorption (b) after biosorption of Cd^{2+} ions.

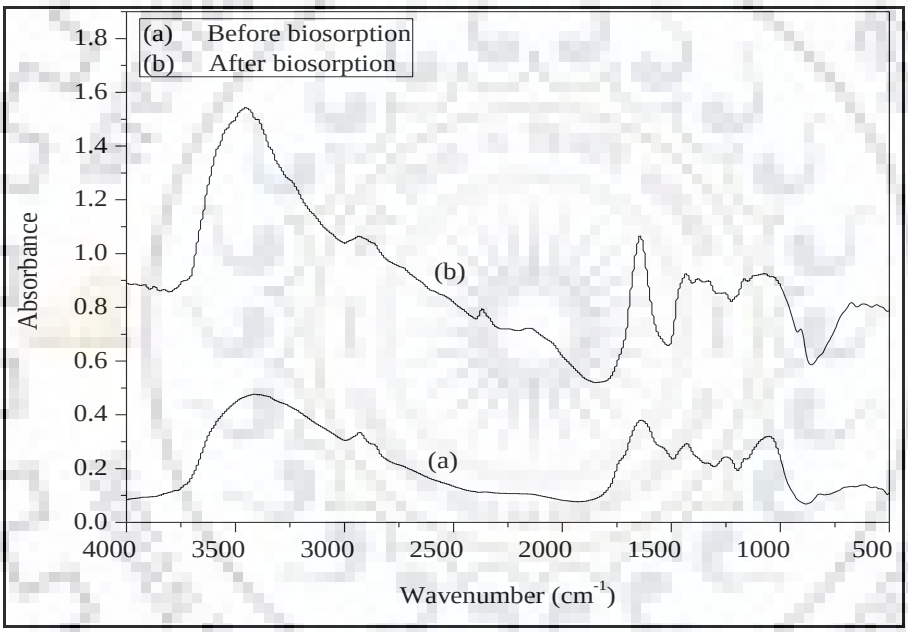

Fig. 4.13 FTIR image before and after Cd^{2+} ions biosorption on *S. filipendula*.

4.2.2 Analysis of results of experiments

The biosorption of Cd^{2+} ions was carried out by using CCD to obtain the optimized conditions for maximum removal of Cd^{2+} ions using *S. filipendula*.

4.2.2.1 Experimental design and factorial model for Cd^{2+} ions biosorption process

The matrix of four variables pH, initial Cd^{2+} ions concentration, biosorbent dosage, and temperature were varied at 5 levels (-α, -1, 0, +1, +α) as shown in **Table 4.7**. The complete experimental design with predicted and experimental response data in terms of removal percent is given in **Table 4.8**. The statistical significance and adequacy of obtained regression model were checked by using ANOVA. The significance of each coefficient term and regression model were examined by *p-value* and *F-value.* The large *F-value* and small *p-value* indicates the high significance of regression model and coefficient terms [7, 323]. The analysis of variance of second order polynomial models and regression coefficient are shown in **Table 4.9**. *F-value* of 32.01 and *p-value* less than 0.0001 implies that the model obtained by RSM was significant. Lack of fit compares the pure error with residual error. The large *F- value* of "Lack of Fit" (554.1) shows that lack of fit was significant. There was only 0.01 % possibility that a "Lack of Fit *F- value*" this large could occur due to noise. A small value of coefficient of variance (CV = 8.57) implies that deviation between predicted and experimental data values was low. The coefficient of determination (R^2) value examines the goodness of fit of the model.

Table 4.7 Range and level of the independent variables for Cd^{2+} ions biosorption

Independent variables	Range and levels (coded)				
	-α	**-1**	**0**	**+1**	**+α**
pH (A)	1.5	3	4.5	6	7.5
Initial Cd^{2+} ion concentration, mg/L (B)	25	50	75	100	125
Biosorbent dosage, g/L (C)	0.25	0.5	0.75	1.0	1.25
Temperature, ºC (D)	20	25	30	35	40

Table 4.8 Experimental design based on CCD and its response for Cd^{2+} ions biosorption on *S. filipendula*

Run	Temperature (°C)	Initial Cd^{2+} ions concentration (mg/L)	Biosorbent dosage (g/L)	pH	Removal %	
					Actual	Predicted
1	25	50	0.5	3	34.4	27.68
2	25	50	0.5	6	63.5	62.07
3	25	100	0.5	3	14	9.87
4	25	100	0.5	6	47.3	46.94
5	25	50	1	3	59.58	48.46
6	25	50	1	6	83.5	76.34
7	25	100	1	3	28	23.08
8	25	100	1	6	60	53.64
9	35	50	0.5	3	56	48.73
10	35	50	0.5	6	81.73	75.32
11	35	100	0.5	3	43.52	39.36
12	35	100	0.5	6	71.14	68.63
13	35	50	1	3	80.32	67.84
14	35	50	1	6	98.92	87.91
15	35	100	1	3	64.6	50.89
16	35	100	1	6	79.76	73.65
17	30	75	0.75	1.5	3.76	2.42
18	30	75	0.75	7.5	72.46	59.56
19	30	25	0.75	4.5	88	86.21
20	30	125	0.75	4.5	66.6	54.14
21	30	75	0.25	4.5	50.8	47.27
22	30	75	1.25	4.5	83.8	73.08
23	20	75	0.75	4.5	38.94	33.24
24	40	75	0.75	4.5	82.84	74.30
25	30	75	0.75	4.5	79.01	72.22
26	30	75	0.75	4.5	79.01	72.22
27	30	75	0.75	4.5	79.01	72.22
28	30	75	0.75	4.5	79.01	72.22
29	30	75	0.75	4.5	79.01	72.22
30	30	75	0.75	4.5	79.01	72.22

Table 4.9 ANOVA for response surface quadratic model of Cd^{2+} ions biosorption

Source	Sum of squares	df	Mean square	*F- value*	*p - value*	Remarks
Model	13878.31	14	991.31	32.01	< 0.0001	Significant
A	4671.30	1	4671.30	150.85	< 0.0001	Significant
B	1238.84	1	1238.84	40.01	< 0.0001	Significant
C	1684.88	1	1684.88	54.41	< 0.0001	Significant
D	2511.47	1	2511.47	81.10	< 0.0001	Significant
AB	59.02	1	59.02	1.91	0.1876	Not Significant
AC	182.72	1	182.72	5.90	0.0282	Significant
AD	219.11	1	219.11	7.08	0.0178	Significant
BC	158.07	1	158.07	5.10	0.0392	Significant
BD	11.78	1	11.78	0.38	0.5466	Not Significant
CD	8.02	1	8.02	0.26	0.6182	Not Significant
A^2	2798.74	1	2798.74	90.38	< 0.0001	Significant
B^2	24.55	1	24.55	0.79	0.3873	Not Significant
C^2	215.63	1	215.63	6.96	0.0186	Significant
D^2	273.26	1	273.26	8.82	0.0095	Significant
Residual	464.51	15	30.97	-	-	-
Lack of Fit	464.51	10	46.45	554.1	<0.0001	Significant
Pure Error	0.000	5	0.000	-	-	-
Total	14342.81	29	-	-	-	-
R^2 = 0.96; *Adjusted* R^2 = 0.93; *Predicted* R^2 = 0.81; *Adequate precision* = 22.09						

For a significant model, R^2 value should be close to unity. The R^2 value for this model was found to be 0.96 shows that more than 96 % of the experimental data was matched with predicted data and only 4 % of total dissimilarity was not explained by the model. The *predicted* R^2 (0.81) was in reasonable agreement with *adjusted* R^2 (0.93) i.e. the difference was less than 0.2. *Adequate precision* determines the signal to noise ratio and a ratio of 4 is desirable [7, 323]. Here, this ratio was 22.09 which imply an adequate signal of biosorption. The value of "Prob > F" less than 0.05 indicates that model terms were significant. In this case A, B, C, D, AC, AD, BC, A^2, C^2, and D^2 were significant model terms. The modified reduced quadratic equation which determine the relationship between response and four independent process variables was obtained by deleting statistically insignificant terms (*p-value* > 0.05) based on *F-value* and *p-value* were given as:

$$Y = +77.01 + 13.95\,A - 7.18\,B + 8.38\,C + 10.23\,D - 3.38\,AC - 3.7\,AD - 3.14\,BC - 10.10\,A^2 - 2.8\,C^2 - 3.16\,D^2 \quad (4.2)$$

where *Y* represents removal percent of Cd^{2+} ions and A, B, C, D were coded values of pH, initial Cd^{2+} ions concentration (mg/L), biosorbent dosage (g/L), temperature (^oC) respectively. The positive sign indicates synergistic effect and negative sign indicates antagonistic effect on removal of Cd^{2+} ions.

Fig. 4.14 (a) shows the plot of normal probability *vs.* studentized residuals which determines the number of standard deviations separating the predicted and experimental data value. Normal probability plot shows whether the residuals follow a normal distribution of points along a straight line. **Fig. 4.14 (b)** shows that the predicted data values of reduces quadratic model was in well agreement with actual values.

4.2.2.2 Variation of process parameters on maximum Cd^{2+} ions removal efficiency

The biosorption efficiency of Cd^{2+} ions depends on various parameters such as pH, temperature, initial Cd^{2+} ions concentration, and biosorbent dosage. **Fig. 4.15 (a-d)** shows the 3D response surface plots which are graphical representation of regression equation showing the interaction effect of variables.

(i) Effect of time at different temperature

The removal efficiency of Cd^{2+} ions after a regular interval of time at different temperature (25- 45 °C) with constant pH (6.0), biosorbent dosage (0.5 g/L), and initial Cd^{2+} ions concentration (50 mg/L) was examined which is shown in **Fig. 4.16**. It was increased with increasing contact time and temperature. Initially increase in removal efficiency was very high and a large amount of Cd^{2+} ions (95 %) was removed by *S. filipendula* in first 10 min of biosorption process. It may be due to rapid transfer of Cd^{2+} ions onto active sites of biosorbent surface. Afterwards, the removal rate was slow down and equilibrium was achieved in 60 min for all the temperatures. When equilibrium condition was attained, no more Cd^{2+} ions was biosorbed due to repulsive forces between the Cd^{2+} ions present on solid and bulk phase [173]. **Fig. 4.16** shows the removal percent of Cd^{2+} ions at equilibrium was increased with increase in temperature from 25-45 °C while the equilibrium time was not affected by temperature [14, 93, 231].

(a)

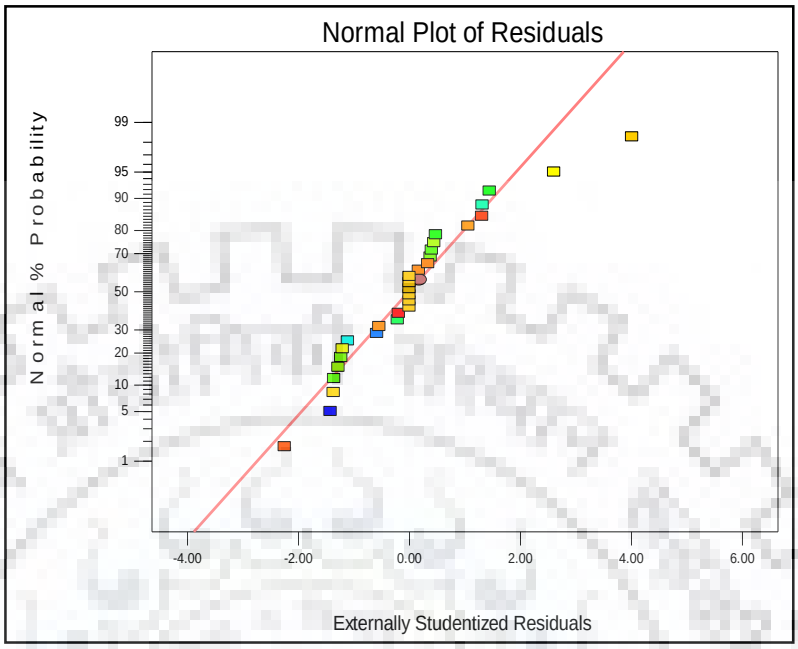

(b)

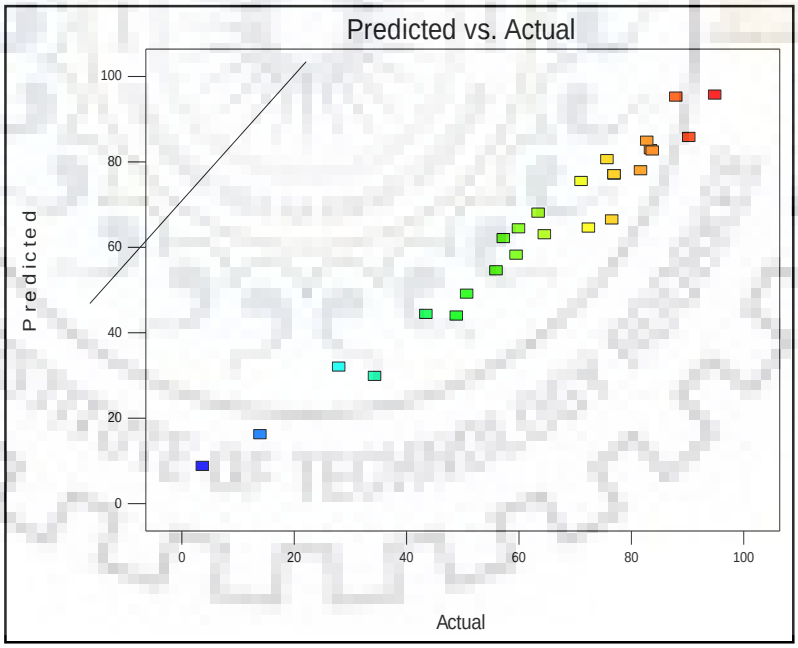

Fig. 4.14 (a) Normal probability plot (b) correlation between actual and predicted values.

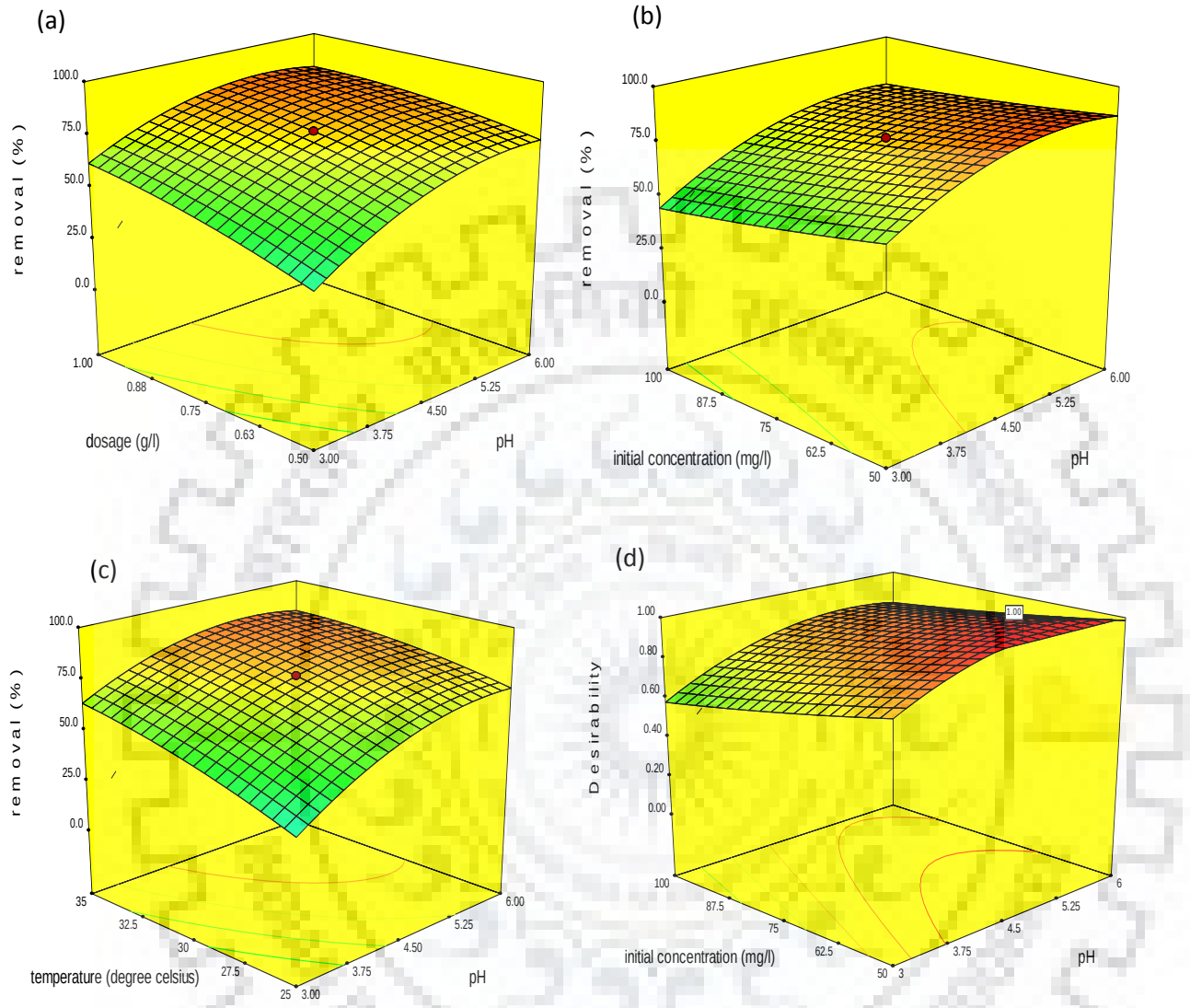

Fig. 4.15 (a) Interactive effect of pH and biosorbent dosage (b) Interactive effect of pH and initial Cd^{2+} ions concentration (c) Interactive effect of pH and temperature (d) Desirability ramp for numerical optimization of four independent variables and the responses.

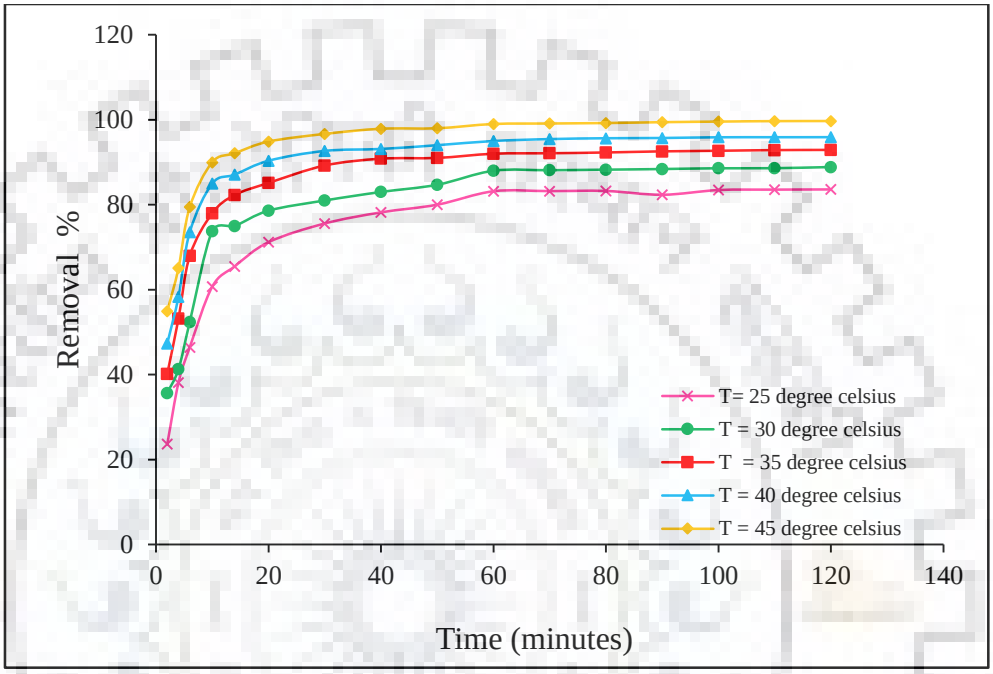

Fig. 4.16 Effect of contact time on Cd^{2+} ions biosorption using *S. filipendula* at different temperatures (pH: 6.0, initial Cd^{2+} ions concentration: 50 mg/L, biosorbent dosage: 0.5 g/L).

(ii) Effect of pH

The pH of solution is a significant parameter which governed the extent of metal ions biosorption. The pH of solution influences the surface charge of biosorbents, degree of ionization and species distribution of metal ions in aqueous solution [153]. In aqueous solution Cd^{2+} ions were present as Cd^{2+}, $Cd(OH)^{+}$, $Cd(OH)_2$ etc. The effect of pH on Cd^{2+} ions biosorption onto raw *S. filipendula* was examined by varying the pH from 1.5 to 7.5. As shown in **Fig. 4.15 (a)** the removal of Cd^{2+} ions increased with increase in pH of the solution. At pH 1.5, biosorption of Cd^{2+} ions was very low, due to repulsion of metal ions by the proton (H_3O^{+}) present at binding sites of *S. filipendula* biomass [7]. The removal efficiency was increased with increase in pH from 1.5 to 6.0 which can be explained in terms of pH_{PZC}. The pH_{PZC} is pH value at which the net charge on *S. filipendula* surface was zero and where the electrostatic forces between Cd^{2+} ions and *S. filipendula* surface were balanced. At pH > pH_{PZC}, the total charge on *S. filipendula* was negative which attracts positively charged Cd^{2+} ions. **Fig. 4.17** shows that the value of pH_{PZC} for *S. filipendula* was found to be 4.3. Due to electrostatic attraction the removal of Cd^{2+} ions was increased at pH > 4.3. While at pH < pH_{PZC}, the overall surface charge on *S. filipendula* was positive which results in decrease of Cd^{2+} ions removal efficiency due to high concentration of H^{+} ions in the solution that were competing with positively charged Cd^{2+} ions for biosorption sites of *S. filipendula*. The removal efficiency of Cd^{2+} ions was also decreased at pH > 6.0 due to precipitation of Cd^{2+} ions occurred as their hydroxides [7, 323]. Therefore, all the other experiments were performed at pH 6.0. Similar pH effects were reported in literatures by using different adsorbents [7, 108].

(iii) Effect of initial Cd^{2+} ions concentration

The effect of initial Cd^{2+} ions concentration was studied by varying from 50 to 100 mg/L. **Fig. 4.15 (b)** shows that with increase in initial Cd^{2+} ions concentration the percent removal was decreased from 98 to 76 %. It may be due to saturation of biosorption sites by Cd^{2+} ions at fixed biosorbent dosage [7]. While the biosorption capacity of *S. filipendula* for Cd^{2+} ions was increased from 51.58 to 80.24 mg/g with increase in initial Cd^{2+} ions concentration. It may be due to the fact that driving force increases with increasing initial Cd^{2+} ions concentration which results in decrease of resistances to mass transfer of Cd^{2+} ions between liquid phase and biosorbent [7, 254, 323].

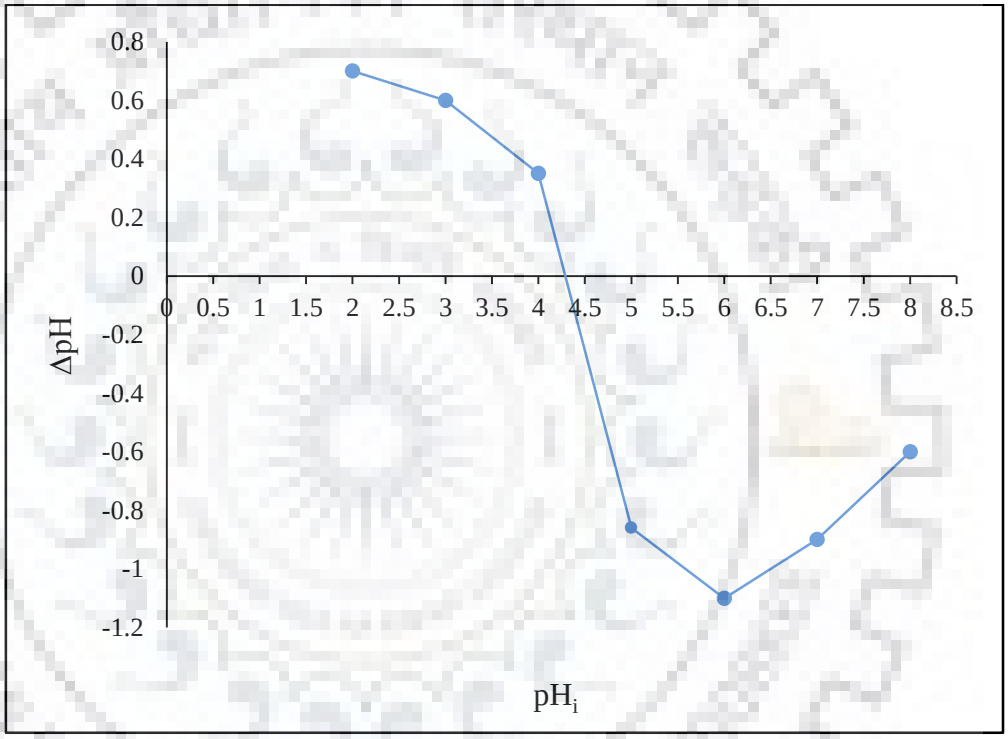

Fig. 4.17 Point of zero charge plot (pH_{PZC}) of *S. filipendula*.

(iv) Effect of temperature

The temperature is an important parameter that influences the rate of biosorption process. The effect of temperature (25, 30, 35, and 40 °C) on the Cd^{2+} ions biosorption was examined. **Fig. 4.15 (b)** shows that the percent removal of Cd^{2+} ions was increased from 50.9 to 99.2 % with rise in temperature from 25 to 40 °C [51, 254]. The increase in biosorption of Cd^{2+} ions on *S. filipendula* with increase in temperature can be due to the enlargement of pore size or activation of the biosorbent surface. In addition to this on increasing temperature the mobility of metal ion increases from the liquid phase towards biosorbent surface which improved the accessibility to binding sites of biosorbent at higher temperature [323].

(v) Effect of biosorbent dosage

Biosorbent dosage is a significant process parameter as it examines the biosorbent capacity for a given initial metal ion concentration. The influence of biosorbent dosage on the removal efficiency of Cd^{2+} ions was observed in range of 0.5–1.0 g/L. **Fig. 4.15 (a)** shows that the removal efficiency of Cd^{2+} ions increased with increase in biosorbent dosage and pH. The maximum removal efficiency of Cd^{2+} ions was observed at biosorbent dosage of 1.0 g/L. Increase in the removal efficiency with biosorbent dosage might be due to increase in surface area of biosorbent and more availability of biosorption sites [196, 323]. While biosorption capacity decreased with increase in biosorbent dosage. It may be due to unsaturation of biosorption site during biosorption process while the total number of available sites for biosorption increases on increasing biosorbent dosage [196].

4.2.3 Optimization and validation

Fig. 4.15 (d) shows desirability plot which was obtained from 10 optimum points by numerical optimization. The best local maxima was observed at pH 5.7, initial Cd^{2+} ions concentration 50.8 mg/L, biosorbent dosage 0.99 g/L, and temperature 34.5 °C where 99.56 % removal of Cd^{2+} ions with desirability value of 1 was achieved. The desirability value of 1 for Cd^{2+} ions removal indicates that the estimated function represents the experimental model and desired conditions.

The validation of model was done by conducting experiments under the optimal conditions obtained by software to find out experimental removal percentage of Cd^{2+} ions. The Cd^{2+} ions removal efficiency from the confirmation experiments was obtained as 97.98 %. It has been noticed that the value generated by the software was in conformity with the experimental values. Thus, the RSM approach could be appropriate for the optimization of the Cd^{2+} ions biosorption process from aqueous solution.

4.2.4 Kinetic results interpretation

The experiments for kinetic study of Cd^{2+} ions biosorption on *S. filipendula* were performed at 35 °C by using five different initial Cd^{2+} ions concentrations: 10, 30, 50, 70, 90 and 100 mg/L. In each flask, a fixed amount of biosorbent (1.0 g/L) was added in solution of pH 5.7. In the biosorption process it is important to find the rate-limiting step. Kinetic studies assist to identify the mechanism involve in biosorption process and to examine the required economical design of wastewater treatment method. For a solid-liquid biosorption process, the transfer of biosorbate may be either through intra-particle diffusion for porous medium or external mass transfer for nonporous medium or both mechanisms. The results of kinetic models with their parameters, coefficient of determination, and normalized standard deviation values are given in **Table 4.10**.

The pseudo second order kinetic model has highest R^2 value (> 0.99) and smaller value of Δq % as comparison to other models for all the initial Cd^{2+} ions concentrations (**Table 4.10**). It indicates that for this model calculated value of q_e was very well matched with the experimental value of q_e. Thus, it can be concluded that Cd^{2+} ions biosorption on *S. filipendula* follows pseudo second order kinetics. It confirmed that chemisorption was the rate limiting mechanism which involves valence forces through exchange and sharing of electrons between biosorbate and biosorbent [90, 97, 209]. The values of h was also increased with the increase in initial Cd^{2+} ions concentration. It indicates that the driving force for mass transfer was increased due to which more Cd^{2+} ions reached the surface of *S. filipendula* in short time period. Similar results were reported for the biosorption of different metal ions using different adsorbents [144, 201, 74].

Table 4.10 Kinetic model parameters for Cd^{2+} ions biosorption using *S. filipendula* at different initial Cd^{2+} ions concentrations

Kinetics models and Parameters	Initial Cd^{2+} ions concentration (mg/L)					
$q_{e\ exp}$ (mg/g)	10	30	50	70	90	100
Pseudo first order						
$q_{e\ cal}$ (mg/g)	10.439	31.065	49.274	67.230	83.230	85.967
$q_{e\ cal}$ (mg/g)	7.61	27.68	46.37	31.81	49.15	42.64
k_o (min^{-1})	0.0826	0.118	0.124	0.118	0.102	0.103
R^2	0.993	0.858	0.840	0.959	0.748	0.954
Δq %	41.78	24.08	25.86	60.39	54.12	61.64
Pseudo second order						
$q_{e\ cal}$ (mg/g)	11.42	33.33	53.76	70.92	84.74	89.28
K (g/mg.min)	$16.37x10^{-3}$	$7.58x10^{-3}$	$6x10^{-3}$	$5.61x10^{-3}$	$5.52x10^{-3}$	$5.4x10^{-3}$
h (mg/g.min)	2.134	8.42	17.34	28.21	39.63	43.04
R^2	0.998	0.999	0.994	0.997	0.998	0.999
Δq %	6.60	4.59	11.79	12.19	3.30	3.78
Elovich						
α	6.507	24.97	22.64	77.08	511.30	607.35
β	0.482	0.164	0.085	0.077	0.092	0.089
R^2	0.973	0.962	0.917	0.830	0.935	0.956
Δq %	9.24	6.47	11.82	13.57	4.99	5.94
Bangham						
α_o	0.033	0.030	0.032	0.030	0.02	0.017
k_b	67.151	76.93	74.21	93.86	90.44	92.81
R^2	0.821	0.749	0.676	0.594	0.751	0.759
Δq %	35.41	34.02	47.90	34.51	22.97	18.59
Intra particle diffusion						
K_{id} ($mg.min^{0.5}/g$)	1.039	3.17	5.93	6.39	5.546	5.844
C	3.391	11.28	13.44	30.22	46.95	49.67
R^2	0.912	0.856	0.776	0.661	0.806	0.863
Δq %	10.09	13.06	25.67	21.43	9.29	6.75
Modified Freundlich						
k_3 (L/g.min)	0.345	0.368	0.251	0.372	0.48	0.479
m_1	3.415	3.45	2.522	3.54	5.85	6.211
R^2	0.957	0.928	0.863	0.787	0.891	0.944
Δq %	6.89	9.37	17.97	15.93	6.24	4.52

For Elovich kinetic model the values of R^2 (< 0.99) and Δq % suggested that this model was not fitted to experimental data. The values of α and β constants helps to understand the initial rate of biosorption process with the nature of biosorbent active sites involved in the biosorption process. It can be described by two assumptions: (i) difference in the energy released during chemisorption in proportion to the degree of coverage (ii) difference in activation energies needs for chemisorption linked to the heterogeneity of active sites [332]. With the increase in initial Cd^{2+} ions concentration from 10 to 100 mg/L, the values of α (increased) and β (decreased) were varied. According to Teng and Hsieh, the parameter α is related to the rate of chemisorption with zero surface coverage which should increase with the increase in initial Cd^{2+} ions concentration [316]. While the parameter β is related to level of surface coverage and activation energy required for chemisorption which should decrease with increase in initial Cd^{2+} ions concentration [200]. Biosorption of Cd^{2+} ions follows the conditions proposed by Teng and Hsieh but the values of R^2 and Δq % do not show the best fitting of Elovich kinetic model with the experimental data.

The intraparticle diffusion model was plotted to confirm the mass transfer influence on Cd^{2+} ions biosorption by *S. filipendula*. The intercept value of q_t *vs* $t^{0.5}$ plot for each initial Cd^{2+} ions concentration shows that the line was not passing through the origin it verifies that intra particle diffusion was not the rate limiting step solely. It may be due to the variation of mass transfer rate in initial and final stage of biosorption. This indicates the involvement of boundary layer control for Cd^{2+} ions biosorption on *S. filipendula*. The values of R^2 and Δq % shows that the fitting of intra particle diffusion kinetic model was not good with experimental data.

Bangham kinetic model was used to verify whether the pore diffusion was only the rate controlling step. The plot of double logarithm was not a linear curve for Cd^{2+} ions biosorption by *S. filipendula*. The small R^2 value and high Δq % (**Table 4.10**) shows that Bangham kinetic model was not matched with the experimental data. Graphical representation of kinetic models for biosorption of Cd^{2+} ions on *S. filipendula* at different initial Cd^{2+} ions concentrations are shown in **Fig. 4.18 (1-30)**. It was confirmed that the pore diffusion was not only the rate controlling step. Likewise, the values of R^2 and Δq % for Modified Freundlich model shows that this model was not fitted with the experimental data (**Table 4.10**). Therefore, it was concluded that the pseudo second order kinetic model was the best fitted model and the rate controlling step was chemisorption for Cd^{2+} ions biosorption by *S. filipendula*.

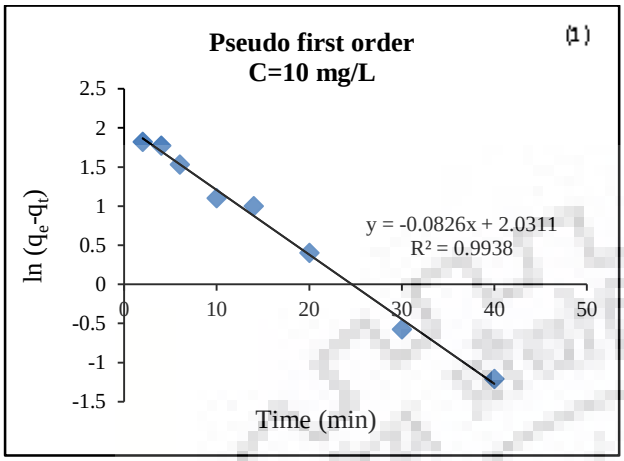
Pseudo first order
C=10 mg/L
(1)
ln (qe-qt)
y = -0.0826x + 2.0311
R² = 0.9938
Time (min)

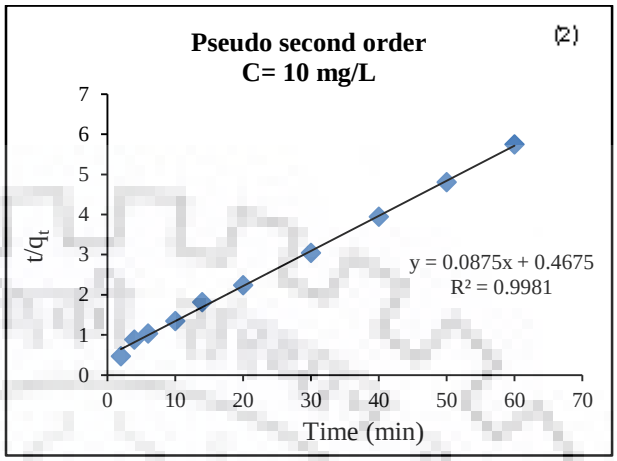
Pseudo second order
C= 10 mg/L
(2)
t/qt
y = 0.0875x + 0.4675
R² = 0.9981
Time (min)

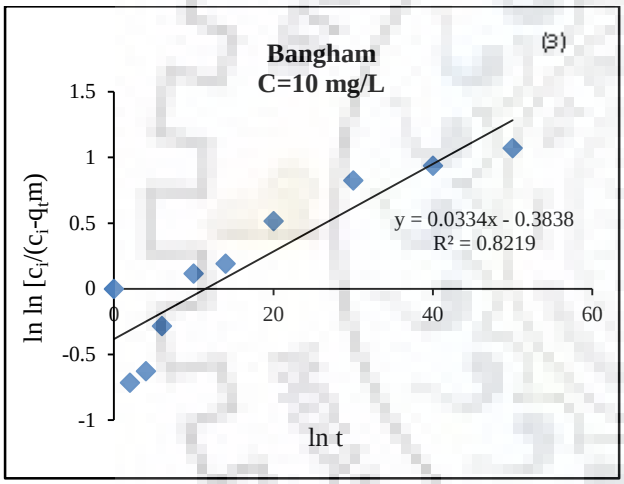
Bangham
C=10 mg/L
(3)
ln ln [Ci/(Ci-qtm)
y = 0.0334x - 0.3838
R² = 0.8219
ln t

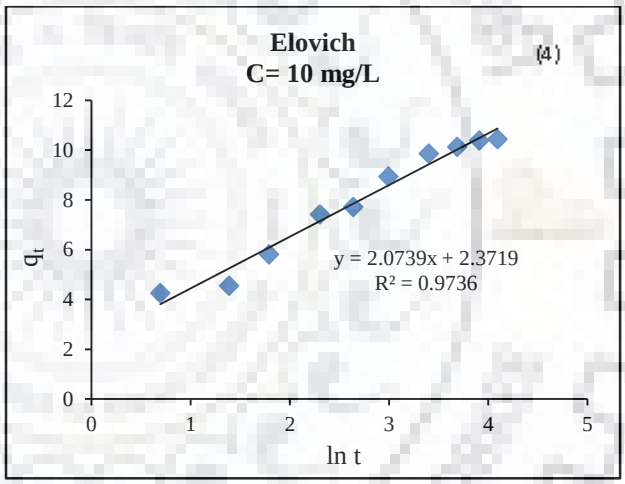
Elovich
C= 10 mg/L
(4)
qt
y = 2.0739x + 2.3719
R² = 0.9736
ln t

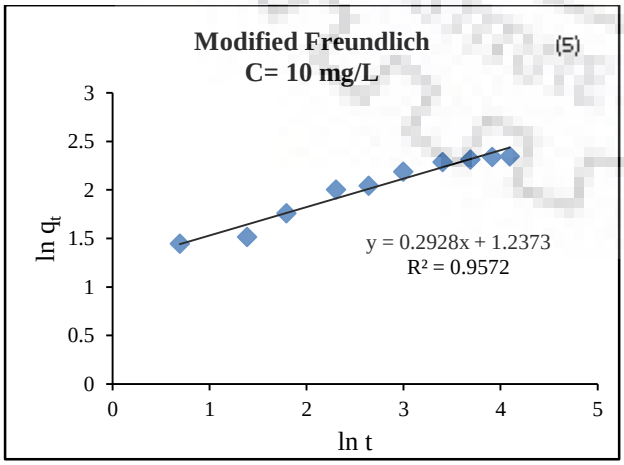
Modified Freundlich
C= 10 mg/L
(5)
ln qt
y = 0.2928x + 1.2373
R² = 0.9572
ln t

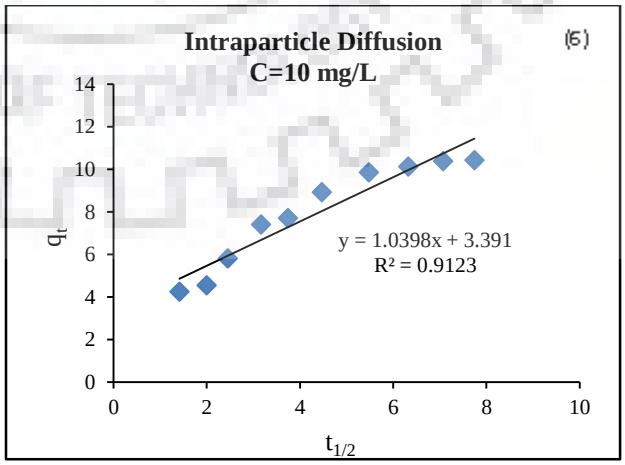
Intraparticle Diffusion
C=10 mg/L
(6)
qt
y = 1.0398x + 3.391
R² = 0.9123
t1/2

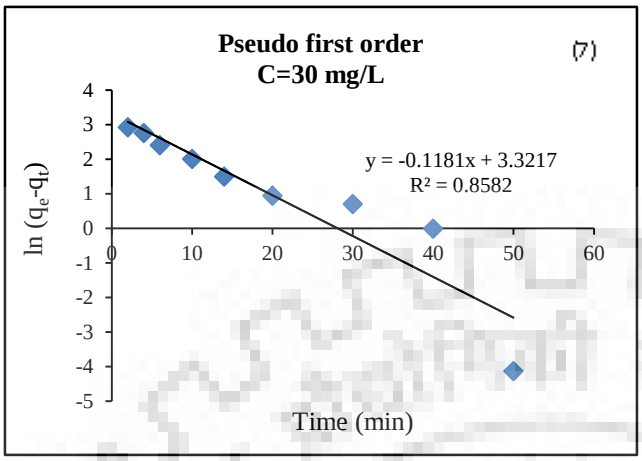
Pseudo first order
C=30 mg/L
(7)
y = -0.1181x + 3.3217
R² = 0.8582
ln (qe-qt)
Time (min)

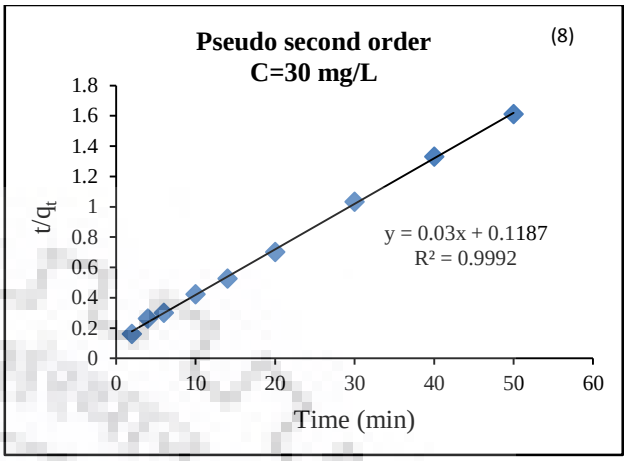
Pseudo second order
C=30 mg/L
(8)
y = 0.03x + 0.1187
R² = 0.9992
t/qt
Time (min)

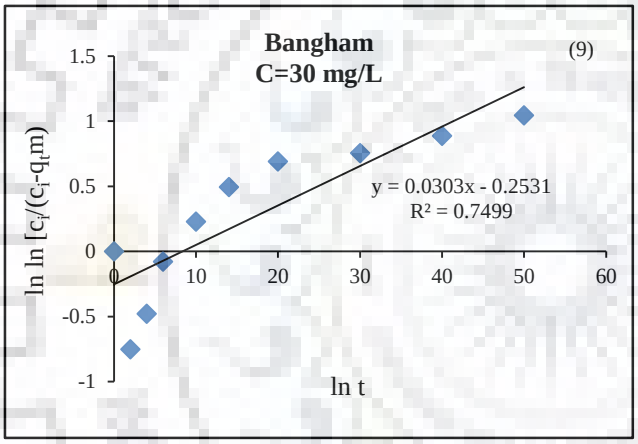
Bangham
C=30 mg/L
(9)
y = 0.0303x - 0.2531
R² = 0.7499
ln ln [Ci/(Ci-qtm)
ln t

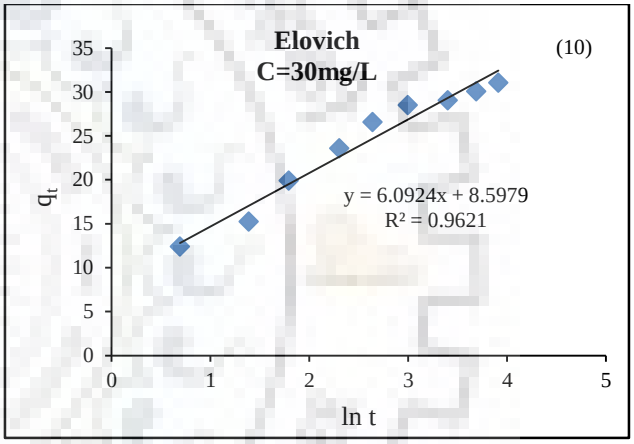
Elovich
C=30mg/L
(10)
y = 6.0924x + 8.5979
R² = 0.9621
qt
ln t

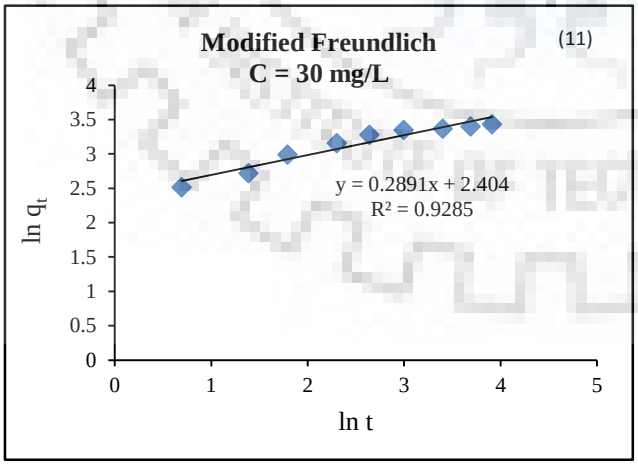
Modified Freundlich
C = 30 mg/L
(11)
y = 0.2891x + 2.404
R² = 0.9285
ln qt
ln t

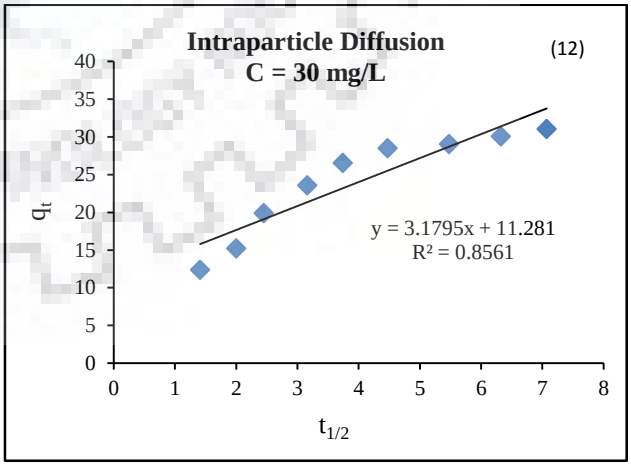
Intraparticle Diffusion
C = 30 mg/L
(12)
y = 3.1795x + 11.281
R² = 0.8561
qt
t1/2

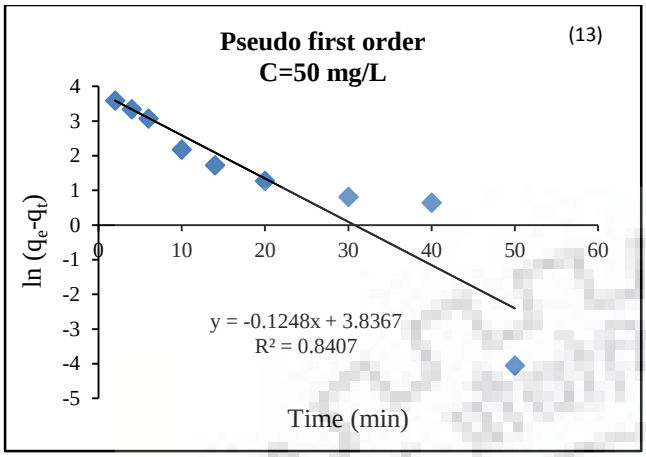
Pseudo first order
C=50 mg/L
(13)
ln (qe-qt)
y = -0.1248x + 3.8367
R² = 0.8407
Time (min)

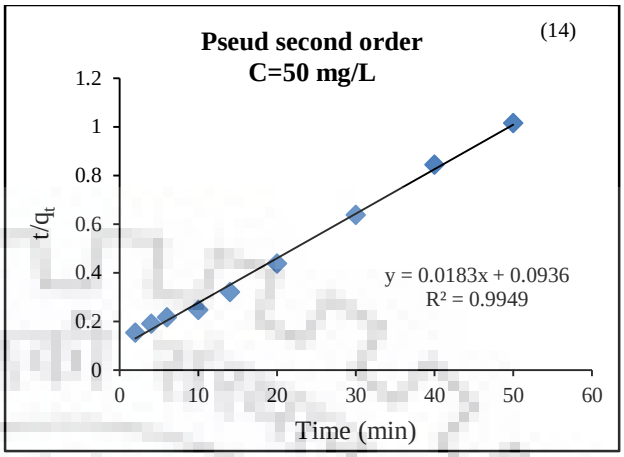
Pseud second order
C=50 mg/L
(14)
t/qt
y = 0.0183x + 0.0936
R² = 0.9949
Time (min)

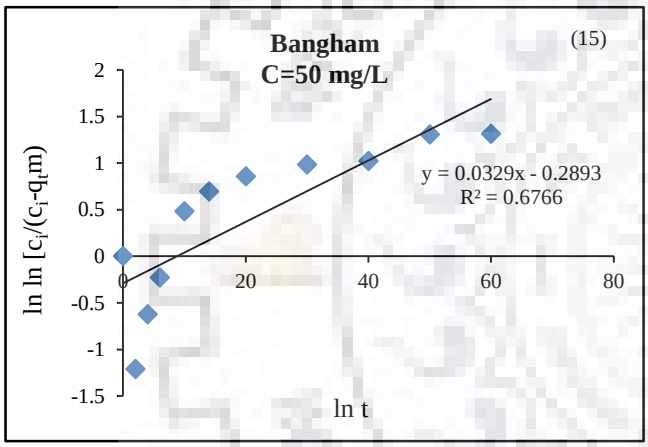
Bangham
C=50 mg/L
(15)
ln ln [Ci/(Ci-qtm)
y = 0.0329x - 0.2893
R² = 0.6766
ln t

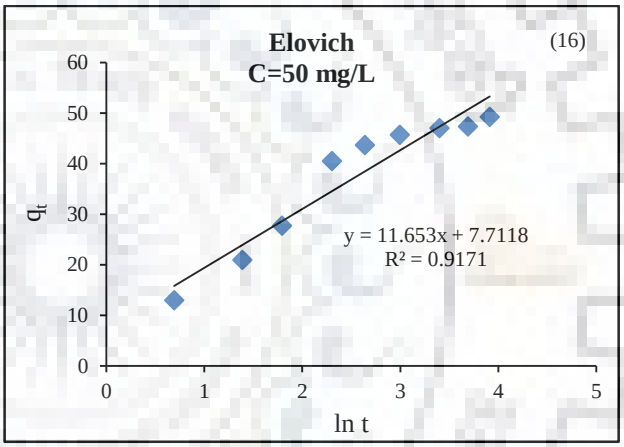
Elovich
C=50 mg/L
(16)
qt
y = 11.653x + 7.7118
R² = 0.9171
ln t

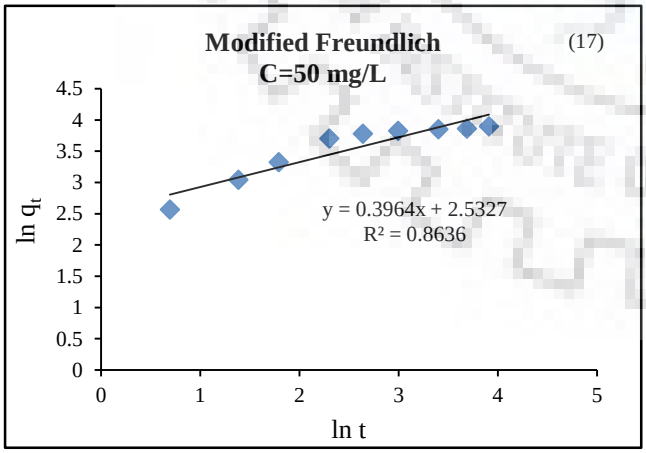
Modified Freundlich
C=50 mg/L
(17)
ln qt
y = 0.3964x + 2.5327
R² = 0.8636
ln t

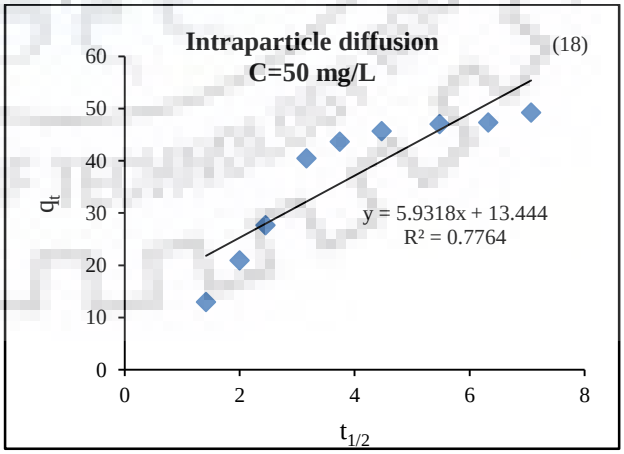
Intraparticle diffusion
C=50 mg/L
(18)
qt
y = 5.9318x + 13.444
R² = 0.7764
t1/2

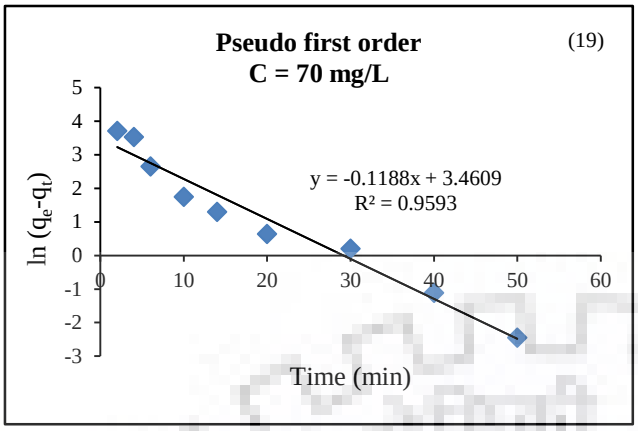
Pseudo first order
C = 70 mg/L
(19)
y = -0.1188x + 3.4609
R² = 0.9593
ln (qe-qt)
Time (min)

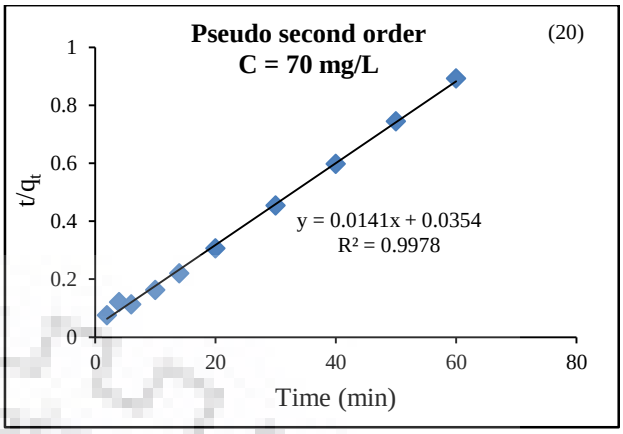
Pseudo second order
C = 70 mg/L
(20)
y = 0.0141x + 0.0354
R² = 0.9978
t/qt
Time (min)

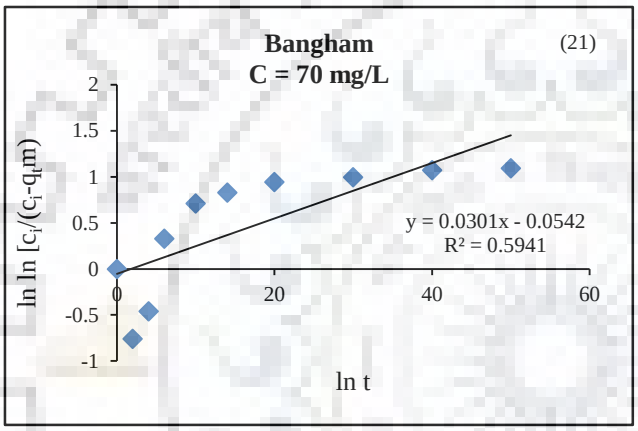
Bangham
C = 70 mg/L
(21)
y = 0.0301x - 0.0542
R² = 0.5941
ln ln [Ci/(Ci-qtm)]
ln t

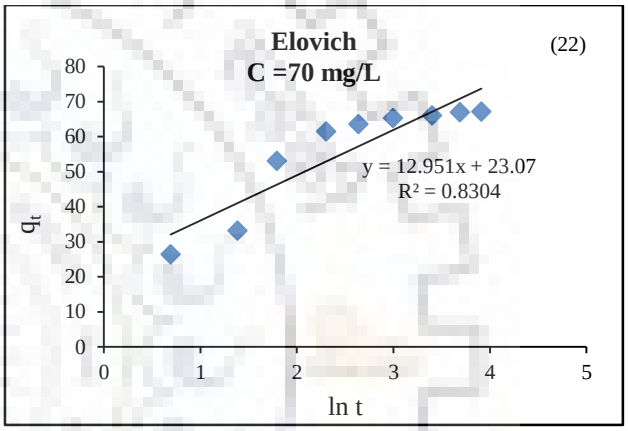
Elovich
C =70 mg/L
(22)
y = 12.951x + 23.07
R² = 0.8304
qt
ln t

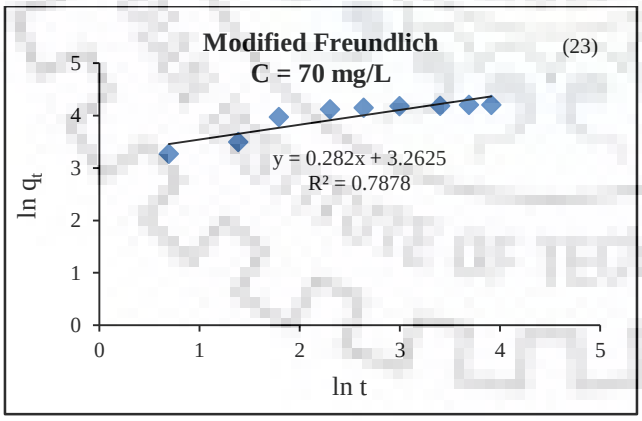
Modified Freundlich
C = 70 mg/L
(23)
y = 0.282x + 3.2625
R² = 0.7878
ln qt
ln t

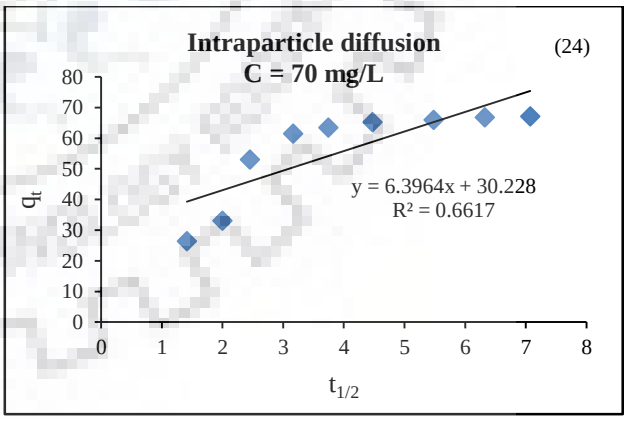
Intraparticle diffusion
C = 70 mg/L
(24)
y = 6.3964x + 30.228
R² = 0.6617
qt
t1/2

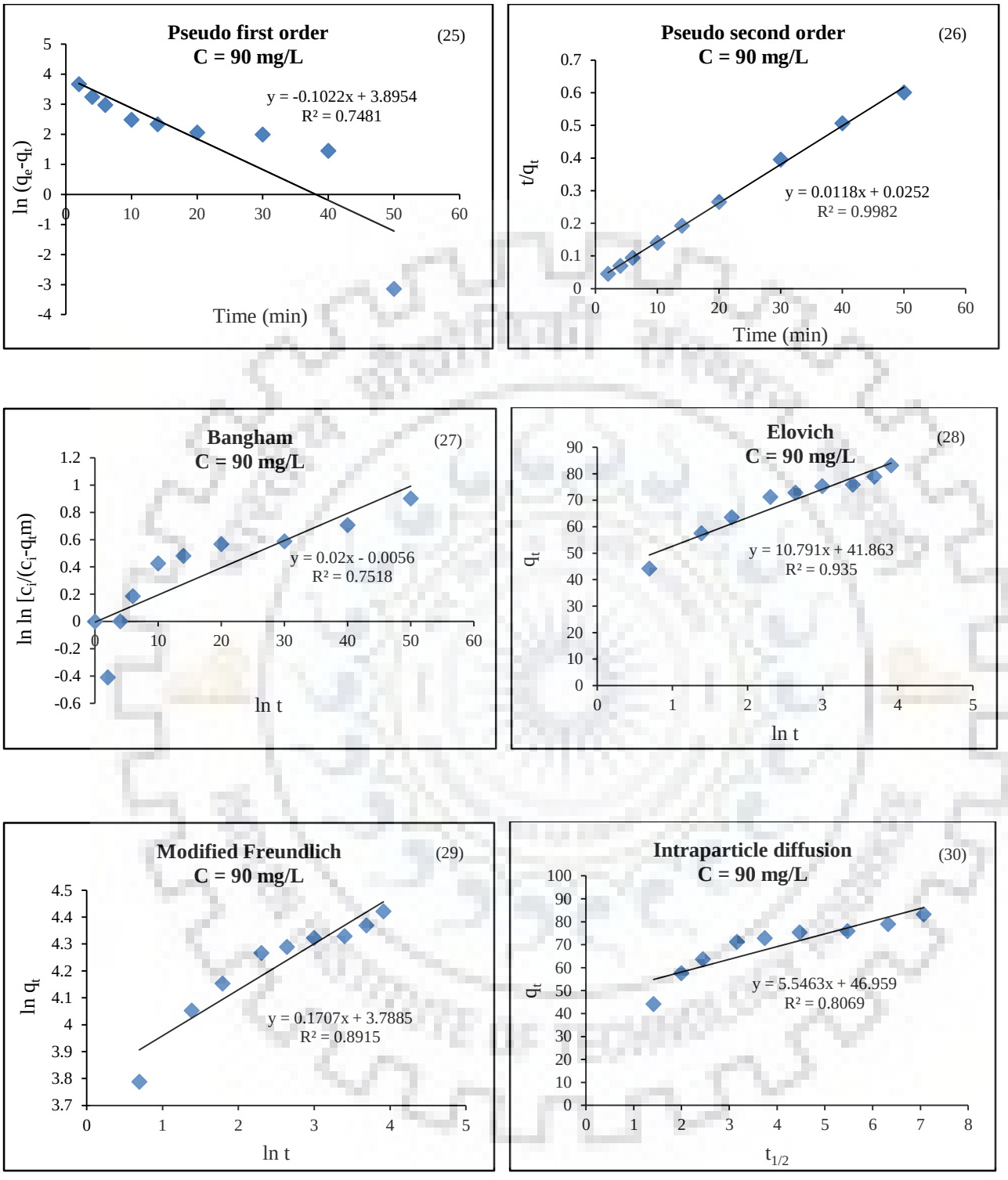

Fig. 4.18 (1-30) Graphical representation of kinetic models for biosorption of Cd^{2+} ions on *S. filipendula* at different initial Cd^{2+} ions concentrations.

Table 4.11 Isotherm model parameters for Cd^{2+} ions biosorption onto *S. filipendula* at different temperatures

Isotherm model	Parameters	Temperature (^{0}C)			
		20	25	30	35
Langmuir	q_o	17.86	59.69	70.36	103.5
	b	0.0419	0.024	0.159	0.193
	R^2	0.946	0.99	0.989	0.987
	Δq %	7.498	13.47	7.313	7.691
	χ^2	0.37	1.43	0.69	1.25
Freundlich	k_f	2.072	4.327	17.24	23.04
	n	2.281	2.07	2.838	2.28
	R^2	0.948	0.9835	0.924	0.964
	Δq %	12.73	12.14	29.61	29.068
	χ^2	0.54	0.61	5.2	4.18
Radke-Prausnitz	q	0.226	0.146	0.055	0.339
	K_o	5.635	17.11	148.8	72.03
	a	0.759	0.797	1.193	0.891
	R^2	0.956	0.993	0.994	0.988
	Δq %	8.92	3.555	12.439	5.641
	$\chi 2$	0.374	0.137	1.42	0.91
Redlich - Peterson	K_1	1.275	2.506	8.328	24.17
	K_2	0.226	0.146	0.055	0.339
	b_o	0.759	0.797	1.193	0.891
	R^2	0.956	0.995	0.994	0.998
	Δq %	0.089	0.035	0.124	0.056
	$\chi 2$	0.35	0.109	0.47	0.86
Toth	q_o	4.024	10.62	388.1	60.44
	a_T	6.732	8.671	15.19	3.112
	n_1	1.422	1.4	0.721	1.171
	R^2	0.971	0.996	0.996	0.992
	Δq %	8.68	3.389	11.287	5.612
	$\chi 2$	0.36	0.131	1.08	0.89
Fritz	α_1	0.00053	0.689	9.944	19.33
	α_2	0.000362	0.118	0.012	7.144×10^{-6}
	β_1	5.582	2.426	0.745	0.559
	β_2	5.062	2.016	1.308	3.47
	R^2	0.925	0.994	0.996	0.984
	Δq %	11.502	2.604	4.678	13.626
	$\chi 2$	0.859	0.140	1.36	1.22

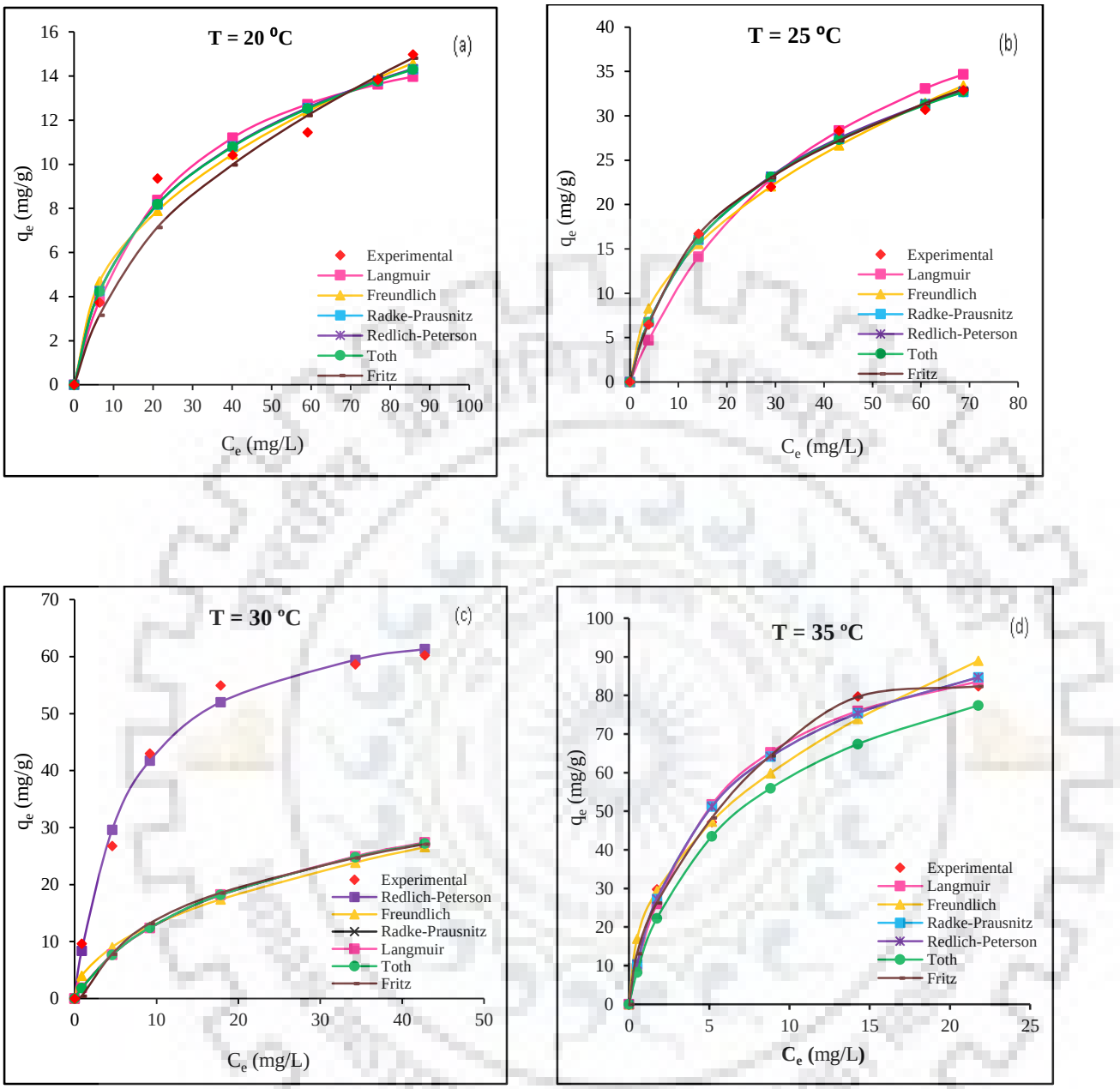

Fig. 4.19 Comparison of different isotherm models for Cd^{2+} ions biosorption on *S. filipendula*: (a) T = 20 °C (b) T = 25 °C (c) T = 30 °C (d) T = 35 °C.

4.2.5 Isotherm results interpretation

In order to determine Cd^{2+} ions biosorption isotherms at different temperatures, experiments were performed at four different temperatures (20, 25, 30 and 35 °C) by varying initial concentration from 10 to 100 mg/L with constant biosorbent dosage of 1.0 g/L. All models' parameters were calculated by non-linear regression using the MATLAB 2013 software. The best fitted isotherm model was selected on the basis of coefficient of determination (R^2), chi square test (χ^2) and normalized standard deviation (Δq %). The values of different isotherm model parameters with their R^2, and Δq % values are given in **Table 4.11.** The R^2 value for all the isotherm models of all four temperatures were greater than 0.90 while the values of chi square test (χ^2) and normalized standard deviation Δq % were smaller in case of Redlich-Peterson model as comparison to other isotherm models (**Table 4.11**). According to these results, it can be decided that Redlich-Peterson model gives a good correlation for Cd^{2+} ions biosorption on *S. filipendula*. The comparison of different isotherm model with experimental results for all the four temperatures are given in **Fig. 4.19 (a-d).** The favorable biosorption system can be confirmed by the shape of isotherm models.

4.2.6 Thermodynamic study

The spontaneity of biosorption process was examined by thermodynamic parameters like free energy change ($\Delta G°$), enthalpy change ($\Delta H°$), and entropy change ($\Delta S°$). The values of thermodynamic parameters are given in **Table 4.12**. The value of $\Delta H°$ and $\Delta S°$ were calculated from intercept and slope of a plot of ΔG^o *vs. T* (**Fig. 4.20**). The positive value of $\Delta H°$ (260.47 J/mol) specifies the endothermic nature of Cd^{2+} ions biosorption which indicate the increase in removal efficiency of Cd^{2+} ions with rise in temperature [139]. The scale of the $\Delta H°$ value gives information about the type of biosorption, which can be either chemical or physical. The heat of biosorption, varying from 0.5 to 5 kcal/mol (2.1-20.9 kJ/mol), indicates physical biosorption, and the activation energy for chemical biosorption is of the same level as the heat of chemical reactions, 5-100 kcal/mol (20.9-418.4 kJ/mol) [317]. The biosorption heat of Cd^{2+} ions onto *S. filipenudla* was of the same level as the heat of chemisorption. The positive value of entropy change, $\Delta S°$ (0.8743 J/mol.K) shows the increase in disorderness at the solid / liquid interface

during Cd^{2+} ions biosorption onto *S. filipendula*. The negative value of $\Delta G°$ reveals that Cd^{2+} ions biosorption process was feasible and spontaneous which does not require any external source of energy for the system. Similar results were found for Cd^{2+} ions biosorption using *Annona squamosa* shell [146].

Table 4.12 Thermodynamic parameters for biosorption of Cd^{2+} ions on *S. filipendula*

T (K)	$\Delta G°$ (kJ/mol)	$\Delta H°$ (J/mol)	$\Delta S°$ (J/mol.K)
293	-0.091	260.47	0.874
303	-3.82		
308	-5.58		
313	-8.51		

4.2.7 Desorption study

For this study, 0.2 M HCl was used as eluent to recover Cd^{2+} ions from *S. filipendula*. The desorption of metal ions from the biosorbent depends on ion-exchange mechanism between the metal ions and H^+ ions released from the acid [149]. After four successive biosorption/desorption cycles, the biosorption and desorption efficiency was evaluated. It was observed that after four cycles, the biosorption and desorption efficiency was decreased by 7.18 % and 9.62 %, respectively (**Fig. 4.21**). The biosorption / desorption cycle was stopped at fourth cycle to avoid any loss of biosorbent mass. Hence, from economical point of view four cycles of biosorption/desorption process were suitable for the recovery of Cd^{2+} ions.

4.2.8 Specific surface area of *S. filipendula* for Cd^{2+} ions biosorption

As the molecular weight of Cd^{2+} ions is 112 and the cross sectional area is 3.73 m^2 [16, 96]. The specific surface area of *S. filipendula* for Cd^{2+} ions biosorption was found to be 20.75 m^2/g. **Table 4.13** shows the comparison of specific surface area of different adsorbents for Cd^{2+} ions adsorption.

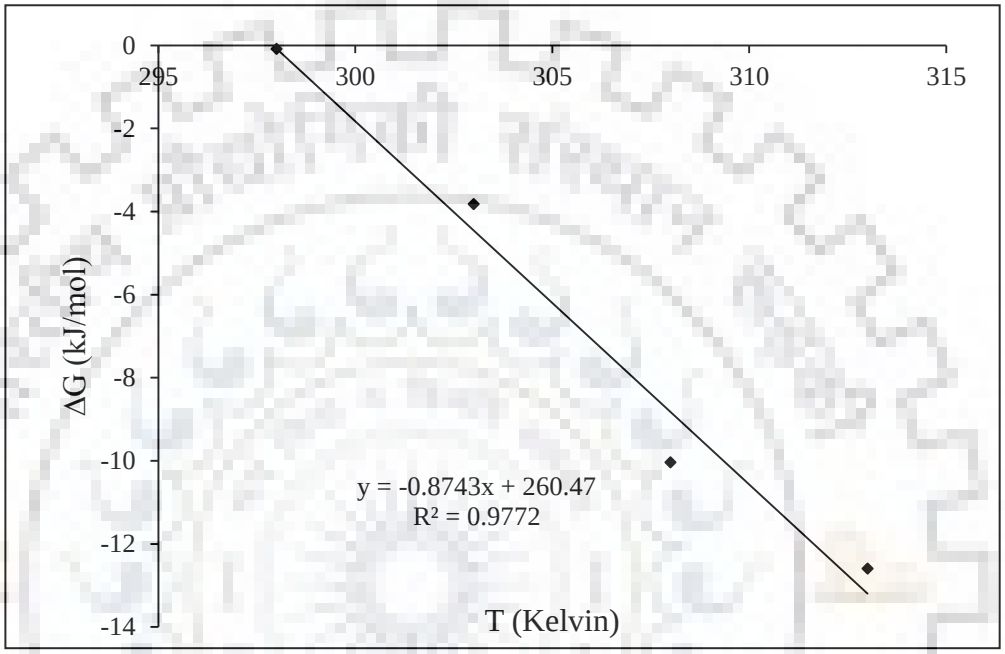

Fig. 4.20 Plot of $\Delta G°$ *vs.* temperature for the evaluation of thermodynamic parameters of Cd^{2+} ions biosorption by *S. filipendula*.

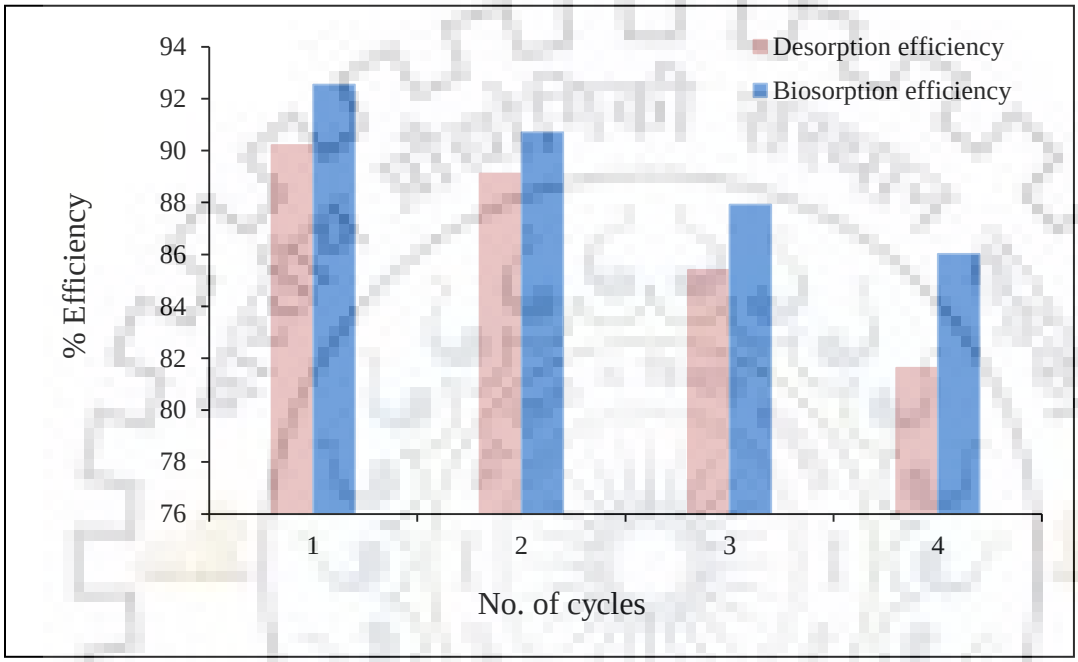

Fig. 4.21 Biosorption-desorption efficiency with cycle number.

Table 4.13 The specific surface area of different adsorbents for Cd^{2+} ions adsorption

Adsorbent	q_m (mg/g)	S (m^2/g)	Reference
Rice husk	5.12	11.3	[158]
Oryza sativa	20.7	4.15	[16]
Wheat straw	39.22	7.88	[96]
Sargassum filipendula	103.5	20.75	This study

4.2.9 Conclusions

The biosorption of Cd^{2+} ions on *S. filipendula* was examined by performing batch experiments. RSM was used to optimize the process parameters of Cd^{2+} ions biosorption on *S. filipendula*. The relationship between the response (% removal) and the independent variables was obtained by the quadratic model. The optimum conditions at which 99.56 % removal efficiency of Cd^{2+} ions was achieved were obtained as pH (5.7), temperature (34.2 °C), initial Cd^{2+} ions concentration (50.8 mg/L), and biosorbent dosage (0.99 g/L). ANOVA results showed that biosorption of Cd^{2+} ions was significantly affected by the linear terms of pH, temperature, initial Cd^{2+} ions concentration, biosorbent dosage and square terms of pH, temperature, biosorbent dosage. Moreover, interactive effect of initial Cd^{2+} ions concentration and biosorbent dosage, pH and biosorbent dosage, and pH and temperature were also significant. The biosorption of Cd^{2+} ions follows a pseudo second order kinetic model ($R^2 > 0.98$) for all the initial Cd^{2+} ions concentration suggesting that chemisorption was the rate limiting step. Experimental data were fitted to six isotherms for four different temperatures and it was found that the Redlich-Peterson was the best fitted model with higher value of R^2 and small value of Δq % for all the four temperatures. The maximum monolayer biosorption capacity of Cd^{2+} ions at all four temperatures were obtained as 17.86 mg/g at 20 °C, 59.69 mg/g at 25 °C, 70.36 mg/g at 30 °C and 103.5 at 35 °C. FESEM-EDS and FTIR analysis of biosorbent confirms the presence of Cd^{2+} ions on the surface of *S. filipendula* after biosorption. Thermodynamic parameters (ΔG^o = -0.091 to -8.51 kJ/mol, ΔH^o = 260.47 J/mol, ΔS^o = 0.874 J/mol.K) revealed that the reaction for Cd^{2+} ions biosorption was spontaneous, feasible and endothermic in nature. After four successive biosorption/desorption cycles, 81.63 % of Cd^{2+} ions was recovered. The results suggested that *S. filipendula* could be used as a potential biosorbent for Cd^{2+} ions biosorption from aqueous solution.

4.3 REMOVAL OF Ni^{2+} IONS FROM AQUEOUS SOLUTION USING *S. FILIPENDULA*

4.3.1 FESEM-EDS Analysis of *S. filipendula*

Fig. 4.22 (a) shows the rough and porous form of *S. filipendula* before biosorption. **Fig. 4.22 (b)** shows that after biosorption of Ni^{2+} ions the pores and surface of *S. filipendula* were covered and the surface becomes smooth. It was evident that the structure of *S. filipendula* has changed after Ni^{2+} ions biosorption.

EDS analysis of biosorbent before and after Ni^{2+} ions biosorption confirms the biosorption of Ni^{2+} ions on the surface of *S. filipendula* as shown in **Fig. 4.23 (a & b)**. A peak of Ni^{2+} ions was noticed after biosorption process. Some of the cations initially present on cell wall matrix were replaced with Ni^{2+} ions present in solution and created a strong cross linkage.

4.3.2 Analysis of results of experiments

For the optimization of Ni^{2+} ions biosorption on *S. filipendula*, the effects of four operating parameters namely temperature, pH, biosorbent dosage, and initial Ni^{2+} ions concentration on removal efficiency of Ni^{2+} ions were studied using RSM. The batch runs were conducted according to CCD designed experiments in order to investigate the optimum combination of aforementioned four biosorption process parameters on removal of Ni^{2+} ions. The detailed results and discussion of the designed experiments carried out are given in the following subsections.

4.3.2.1 Experimental design and factorial model for Ni^{2+} ions biosorption process

The matrix of four variables pH, initial Ni^{2+} ions concentration, biosorbent dosage, and temperature were varied at 5 levels ($-\alpha$, -1, 0, +1, $+\alpha$) as shown in **Table 4.14**. The higher and lower levels of variables were symbolized as '+' and '-', respectively. **Table 4.15** shows the result of CCD experiments for analyzing the effect of four independent parameters along with the response as % removal efficiency.

(a)

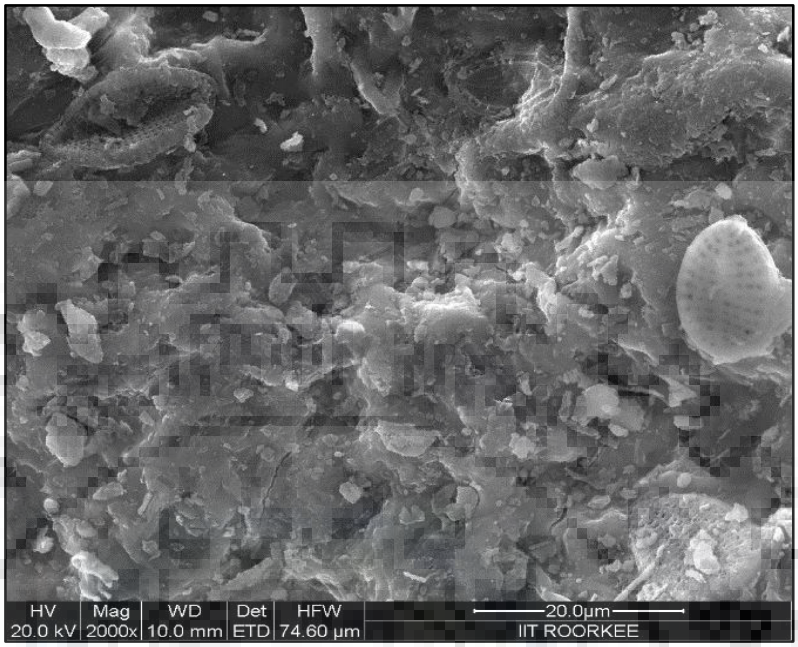

(b)

Fig. 4.22 FESEM images for Ni^{2+} ions biosorption on *S. filipendula* (a) before biosorption (b) after biosorption.

(a)

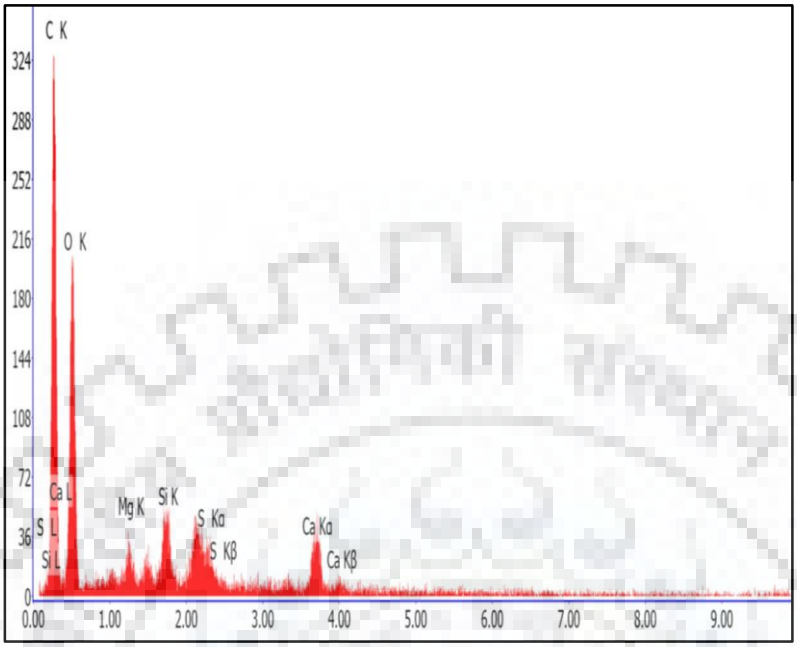

(b)

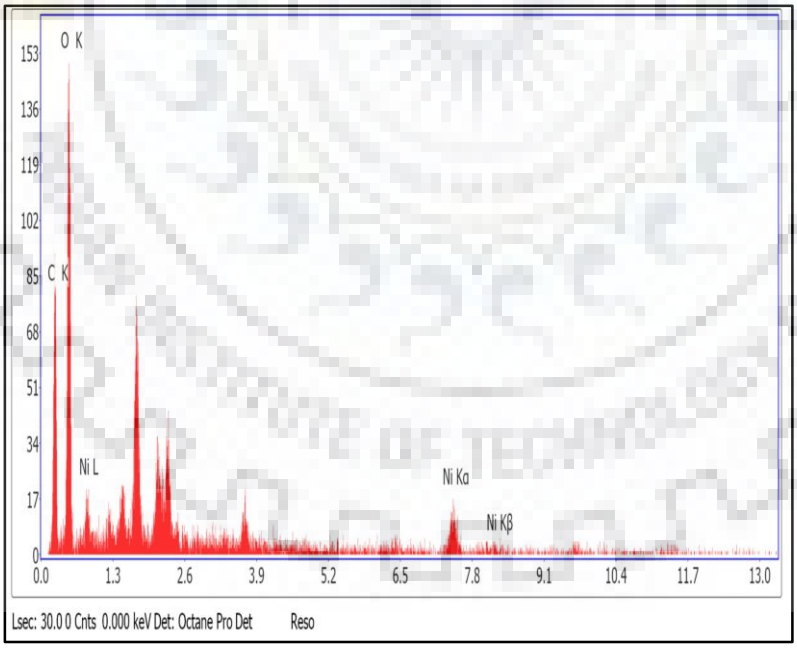

Fig. 4.23 EDS images for Ni^{2+} ions biosorption on *S. filipendula* (a) before biosorption (b) after biosorption.

Table 4.14 Range and level of the independent variables for Ni^{2+} ions biosorption

Independent variables	Range and levels (coded)				
	-α	**-1**	**0**	**+α**	**+1**
Temperature, °C (A)	10	20	30	50	40
pH (B)	1.5	3.0	4.5	7.5	6.0
Biosorbent dosage, g/L (C)	0.25	1.0	1.75	3.25	2.5
Initial Ni^{2+} ions concentration, mg/L (D)	25	50	100	200	150

The experimental results were determined and approximating functions of percent removal of Ni^{2+} ions were expressed by the following second order polynomial equation:

$$Y\ (\%) = +\ 57.2 + 12.88\ A + 8.86\ B + 3.5\ C - 3.21\ D + 3.24\ AB + 0.49\ AC - 1.49\ AD + 0.12\ BC - 1.36\ BD - 0.87\ CD - 6.78\ A^2 - 10.39\ B^2 - 7.35\ C^2 - 8.97\ D^2 \quad (4.3)$$

where, Y represents removal percent of Ni^{2+} ions. A, B, C, and D represents the coded values of temperature, pH, biosorbent dosage and initial Ni^{2+} ions concentration, respectively. The negative sign indicates antagonistic and positive sign indicates synergistic effect of process parameters on removal of Ni^{2+} ions. The statistical significance of the quadratic model was determined by analysis of variance as given in **Table 4.16**. The significant of each coefficient was evaluated by *p-values* and *F-values*. The model term which has smaller *p-value* and larger *F-value* will be more significant. For this model the *p-value* was <0.0001 and *F-value* was 11.37 implies that the model was significant for removal of Ni^{2+} ions. The value of "Prob>F" less than 0.0500 shows that model terms were significant. In this case A, B, A^2, B^2, C^2, and D^2 were significant model terms. The determination coefficient (R^2 = 0.91) was reasonability good which explained 91 % of the total variation in the response. The "Lack of Fit F-value" of 17.69 implies that the Lack of Fit was significant. There was only 0.28 % chance that a "Lack of Fit F-value" this large could occur due to noise. The "*Adequate precision*" ration of this model was 9.78 which was an adequate signal for the model.

Table 4.15 Experimental design based on CCD and its response for Ni^{2+} ions biosorption on *S. filipendula*

Run	Temperature (°C)	pH	Biosorbent dosage (g/L)	Initial Ni^{2+} ions concentration (mg/L)	Removal (%)
1	40	3.0	2.5	150	13
2	30	4.5	1.75	200	28.3
3	20	6.0	2.5	50	26
4	30	4.5	1.75	100	58
5	30	4.5	1.75	100	58.7
6	30	4.5	1.75	100	58.5
7	40	6.0	1.0	50	48
8	40	3.0	2.5	50	30
9	30	1.5	1.75	100	6.7
10	30	4.5	1.75	100	57.8
11	50	4.5	1.75	100	71
12	40	3.0	1.0	50	20
13	10	4.5	1.75	100	2.54
14	20	3.0	1.0	50	3
15	30	4.5	0.25	100	22
16	30	4.5	1.5	25	70
17	30	4.5	1.75	100	58
18	20	3.0	2.5	150	3.98
19	30	4.5	1.75	100	58
20	30	4.5	3.25	100	47
21	20	6.0	1.0	50	18
22	40	6.0	2.5	50	52
23	40	6.0	2.5	150	40
24	20	3.0	2.5	50	5
25	30	7.5	1.75	100	38
26	20	6.0	1.0	150	9
27	20	6.0	2.5	150	10
28	20	3.0	1.0	150	1.86
29	40	3.0	1.0	150	11
30	40	6.0	1.0	150	35

Table 4.16 ANOVA for response surface quadratic model of Ni^{2+} ions biosorption

Source	Sum of Squares	df	Mean Square	*F-value*	*p-value*	Remarks
Model	12288.97	14	877.78	11.37	< 0.0001	Significant
A	3980.44	1	3980.44	51.58	< 0.0001	Significant
B	1886.12	1	1886.12	24.44	0.0002	Significant
C	294.84	1	294.84	3.82	0.0709	Not Significant
D	176.72	1	176.72	2.29	0.1525	Not Significant
AB	167.96	1	167.96	2.18	0.1000	Not Significant
AC	3.88	1	3.88	0.050	0.8258	Not Significant
AD	35.52	1	35.52	0.46	0.5085	Not Significant
BC	0.22	1	0.22	$2.863x10^{-3}$	0.9581	Not Significant
BD	29.81	1	29.81	0.39	0.5442	Not Significant
CD	12.04	1	12.04	0.16	0.6988	Not Significant
A^2	1226.49	1	1226.49	15.89	0.0014	Significant
B^2	2876.97	1	2876.97	37.28	< 0.0001	Significant
C^2	1440.34	1	1440.34	18.66	0.0007	Significant
D^2	1286.90	1	1286.90	16.68	0.0011	Significant
Residual	1080.37	14	77.17	-	-	-
Lack of Fit	1047.47	9	116.39	17.69	0.0028	Significant
Pure Error	32.90	5	6.58	-	-	-
Total	13369.34	28	-	-	-	-
R^2 = 0.9192; *Adjusted* R^2 = 0.8384; *Predicted* R^2 = 0.80; *Adequate precision* = 9.785						

Fig. 4.24 (a) shows the plot of normal probability *vs.* studentized residuals which shows whether the residuals follow a normal distribution of points along a straight line. **Fig. 4.24 (b)** shows that the predicted data values of reduces quadratic model was in well agreement with actual values.

4.3.2.2 Variation of process parameters on Ni^{2+} ions maximum removal efficiency

The optimum levels of different process parameters for Ni^{2+} ions biosorption were predicted from 3D graph as shown in **Fig. 4.25 (a-d)**. The 3D response surface plots are graphical representation of regression equation which shows the interaction effect of variables.

(a)

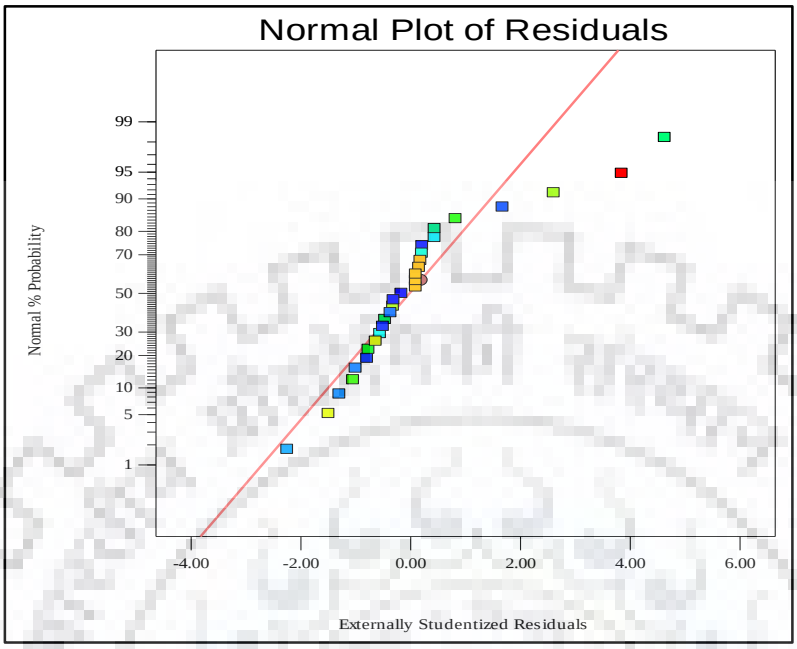

(b)

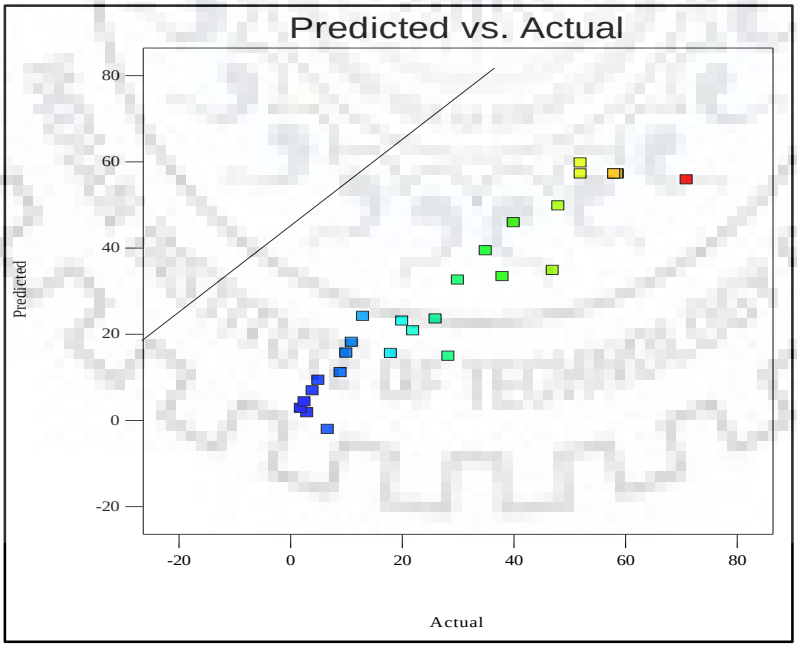

Fig. 4.24 (a) Normal probability plot (b) correlation between actual and predicted values.

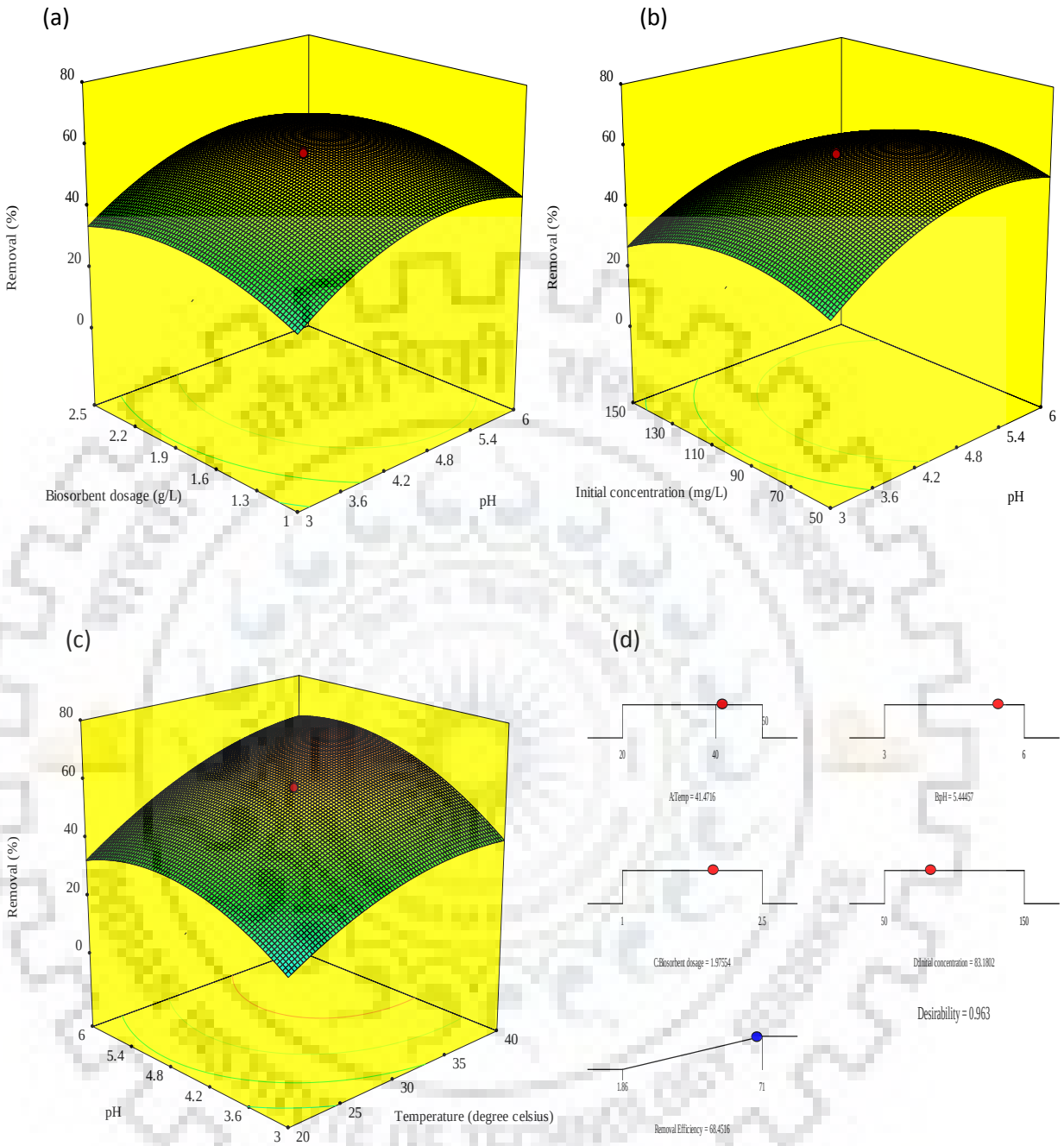

Fig. 4.25 (a) Interactive effect of pH and biosorbent dosage (b) Interactive effect of pH and initial concentration of Ni^{2+} ions (c) Interactive effect of pH and temperature (d) Desirability ramp for numerical optimization of four independent variables and the responses.

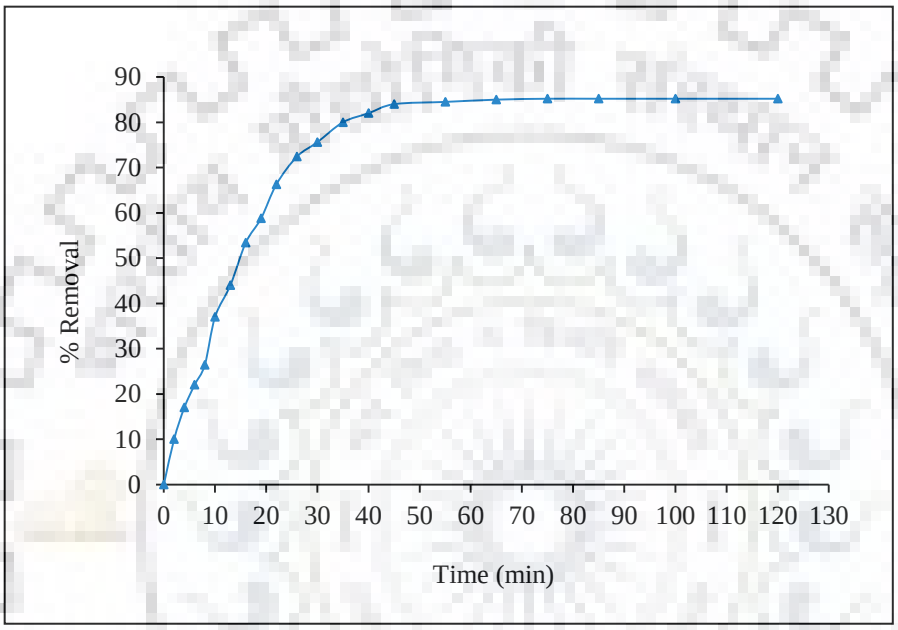

Fig. 4.26 Effect of contact time on removal efficiency of Ni^{2+} ions at T = 25 ºC, m = 2 g/L, C_o = 50 mg/L, pH = 5.0).

(i) Effect of contact time

Fig. 4.26 shows that the biosorption of Ni^{2+} ions gradually increased with contact time until equilibrium condition was reached after which there was no change in removal percent. Initially the removal rate of Ni^{2+} ions was very fast for first 10 min. In initial stage, the biosorption of metal ions occurs generally on biosorbent surface instead of pores, whereas ion exchange processes occur between the ions available on the solid and liquid phase. Fast diffusion on outer surface was followed by slow pore diffusion [207]. The equilibrium time for Ni^{2+} ions was found to be 60 min and beyond this time no further significant removal was noted. The fast biosorption rate at the initial stage may be due to the availability of a large number of vacant surface active sites while after a certain time period accessibility of active sites on biosorbent surface decreases which slows down the biosorption rate [323].

(ii) Effect of pH

The solution pH is an important factor which governed the extent of metal ions biosorption. The optimal pH value may be different for different metal ions depend on solution chemistry of the species [125]. The pH of solution influences the degree of ionization, species distribution of metal ions in aqueous solution, and surface charge of biosorbent [153]. The biosorption characteristic of Ni^{2+} ions was studied at different pH values varied from 1.5 to 7.5. For this study the range of pH was selected based on the reported data given in the literature [253]. At acidic pH, the surface of *S. filipendula* becomes positively charged with H^+ ions which cause electrostatic repulsion of Ni^{2+} ions for binding site of *S. filipendula*. While at higher pH, H^+ ions desorbs from binding sites which results in exposure of negatively charged ligands of *S. filipendula* for Ni^{2+} ions biosorption. Hence with increase in pH the percent removal of Ni^{2+} ions ions was increased, **Fig. 4.25 (a)**. While beyond pH value of 6.0, precipitation of Ni^{2+} ions was occured in form of hydroxides $Ni(OH)_2$ which results in decrease of removal efficiency [323].

(iii) Effect of biosorbent dosage

The biosorption process is greatly influenced by biosorbent dosage as it examined the biosorbent potential by the number of available binding sites for removal of metal ions. The selected range of biosorbent dosage was 0.25 to 3.25 g/L. **Fig. 4.25 (a)** shows that the percent

removal of Ni^{2+} ions was increased with increasing the *S. filipendula* dose. It can be explained as for fixed initial metal ion concentration an increase in biosorbent dosage provides large number of active sites and available surface area [207, 253]. Biosorption of Ni^{2+} ions reached an equilibrium at 2.0 g/L dose of *S. filipendula*, respectively. Further increase in biomass does not show any significant increase in removal efficiency of Ni^{2+} ions which may be due to the saturation of the *S. filipendula* surface [253]. Similar results were given in the literature [237, 255, 271].

(iv) Effect of initial Ni^{2+} ion concentration

The removal efficiency of *S. filipendula* as a function of the initial Ni^{2+} ions concentration was studied for 50 to 200 mg/L range in batch experiments. **Fig. 4.25 (b)** shows that the percent removal of Ni^{2+} ions was decreased from 70 to 28 % with increase in the initial Ni^{2+} ions concentration. It can be explained that all biosorbents have fixed number of binding sites which are available for binding of metal ions at low initial metal ions concentration but at high initial metal ions concentration the binding sites become saturated [308]. On the other hand, metal ions uptake capacity was increased with increasing initial metal ions concentration. It may be due to the fact that increase in the initial metal ions concentration provides a larger driving force to overcome mass transfer resistances between the solid and the liquid phase. Similar results were reported in literature [253, 323].

(v) Effect of temperature

The effect of temperature over the range of 20 to 50 ºC was examined to determine whether the biosorption process was exothermic or endothermic in nature. **Fig. 4.25 (c)** shows that the removal percent of Ni^{2+} ions was increased from 26 to 71 % with rise in temperature from 20 to 50 ºC. It indicates the endothermic nature of Ni^{2+} ions biosorption process. With increase in temperature the boundary layer thickness of biosorbent decreases which results in decrease of external layer resistance. The more surface area for biosorption was available due to widening of micro-pores and the increased accessibility for binding sites [323].

4.3.3 Optimization using the desirability function

The maximum point for desirability function was obtained by numerical optimization in which the values of reaction parameters were fixed within their ranges and maximizing the removal efficiency of Ni^{2+} ions [68]. It shows in **Fig. 4.25 (d)**, that the best local maximum value was found at temperature of 41.47 °C, pH of 5.4, biosorbent dosage of 1.97 g/L and initial Ni^{2+} ions concentration of 83.18 mg/L. In these conditions, Ni^{2+} ions removal efficiency and the desirability value were found to be 68.45 % and 1.0, respectively. This optimum condition was experimentally tested and results revealed that removal efficiency was achieved as 70 %. The high degree of agreement between the repeated experimental results and predicted optimum conditions indicates that RSM can be used as a reliable and effective tool to assess and optimize the effects of different biosorption process parameters on Ni^{2+} ions removal efficiency using *S. filipendula*.

4.3.4 Kinetic study

The experiments for kinetic study of Ni^{2+} ions biosorption on *S. filipendula* were performed at temperature of 35 °C, pH of 5.5, biosorbent dosage of 2.0 g/L, and initial Ni^{2+} ion concentration of 100 mg/L. The best fitted kinetic model was determined by the values of coefficient of determination (R^2) and normalized standard deviation (Δq %) which are given in **Table 4.17.** Graphical representation of kinetic models for Ni^{2+} ions biosorption on *S. filipendula* at different initial Ni^{2+} ions concentrations are shown in **Fig. 4.27 (1-6)**. The higher R^2 and small Δq % value of pseudo first order shows the best fitted kinetic model for Ni^{2+} ions biosorption. It indicates that Ni^{2+} ions biosorption process on *S. filipendula* was more inclined towards physisorption.

4.3.5 Equilibrium study

In order to determine Ni^{2+} ions biosorption isotherms, experiments were performed at pH 5.5, temperature 40 °C by varying initial Ni^{2+} ions concentration from 50 to 100 mg/L with constant biosorbent dosage of 2.0 g/L. The value of each isotherm model with their values of normalized standard deviation Δq % and correlation coefficient (R^2) are shown in **Table 4.18**. For Redlich-Peterson model the R^2 value was > 0.99 with smallest Δq % value. It indicates that Redlich-Peterson model was the best fitted isotherm model for Ni^{2+} ions biosorption on *S. filipendula*.

Table 4.17 Kinetic model parameters for Ni^{2+} ions biosorption using *S. filipendula*

Kinetic model parameters	Parameters value
$q_{e\ exp}$ (mg/g)	83.230
Pseudo first order	
$q_{e\ cal}$ (mg/g)	88.25
k_o (min^{-1})	0.057
R^2	0.989
$\Delta q\%$	6.78
Pseudo second order	
$q_{e\ cal}$ (mg/g)	108.7
K_2 (g/mg.min)	$5.47x10^{-4}$
R^2	0.963
$\Delta q\%$	12.13
Elovich	
α	13.81
β	0.042
R^2	0.938
$\Delta q\%$	20.12
Bangham	
α_o	0.842
k_b	6.97
R^2	0.957
$\Delta q\%$	15.43
Intra particle diffusion	
K_{id} ($mg.min^{0.5}/g$)	9.58
C	9.612
R^2	0.826
$\Delta q\%$	32.34
Modified Freundlich	
k_3 (L/g.min)	0.173
m_1	2.612
R^2	0.857
$\Delta q\%$	35.43

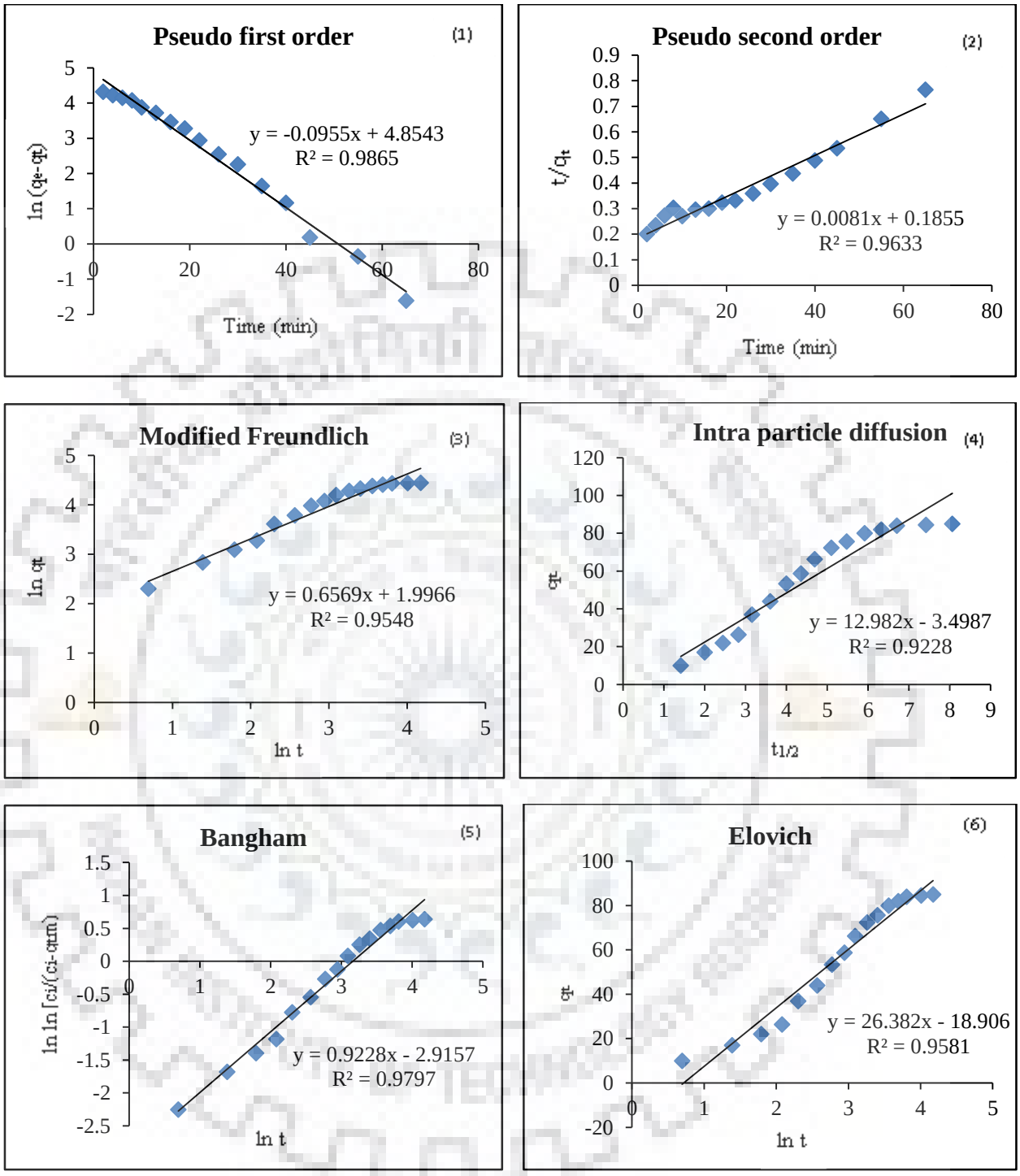

Fig. 4.27 (1-6) Graphical representation of kinetic models for biosorption of Ni^{2+} ions on *S. filipendula* (T = 40 ˚C, pH = 5.5, biosorbent dosage = 2.0 g/L, initial Ni^{2+} ions concentration = 100 mg/L).

Table 4.18 Isotherm model parameters for Ni^{2+} ions biosorption onto *S. filipendula*

Isotherm models	Parameters	Parameters values
Langmuir	q_o	34.3
	b	0.343
	R^2	0.81
	Δq %	39.27
Freundlich	k_f	23.04
	n	2.28
	R^2	0.994
	Δq %	1.039
Radke-Prausnitz	q	26.27
	K_o	6.19×10^{-4}
	a_R	0.187
	R^2	0.994
	Δq %	3.352
Redlich - Peterson	K_1	-0.0162
	K_2	26.27
	b_o	0.187
	R^2	0.994
	Δq %	0.988
Toth	q_e^{∞}	61.33
	a	5.78
	n_1	40.1
	R^2	0.949
	Δq %	39.27
Fritz	α_1	25.93
	α_2	3.56×10^{-13}
	β_1	0.1776
	β_2	6.575
	R^2	0.957
	Δq %	3.462

4.3.6 Thermodynamic study

The negative values of $\Delta G°$ shows the spontaneous nature of Ni^{2+} ions biosorption process and positive values of $\Delta H°$ (+ 79.175 J/mol) indicates the endothermic nature of Ni^{2+} ions biosorption on *S. filipendula* [210]. The positive values of entropy change, $\Delta S°$ (+ 0.270 J/mol.K) shows the increase in randomness at the solid/liquid interface during Ni^{2+} ions biosorption onto *S. filipendula* (**Table 4.19**).

Table 4.19 Thermodynamic parameters of Ni^{2+} ions biosorption process using *S. filipendula*

T (K)	$\Delta G°$ (kJ/mol)	$\Delta H°$ (J/mol)	$\Delta S°$ (J/mol.K)
298	- 0.097	79.175	0.270
303	-1.533		
308	-3.188		
313	-4.060		

4.3.7 Specific surface area of *S. filipendula* for Ni^{2+} ions biosorption

As the molecular weight of Ni^{2+} ions is 58.6 and the cross sectional area is 0.69 m^2. The specific surface area of *S. filipendula* for Ni^{2+} ions biosorption was found to be 2.43 m^2/g.

4.3.8 Conclusions

The biosorption of Ni^{2+} ions on *S. filipendula* was studied by conducting batch experiments. The optimization of process parameters for Ni^{2+} ions biosorption on *S. filipendula* was done by using RSM. The relationship between independent variables and response (% removal) was achieved by the quadratic model. The optimum conditions at which 68.45 % removal efficiency of Ni^{2+} ions were obtained as temperature of 41.47 °C, pH of 5.4, biosorbent dosage of 1.97 g/L, and initial Ni^{2+} ions concentration of 83.18 mg/L. ANOVA results showed that biosorption of Ni^{2+} ions was significantly affected by the linear terms of temperature, pH and square terms of temperature, pH, biosorbent dosage, initial Ni^{2+} ions concentration. Experimental data were fitted to six isotherm models and it was noticed that the Redlich-Peterson was the best fitted isotherm model with higher value of R^2 and small value of Δq %. The biosorption of Ni^{2+} ions follows a pseudo

first order kinetic model ($R^2 > 0.98$) indicating that physisorption was the rate limiting step. FESEM-EDS analysis of *S. filipendula* confirms the presence of Ni^{2+} ions on the surface of *S. filipendula* after biosorption. Thermodynamic parameters (ΔG^o = - 0.097 to -4.060kJ/mol, ΔH^o = 79.175 J/mol, ΔS^o = 0.270 J/mol.K) showed that Ni^{2+} ions biosorption process was feasible, spontaneous, and endothermic in nature.

4.4 COMPARISON OF DIFFERENT BIOSORBENTS EFFICACY FOR Pb^{2+}, Cd^{2+} AND Ni^{2+} IONS BIOSORPTION

The comparison of different biosorbents for Pb^{2+}, Cd^{2+}, and Ni^{2+} ions biosorption capacities is shown in **Table 4.20**. The biosorption affinity of a biosorbent for a metal ions correlate with physiochemical properties of metal ions [279]. The order of ionic radii: Pb^{2+} (133) > Cd^{2+} (109) >Ni^{2+} (83); electro negativity: Pb^{2+} (2.33) > Ni^{2+} (1.91) > Cd^{2+} (1.69); and atomic weight: Pb^{2+} (207.2) > Cd^{2+} (112.4) > Ni^{2+} (58.7). In reported literature similar order of affinity for Pb^{2+}, Cd^{2+}, and Ni^{2+} ions was shown by different biosorbents. Hence it shows a clear correlation between the amount of metal ions biosorbed and metals ion properties (ionic radii and atomic weight). Although electro negativity of Cd^{2+} ions found to be least as comparison to Ni^{2+} ions, instead of this the ionic radii and atomic weight favored Cd^{2+} ions to be biosorbed more than Ni^{2+} ions.

The value of biosorption capacity for Pb^{2+}, Cd^{2+}, and Ni^{2+} ions in this work was much greater than other reported biosorbents. Therefore, *S. filipendula* can be used as an effective biosorbent for metal ions uptake in the following order $Pb^{2+} > Cd^{2+} > Ni^{2+}$. Similar sequence was reported in literature for other adsorbents [348].

Table 4.20 Comparison of different biosorbents for biosorption capacities (mg/g) with affinity order of $Pb^{2+} > Cd^{2+} > Ni^{2+}$

S.No.	Biosorbent	Pb^{2+}	Cd^{2+}	Ni^{2+}	pH	Reference
1	*Nizimuddinia zanardini*	29.3	3.15	2.11	4.0	[253]
2	*Padina australis*	21.53	3.07	2.44	4.0	[253]
3	*Sargassum gluacescens*	21.53	5.72	3.08	4.0	[253]
4	*Padina* sp.	258.75	84	36.3	5.5	[284]
5	*Sargassum* sp.	240	85.12	35.74	5.5	[284]
6	*Spirulina platensis*	75	54	31	6.0	[276]
7	Anaerobic biomass	255	60	26	5.5	[137]
8	Sugar beet pulp	74.52	24.64	11.72	5.5	[258]
9	Activated sludge	89.01	68.32	18.16	5.5	[129]
10	*Sargassum filipendula*	367.94	103.5	34.3	5.0	This study

CHAPTER V

BIOSORPTION OF Pb^{2+} AND Cd^{2+} IONS FROM DUAL METAL IONS SYSTEM

5.0 INTRODUCTION

This Chapter deals with the competitive biosorption of Pb^{2+} and Cd^{2+} ions onto *S. filipendula* from dual metal ions systems. The main aim of this work was to determine the multicomponent isotherms for simultaneous removal of Pb^{2+} and Cd^{2+} ions by *S. filipendula* using equilibrium data. The effect of temperature, pH, initial metal ions concentration, and biosorbent dosage were investigated for simultaneous removal of Pb^{2+} and Cd^{2+} ions from dual metal ions system. The applicability of non-competitive biosorption isotherm models (i.e., Freundlich, Langmuir, Radke-Prausnitz, Redlich-Peterson, and Fritz) based on the regression analysis for single component were tested. The experimental data on biosorption equilibrium for the binary system containing Pb^{2+} and Cd^{2+} ions were gathered and examined for the applicability of the multicomponent biosorption isotherm equations. The parameters obtained from single metal ion isotherm modeling were used for multicomponent isotherm modeling. These isotherms may provide useful information for the design of processes to remove these metal ions from industrial effluents at low concentrations.

5.1 INVESTIGATION OF EFFECT OF VARIOUS BIOSORPTION PROCESS PARAMETERS ON SIMULTANEOUS REMOVAL OF Pb^{2+}-Cd^{2+} IONS FROM DUAL METAL IONS SYSTEM

(i) Effect of pH

In this study, pH varied from 2.0 to 6.0 was used for Cd^{2+} and Pb^{2+} ions biosorption. **Fig. 5.1**

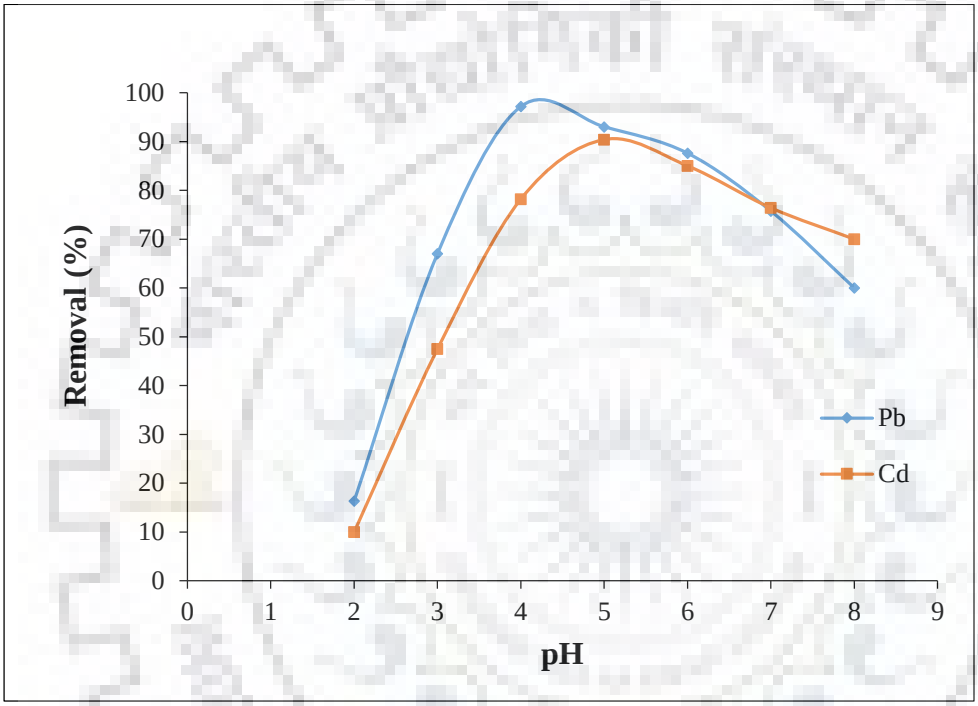

Fig. 5.1 Effect of pH on removal of Cd^{2+} and Pb^{2+} ions using *S. filipendula* (T = 35 °C, C_o = 150 mg/L, and m = 3 g/L).

shows the effect of pH on the simultaneous removal of Cd^{2+} and Pb^{2+} ions from aqueous solution. At pH = 2.0, the removal percent of Cd^{2+} and Pb^{2+} ions were very low 10 % and 16.35 %, respectively. The positively charged surface of biosorbent inhibits the binding of Cd^{2+} and Pb^{2+} ions on *S. filipendula* surface. With increase in solution pH, the removal percent of both the metal ions was increased. The increase in removal of Pb^{2+} ions was more as comparison to Cd^{2+} ions. The greatest removal efficiency of Pb^{2+} ions (97.82 %) and Cd^{2+} ions (86.73 %) was observed at pH 4.0 and 5.0, respectively. Above pH 6.0, Pb^{2+} and Cd^{2+} ions were precipitate in form of their hydroxides. Thus, solution pH 5.0 was chosen to conduct further experiments.

(ii) Effect of biosorbent dosage

The effect of biosorbent dosage on simultaneous uptake of Pb^{2+} and Cd^{2+} ions by *S. filipendula* was studied. **Fig. 5.2** indicates that removal efficiency of Pb^{2+} and Cd^{2+} ions was increased with increase in biosorbent dosage from 0.2 to 3 g/L. At m < 0.75 g/L, saturation of *S. filipendula* surface was occurred with metal ions while in liquid phase the remaining concentration of metal ions was become high. It was noticed that the removal efficiency of both metal ions was increasing with increase in biosorbent dosage due to increase in uptake of metal ions. While at m > 0.75 g/L, the increase in removal efficiency became very slow and at m = 1 g/L, this change becomes negligible. Therefore, 1 g/L of biosorbent dosage was selected for kinetic and equilibrium studies.

(iii) Effect of time

In order to examine the equilibrium time for simultaneous removal of Pb^{2+} and Cd^{2+} ions on *S. filipendula*, the experiments were performed for 100 min. **Fig. 5.3** shows the effect of time on removal efficiency of Pb^{2+} and Cd^{2+} ions. Initially, the rate of Pb^{2+} and Cd^{2+} ions removal was very high up to 15 min beyond this the removal rate was decreased. After 60 min, the change in removal efficiency of metal ions was negligible. The equilibrium time was found to be 60 min for removal of both Pb^{2+} and Cd^{2+} ions in multicomponent biosorption system.

(iv) Effect of temperature

The experiments were performed to examine the temperature effect on simultaneous removal of Pb^{2+} and Cd^{2+} ions. **Fig. 5.4** shows that removal of Pb^{2+} and Cd^{2+} ions increased with increase in

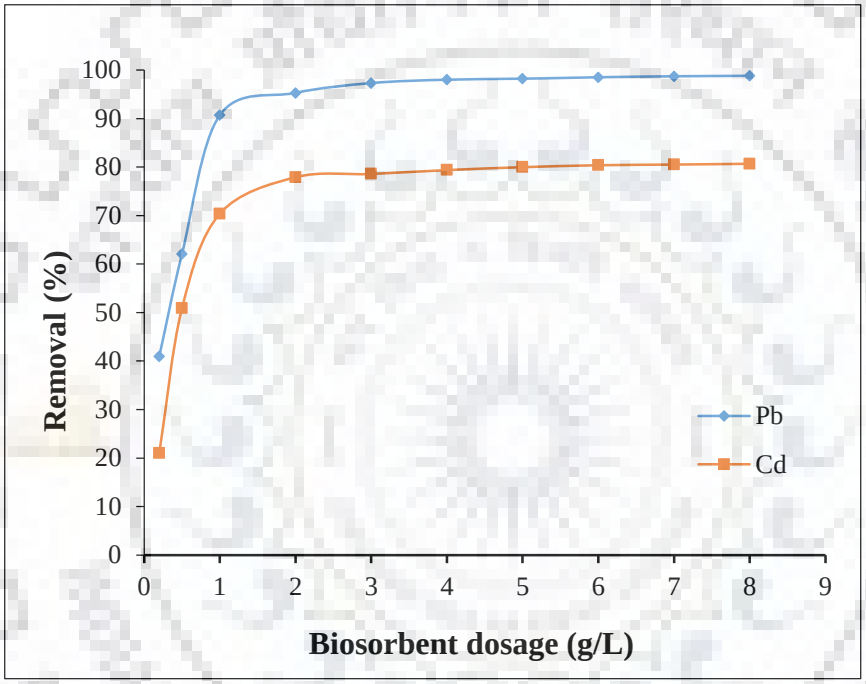

Fig. 5.2 Effect of biosorbent dosage on Pb^{2+} and Cd^{2+} ions biosorption using *S. filipendula* (T = 35 °C, C_o = 150 mg/L, pH = 5.0).

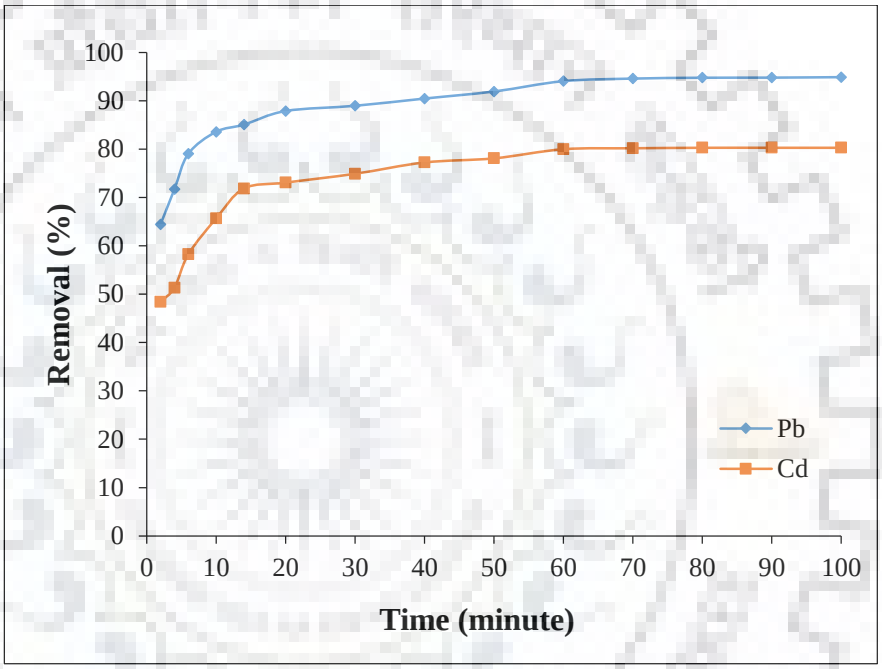

Fig. 5.3 Effect of contact time on Pb^{2+} and Cd^{2+} ions biosorption using *S. filipendula* (T = 35 °C, C_o = 150 mg/L, pH = 5.0, m = 1 g/L).

temperature from 20 ºC to 40 ºC. But, the increase in percentage of removal was more when the temperature was raised from 20 ºC to 30 ºC and beyond 30 ºC this change become more gradual. So for further experimental study 30 ºC temperature was selected.

5.2 COMPARISON OF Cd^{2+} AND Pb^{2+} IONS BIOSORPTION IN SINGLE AND DUAL METAL IONS SYSTEM

Table 5.1 shows the equilibrium uptake of metal ion, removal percent of single metal ion, and total metal ions in single and dual metal ions biosorption systems on *S. filipendula*. It was noticed that on increasing initial metal ion concentration (50 to 300 mg/L) the uptake of Cd^{2+} and Pb^{2+} ions was increased from 44 to 111.1 mg/g and 49.79 to 193.53 mg/g, respectively. While removal percent of both the metal ions was decreased from 88 % to 37.03 % for Cd^{2+} ions and from 99.58 % to 64.5 % for Pb^{2+} ions. The initial concentration of metal ion offers the required driving force which helps to overcome the mass transfer resistance of Cd^{2+} and Pb^{2+} ions between the solid and liquid phases. The rise in metal ion concentration also enhances the interaction between the metal ion present in solution and on *S. filipendula* surface [35, 50]. Thus, equilibrium uptake of Cd^{2+} and Pb^{2+} ions biosorption was increased with increase in initial concentration of metal ions. The simultaneous biosorption of Cd^{2+} and Pb^{2+} ions from dual metal ions solution was also examined. It was observed that the amount of metal ions biosorbed increased with increasing the initial concentration of one metal ion from 50 to 300 mg/L on addition of 50 mg/L of other metal ion. While the uptake of metal ion biosorbed in dual metal ions system decreased as comparison to single metal ion system. At 300 mg/L initial Pb^{2+} ions concentration, in absence and presence of Cd^{2+} ions (50 mg/L) the amount of Pb^{2+} ions biosorbed was 193.52 mg/g and 151.98 mg/g, respectively. Similar pattern of biosorption was followed by Cd^{2+} ions biosorption in absence and presence of Pb^{2+} ions (50 mg/L), the amount of Cd^{2+} ions biosorbed was 111.1 mg/g and 61.11 mg/g, respectively. It was noticed that with rise in initial concentration of one metal ion the removal percent of other metal ion was decreased.

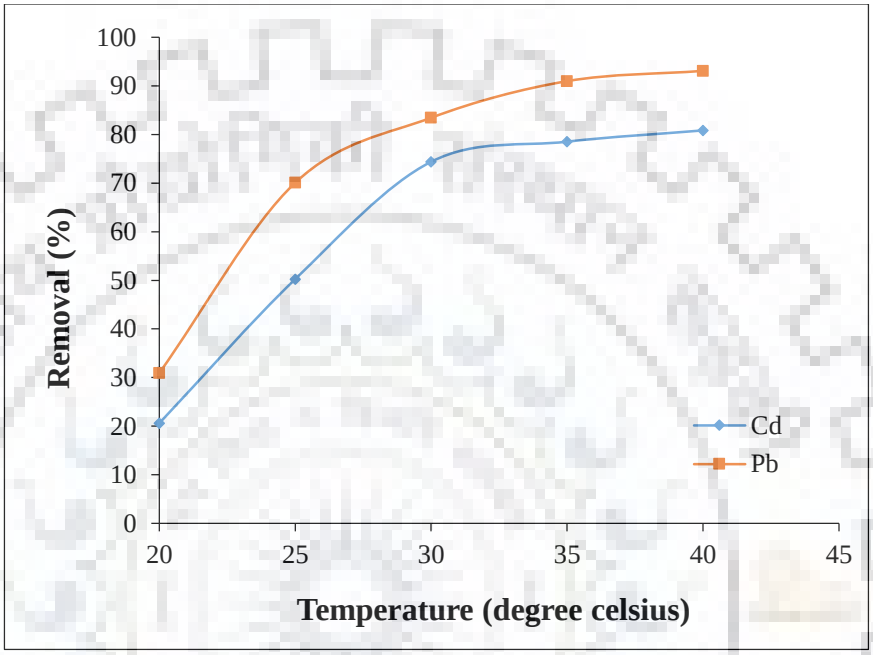

Fig. 5.4 Effect of temperature on Pb^{2+} and Cd^{2+} ions biosorption using *S. filipendula* (C_o = 150 mg/L, pH = 5.0, m = 1 g/L).

Table 5.1 Comparison of single and binary metal ion uptake capacity and removal percent

C_{oPb} (mg/L)	C_{oCd} (mg/L)	q_{ePb} (mg/g)	q_{eCd} (mg/g)	$Removal_{Pb}$ (%)	$Removal_{Cd}$ (%)	$Removal_{Total}$ (%)
50	0	49.79	0	99.58	0	99.58
75	0	74.01	0	98.69	0	98.69
100	0	96.2	0	96.2	0	96.2
150	0	143.95	0	95.97	0	95.97
200	0	165.92	0	82.96	0	82.96
250	0	180	0	72	0	72
300	0	193.5	0	64.50	0	64.5
0	50	0	44	0	88	88
50	50	48.91	37.87	97.82	75.74	86.78
75	50	71.04	32.33	94.73	64.66	82.70
100	50	91.12	29.46	91.12	58.92	80.38
150	50	131.67	23.91	87.78	47.82	77.79
200	50	158.9	16.91	79.45	33.82	70.32
250	50	174.32	11.8	69.73	23.6	62.04
300	50	151.98	8.24	50.66	16.48	45.77
0	50	0	44	0	88	88
0	75	0	60.30	0	80.41	80.41
0	100	0	76.2	0	76.2	76.2
0	150	0	86.73	0	57.82	57.82
0	200	0	91.24	0	45.62	45.62
0	250	0	101.9	0	40.76	40.76
0	300	0	111.09	0	37.03	37.03
50	0	49.79	0	99.58	0	99.58
50	50	48.91	37.87	97.82	75.74	86.78
50	75	42.91	52.84	85.82	70.46	76.60
50	100	39.66	60.91	79.32	60.91	67.04
50	150	34.82	75.45	69.64	50.30	55.13
50	200	31.11	79.9	62.22	39.95	44.40
50	250	26.99	81.95	53.98	32.78	36.31
50	300	24.87	61.11	49.74	20.37	24.56

Generally, three types of behaviors are possible in multicomponent biosorbates - biosorbent system: synergism (total removal efficiency was increased in presence of other metal ion), antagonism (total removal efficiency was decreased in presence of other metal ion), and non-interaction (no effect of other metal ion) [35, 267]. The biosorption behavior of two metal ions was examined by comparing the removal percent of single and dual metal ions systems. From **Table 5.1** it was supposed that the total removal percent should be 67.86 % for the total metal ion concentration

of 350 mg/L having 300 mg/L of Pb^{2+} ions and 50 mg/L of Cd^{2+} ions in the mixture [Total removal percent (%) = 67.86 = 100 x ((193.52 mg/L Pb^{2+} ions + 44 mg/L Cd^{2+} ions) / 350 mg/L initial total concentration)], but it was found that from **Table 5.1**, experimental total removal percent was 45.77 % for total 350 mg/L Pb^{2+} and Cd^{2+} ions mixture [Total removal percent (%) = 45.77 = 100 x ((151.98 mg/L Pb^{2+} ions + 8.24 mg/L Cd^{2+} ions) / 350 mg/L initial total concentration)]. Therefore, it was cleared that the dual metal ions solution of Pb^{2+} and Cd^{2+} ions showing antagonistic effect on biosorption of each metal ion which results in less removal [345]. The results obtained for single and dual metal ions biosorption systems shows that the uptake capacity of *S. filipendula* for Cd^{2+} ions was less than that of Pb^{2+} ions. It can be due to possible interaction effects between different metal ions in the solution and interactions on biosorbent surface depend on the biosorption mechanism. The factors on the basis of which biosorbates binds to the binding sites of biosorbent are properties (like surface properties, functional groups, and structure etc), biosorbate characteristics (like ionic size, ionic charge, ionic weight, concentration, ionic nature, standard redox potential or molecular size), and chemistry of the solution (like ionic strength, pH etc). But it is not easy to examine a common factor which can explain the interaction mechanism and selectivity of biosorption for a biosorbate from dual metal ions system.

5.3 MONOCOMPONENT EQUILIBRIUM ISOTHERM

In batch biosorption studies, experimental data shows that *S. filipendula* can be significantly used for Cd^{2+} and Pb^{2+} ions biosorption from aqueous solution. The equilibrium analysis for Cd^{2+} and Pb^{2+} ions biosorption on *S. filipendula* was examined with monocomponent biosorption isotherm models. **Table 5.2** shows the value of parameters and statistical indices of Pb^{2+} and Cd^{2+} ions for six different monocomponent isotherm models.

5.4 MULTICOMPONENT EQUILIBRIUM ISOTHERM

The simultaneous biosorption data of Pb^{2+} and Cd^{2+} ions on *S. filipendula* was analyzed by using five multicomponent isotherm models (non-modified Langmuir, modified Langmuir, extended Freundlich, non-modified Redlich Peterson, and modified Redlich Peterson). The parameters obtained from monocomponent isotherm model were used for modified models which are given in **Table 5.2**.The parameters of monocomponent isotherm models with correction factors were used

Table 5.2 Monocomponent isotherm model parameters for simultaneous removal of Cd^{2+} and Pb^{2+} ions

S. No.	Isotherm Models	Parameters	Cd^{2+}	Pb^{2+}
1	Langmuir	q_o	102.295	176.833
		b	0.127	0.709
		B_f	0.992	0.566
		NSD	7.028	31.880
		RMSE	6.238	17.735
		R^2	0.94	0.96
		R_L	1	1
2	Freundlich	k_f	32.2694	78.575
		n	4.253	4.777
		B_f	0.992	0.982
		NSD	7.202	10.596
		RMSE	4.588	13.373
		R^2	0.92	0.98
3	Redlich-Peterson	K	21.492	556.907
		a	0.3672	5.547
		b	0.883	0.856
		B_f	0.995	0.992
		NSD	5.62	6.851
		RMSE	4.33	7.668
		R^2	0.989	0.978
4	Radke-Prausnitz	q	0.366	0.608
		K	58.551	217.938
		A	0.883	0.490
		B_f	0.9947	0.995
		NSD	5.861	5.521
		RMSE	4.344	6.933
		R^2	0.96	0.999
5	Toth	a_T	0.4162	0.422
		n	0.085	0.317
		B_f	0.99	0.99
		NSD	6.287	5.927
		RMSE	4.372	6.93
		R^2	0.954	0.985
6	Fritz	a_1	0.0176	121.462
		a_2	0.0003	0.4768
		b_1	4.978	0.464
		b_2	4.817	0.490
		B_f	0.99	0.995
		NSD	3.3809	5.710
		RMSE	3.123	7.060
		R^2	0.998	0.987

for multicomponent non-modified models parameters. The biosorption equilibrium data from batch studies were analyzed by using Solver function of MS Excel (2010). The parameters of multicomponent isotherm models and average relative error 'q_e' values of Pb^{2+} and Cd^{2+} ions in the aqueous solution are given in **Table 5.3**.

Table 5.3 Multicomponent isotherm model parameters for simultaneous removal of Cd^{2+} and Pb^{2+} ions

S. No.	Isotherm Models	Parameters	Cd^{2+}	Pb^{2+}
1	Non modified Langmuir	q_o	102.295	176.833
		b	0.127	0.709
		ARE	50.62	33.045
2	Modified Langmuir	q_o	102.295	176.833
		b	0.1278	0.709
		n_i	0.3702	0.4712
		ARE	44.72	29.55
3	Extended Freundlich	k_f	32.269	78.57
		n_i	4.253	4.7775
		x_i	0.00057	0
		y_i	0.123	0.1529
		z_i	0.00502	0
		ARE	6.924	16.219
4	Non modified Redlich-Peterson	K_1	21.492	556.907
		K_2	0.3672	5.5475
		b_o	0.8836	0.8564
		ARE	74.827	17.099
5	Modified Redlich-Peterson	K_1	21.492	556.907
		K_2	0.3672	5.5475
		b_o	0.8836	0.8564
		n	0.0234	0.0857
		ARE	33.744	19.533

The comparison of multicomponent biosorption isotherm models with the experimental data is shown in **Fig. 5.5 (a & b)** for Cd^{2+} and Pb^{2+} ions, respectively. It was clear from **Fig. 5.5 (a & b)** that extended Freundlich model represents the best fit for experimental biosorption data in dual metal ions system with low value of average relative error (ARE = 16.21 and ARE = 6.92 for Pb^{2+} and Cd^{2+} ions, respectively). The sequence of best fitted model based on ARE values for Cd^{2+} ions: (extended Freundlich > extended Langmuir > modified Redlich-Peterson > modified Langmuir > non modified Langmuir > non modified Redlich-Peterson) and for Pb^{2+} ions: (extended Freundlich > modified Redlich-Peterson > non modified Redlich-Peterson > modified Langmuir > non modified

Langmuir > extended Langmuir). As extended Freundlich was the best fitted multicomponent isotherm model, it was expected that *S. filipendula* has a heterogenous surface [35].

5.5 CONCLUSIONS

The brown algae *S. filipendula* was proved to be an effective biosorbent for the simultaneous biosorption of Pb^{2+} and Cd^{2+} ions from aqueous solution. In case of both the single and dual metal ions systems under the same experimental conditions, the affinity of *S. filipendula* for Pb^{2+} ions was marginally greater than that for Cd^{2+} ions. The affinity of metal ions for binding sites was represented by Langmuir isotherm constant 'b' which also shows that *S. filipendula* has more affinity for Pb^{2+} ions as comparison to Cd^{2+} ions. It may be explained as a function of chemical characteristics of metal ion and bigger ionic size of Cd^{2+} ions reduces its sorption on *S. filipendula* surface as comparison to Pb^{2+} ions. The effect of presence of Pb^{2+} and Cd^{2+} ions on each other was found to be antagonistic [41]. The simultaneous biosorption of Pb^{2+} and Cd^{2+} ions on *S. filipendula* were described by five multicomponent isotherm models. Based on ARE values, the extended Freundlich isotherm model showed the best fit to experimental data of dual metal ions biosorption system.

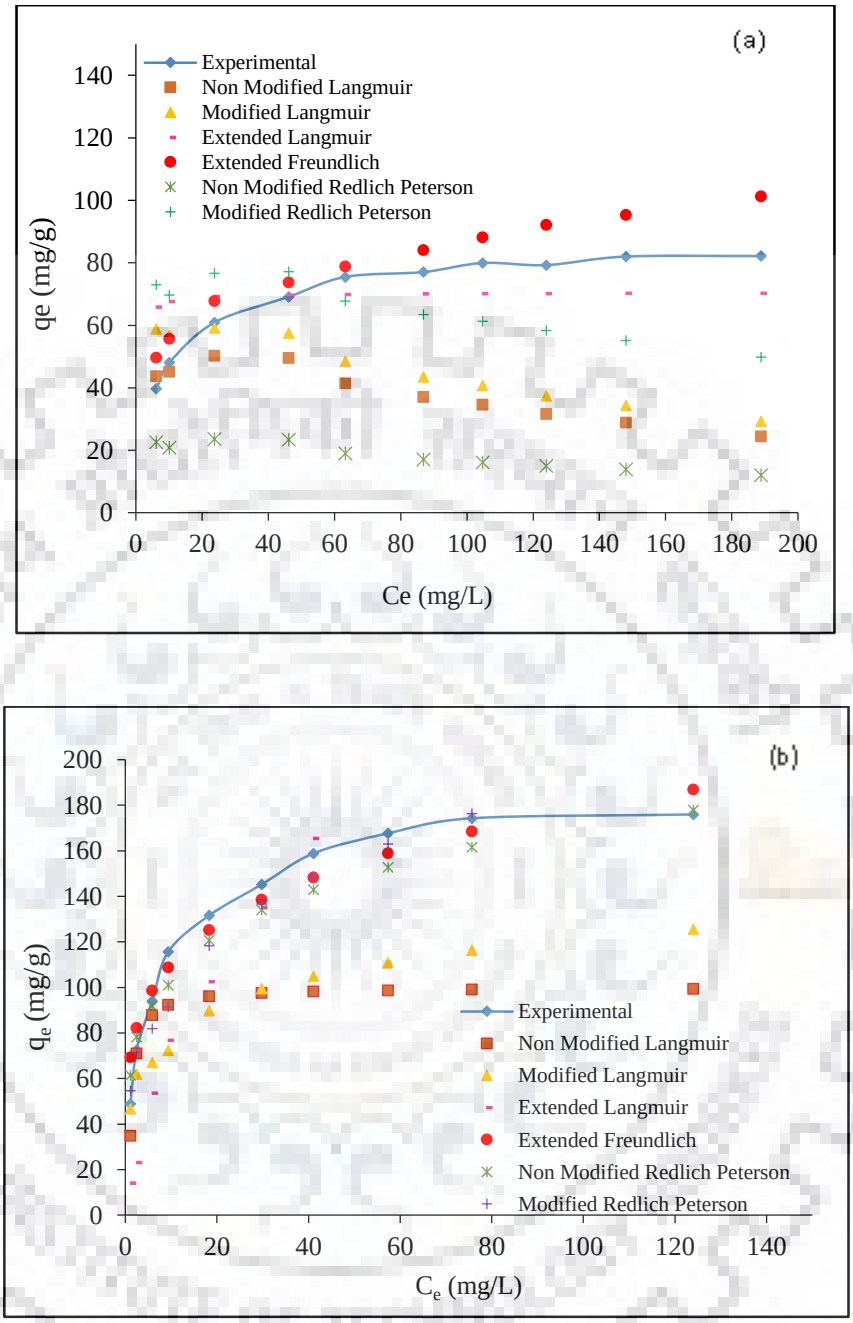

Fig. 5.5 Comparison of multicomponent isotherm models (a) Cd^{2+} ions (b) Pb^{2+} ions.

CHAPTER VI

CONCLUSIONS AND RECOMMENDATIONS

6.0 INTRODUCTION

The present research program is concerned with the removal of Pb^{2+}, Cd^{2+}, and Ni^{2+} ions from the synthetic wastewater in single and dual metal ion systems by biosorption process using brown seaweed *S. filipendula*. The results of biosorption studies related to single metal ion and dual metal ions biosorption systems have been summarized separately. According to the objectives mentioned in the section 1.5 of Chapter I, the summary of conclusions are compiled section wise as given below.

6.1 SINGLE METAL ION BIOSORPTION STUDIES

1. FESEM-EDS studies confirmed that ion exchange process was responsible for the uptake of Pb^{2+}, Cd^{2+}, and Ni^{2+} ions on *S. filipendula*.

2. The FTIR analysis describes the chelating characteristics of Pb^{2+}, Cd^{2+}, and Ni^{2+} ions. The main functional groups namely carboxyl, amide, and hydroxyl groups were involved in the binding of Pb^{2+}, Cd^{2+}, and Ni^{2+} ions on the surface of *S. filipendula*.

3. The batch biosorption experiments were conducted according to Central Composite Design.

4. Removal of Pb^{2+} ions by *S. filipendula* was found to be 96.0 % at pH of 4.99, temperature of 34.85 ^{o}C, biosorbent dosage of 0.5 g/L, and initial Pb^{2+} ions concentration of 152.10 mg/L.

5. Removal of Cd^{2+} ions by *S. filipendula* was found to be 99.56 % at pH of 5.7, temperature of 34.5 ºC, initial Cd^{2+} ions concentration of 50.8 mg/L, and biosorbent dosage of 0.99 g/L.

6. Removal of Ni^{2+} ions by *S. filipendula* was found to be 68.45 % at temperature of 41.47 ºC, pH of 5.4, biosorbent dosage of 1.97 g/L, and initial Ni^{2+} ions concentration of 83.18 mg/L.

7. The biosorption kinetic data for Pb^{2+}, Cd^{2+}, and Ni^{2+} ions followed Bangham, pseudo second order, and pseudo first order kinetic models, respectively. It shows that the nature of the process for Cd^{2+} , and Ni^{2+} ions biosorption were chemisorption and physisorption, respectively.

8. On the basis of large R^2 value and small $\Delta q\ \%$, the best fitted isotherm models were found to be Fritz for Pb^{2+} ions biosorption while Redlich-Peterson for Cd^{2+} and Ni^{2+} ions.

9. Desorption study shows the better reusability of *S. filipendula* upto four consecutive cycles of biosorption and desorption without any significant loss of their biosorption capacity.

10. Thermodynamic parameters (i.e. $\Delta G°$, $\Delta H°$ and $\Delta S°$) were also estimated for Pb^{2+}, Cd^{2+}, and Ni^{2+} ions biosorption. These values revealed that the biosorption processes of Pb^{2+}, Cd^{2+}, and Ni^{2+} ions were spontaneous, endothermic, and feasible in nature.

6.2 DUAL METAL IONS BIOSORPTION STUDIES

1. The affinity of the *S. filipendula* for Pb^{2+} ions was more than that for Cd^{2+} ions for both the single and dual metal ions solutions under the same experimental conditions. It may be explained as a function of chemical characteristics of metal ions and bigger ionic size of Cd^{2+} ions reduces its sorption on *S. filipendula* surface in comparison to Pb^{2+} ions.

2. The effect of presence of Pb^{2+} and Cd^{2+} ions on each other was found to be antagonistic which results in less removal. The results obtained for single and binary metal ion biosorption system shows that the uptake capacity of *S. filipendula* for Cd^{2+} ions was less than Pb^{2+} ions.

3. The simultaneous biosorption of Pb^{2+} and Cd^{2+} ions on *S. filipendula* were described by five multicomponent isotherm models. Based on ARE values, the extended Freundlich isotherm model showed the best fit to dual metal ions biosorption experimental data.

The statistical modeling and experimental studies on biosorption of Pb^{2+}, Cd^{2+} and Ni^{2+} ions from single and dual metal ions systems revealed that the brown seaweed *S. filipendula* has potential to be used in wastewater treatment for the removal of metal ions.

6.3 RECOMMENDATIONS FOR FURTHER INVESTIGATION

On the basis of present investigations, the following recommendations have been made for future studies:

1. As the present research work pertains to batch study of Pb^{2+}, Cd^{2+} and Ni^{2+} ions biosorption in single and dual metal ion systems, the biosorption studies in continuous systems like fixed or fluidized bed reactors are desirable.

2. Removal of metal ions from real industrial wastewater using various biosorbents can be practiced.

3. The biosorption capacity of biosorbents using more surface modifying agents can be examined.

4. Comparative study of bioremediation, phytoremediation and biosorption of metal ions should be carried out.

LIST OF RESEARCH PUBLICATIONS

International Refereed Journals

1. **Ayushi Verma**, Shashi Kumar, Surendra Kumar, Statistical modeling, equilibrium and kinetic studies of cadmium ions biosorption from aqueous solution using *S. filipendula*, Journal of Environmental Chemical Engineering 5, 2290–2304, 2017.

2. **Ayushi Verma**, Shashi Kumar, Surendra Kumar, Biosorption of lead ions from the aqueous solution by *Sargassum filipendula*: Equilibrium and kinetic studies, Journal of Environmental Chemical Engineering 4, 4587–4599, 2016.

3. **Ayushi Verma**, Shashi Kumar, Surendra Kumar, Chandrajit Balomajumder, Efficacy of *Sargassum filipendula* for the removal of Pb^{2+}, Cd^{2+} and Ni^{2+} ions from aqueous solution: A Comparative Study, Desalination and Water Treatment, Under review.

4. **Ayushi Verma**, Shashi Kumar, Chandrajit Balomajumder, Binary biosorption of lead and cadmium ions onto *Sargassum filipendula*: Co-ion effect on single component isotherm parameters, New Biotechnology Journal, Under review.

5. **Ayushi Verma**, Shashi Kumar, Chandrajit Balomajumder, Application of response surface methodology for the optimization of Ni^{2+} ions biosorption from aqueous solution using *Sargassum filipendula*, Journal of Molecular Liquids, Under review.

International Conferences

1. **Ayushi Verma**, Shashi Kumar, Surendra Kumar, Chandrajit Balomajumder, Equilibrium studies of Pb^{2+} ions biosorption from aqueous solution using *S. filipendula*, Oral Presentation, International Conference on Advances in Biosciences and Biotechnology, ICABB-2018, Feburary 1-3, 2018, at Jaypee Institute of Information Technology, Noida (INDIA).

2. **Ayushi Verma**, Shashi Kumar, Surendra Kumar, Investigation of Ni^{2+} ions biosorption from aqueous solution on *S. filipendula*, International Conference on Sustainable Technologies for Intelligent Water Management (STIWM-2018) Indian Institute of Technology Roorkee February 16-19 (2018).

3. **Ayushi Verma**, Shashi Kumar, Surendra Kumar, Equilibrium studies of Ni^{2+} ions biosorption from aqueous solution using *S. filipendula*, Poster Presentation, International Conference "Advancing Green Chemistry: Building a Sustainable Tomorrow ", New Delhi, October 3 (2017).

4. **Ayushi Verma**, Shashi Kumar, Biosorption isotherm study for Pb^{2+} ions recovery from aqueous solution by *Sargassum* sp., CHEMCON 2014, Punjab University, Chandigarh, India, December 27-30 (2014).

REFERENCES

1. Abbas SH, Ismail IM, Mostafa TM, and Abbas SH, Biosorption of heavy metals: A review, *J Chem Sci Tech, 3, 74-102, 2014.*

2. Abdia O, and Kazemia M, A review study of biosorption of heavy metals and comparison between different biosorbents, *J Mater Environ Sci, 6, 1386-1399, 2015.*

3. Acheampong MA, Sustainable gold mining wastewater treatment by sorption using low cost materials, *Ph.D Thesis, Wageningen University, Netherland, 2013.*

4. Aggarwal D, Goyal M, and Bansal RC, Adsorption of chromium by activated carbon from aqueous solution, *Carbon, 37, 1989-1997, 1999.*

5. Agrawal A, Pandey RS, and Sharma B, Water pollution with special reference to pesticide contamination in India, *J Water Resource Prot, 2, 432-448, 2010.*

6. Ahmad MA, Afandi NS, and Bello OS, Optimization of process variables by response surface methodology for malachite green dye removal using lime peel activated carbon, *Appl Water Sci, 284, 1-11, 2015.*

7. Ahmad R, and Hasan I, Optimization of the adsorption of Pb (II) from aqueous solution onto PAB nanocomposite using response surface methodology, *Environ Nanotechnol Monit Manage, 6, 116-129, 2016.*

8. Ahmadi A, Heidarzadeh S, Mokhtari AR, Darezereshki E, and Harouni HA, Optimization of heavy metal removal from aqueous solutions by maghemite (-Fe_2O_3) nanoparticles using response surface methodology, *J Geochem Explor, 147, 151-158, 2014.*

9. Ahmaruzzaman M, Industrial wastes as low-cost potential adsorbents for the treatment of wastewater laden with heavy metals, *Adv Colloid Interface Sci, 166, 36-59, 2011*.

10. Akbari M, Hallajisani A, Keshtkar AR, Shahbeig H, and Ghorbanian SA, Equilibrium and kinetic study and modeling of Cu (II) and Co (II) synergistic biosorption from Cu (II)-Co (II) single and binary mixtures on brown algae *C. indica, J Environ Chem Eng, 3, 140-149, 2015.*

11. Aksu Z, and Donmez G, Binary biosorption of cadmium (II) and nickel (II) onto dried *Chlorella vulgaris*: Co-ion effect on mono-component isotherm parameters, *Process Biochem, 41, 860-868, 2006.*

12. Aksu Z, Acikel U, Kabasakal E, and Tezer S, Equilibrium modelling of individual and simultaneous biosorption of chromium (VI) and nickel (II) onto dried activated sludge, *Water Res, 36, 3063-3073, 2002.*

13. Aksu Z, and Akinar D, Modelling of simultaneous biosorption of phenol and nickel onto dried aerobic activated sludge, *Sep Purif Technol, 21 (1-2), 87-99, 2000.*

14. Aksu Z, Determination of the equilibrium, kinetic and thermodynamic parameters of the batch biosorption of nickel (II) ions onto *Chlorella vulgaris*, *Process Biochem, 38, 89-99, 2002.*

15. Ali SM, Khalid AR, and Majid RM, The removal of zinc, chromium and nickel from industrial wastewater using corn cobs, *Iraqi J Sci, 55, 123-131, 2014.*

16. Ali SZ, Athar M, Farooq U, and Salman M, Insight into equilibrium and kinetics of the binding of cadmium ions on radiation-modified straw from *Oryza sativa*, *J Appl Chem (Article ID 417180), 2013.*

17. Aloma IC, Rodriguez I, Calero M, and Blazquez G, Biosorption of Cr^{6+} from aqueous solution by sugarcane bagasse, *Desalin Water Treat, 52, 5912-5922, 2014.*

18. Amini M, Younesi H, and Bahramifar N, Biosorption of nickel (II) from aqueous solution by *Aspergillus niger*: Response surface methodology and isotherm study, *Chemosphere, 75 1483-1491, 2009.*

19. Amini M, Younesi H, and Bahramifar N, Statistical modeling and optimization of the cadmium biosorption process in an aqueous solution using *Aspergillus niger, Colloids and Surf A, 337, 67-73, 2009.*

20. Amini M, Younesi H, Bahramifar N, Lorestani AAZ, Ghorbani F, Daneshi A, and Sharfizadeh M, Application of response surface methodology for optimization of lead biosorption in an aqueous solution by *Aspergillus niger, J Hazard Mater, 154 (1-3), 694-702, 2008.*

21. Amirnia S, Ray MB, and Margaritis A, Heavy metals removal from aqueous solutions using *Saccharomyces cerevisiae* in a novel continuous bioreactor-biosorption system, *Chem Eng J, 264, 863-872, 2015.*

22. Anayurt RA, Sari A, and Tuzen M, Equilibrium, thermodynamic and kinetic studies on biosorption of Pb (II) and Cd (II) from aqueous solution by macrofungus (*Lactarius scrobiculatus*) biomass, *Chem Eng J, 151, 255-261, 2009.*

23. Apiratikul R, and Pavasant P, Batch and column studies of biosorption of heavy metals by *Caulerpa lentillifera*, *Bioresour Technol, 99, 2766-2777, 2008.*

24. Arbabi M, Hemati S, and Amiri M, Removal of lead ions from industrial wastewater: A review of removal methods, *Int J Epidemiol, 2, 105-109, 2015.*

25. Arikawei AR, Owede KE, and Onokpite JO, Effects of industrial pollution on well-being of residents in trans-amadi industrial layout, Port Harcourt, Rivers State, *J Educ Real, 2, 80-93, 2017.*

26. Arivalagan P, Singaraj D, Haridass V, and Kaliannan T, Removal of cadmium from aqueous solution by batch studies using *Bacillus cereus*, *Ecol Eng, 71, 728-735, 2014.*

27. Arya SK, and Srivastava SK, Kinetics of immobilized cyclodextrin gluconotransferase produced by *Bacillus macerans* ATCC 8244, *Enzyme Microb Technol, 39, 507-510, 2006.*

28. Aryal M, Removal and recovery of nickel ions from aqueous solutions using *Bacillus Sphaericus, Biomass Int J Environ Res, 9, 1147-1156, 2015.*

29. Association Europeenne Oceanique, Metallic effluents of industrial origin in the marine environment, *Springer Netherlands, 1977.*

30. Asuquo ED, and Martin AD, Sorption of cadmium (II) ion from aqueous solution onto sweet potato (*Ipomoea batatas L.*) peel adsorbent: Characterisation, kinetic and isotherm studies, *J Environ Chem Eng, 4, 4207-4228, 2016.*

31. Atkinson BW, Bux F, and Kasan HC, Considerations for application of biosorption technology to remediate metal-contaminated industrial effluents, *Water SA, 24, 129-135, 1998.*

32. Aty AMA, Ammar NS, Ghafar HHA, and Ali RK, Biosorption of cadmium and lead from aqueous solution by fresh water alga *Anabaena sphaerica* biomass, *J Adv Res, 4, 367-374, 2013.*

33. Awwad AM, and Salem NM, Kinetics and thermodynamics of Cd (II) biosorption onto loquat (*Eriobotrya japonica*) leaves, *J Saudi Chem Soc, 18, 486-493, 2014.*

34. Azila YY, Mashitah MD, and Bhatia S, Process optimization studies of lead Pb (II) biosorption onto immobilized cells of *Pycnoporus sanguineus* using response surface methodology, *Bioresour Technol, 99, 8549-8552, 2008.*

35. Babu BV, and Gupta S, Adsorption of Cr (VI) using activated neem leaves: Kinetic studies, *Adsorption, 14, 85-92, 2008.*

36. Badmus MAO, Audu TOK, and Anyata BU, Removal of lead ion from industrial wastewaters by activated carbon prepared from periwinkle shells (*Typanotonus fuscatus*), *Turk J Eng Env Sci, 31, 251-263, 2007.*

37. Bandhyopadhyay K, Das D, Bhattacharyya P, and Maiti BR, Reaction engineering studies on biodegradation of phenol by *Pseudomonas putida* MTCC 1194 immobilized on calcium alginate, *Biochem Eng J, 8, 179-186, 2001.*

38. Barbosa JJM, Velandia CL, Maldonado AP, Giraldo L, and Piraja'n JCM, Removal of lead (II) and zinc (II) ions from aqueous solutions by adsorption onto activated carbon synthesized from watermelon shell and walnut shell, *Adsorption, 19, 675-685, 2013.*

39. Barquilha CER, Cossich ES, Tavares CRG, and Silva EA, Biosorption of nickel (II) and copper (II) ions in batch and fixed-bed columns by free and immobilized marine algae *Sargassum s*p, *J Clean Prod, 150, 58-64, 2017.*

40. Basha S, and Murthy ZVP, Kinetic and equilibrium models for biosorption of Cr (VI) on chemically modified seaweed, *Cystoseira indica, Process Biochem, 42, 1521-1529, 2007.*

41. Bayo J, Kinetic studies for Cd (II) biosorption from treated urban effluents by native grapefruit biomass (*Citrus paradisi* L.): The competitive effect of Pb (II), Cu (II) and Ni (II), *Chem Eng J, 191, 278-287, 2012.*

42. Belhachemi M, and Addoun F, Comparative adsorption isotherms and modeling of methylene blue onto activated carbon, *Appl Water Sci, 1, 111-117, 2011.*

43. Bermudez YG, Rico ILR, Bermudez OG, and Guibal E, Nickel biosorption using *Gracilaria caudata* and *Sargassum muticum, Chem Eng J, 166, 122-131, 2011.*

44. Bermudez YG, Rico ILR, Guibal E, de Hoces MC, and Martin-Lara MA, Biosorption of hexavalent chromium from aqueous solution by *Sargassum muticum* brown alga: Application of statistical design for process optimization, *Chem Eng J, 183, 68-76, 2012.*

45. Beveridge TJ, The role of cellular design in bacterial metal accumulation and mineralization, *Annu Rev Microbiol*, 43, 147-171, 1989.

46. Bhatnagar A, Vilar VJP, Ferreira C, Botelho CMS, and Boaventura RAR, Optimization of nickel biosorption by chemically modified brown macroalgae *(Pelvetia canaliculata), Chem Eng J, 193-194, 256-266, 2012.*

47. Bhatt P, Vyas RK, Pandit P, and Sharma M, Adsorption of reactive blue and direct red dyes on PAC: Equilibrium kinetics and thermodynamic studies, *Nat Env Poll Tech, 12, 397-405, 2013.*

48. Bilal M, Shah JA, Ashfaq T, Gardazi SMH, Tahir AA, Pervez A, Haroon H, and Mahmood Q, Waste biomass adsorbents for copper removal from industrial wastewater-A review, *J Hazard Mater, 263, 322-333, 2013.*

49. Blazquez G, Martin-Lara MA, Tenorio G, and Calero M, Batch biosorption of lead (II) from aqueous solutions by olive tree pruning waste: Equilibrium, kinetics and thermodynamic study, *Chem Eng J, 168, 170-177, 2011.*

50. Blazquez G, Ronda A, Martin-Lara MA, Perez A, and Calero M, Comparative study of isotherm parameters of lead biosorption by two wastes of olive-oil production, *Wat Sci Tech,72 (5), 711-720, 2015.*

51. Boparai HK, Joseph M, and Caroll DMO, Kinetics and thermodynamics of cadmium ion removal by adsorption onto nano zerovalent iron particles, *J Hazard Mater, 186, 458-465, 2011.*

52. Bulgariu D, and Bulgariu L, Potential use of alkaline treated algae waste biomass as sustainable biosorbent for clean recovery of cadmium (II) from aqueous media: Batch and column studied, *J Clean Prod, 112, 4525-4533, 2016.*

53. Cameselle C, and KR Reddy, Effects of periodic electric potential and electrolyte recirculation on integrated electrochemical remediation of contaminant mixtures, *Water, Air, Soil Pollut, 224 (8), 1-13, 2013.*

54. Carvalho MF, Duque AF, Goncalyes, and Castro PML, Adsorption of fluorobenzene onto granular activated carbon: Isotherm and bioavailability studies, *Bioresour Technol, 98, 3424-3430, 2007.*

55. Cayllahua JEB, Carvalho RJ, and Torem ML, Evaluation of equilibrium, kinetic and thermodynamic parameters for biosorption of nickel (II) ions onto bacteria strain, *Rhodococcus opacus, Miner Eng, 22, 1318-1325, 2009.*

56. Cechinel MAP, Mayer DA, Pozdniakova TA, LP Mazur, Boaventura RAR, de Souza AAU, de Souza SMAGU, and Vilar VJP, Removal of metal ions from a petrochemical wastewater using brown macro-algae as natural cation-exchangers, *Chem Eng J, 286, 1-15, 2016.*

57. Celekli A, and Bozkurt H, Biosorption of cadmium and nickel ions using *Spirulina platensis*: Kinetic and equilibrium studies, *Desalination, 275, 141-147, 2011.*

58. Chaisongkroh N, Chungsiriporn J, and Bunyakan C, Modeling and optimization of ammonia treatment by acidic biochar using response surface methodology, *Songklanakarin J Sci Technol, 34, 423-432, 2012.*

59. Chang LW, Magos L, and Suzuki T, Toxicology of Metals, *Boca Raton FL, USA: CRC Press, 1996.*

60. Charerntanyarak L, Heavy metals removal by chemical coagulation and precipitation, *Water Sci Technol, 39, 135-138, 1999.*

61. Chauhan D, Jaiswal M, and Sankararamakrishnan N, Removal of cadmium and hexavalent chromium from electroplating waste water using thiocarbamoyl chitosan, *Carbohydr Polym, 88, 670-675, 2012.*

62. Chen G, Zeng G, Tang L, Du C, Jiang X, Huang G, Liu H, and Shen G, Cadmium removal from simulated wastewater to biomass byproduct of *Lentinus edodes, Bioresour Technol, 99 (15), 7034-7040, 2008.*

63. Chen JP, Decontamination of heavy metals: Processes, mechanisms, and applications, *CRC Press, 2012.*

64. Chen Z, Ma W, and Han M, Biosorption of nickel and copper onto treated alga (*Undaria pinnatifida*): Application of isotherm and kinetic models, *J Hazard Mate, 155, 327-333, 2008.*

65. Cheng RC, Liang S, Wang HC, and Beuhler MD, Enhanced coagulation for arsenic removal, *J Am Water Works Assoc, 86, 7-90 1994.*

66. Cheung CW, Porter JF, and Mckay G, Sorption kinetic analysis for the removal of cadmium ions from effluents using bone char, *Water Res, 35, 605-612, 2001.*

67. Chien SH, and Clayton WR, Application of Elovich equation to the kinetics of phosphate release and sorption on soils, *Soil Sci Soc Am J, 44, 265-268, 1980.*

68. Chowdhury S, and Saha PD, Scale-up of a dye adsorption process using chemically modified rice husk: Optimization using response surface methodology, *Desalin Water Treat, 37, 331-336, 2012.*

69. Colak F, Necip A, Yazicioglu D, and Olgun A, Biosorption of lead from aqueous solutions by *Bacillus* strains heavy-metal resistance, *Chem Eng J, 173, 422-428, 2011.*

70. Collins YE, and Stotzky G, Heavy metals alter the electrokinetic properties of bacteria, yeast, and clay minerals, *Appl Environ Microbiol, 58, 1592-1600, 1992.*

71. Cordero B, Lodeiro P, Herrero R, and de Vicente MES, Biosorption of cadmium by *Fucus spiralis, Environ Chem, 1, 180-187, 2004.*

72. Coskun R, Soykan C, and Sac M, Adsorption of copper (II), nickel (II) and cobalt (II) ions from aqueous solution by methacrylic acid/acrylamide monomer mixture grafted poly (ethylene terephthalate) fiber, *Sep Purif Technol, 49, 107-114, 2006.*

73. Costa ACA, Tavares APM, and Franc FP, The release of light metals from an brown seaweed (*Sargassum* sp.) during zinc biosorption in a continuous system, *Egypt J Biotechnol, 4, 125-129, 2001.*

74. Costodes VC, Fauduet H, Porte C, and Delacroix A, Removal of Cd (II) and Pb (II) ions, from aqueous solutions, by adsorption onto sawdust of *Pinus sylvestris, J Hazard Mater, 105, 121-142, 2003.*

75. Crist RH, Oberholser K, Shank N, and Nguyen M, Nature of bonding between metallic ions and algal cell walls, *Environ Sci Technol, 15, 1212-1217, 1981.*

76. Cruz CCV, da Costa ACA, Henriques CA, and Luna AS, Kinetic modeling and equilibrium studies during cadmium biosorption by dead *Sargassum* sp. biomass, *Bioresour Technol, 91, 249-257, 2004.*

77. Curkovi L, Stefanovi SC, and Filipan T, Metal ion exchange by natural and modified zeolites, *Water Res, 31, 1379-1382, 1997.*

78. da Costa ACA, and de Franca FP, Cadmium uptake by biosorbent seaweeds: Adsorption isotherms and some process conditions, *Separ Sci Technol, 31, 2373-2393, 1996.*

79. da Motaa IO, de Castro JA, Casqueirab RG, and Junior AGO, Study of electroflotation method for treatment of wastewater from washing soil contaminated by heavy metals, *J Mater Res Technol, 4, 109-113, 2015.*

80. Dada AO, Olalekan AP, Olatunya AM, and Dada O, Langmuir, Freundlich, Temkin and Dubinin-Radushkevich isotherms studies of equilibrium sorption of Zn^{+2} onto phosphoric acid modified rice husk, *J Appl Chem, 3, 38-45, 2012.*

81. Das D, Basak G, Lakshmi V, and Das N, Kinetics and equilibrium studies on removal of zinc (II) by untreated and anionic surfactant treated dead biomass of yeast: batch and column mode, *Biochem Eng J, 64, 30-47, 2012.*

82. Davis TA, Volesky B, and Mucci A, A review of the biochemistry of heavy metal biosorption by brown algae, *Water Res, 37, 4311-4330, 2003.*

83. de Britto, da Costa ACA, Luna AS, and Henriques CA, Comparative study of ion- exchange and biosorption processes for the removal of Cd^{2+} and Zn^{2+} ions from aqueous effluents, *Adsorpt. Sci Technol, 25, 661-671, 2007.*

84. De M, Azargohar R, Dalai AK, and Shewchuk, SR, Mercury removal by bio-char based modified activated carbons. *Fuel, 103, 570-578, 2013.*

85. Deepa CN, and Suresha S. Biosorption of lead (II) from aqueous solution and industrial effluent by using leaves of *Araucaria cookii*: Application of response surface methodology, *J Environ Sci Toxicol Food Technol, 8, 67-79, 2014.*

86. Delshab S, Kouhgardi E, and Ramavandi B, Data of heavy metals biosorption onto *Sargassum oligocystum* collected from the northern coast of Persian Gulf, *Data Brief, 8, 235-241, 2016.*

87. Deng L, Su Y, Su H, Wang X, and Zhu X, Biosorption of copper (II) and lead (II) from aqueous solutions by nonliving green algae *Cladophora fascicularis*: Equilibrium, kinetics and environmental effects, *Adsorption, 12, 267-277, 2006.*

88. Dermentzis K, Valsamidou E, and Marmanis D, Simultaneous removal of acidity and lead from acid lead battery wastewater by aluminum and iron electrocoagulation, *J Eng Sci Technol, 5, 1-5, 2012.*

89. Dhabhai R, Ahmadifeijani E, Dalai AK, and Reaney M, Purification of crude glycerol using a sequential physico-chemical treatment, membrane filtration, and activated charcoal adsorption, *Sep Puri Technol, 168, 101-106, 2016.*

90. Din ATM, Hameed BH, and Ahmad AL, Batch adsorption of phenol onto physiochemical activated coconut shell, *J Hazard Mater, 161, 1522-1529, 2009.*

91. Doshi H, Ray A, and Kothari IL, Bioremediation potential of live and dead *Spirulina*: Spectroscopic, kinetics and SEM studies, *Biotechnol Bioeng, 96 (6), 1051-1063, 2007.*

92. Edwards M, Chemistry of arsenic removal during coagulation and Fe–Mn oxidation, *J Am Water Works Assoc, 86, 64-78, 1994.*

93. El-Kamash AM, Zaki AA, and Geleel MAE, Modeling batch kinetics and thermodynamics of zinc and cadmium ions removal from waste solutions using synthetic zeolite A, *J Hazard Mater, 127, 211-220, 2005.*

94. Fan WH, Xu ZZ, and Li Q, Kinetics and mechanism of nickel (II) ion biosorption by immobilized brown *Laminaria japonica* algae, *Adsorpt Sci Technol, 28, 499-504, 2010.*

95. Fanun M, The role of colloidal systems in environmental protection, *Elsevier, The Netherland, 2014.*

96. Farooq U, Khan MA, Athar M, and Kozinski JA, Effect of modification of environmentally friendly biosorbent wheat (*Triticum aestivum*) on the biosorptive removal of cadmium (II) ions from aqueous solution, *Chem Eng J, 171, 400- 410, 2011*.

97. Febriantoa J, Kosasih AN, Sunarso J, Ju YH, Indraswati N, and Ismadji S, Equilibrium and kinetic studies in adsorption of heavy metals using biosorbent: A summary of recent studies, *J Hazard Mater, 162, 616-645, 2009.*

98. Feijoo F, and Das TK, Design of pareto optimal CO_2 cap-and-trade policies for deregulated electricity networks, *Appl Energ, 119, 371-383, 2014.*

99. Fein JB, Daughney CJ, Yee N, and Davis TA, A chemical equilibrium model for metal adsorption onto bacterial surfaces, *Geochim Cosmochim Acta, 61, 3319-3328, 1997.*

100. Fenglian F, and Qi W, Removal of heavy metal ions from wastewaters: A review, *J. Environ Manage, 92, 407-418, 2011*.

101. Ferreira LS, Rodriguesa MS, de Carvalho JCM, Lodi A, Finocchio E, Perego P, and Converti A, Adsorption of Ni^{2+}, Zn^{2+} and Pb^{2+} onto dry biomass of *Arthrospira (Spirulina) platensis* and *Chlorella vulgaris*. I. single metal systems, *Chem Eng J, 173, 326-333, 2011*.

102. Flickinger MC, and Drew SW, Encyclopaedia of bioprocess technology: Fermentation, biocatalysis, and bioseparation, *John Wiley and Sons, Inc, USA, 1999.*

103. Foo KY, and Hameed BH, Insights into the modeling of adsorption isotherm systems, *Chem Eng J, 156, 2-10, 2010.*

104. Fourest E, and Volesky B, Alginate properties and heavy metal biosorption by marine algae, *Appl Biochem Biotechnol, 67, 33-44, 1997.*

105. Freitas OMM, Martins RJE, Delerue-Matos CM, and Boaventura RAR, Removal of Cd (II), Zn (II) and Pb (II) from aqueous solutions by brown marine macro algae: Kinetic modeling, *J Hazard Mate, 153, 493-501, 2008.*

106. Friis RH, Essentials of Environmental Health, *Jones and Barlett Publishers, 2008.*

107. Garba ZN, Bello I, Galadima A, and Lawal AY, Optimization of adsorption conditions using central composite design for the removal of copper (II) and lead (II) by defatted papaya seed, *Karbala Int J Mod Sci, 2, 20-28, 2016.*

108. Garg U, Kaur MP, Jawa GK, Sud D, and Garg VK, Removal of cadmium (II) from aqueous solutions by adsorption on agricultural waste biomass, *J Hazard Mater, 154, 1149-1157, 2008.*

109. Garnica JGF, Barrera LM, Camacho GP, and Urbina EC, Biosorption of Ni (II) from aqueous solutions by *Litchi chinensis* seeds, *Bioresour Technol, 136, 635-643, 2013.*

110. Garud RM, Kore SV, Kore VS, and Kulkarni GS, A short review on process and applications of reverse osmosis, *Univer J Environ Res Technol, 1, 233-238, 2011.*

111. Ghaedi M, Hajati S, Karimi F, Barazesh B, and Ghezelbash G, Equilibrium, kinetic and isotherm of some metal ion biosorption, *J Ind Eng Chem, 19, 987-992, 2013.*

112. Ghani NTA, Hefny M, and Chaghaby GAFE, Removal of lead from aqueous solution using low cost abundantly available adsorbents, *Int J Environ Sci Tech, 4, 67-73, 2007.*

113. Ghoneim MM, El-Desoky HS, El-Moselhy KM, Amer A, El-Naga EHA, Mohamedein LI, and Al-Prol AE, Removal of cadmium from aqueous solution using marine green algae, *Ulva lactuca, Egyptian J Aquat Res, 40, 235-242, 2014.*

114. Ghorbani F, Younesi H, Ghasempouri SM, Zinatizadeh AA, Amini M, and Daneshi A, Application of response surface methodology for optimization of cadmium biosorption in an aqueous solution by *Saccharomyces cerevisiae*, *Chem Eng J, 145, 267-275, 2008.*

115. Goel J, Kadirvelu, Rajagopal C, and Garg VK, Removal of lead (II) by adsorption using treated granular activated carbon: Batch and column studies, *J Hazard Mater, 125, 211-220, 2005.*

116. Gomez-Gonzalez R, Cerino-Cordova FJ, Garcia-Leon AM, Soto-Regalado E, Davila-Guzman NE, and Salazar-Rabago JJ, Lead biosorption onto coffee grounds: Comparative analysis of several optimization techniques using equilibrium adsorption models and ANN, *J Taiwan Inst Chem Eng, 68, 201-210, 2016.*

117. Goyal M, Rattan VK, Aggarwal D, and Bansal RC, Removal of copper from aqueous solutions by adsorption on activated carbons, *Colloids Surf A, 190, 229-238, 2001.*

118. Goyal M, Rattan VK, and Bansal RC, Adsorption of nickel from aqueous solutions by activated carbons, *Sep Purif Technol, 6, 305-312, 1999.*

119. Gunatilake SK, Methods of removing heavy metals from industrial wastewater, *J Multidiscip Eng Sci Stud, 1, 12-18, 2015.*

120. Gunda NSK, Choi HW, Berson A, Kenney B, Karan K, Pharoah JG, and Mitra SK, Focused ion beam-scanning electron microscopy on solid-oxide fuel-cell electrode: Image analysis and computing effective transport properties, *J Power Sources, 196 (7), 3592-3603, 2011.*

121. Gupta S, and Babu BV, Removal of toxic metal Cr (VI) from aqueous solutions using sawdust as adsorbent: Equilibrium, kinetics and regeneration studies, *Chem Eng J,150, 352-365,2009.*

122. Gupta S, and Babu BV, Modeling, simulation, and experimental validation for continuous Cr (VI) removal from aqueous solutions using sawdust as an adsorbent, *Bioresour Technol, 100, 5633-5640, 2009.*

123. Gupta VK, and Rastogi A, Biosorption of lead (II) from aqueous solutions by non-living algal biomass *Oedogonium* sp. and *Nostoc* sp. - A comparative study, *Colloids Surf B, 64, 170-178, 2008.*

124. Gupta VK, and Rastogi A, Biosorption of lead from aqueous solutions by green algae *Spirogyra* species: Kinetics and equilibrium studies, *J Hazard Mater, 152, 407-414, 2008.*

125. Gupta VK, Rastogi A, and Nayak A, Biosorption of nickel onto treated alga (*Oedogonium hatei*): Application of isotherm and kinetic models, *J Colloid Interface Sci, 342, 533-539, 2010.*

126. Gupta VK, Suhas, Nayak A, Agarwal S, Chaudhary M, and Tyagi I, Removal of Ni (II) ions from water using scrap tire, *J Mol Liq, 190, 215-222, 2014.*

127. Gutierrez C, Hansen HK, Hernandez P, and Pinilla C, Biosorption of cadmium with brown macroalgae, *Chemosphere, 138,164-169, 2015.*

128. Hackbarth FV, Girardi F, de Souza SMAGU, de Souza AAU, Boaventura RAR, and Vilar VJP, Marine macroalgae *Pelvetia canaliculata* (Phaeophyceae) as a natural cation exchanger for cadmium and lead ions separation in aqueous solutions, *Chem Eng J, 242, 294-305, 2014.*

129. Hammaini A, Ballester A, Gonzalez F, Blazquez ML, and Munoz JA, Activated sludge as biosorbent of heavy metals, *Process Metall, 9, 185-192, 1999.*

130. Hammer MJ, Water and wastewater technology, *3rd edition, Prentice Hall Collefe Div, 1995.*

131. Hannachi Y, Rezgui A, Dekhil AB, and Boubaker T, Removal of cadmium (II) from aqueous solutions by biosorption onto the brown macroalga (*Dictyota dichotoma*), *Desalin Water Treat, 54, 1663-1673, 2015.*

132. Hansen HK, Gutierrez C, Callejas J, and Cameselle C, Biosorption of lead from acidic aqueous solutions using *Durvillaea Antarctica* as adsorbent, *Miner Eng, 46-47, 95-99, 2013.*

133. Harja M, Buema G, Bulgariu L, Bulgariu D, Sutiman DM, and Ciobanu G, Removal of cadmium (II) from aqueous solution by adsorption onto modified algae and ash, *Korean J Chem Eng, 32, 1804-1811, 2015.*

134. Hasan SH, Srivastava P, and Talat M, Biosorption of Pb (II) from water using biomass of *Aeromonas hydrophila*: Central composite design for optimization of process variables, *J Hazard Mate, 168, 1155-1162, 2009.*

135. Hashem MA, Adsorption of lead ions from aqueous solution by okra wastes, *Int J Phys Sci, 2, 178-184, 2007.*

136. Hashim MA, and Chu KH, Biosorption of cadmium by brown green, and red seaweeds, *Chem Eng J, 97, 249-255, 2004.*

137. Hawari AH, and Mulligan CN, Biosorption of lead (II), cadmium (II), copper (II) and nickel (II) by anaerobic granular biomass, *Bioresour Technol*, 97, 692-700, 2006.

138. Hess K, and Straub PW, Chronic lead poisoning, *Schweiz Rundsch Med Prax, 63, 177-183, 1974.*

139. Ho YS, and McKay G, Application of kinetic models to the sorption of copper (II) on to peat, *Adsorpt Sci Technol, 20, 797-815, 2002.*

140. Ho YS, and McKay G, The kinetics of sorption of divalent metal ions onto sphagnum moss peat, *Water Res, 34, 735-742, 2000.*

141. Homaidan AAA, Alabdullatif JA, Hazzani AAA, Ghanayem AAA, and Alabbad AF, Adsorptive removal of cadmium ions by *Spirulina platensis* dry biomass, *Saudi J Biol Sci, 22, 795-800, 2015.*

142. Huang W, and Liu Z, Biosorption of Cd (II) / Pb (II) from aqueous solution by biosurfactant-producing bacteria: Isotherm kinetic characteristic and mechanism studies, *Colloids Surf B, 105, 113-119, 2013.*

143. Ibrahim WM, Biosorption of heavy metal ions from aqueous solution by red macro algae, *J Hazard Mater, 192, 1827-1835, 2011.*

144. Inyinbor AA, Adekola FA, and Olatunji GA, Kinetics, isotherms and thermodynamic modeling of liquid phase adsorption of Rhodamine B dye onto *Raphia hookerie* fruit epicarp, *Water Res Ind, 15, 14-27, 2016.*

145. Iqbala M, Saeeda A, and Zafar SI, FTIR spectrophotometry, kinetics and adsorption isotherms modeling, ion exchange, and EDX analysis for understanding the mechanism of Cd and Pb removal by mango peel waste, *J Hazard Mate, 164, 161-171, 2009.*

146. Isaac CPJ, and Sivakumar A, Removal of lead and cadmium ions from water using *Annona squamosa* shell: kinetic and equilibrium studies, *Desalin* Water Treat, *51, 7700-7709, 2013*.

147. Jain M, Garg VK, and Kadrivelu K, Investigation of Cr (VI) adsorption onto chemically treated *Helianthus annus*: Optimization using response surface methodology, *Bioresour Technol, 102 600-605, 2011.*

148. Jain S, Kumar P, Vyas RK, Pandit P, and Dalai AK, Adsorption optimization of acyclovir on prepared activated carbon, *Can J Chem Eng, 92, 1627-1635, 2014*.

149. Jalali R, Ghafourian H, Asef Y, Davarpanah SJ, and Sepehr S, Removal and recovery of lead using nonliving biomass of marine algae, *J Hazard Mater, 92, 253-262, 2002.*

150. Javanbakht V, Zilouei H, and Karimi K, Lead biosorption by different morphologies of fungus *Mucor indicus, Internat Biodeter Biodegr, 65, 294-300, 2011.*

151. Jellali S, Diamantopoulos E, Haddad K, Anane M, Durner W, and Mlayah A, Lead removal from aqueous solutions by raw sawdust and magnesium pretreated biochar: Experimental investigations and numerical modeling, *J Environ Manage, 180, 439-449, 2016.*

152. Jing-ming L, Xiao X, and Sheng-lian L, Biosorption of cadmium from aqueous solutions by industrial fungus *Rhizopus cohnii, Trans. Nonferrous Met Soc China 20, 1104-1111, 2010.*

153. Jnr MH, and Spiff AI, Studies on the effect of pH on the sorption of Pb^{2+} and Cd^{2+} ions from aqueous solutions by *Caladium bicolor* (Wild Cocoyam) biomass, *Electron J Biotechnol, 7, 313-323, 2004.*

154. Jo SW, Sherif SA, and Lear WE, Numerical simulation of saturated flow boiling heat transfer of ammonia/water mixture in bubble pumps for absorption–diffusion refrigerators, *J Thermal Sci Eng Appl*, 6 (1), 011007, 2014.

155. Kadirvelu K, Thamaraiselvi K, and Namasivayam C, Removal of heavy metal from industrial wastewaters by adsorption onto activated carbon prepared from an agricultural solid waste, *Bioresour Technol, 76, 63-65, 2001.*

156. Kalsi AS, and Srivastava AK, Biological phosphorous removal by *Acinetobacter* bacteria, Presented in CHEMCON 98 (Indian Chemical Engineering Congress 1998) Dec 16 – 19, 1998 at Visakhapatnam (Andhra Pradesh).

157. Kamsonlian S, and Shukla B, Optimization of process parameters using Response Surface Methodology (RSM): Removal of Cr (VI) from aqueous solution by wood apple shell activated carbon (WASAC), *Res J Chem Sci, 3, 31-37, 2013.*

158. Kanwal F, Rehman R, Anwar J, and Mahmud T, Adsorption studies of cadmium (II) using novel composites of polyaniline with rice husk and saw dust of *Eucalyptus camaldulensis, Electron J Environ Agric Food Chem, 10, 2972-2985, 2011.*

159. Khan AR, Ataullah R, and Al-Haddad A, Equilibrium adsorption studies of some aromatic pollutants from dilute aqueous solutions on activated carbon at different temperatures, *J Colloid Interface Sci, 194, 154-165, 1997.*

160. Khani MH, Pahlavanzadeh H, and Alizadeh K, Biosorption of strontium from aqueous solution by fungus *Aspergillus terreus, Environ Sci Pollut Res, 19, 2408-2418, 2012.*

161. Kim SY, Jin MR, Chung CH, Yun YS, Jahng KY, and Yu KY, Biosorption of cationic basic dye and cadmium by the novel biosorbent *Bacillus catenulatus* JB-022 strain, *J Biosci Bioeng, 119 (4), 433-439, 2015.*

162. Kleinubing SJ, da Silva EA, da Silva MGC, and Guibal E, Equilibrium of Cu (II) and Ni (II) biosorption by marine alga *Sargassum filipendula* in a dynamic system: Competitiveness and selectivity, *Bioresour Technol, 102, 4610-4617, 2011.*

163. Kleinubing SJ, Vieira RS, Beppu MM, Guibal E, and da Silv MGC, Characterization and evaluation of copper and nickel biosorption on acidic algae *Sargassum filipendula, Mat Res, 13 (4), 541-550, 2010.*

164. Kowanga K, Mauti GO, and Mauti EM, Biosorption for lead (II) ions from aqueous solutions by the biomass of *Spyridia filamentosa* algal species found in Indian Ocean, *J Inno Sci Res, 4 (5), 218-220, 2015.*

165. Kratochvil D, and Volesky B, Advances in the biosorption of heavy metals, *Trends Biotechnol, 16, 291-300, 1998.*

166. Kulkarni RM, Shetty KV, and Srinikethan G, Cadmium (II) and nickel (II) biosorption by *Bacillus laterosporus* (MTCC 1628), *J Taiwan Inst Chem Eng 45, 1628-1635, 2014.*

167. Kulkarni SJ, and Kaware JP, A review on research for cadmium removal from effluent, *Int J Innov Sci Eng Technol, 2, 465-469, 2013*.

168. Kumar A, Kumar S, and Kumar S, Adsorption of resorcinol and catechol on granular activated carbon: Equilibrium and kinetics, *Carbon, 41, 3015-3025, 2003.*

169. Kumar A, Kumar S, Kumar S, and Gupta DV, Adsorption of phenol and 4-nitrophenol on granular activated carbon in basal salt medium: Equilibrium and kinetics, *J Hazard Mater, 147,155-166, 2007.*

170. Kumar JIN, and Oommen C, Removal of heavy metals by biosorption using freshwater alga *Spirogyra hyaline, J Environ Biol, 33, 27-31, 2012.*

171. Kumar M, and Puri A, A review of permissible limits of drinking water, *Indian J Occup Envrion Med, 16, 40-44, 2012.*

172. Kumar P, Headley J, Peru K, Bailey J, and Dalai A, Removal of dicyclohexyl acetic acid from aqueous solution using ultrasound, ozone and their combination, *J Environ Sci Health A, 49 (13), 1512-1519, 2014.*

173. Kumar R, Bishnoi NR, Garima, and Bishnoi K, Biosorption of chromium (VI) from aqueous solution and electroplating wastewater using fungal biomass, *Chem Eng J, 135, 202-208, 2008.*

174. Kumar S, Zafar M, Prajapati J, Kumar S, and Kannepalli S, Modeling studies on simultaneous adsorption of phenol and resorcinol onto granular activated carbon from simulated aqueous solution, *J Hazard Mater, 185, 287-294, 2011.*

175. Kumari AR, and Sobha K, Removal of lead by adsorption with the renewable biopolymer composite of feather (*Dromaius novaehollandiae*) and chitosan (*Agaricus bisporus*), *Environ Tech Innov, 6, 11-26, 2016.*

176. Kuo S, and Lotse EG, Kinetics of phosphate adsorption and desorption by hematite and gibbsite, *Soil Sci, 116, 400-406, 1973.*

177. Kurniawan TA, Chan GYS, Lo WH, and Babel S, Physico–chemical treatment techniques for wastewater laden with heavy metals, *Chem Eng J, 118, 83-98, 2006.*

178. Kushwaha AK, Gupta N, and Chattopadhyaya MC, Adsorption behavior of lead onto a new class of functionalized silica gel, *Arab J Chem, 10, S81-S89, 2017.*

179. Lagergren S, Zur theorie der sogenannten adsorption gelo ster stoffe. Kungliga Svenska Vetenskapsakademiens, *Handlingar, 24, 1-39, 1898.*

180. Lalhmunsiama, Gupta PL, Jung H, Tiwari D, Kong SH, and Lee SM, Insight into the mechanism of Cd (II) and Pb (II) removal by sustainable magnetic biosorbent precursor to *Chlorella vulgaris, J Taiwan Inst Chem E, 71, 206-213, 2017.*

181. Lee SF, and Sherif SA, Thermodynamic analysis of a lithium bromide/water absorption system for cooling and heating applications, *Internat J Energy Res, 25 (11), 1019-1031, 2001.*

182. Lee YC, and Chang SP, The biosorption of heavy metals from aqueous solution by *Spirogyra* and *Cladophora* filamentous macroalgae, *Bioresour Technol, 102, 5297-5304, 2011.*

183. Leitao A, and Serrao R, Adsorption of phenolic compounds from water on activated carbon: Prediction of multicomponent equilibrium isotherms using single component data, *Adsorption, 11,167-179, 2005.*

184. Li Q, Wu S, Liu G, Liao X, Deng X, Sun D, Hu Y, and Huang Y, Simultaneous biosorption of cadmium (II) and lead (II) ions by pretreated biomass of *Phanerochaete chrysosporium, Sep Purif Technol, 34, 135-142, 2004.*

185. Li Z, and Yuan H, Characterization of cadmium removal by Rhodotorula sp. Y11, *Appl Microbiol Biotechnol, 73 (2), 458-463, 2006.*

186. Liu Y, Luo QCF, and Chen J, Biosorption of Cd^{2+}, Cu^{2+}, Ni^{2+} and Zn^{2+} ions from aqueous solutions by pretreated biomass of brown algae, *J Hazard Mater, 163, 931-938, 2009.*

187. Liu YG, Fan T, Zeng GM, Li X, Tong Q, Ye F, Zhou M, Xu WH, and Huang Y, Removal of cadmium and zinc ions from aqueous solution by living *Aspergillus niger*, *Tran Non ferr Metal Soc China, 16, 681-686, 2006.*

188. Lodeiro P, Cordero B, Barriada JL, Herrero R, and de Vicente MES, Biosorption of cadmium by biomass of brown marine macroalgae, *Bioresour Technol, 96 (16), 1796-1803, 2005.*

189. Lodeiro P, Herrero R, and de Vicente MES, The use of protonated *Sargassum muticum* as biosorbent for cadmium removal in a fixed-bed column, *J Hazard Mater, 137, 244-253, 2006.*

190. Loukidou MX, Karapantsios TD, Zouboulis AI, and Matis KA, Cadmium (II) biosorption by *Aeromonas caviae*: Kinetic modeling, *Sep Sci Technol, 40, 1293-1311, 2005.*

191. Low MJD, Kinetics of chemisorption of gases on solids, *Chem Rev, 60, 267-312, 1960.*

192. Lu WB, Shi JJ, Wang CH, and Chang JS, Biosorption of lead, copper and cadmium by an indigenous isolate *Enterobacter* sp. J1 possessing high heavy-metal resistance, *J Hazard Mater, 134, 80-86, 2006.*

193. Luna AS, Costa ALH, da Costa ACA, and Henriques CA, Competitive biosorption of cadmium (II) and zinc (II) ions from binary systems by *Sargassum filipendula*, *Bioresour Technol, 101, 5104-5111, 2010.*

194. Mahamadi C, and Nharingo T, Competitive adsorption of Pb^{2+}, Cd^{2+} and Zn^{2+} ions onto *Eichhornia crassipes* in binary and ternary systems, *Bioresour Technol, 101, 859-864, 2010.*

195. Maheshwari M, Vyas RK, and Sharma M, Kinetics, equilibrium and thermodynamics of ciprofloxacin hydrochloride removal by adsorption on coal fly ash and activated alumina, *Desalin Water Treat, 51, 7241-7254, 2013.*

196. Malik R, Ramteke DS, and Wate SR, Adsorption of malachite green on groundnut shell waste based powdered activated carbon, *Waste Manage, 27, 1129-1138, 2007.*

197. Malkoc E, and Nutoglu Y, Investigation of nickel II removal from aqueous solution using factory waste, *J Hazard Mater, 127, 120-128, 2005.*

198. Manasi, Rajesh V, Kumar ASK, and Rajesh N, Biosorption of cadmium using a novel bacterium isolated from an electronic industry effluent, *Chem Eng J, 235, 176-185, 2014.*

199. Martins BL, Cruz CCV, Luna AS, and Henriques CA, Sorption and desorption of Pb^{2+} ions by dead *Sargassum* sp. biomass, *Biochem Eng J, 27, 310-314, 2006.*

200. Martins RJE, Vilar VJP, and Boaventura RAR, Kinetic modelling of cadmium and lead removal by aquatic mosses, *Braz J Chem, 31, 229-242, 2014.*

201. Mathialagan T, and Viraraghavan T, Adsorption of cadmium from aqueous solutions by perlite, *J Hazard Mater, 94, 291-303, 2002.*

202. Matis KA, Zouboulis AI, Gallios GP, Erwe T, and Blocher C, Application of flotation for the separation of metal-loaded zeolite, *Chemosphere, 55, 65-72, 2004.*

203. Matis KA, Zouboulis AI, Lazaridis NK, and Hancock IC, Sorptive flotation for metal ions recovery, *Int J Miner Process, 70, 99-108, 2003.*

204. McKay G, and Ho YS, Pseudo-second order model for sorption processes, *Process Biochem, 34, 451-465, 1999.*

205. Meena AK, Mishra GK, Rai PK, Rajagopal C, and Nagar PN, Removal of heavy metal ions from aqueous solutions using carbon aerogel as an adsorbent, *J Hazard Mater, 122 161-170, 2005.*

206. Mengistie AA, Rao TS, Rao AVP, and Singanan M, Removal of lead (II) ions from aqueous solutions using activated carbon from *Militia ferruginea* plant leaves, *Bull Chem Soc Ethiop, 22, 349-360, 2008.*

207. Merrikhpour H, and Jalali M, Comparative and competitive adsorption of cadmium, copper, nickel, and lead ions by Iranian natural zeolite, *Clean Techn Environ Policy, 15 303-316, 2013.*

208. Mesas ML, Navarrete ER, Carrillo F, and Palet C, Bioseparation of Pb (II) and Cd (II) from aqueous solution using cork waste biomass. Modeling and optimization of the parameters of the biosorption step, *Chem Eng J, 174, 9-17, 2011*.

209. Miretzky P, Munoz C, and Carrillo-Chavez A, Experimental binding of lead to a low cost on biosorbent: Nopal (*Opuntia streptacantha*), *Bioresour Technol, 99, 1211-1217, 2008.*

210. Mishra A, Tripathi BD, and Rai AK, Biosorption of Cr (VI) and Ni (II) onto *Hyderilla verti cillata* dried biomass, *Ecol Eng, 73, 713-723, 2014.*

211. Moghal AAB, Reddy KR, Mohammed SAS, Al-Shamrani MA and Zahid WM, Lime-amended semi-arid soils in retaining copper, lead, and zinc from aqueous solutions, *Water Air Soil Pollut, 227 (372), 1-19, 2016.*

212. Mohammadpour A, Waghmare PR, Mitra SK, and Shankar K, Anodic growth of large-diameter multipodal TiO_2 nanotubes, *Acs Nano, 4 (12), 7421-7430, 2010.*

213. Mohan S, and Karthikeyan J, Removal of lignin and tannin color from aqueous solution by adsorption onto activated carbon solution by adsorption onto activated charcoal, Environ Pollul, 97, 183-187, 1997.

214. Mohanty K, Das D, and Biswas MN, Adsorption of phenol from aqueous solutions using activated carbons prepared from *Tectona grandis* sawdust by $ZnCl_2$ activation, *Chem Eng J, 115, 121-131, 2005.*

215. Mohanty. K, Das D, and Biswas MN, Preparation and characterization of activated carbons from *Sterculia alata* nutshell by chemical activation with zinc chloride to remove phenol from wastewater, *Adsorption, 12, 119-132, 2006.*

216. Mokaddem H, Sadaoui Z, Boukhelata N, Azouaoua N, and Kaci Y, Removal of cadmium from aqueous solution by polysaccharide produced from *Paenibacillus polymyxa*, *J Hazard Mater, 172, 1150-1155, 2009.*

217. Momcilovic MZ, Randelovic MS, Purenovic M, Onjia AE, Babic BM, and Matovic BZ, Synthesis and characterization of resorcinol formaldehyde carbon cryogel as efficient sorbent for imidacloprid removal, *Desalin Water Treat, 52, 7306-7316*, 2014.

218. Monteiro CM, Castro PML, and Malcata FX, Capacity of simultaneous removal of zinc and cadmium from contaminated media, by two microalgae isolated from a polluted site, *Environ Chem Lett, 9, 511-517, 2011.*

219. Montgomery DC, Introduction to Statistical Quality Control, fourth edition, *Wiley, New York, 2011.*

220. Montgomery JM, Water treatment principles and design, *John Wiley and Sons Inc, NY, USA, 1985.*

221. Morera MT, Echeverria JC, Mazkiaran C, and Garrido JJ, Isotherms and sequential extraction procedures for evaluating sorption and distribution of heavy metals in soils, *Environ Pollut, 113 135-144, 2001.*

222. Morshedi A, and Akbarian M, Application of response surface methodology: Design of experiments and optimization: A mini review, *Ind J Fund Appl Life Sci, 4, 2434-2439, 2014.*

223. Moussavi G, and Khosravi R, Removal of cyanide from wastewater by adsorption onto pistachio hull wastes: Parametric experiments, kinetics and equilibrium analysis, *J Hazard Mater, 183, 724-730, 2010.*

224. Munoz AJ, Espinola F, and Ruiz E, Removal of Pb (II) in a packed-bed column by a *Klebsiella* sp. 3S1 biofilm supported on porous ceramic raschig rings, *Ind Eng Chem Res, 40, 118-127, 2016.*

225. Murthy ZVP, Vijayaragavan K, and Pant KK, Kinetic and thermodynamic studies of Ni (II) adsorption onto activated carbon of *Abelmoschus manihot* from aqueous solutions, *J Disper Sci Technol, 34, 923-931, 2013.*

226. Nagajyoti PC, Lee KD, and Sreekanth TVM, Heavy metals, occurrence and toxicity for plants: A review, *Environ Chem Lett, 8, 199-216, 2010.*

227. Naiya TK, Bhattacharya AK, Mandal S, and Das SK, The sorption of lead (II) ions on rice husk ash, *J Hazard Mater, 163, 1254-1264, 2009.*

228. Netpae T, Removal of lead from aqueous solutions by *Aspergillus niger* from artificial vinegar factory, *Electron J Biol, 8 (1), 7-10, 2012.*

229. Nicklowitz WJ, and Mandybur TI, Neurofibrillaary changes following childhood lead encephalopathy, *J Neuropathol Exp Neurol, 34, 445-455, 1975.*

230. Njau KN, Woude M, Visser GJ, and Janssen LJJ, Electrochemical removal of nickel ions from industrial wastewater, *Chem Eng J, 79, 187-195, 2000.*

231. Nouri L, Ghodbane I, Hamdaoui O, and Chiha M, Batch sorption dynamics and equilibrium for the removal of cadmium ions from aqueous phase using wheat bran, *J Hazard Mater, 149, 115-125, 2007.*

232. Ofomaja AE, Unuabonah EI, and Oladoja NA, Competitive modeling for the biosorptive removal of copper and lead ions from aqueous solution by mansonia wood sawdust, *Bioresour Technol, 101, 3844-3852, 2010.*

233. Okoli CP, Diagboya, Anigbogu IO, Owolabi BIO, and Adebowale KO, Competitive biosorption of Pb (II) and Cd (II) ions from aqueous solutions using chemically modified moss biomass (*Barbula lambarenensis*), *Environ Earth Sci, 76, 1-10, 2017*.

234. Onal Y, Kinetics of adsorption of dyes from aqueous solution using activated carbon prepared from waste apricot, *J Hazard Mater, 137, 1719-1728, 2006.*

235. Ossman ME, and Mansour MS, Removal of Cd (II) ion from wastewater by adsorption onto treated old newspaper: Kinetic modeling and isotherm studies, *Int J Ind Chem, 4, 1-7, 2013.*

236. Oubagaranadin JUK and Murthy ZVP, Adsorption of divalent lead on a montmorillonite-illite type of clay, *Ind Eng Chem Res, 48, 10627-10636, 2009*.

237. Ozdemir S, Kilinc E, Poli A, Nicolaus B, and Guven K, Biosorption of Cd, Cu, Ni, Mn and Zn from aqueous solutions by thermophilic bacteria, *Geobacillus toebii* sub sp. *decanicus* and *Geobacillus thermoleovorans* sub sp. *stromboliensis*: Equilibrium, kinetic and thermodynamic studies, *Chem Eng J, 152, 195-206, 2009.*

238. Ozer A, Akkaya G, and Turabik M, Biosorption of acid blue 290 (AB 290) and acid blue 324 (AB 324) dyes on *Spirogyra rhizopus, J Hazard Mater, 135, 355-364, 2006.*

239. Ozer A, Gurbuz G, Calimli A, and Korbahti BK, Biosorption of copper (II) ions on *Enteromorpha prolifera*: Application of response surface methodology (RSM), *Chem Eng J, 146, 377-387, 2009.*

240. Ozer A, Gurbuz G, Calimli A, and Korbahti BK, Investigation of nickel (II) biosorption on *Enteromorpha prolifera*: Optimization using response surface analysis, *J Hazard Mater, 152, 778-788, 2008.*

241. Padmavathy V, Biosorption of nickel (II) ions by baker's yeast: Kinetic, thermodynamic and desorption studies, *Bioresour Technol, 99, 3100-3109, 2008.*

242. Padmavathy V, Vasudevan P, and Dhingra SC, Biosorption of nickel (II) ions on baker's yeast. *Process Biochem, 38, 1389-1395, 2003.*

243. Pahlavanzadeha H, Keshtkar AR, Safdari J, and Abadi Z, Biosorption of nickel (II) from aqueous solution by brown algae: Equilibrium, dynamic and thermodynamic studies, *J Hazard Mater, 175, 304-310, 2010.*

244. Patron-Prado M, Valdez MC, Zaragoza ES, Savin TZ, Cota DBL, and Rodriguez LM, Biosorption capacity for cadmium of brown seaweed *Sargassum sinicola* and *Sargassum lapazeanum* in the Gulf of California, *Water Air Soil Pollut. 221, 37-144, 2011.*

245. Pavasant P, Apiratikul R, Sungkhum V, Suthiparinyanont P, Wattanachira S, and Marhaba TF, Biosorption of Cu^{+2}, Cd^{+2}, Pb^{+2}, and Zn^{+2} using dried marine green macroalga *Cauler palentillifera, Bioresour Technol, 97, 2321-2329, 2006.*

246. Perez-Marin AB, Zapata VM, Ortuno JF, Aguilar M, Saez J, and Llorens M, Removal of cadmium from aqueous solutions by adsorption onto orange waste, *J Hazard Mater, 139, 122-131, 2007.*

247. Periasamy K, and Namasivayam C, Removal of nickel (II) from aqueous solution and nickel plating industry wastewater using an agricultural waste: Peanut hulls, *Waste Manage, 15, 63-68, 1995.*

248. Prado MP, Valdez MC, Zaragoza ES, Savin TZ, Cota DBL, and Rodriguez LM, Biosorption capacity for cadmium of brown seaweed *Sargassum sinicola* and *Sargassum lapazeanum* in the Gulf of California, *Water Air Soil Pollut, 221 (1-4),137-144, 2011.*

249. Prasad ASA, Varatharaju G, Anushri C, and Dhivyasree S, Biosorption of lead by *Pleurotus florida* and *Trichoderma viride, Br Biotechnol J, 3(1), 66-78, 2013.*

250. Prieto DM, Das TK, Savachkin A, Uribe A, Izurieta R, and Malavade S, A systematic review to identify areas of enhancements of pandemic simulation models for higher practical usability, *BMC Public Health , 12, 251, 2012.*

251. Pundir R, Chary GHVC, and Dastidar MG, Application of Taguchi method for optimizing the process parameters for the removal of copper and nickel by growing *Aspergillus* sp, *Water Resour Ind, in press 2016.*

252. Rabago JJS, and Ramos RL, Novel biosorbent with high adsorption capacity prepared by chemical modification of white pine (*Pinus durangensis*) sawdust, adsorption of Pb (II) from aqueous solutions, *J Environ Manage, 169, 303-312, 2016.*

253. Rahmati MMM, Rabbani P, Abdolali A, and Keshtkar AR, Kinetics and equilibrium studies on biosorption of cadmium lead, and nickel ions from aqueous solutions by intact and chemically modified brown algae, *J Hazard Mater, 185, 401-407, 2011.*

254. Rao KS, Anand S, and Venkateswarlu P, Equilibrium and kinetic studies for Cd (II) adsorption from aqueous solution on *Terminalia catappa L.* leaf powder biosorbent, *Indian J Chem Technol, 17, 329-336, 2010.*

255. Rao RAK, and Khan MA, Biosorption of bivalent metal ions from aqueous solution by an agricultural waste: Kinetics, thermodynamics and environmental effects, *Colloids Surf A Physicochem Eng Asp, 332, 121-128, 2009.*

256. Rathinam A, Maharshi B, Janardhanan SK, Jonnalagadda RR, and Nair BU, Biosorption of cadmium metal ion from simulated wastewaters using *Hypnea valentiae* biomass: A kinetic and thermodynamic study, *Bioresour Technol, 101, 1466-1470, 2010.*

257. Raymond C, Chemistry: Thermodynamics, *McGraw-Hill, Boston, 1998.*

258. Reddad Z, Gerente C, Andres Y, and Cloirec PL, Adsorption of several metal ions onto a low-cost biosorbent: Kinetic and equilibrium studies, *Environ Sci Technol, 36, 2067-2073, 2002.*

259. Reddy KR, Xie T, and Dastgheibi S, Removal of heavy metals from urban stormwater runoff using different filter materials, *J Environ Chem Eng, 2, 282-292, 2014.*

260. Romera E, Gonzalez F, Ballester A, Blazquez ML, and Munoz JA, Comparative study of biosorption of heavy metals using different types of algae, *Bioresour Technol, 98 (17), 3344-3353, 2007.*

261. Ronda, Settalluri VS, Bondili JS, Suryanarayana V, Venkateshwar P, Alluri HK, and Srinivasa, Biosorption: An eco-friendly alternative for heavy metal removal, *Afr J Biotechnol, 6, 2924-2931, 2007.*

262. Rout PR, Bhunia P, and Dash RR, Modeling isotherms, kinetics and understanding the mechanism of phosphate adsorption onto a solid waste: ground burnt patties, *J Environ Chem Eng, 2 (3),1331-1342, 2014.*

263. Rout PR, Bhunia P, and Dash RR, A mechanistic approach to evaluate the effectiveness of red soil as a natural adsorbent for phosphate removal from wastewater, *Desalin Water Treat, 54 (2), 358-373, 2015.*

264. Royer B, Cardoso NF, Lima EC, Vaghetti JCP, Simon NM, Calvete T, and Veses RC, Applications of Brazilian pine-fruit shell in natural and carbonized forms as adsorbents to

removal of methylene blue from aqueous solutions-kinetic and equilibrium study, *J Hazard Mater, 164, 1213-1222, 2009.*

265. Rubio J, Souza ML, and Smith RW, Overview of flotation as a wastewater treatment technique, *Miner Eng, 15, 139-155, 2002.*

266. S Paul, PK Nanda, C Mathoniere, Hearns NGR, Clerac R and Ray D, Aqua bridge cleavage and metal ion extrusion by thiocyanate anions in a dicopper complex, *Inorganica Chimica Acta, 370 108-116, 2011.*

267. Sag Y, and Kutsal T, The selective biosorption of chromium (VI) and copper (II) ions from binary metal mixtures by *Rhizopus arrhizus* biomass, *Process Biochem, 31, 561-572, 1996.*

268. Saleem M, Pirzada T, and Qadeer R, Sorption of acid violet 17 and direct red 80 dyes on cotton fiber from aqueous solutions, *Colloids Surf A, 292, 246-250, 2007.*

269. Salem NM, and Awwad AM, Biosorption of Ni (II) from electroplating wastewater by modified (*Eriobotrya japonica*) loquat bark, *J Saudi Chem Soc, 18, 379-386, 2014.*

270. Sarada B, Prasad MK, Kumar KK, and Murthy CVR, Cadmium removal by macro algae *Caulerpa fastigiata:* Characterisation, kinetic, isotherm and thermodynamic studies, *J Environ Chem Eng*, 2, 1533-1542, 2014.

271. Sari A, and Tuzen M, Biosorption of cadmium (II) from aqueous solution by red algae (*Ceramium virgatum*): Equilibrium, kinetic and thermodynamic studies, *J Hazard Mater, 157, 448-454, 2008.*

272. Sarkar M, Clerac R, Mathoniere C, Hearns NGG, Bertolasi V, and Ray D, New phenoxide-bridged quasi-tetrahedral and rhomboidal [cu4] compounds bearing u4 oxide or u1,1-azido ligands: synthesis, chemical reactivity and magnetic studies, *Inorg Chem, 50, 3922-33, 2011.*

273. Sarkar M, Clerac R, Mathoniere C, Hearns NGG, Bertolasi V, and Ray D, New u4-oxide-bridged copper benzoate quasi-tetrahedron and bis-u3-hydroxido-bridged copper azide and copper thiocyanate stepped cubanes: Core conversion, structural diversity, and magnetic properties, *Inorg Chem, 49, 6575-6585, 2010.*

274. Satarug S, Garrett SH, Ann SM, and Sens DA, Cadmium, environmental exposure, and health outcomes, *Environ Health Perspect, 118, 182-90, 2010.*

275. Sdiri A, Higashi T, Chaabouni R, and Jamoussi F, Binary adsorption of heavy metals from aqueous solution onto natural clays, *Chem Eng J, 225, 535-546, 2013.*

276. Seker A, Shahwan T, Eroglu AE, Yilmaz S, Demirel Z, and Dalay MC, Equilibrium, thermodynamic and kinetic studies for the biosorption of aqueous lead (II), cadmium (II) and nickel (II) ions on *Spirulina platensis, J Hazard Mater, 154, 973-980, 2008.*

277. Selatnia A, Bakhti MZ, Madani A, Kertous L, and Mansouri Y, Biosorption of Cd^{2+} from aqueous solution by a NaOH-treated bacterial dead *Streptomyces rimosus* biomass, *Hydrometallurgy, 75, 11-24, 2004.*

278. Selatnia A, Boukazoula A, Kechid N, Bakhti MZ, Chergui A, and Kerchich Y, Biosorption of lead (II) from aqueous solution by a bacterial dead *Streptomyces rimosus* biomass, *Biochem Eng J, 19 (2), 127-135, 2004.*

279. Sengil IA, and Ozacar MO, Competitive biosorption of Pb^{2+}, Cu^{2+} and Zn^{2+} ions from aqueous solutions onto valonia tannin resin, *J Hazard Mater, 166, 1488-1494, 2009*.

280. Senthilkumar G, and Murugappan A, Kinetic modeling and multicomponent isotherm studies on adsorption of multi heavy metal ions in MSW leachate by alcoffine, *Int J Chem Tech Res, 8, 324-343, 2015.*

281. Shahverdi F, Moghadam SA, Ahmadi M, and Faramarzi MA, Biosorption of nickel (II) from aqueous solution on immobilized fungal biomass of *Aspergillus awamori, Asian J Research Chem, 7, 570-575, 2014.*

282. Shanab S, Essa A, and Shalaby E, Bioremoval capacity of three heavy metals by some microalgae species (Egyptian Isolates), *Plant Signal Behav, 7 (3), 392-399, 2012.*

283. Sharma M, Vyas RK, and Singh K, A review on reactive adsorption for potential environmental applications, *Adsorption, 19, 161-188, 2013.*

284. Sheng PX, Ting YP, Chen JP, and Hong L, Sorption of lead, copper, cadmium, zinc, and nickel by marine algal biomass: Characterization of biosorptive capacity and investigation of mechanisms, *J Colloid Interface Sci, 75, 131-141, 2004.*

285. Sherif SA, Barbir F, and Veziroglu TN, Wind energy and the hydrogen economy-Review of the technology, *Sol Energy, 78 (5), 647-660, 2005.*

286. Shinde NR, Bankar AV, Kumar AR, and Zinjarde SS, Removal of Ni (II) ions from aqueous solutions by biosorption onto two strains of *Yarrowia lipolytica, J Environ Manage, 102, 115-124, 2012.*

287. Shroff KA, and Vaidya VK, Kinetics and equilibrium studies on biosorption of nickel from aqueous solution by dead fungal biomass of *Mucor hiemalis*, *Chem Eng J, 171 1234-1245, 2011*.

288. Shun-Fu L, and Sherif SA, Second law analysis of various double-effect lithium bromide/water absorption chillers/Discussion. *ASHRAE Transactions, 107, 664, 2001*.

289. Siahkamari M, Jamali A, Sabzevari A, and Shakeri A, Removal of lead (II) ions from aqueous solutions using biocompatible polymeric nano-adsorbents: A comparative study, *Carbohydr Polym, 157, 1180-1189, 2017.*

290. Silva JP, Sousa S, Rodrigues J, Antunes H., Porter JJ, Gonçalves I, and Dias SF, Adsorption of acid orange 7 dye in aqueous solutions by spent brewery grains, *Sep Purif Technol, 40, 309-315, 2004.*

291. Singh A, Mehta SK, and Gaur JP, Removal of heavy metals from aqueous solution by common freshwater filamentous algae, *World J Microbiol Biotechnol, 23, 1115-1120, 2007.*

292. Singh H, and Rattan VK, Adsorption of nickel from aqueous solutions using low cost biowaste adsorbents, *Water Qual Res J Can, 6 (1), 239-249, 2011.*

293. Singh KK, Singh AK, and Hasan SH, Low cost biosorbent wheat bran for the removal of cadmium from wastewater: Kinetic and equilibrium studies, *Bioresour Technol, 97, 994-1001, 2006.*

294. Singh RK, Kumar S, Kumar S, and Kumar A, Development of parthenium based activated carbon and its utilization for adsorptive removal of p-cresol from aqueous solution, *J Hazard Mater, 155, 523-535, 2008.*

295. Singh RK, Vats S, and Tyagi P, Industrial wastewater treatment by biological activated carbon-a review industrial wastewater treatment by biological activated carbon-A Review, *Res J Pharm Biol Chem Sci, 2, 1053-1058, 2011.*

296. Singh Y, and Srivastava SK, Performance improvement of *Bacillus aryabhattai* ITBHU02 for high-throughput production of a tumor-inhibitory L-asparaginase using a kinetic model based approach, *J Chem Technol Biotechnol, 89, 117-127, 2014.*

297. Sjahrul M, and Arifin, Phytoremediation of Cd^{2+} by marine phytoplanktons, *Tetracelmis chuii* and *Chaetoceros calcitrans*, *Int J Chem, 4 (1), 69-74, 2012.*

298. Soin N, Roy SS, Mitra SK, Thundat T, and McLaughlin JA, Nanocrystalline ruthenium oxide dispersed Few Layered Graphene (FLG) nanoflakes as supercapacitor electrodes, *J Mater Chem, 22 (30), 14944-14950, 2012.*

299. Soleymani F, Khani MH, Pahlavanzadeh H, and Manteghian M, Study of cobalt (II) biosorption on *Sargassum* sp. by experimental design methodology, *Int J Environ Sci Technol, 12, 1907-1922, 2015.*

300. Soni B, Swami M, and Shah HR, Electrochemical Methods for wastewater treatment, *Indian J Appl Res, 5, 70-73, 2015.*

301. Southichak B, Nakano K, Nomura M, Chiba N, and Nishimura O, Marine macroalga *Sargassum horneri* as biosorbent for heavy metal removal: Roles of calcium in ion exchange mechanism, *Water Sci Technol, 58, 697-704, 2008.*

302. Srivastava NK, and Majumder CB, Novel biofiltration methods for the treatment of heavy metals from industrial wastewater, *J Hazard Mater, 151, 1-8, 2008.*

303. Srivastava NK, Jha MK, and Sreekrishnan TR, Removal of Cr (VI) from waste water using nio nanoparticles, *Int J Sci Environ Tech, 3,395-402, 2014.*

304. Srivastava NK, Parhi SS, Jha MK, and Sreekrishnan TR, Optimization of effect of pre-treatment on chromium removal by algal biomass using response surface methodology, *Int J Eng Res, 3, 167-171, 2014.*

305. Srivastava S, and Srivastava AK, Biological phosphate removal by model based fed-batch cultivation of *Acinetobacter calcoaceticus, Biochem Eng J, 40 (2), 227-232, 2008.*

306. Srivastava S, and Srivastava AK, Biological phosphate removal by model based continuous cultivation of *Acinetobacter calcoaceticus, Process Biochem, 41 (3), 624-630, 2006.*

307. Sud D, Mahajan G, and Kaur MP, Agricultural waste material as potential adsorbent for sequestering heavy metal ions from aqueous solutions – A review, *Bioresour Technol, 99, 6017-6027, 2008.*

308. Sugashini S, and Gopalakrishnan S, Studies on the performance of protonated cross linked chitosan beads (PCCB) for chromium removal, *Res J Chem Sci, 2, 55-59, 2012.*

309. Sulaymon AH, Mohammed AA, and Al-Musawi TJ, Competitive biosorption of lead, cadmium, copper, and arsenic ions using algae, *Environ Sci Pollut Res, 20, 3011-3023, 2013.*

310. Sun YM, Horng CY, Chang FL, Cheng LC, and Tian WX, Biosorption of lead, mercury, and cadmium ions by *Aspergillus terreus* immobilized in a natural matrix, *Pol J Microbiol, 59 (1), 37-44, 2010.*

311. Sunderman Jr FW, Shen SK, Mitchell JM, Allpass PR, and Damjanoy I, Embryotoxicity and fetal toxicity of nickel in rats, *Toxicol Appl Pharmacol, 43, 381-390, 1978.*

312. Sweetly DJ, Sangeetha K, and Suganthi B, Biosorption of heavy metal lead from aqueous solution by non-living biomass of *Sargassum myriocystum*, *Int J Appl Innov Eng Manag, 3, 39-45, 2014.*

313. Tabaraki R, and Nategh A, Multimetal biosorption modeling of Zn^{2+}, Cu^{2+} and Ni^{2+} by *Sargassum ilicifolium*, *Ecolo Eng, 71, 197-205, 2014.*

314. Tabaraki R, Nateghi A, and Ahmady-Asbchin S, Biosorption of lead (II) ions on *Sargassum ilicifolium*: Application of response surface methodology, *Internat Biodeter Biodegradation, 93, 145-152, 2014.*

315. Tasar S, Kaya F, and Ozer A, Biosorption of lead (II) ions from aqueous solution by peanut shells: Equilibrium, thermodynamic and kinetic studies, *J Envrion Chem Eng, 2, 1018-1026, 2014.*

316. Teng H, and Hsieh C, Activation energy for oxygen chemisorption on carbon at low temperatures, *Ind Eng Chem Res, 38, 292-297, 1999.*

317. Treybal RE, Mass-Transfer Operations, *3rd edition, McGraw-Hill, 1981*.

318. Tripathi A, and Ranjan MR, Heavy metal removal from wastewater using low cost adsorbent, *J Bioremed Biodeg, 6, 1-5, 2015.*

319. Tripathi A, and Srivastava SK, Biodegradation of orange G by a novel isolated bacterial strain *Bacillus megaterium* ITBHU01 using response surface methodology, *Afr J Biotechnol, 11 (7), 1768-1781, 2012.*

320. Tuzun I, Bayramoglu G, Yalcin E, Basaran G, Celik G, and Arica MY, Equilibrium and kinetic studies on biosorption of Hg (II), Cd (II) and Pb (II) ions onto microalgae *Chlamydomonas reinhardtii, J Environ Manag, 77, 85-92, 2005.*

321. Uribe A, Savachkin A, Das TK, Santana A, and Prieto D, A predictive decision aid methodology for dynamic mitigation of influenza pandemics, *OR Spectrum, 33 (3), 751-786, 2011 .*

322. Uzunoglu D, Gurel N, Ozkaya N, and Ozer A, The single batch biosorption of copper (II) ions on *Sargassum acinarum, Desalin Water Treat, 52, 1514-1523, 2014.*

323. Verma A, Kumar S, and Kumar S, Biosorption of lead ions from the aqueous solution by *Sargassum filipendula*: Equilibrium and kinetic studies, *J Environ Chem Eng, 4, 4587- 4599, 2016.*

324. Verma AK, Dash RR, and Bhunia P, A review on chemical coagulation/flocculation technologies for removal of colour from textile wastewaters, *J environ manage, 93 (1),154-168, 2012.*

325. Vieira DM, da Costa ACA, Henriques CA, Cardoso VL, and de Franca FP, Biosorption of lead by the brown seaweed *Sargassum filipendula* – Batch and continuous pilot studies, *Electron J Biotechnol, 10, 368-375, 2007.*

326. Vieira RHSF, and Volesky B, Biosorption: Asolution to pollution, *International Microbiol, 3, 17- 24, 2000.*

327. Vilar VJP, Botelho CMS, and Boaventura RAR, Equilibrium and kinetic modelling of Cd (II) biosorption by algae *Gelidium* and agar extraction algal waste, *Water Res, 40, 291-302, 2006.*

328. Vilar VJP, Botelho CMS, and Boaventura RAR, Influence of pH, ionic strength and temperature on lead biosorption by *Gelidium* and agar extraction algal waste, *Process Biochem, 40, 3267-3275, 2005.*

329. Vimala R, and Das N, Biosorption of cadmium (II) and lead (II) from aqueous solutions using mushrooms: A comparative study, *J Hazard Mater, 168, 376-382, 2009.*

330. Vimala R, and Das N, Mechanism of Cd (II) adsorption by macrofungus *Pleurotus platypus, J Environ Sci, 23, 288-293, 2011.*

331. Vinh NV, Zafar M, Behera S. K, and Park HS, Arsenic (III) removal from aqueous solution by raw and zinc loaded pine cone biochar: Equilibrium, kinetics, and thermodynamics studies, *Int J Environ Sci Technol, 12, 1283-1294, 2015.*

332. Viswanathan B, Adsorption of small molecules on metallic surfaces, *Bull Catal Soc India, 3, 43-53, 2004.*

333. Volesky B, and Kuyucak N, Biosorbent for gold, *US Patent No. 4, 769, 233, 1988.*

334. Volesky B, Sorption and Biosorption, *BV-Sorbex, Inc. St. Lambert (Montreal), Quebec, Canada, 2003*.

335. Volesky B, May H, and Holan ZR, Cadmium biosorption by *Saccharomyces cerevisiae, Biotechnol Bioeng, 41(8), 826-9, 1993.*

336. Volesky B, May-Phillips HA, Biosorption of heavy metals by *Saccharomyces cerevisiae*, *Appl Microbiol Biotechnol, 42 (5), 797-806, 1995.*

337. Wang W, Wang X, Wang X, Yang L, Wu Z, Xia S, and Zhao J, Cr (VI) removal from aqueous solution with bamboo charcoal chemically modified by iron and cobalt with the assistance of microwave, *J Environ Sci, 25, 1726-1735, 2013.*

338. Wang Y, Li Y, and Zhao FJ, Biosorption of chromium (VI) from aqueous solutions by *Sargassum thunbergii* Kuntze, *Biotechnol Biotec Equip, 28, 259-265, 2014.*

339. Wierzba S, Biosorption of lead (II) zinc (II) and nickel (II) from industrial wastewater by *Stenotrophomonas maltophilia* and *Bacillus subtilis, Pol J Chem Technol, 17, 7-87, 2015.*

340. Wierzba S, Biosorption of nickel (II) and zinc (II) from aqueous solutions by the biomass of yeast *Yarrowia lipolytica, Pol J Chem Technol, 19 (1), 1-l0, 2017.*

341. World Health Organization (WHO), Guidelines for drinking-water quality, Incorporating First Addendum to 3rd Edition, Recommendations, *World Health Organization, Geneva, 2006.*

342. World Health Organization, Trace Elements in Human Nutrition and Health, *World Health Organization, Switzerland: Geneva, 2006.*

343. Wurster DE, Alkhamis KA, and Matheson LE, Prediction of adsorption from multicomponent solutions by activated carbon using single-solute parameters, *AAPS Pharm Sci Tech, 1, 79-93, 2000.*

344. Xu M, Wang H, Lei D, Qu D, Yujia Z, and Yili W, Removal of Pb (II) from aqueous solution by hydrous manganese dioxide: Adsorption behavior and mechanism, *J Environ Sci, 25, 479-486, 2013.*

345. Yan G, and Viraraghavan T, Heavy metal removal from aqueous solution by fungus *Mucorrouxii, Water Res, 37, 4486-4496, 2003.*

346. Yan G, and Viraraghavan, T, Effect of pretreatment on the bioadsorption of heavy metals on *Mucor rouxii*, *Water SA, 26, 119-123, 2000.*

347. Yan T, Luo X, Lin X, and Yang J, Preparation, characterization and adsorption properties for lead (II) of alkali-activated porous leather particles, *Colloids Surf A, 512 7-16, 2017.*

348. Yasemin B, and Zeki T, Removal of heavy metals from aqueous solution by sawdust adsorption, *J Environ Sci, 19, 160-166, 2007.*

349. Yu B, Zhang Y, Shukla A, Shukla SS, and Dorris KL, The removal of heavy metals from aqueous solutions by sawdust adsorption- removal of lead and comparison of its adsorption with copper, *J Hazard Mater, 84, 83-94, 2001.*

350. Yu JX, Wang LY, Chi RA, Zhang YF, Xu ZG, and Guo J, Competitive adsorption of Pb^{2+} and Cd^{2+} on magnetic modified sugarcane bagasse prepared by two simple steps, *Appl Surf Sci, 268, 163-170, 2013.*

351. Zafar M, Kumar S, Kumar S, and Dhiman AK, Optimization of polyhydroxybutyrate (PHB) production by *Azohydromonas lata* MTCC 2311 by using genetic algorithm based on artificial neural network and response surface methodology, *Biocatal Agric Biotechnol, 1, 70-79, 2012.*

352. Zhang X, Zhao X, Wan C, Chen B, and Bai F , Efficient biosorption of cadmium by the self-flocculating microalga *Scenedesmus obliquus* AS-6-1, *Algal Res, 16, 427-433, 2016.*

353. Zhou H, and Smith DW, Advanced technologies in water and wastewater treatment, *J Environ Eng Sci, 1, 247-264, 2002.*

354. Zhou K, Yang Z, Liu Y, and Kong X, Kinetics and equilibrium studies on biosorption of Pb (II) from aqueous solution by a novel biosorbent: *Cyclosorus interruptus, J Environ Chem Eng, 3, 2219-2228, 2015.*

355. Zolgharnein J, Asanjarani N, and Shariatmanesh T, Taguchi L 16 orthogonal array optimization for Cd (II) removal using *Carpinus betulus* tree leaves: Adsorption characterization, *Int Biodeter Biod, 85, 66-77, 2013.*